

**THE UNIVERSITY OF CALGARY**

**Molecular Studies on the Retinal Rod Na/Ca+K Exchanger**

**by**

**Joseph Edward Lovell Tucker**

**A DISSERTATION**

**SUBMITTED TO THE FACULTY OF GRADUATE STUDIES**

**IN PARTIAL FULFILLMENT OF THE REQUIREMENTS FOR THE**

**DEGREE OF DOCTOR OF PHILOSOPHY**

**DEPARTMENT OF**

**BIOCHEMISTRY AND MOLECULAR BIOLOGY**

**CALGARY, ALBERTA**

**APRIL, 2000**

**© Joseph Edward Lovell Tucker 2000**



**National Library  
of Canada**

**Acquisitions and  
Bibliographic Services**

**395 Wellington Street  
Ottawa ON K1A 0N4  
Canada**

**Bibliothèque nationale  
du Canada**

**Acquisitions et  
services bibliographiques**

**395, rue Wellington  
Ottawa ON K1A 0N4  
Canada**

*Your file Votre référence*

*Our file Notre référence*

**The author has granted a non-exclusive licence allowing the National Library of Canada to reproduce, loan, distribute or sell copies of this thesis in microform, paper or electronic formats.**

**The author retains ownership of the copyright in this thesis. Neither the thesis nor substantial extracts from it may be printed or otherwise reproduced without the author's permission.**

**L'auteur a accordé une licence non exclusive permettant à la Bibliothèque nationale du Canada de reproduire, prêter, distribuer ou vendre des copies de cette thèse sous la forme de microfiche/film, de reproduction sur papier ou sur format électronique.**

**L'auteur conserve la propriété du droit d'auteur qui protège cette thèse. Ni la thèse ni des extraits substantiels de celle-ci ne doivent être imprimés ou autrement reproduits sans son autorisation.**

**0-612-49544-2**

**Canada**

## **ABSTRACT**

The retinal rod Na/Ca+K exchanger couples the extrusion of Ca to the inward Na and outward K gradients, and rapidly lowers cytosolic Ca in the rod outer segment, providing a key cellular signal for the recovery from photoexcitation. At the start of this doctoral project, only the bovine rod Na/Ca+K exchanger had been cloned, and no information was available on structure function relationships.

In this dissertation I report the cloning of the second Na/Ca+K exchanger cDNA, the human rod NCKX1, as well as the determination of the associated chromosomal localization and genomic organization. Comparison of the cDNA sequences reveals unexpectedly low homology between the bovine and human homologues in the extracellular and cytoplasmic loop regions. However, the hydrophobic membrane-spanning domains show strong conservation. Examination of the genomic organization revealed that the human rod NCKX1 exchanger contains nine introns, five of them clustered in a short region that codes for the N-terminal portion of the cytosolic loop. Analysis of human and bovine retinal transcripts found that alternate splicing occurs in the cytoplasmic region where the gene is divided by the multiple introns. The human rod NCKX1 gene was localized to chromosome 15q22-23, and ongoing investigations are looking into the role of NCKX1 in human retinopathy.

Construction and heterologous expression of deletion and chimeric bovine Na/Ca+K exchanger mutants demonstrated that only the two large hydrophobic transmembrane segments are required for Na<sub>i</sub>-dependent Ca influx, ie. reverse exchange. In addition, the Na/Ca+K exchanger characteristic K-dependence is maintained in the heterologously expressed deletion mutant, as measured by K<sub>m</sub> activation constants for Ca and K.

## **ACKNOWLEDGEMENTS**

I wish to take this opportunity to thank my mentors, past and present, for the insights, direction and encouragement I have received from them over the years. In particular, Randy Johnston and Paul Schnetkamp have played pivotal roles in the development and progress of my career.

I would also like to thank my wife and children for their love and support throughout this endeavor, and for the sacrifices they have made on my behalf. As well, I'd like to recognize the steadfast encouragement and unequivocal faith in me displayed by my father Dr. Edward Tucker and my grandmother Margaret Elliott. My mother, Lindis Psutka, always knew I could do it.

It has been my great good fortune to work closely with two of the most skilled and capable technicians the University of Calgary has to offer. For all the years I have known them, Robert Szerencsei and Bob Winkfein have tirelessly contributed their blood, sweat and tears to the endeavors of others, in return for little recognition. Gentlemen, I thank you. Your efforts have meant a great deal to me.

All of the members of my graduate, candidacy and defense committees deserve gratitude for their efforts and support of my project, and for their guidance throughout my graduate career.

## **DEDICATION**

This dissertation is dedicated to:

My wife **Candace**  
and my children **Joshua, Mykaela and Daniel.**

They are my inspiration and my purpose.

## TABLE OF CONTENTS

<b>Approval Page</b>	ii
<b>Abstract</b>	iii
<b>Acknowledgments</b>	iv
<b>Dedication</b>	v
<b>Table of Contents</b>	vi
<b>List of Tables</b>	x
<b>List of Figures</b>	xi
<b>List of Abbreviations</b>	xiv
<b>Epigraph</b>	xvii
<b>CHAPTER ONE: INTRODUCTION</b>	1
1.1 Na/Ca Exchange	2
1.1.1 NCX and NCKX Gene Families	2
1.1.2 Comparisons of NCX and NCKX Exchangers	3
1.1.3 Structural Similarities and Differences	6
1.1.4 Similarities and Differences, at the Amino Acid Level	11
1.1.5 Current Research on NCX	12
1.1.6 Current Research on NCKX	21
1.2 The Role of Calcium in Phototransduction	24
1.2.1 Phototransduction Excitation	27
1.2.2 Recovery from Excitation	31
1.2.3 Calcium and cGMP-gated Channel	34

1.2.4	Calcium and Guanylate Cyclase .....	36
1.2.5	Calcium and Phosphodiesterase .....	38
1.3	Retinitis Pigmentosa .....	42
1.3.1	Rhodopsin Mutants .....	46
1.3.2	RIM/ABCR Mutants .....	48
1.3.3	<i>rds</i> /Peripherin Mutants .....	49
1.3.4	Retinal Rod cGMP Phosphodiesterase .....	50
1.3.5	Retinal Rod cGMP-gated Channel .....	50
1.3.6	Genotypic and Phenotypic Diversity .....	51
1.3.7	Potential Role of NCKX1 in Degenerative Human Retinopathies .....	52
<b>CHAPTER TWO: OBJECTIVES .....</b>		<b>53</b>
<b>CHAPTER THREE: MATERIALS AND METHODS .....</b>		<b>55</b>
3.1	Molecular Techniques .....	56
3.1.1	DNA Preparation .....	56
3.1.2	RNA .....	57
3.1.3	Gel Electrophoresis .....	59
3.1.4	DNA Manipulation .....	61
3.1.5	PCR .....	62
3.1.6	Sequencing Reactions .....	63
3.1.7	Probe Synthesis .....	64
3.1.8	Sample Detection .....	65
3.2	Clone Construction .....	70

3.2.1	Cloning of Bovine NCKX1 / NCX1 Mutants .....	70
3.2.2	Construction of Human NCKX1 Derived Clones .....	75
3.2.3	Construction of RNase Protection Assay Probe Templates .....	77
3.3	Cell Culture .....	78
3.3.1	Bacteria .....	78
3.3.2	CHO Cells .....	80
3.3.3	HEK Cells .....	81
3.3.4	SF9/SF21 Cells .....	82
3.3.5	HighFive Cells .....	83
3.4	Functional Assays .....	84
<b>CHAPTER FOUR: RESULTS .....</b>		<b>91</b>
4.1	cDNA Cloning of the Human Retinal Rod Na-Ca+K Exchanger: Comparison with a Revised Bovine Sequence .....	92
4.2	Chromosomal Localization and Genomic Organization of the Human Retinal Rod Na-Ca+K Exchanger .....	110
	Addendum to Chapter 4.2 .....	121
4.3	Alternate Splicing of the Human Exchanger .....	138
4.3.1	Introduction .....	138
4.3.2	Results .....	141
	4.3.2.1 RT-PCR of Alternately Spliced Transcripts .....	141
	4.3.2.2 RNase Protection Assay .....	151
	4.3.2.3 Human Deletion Constructs .....	161



4.3.3	Discussion	169
4.4	Chimeric / Deletion Mutants of Bovine Na-Ca+K Exchanger	171
4.4.1	Introduction	171
4.4.2	Results	172
4.4.3	Discussion	210
<b>CHAPTER FIVE: DISCUSSION</b>		<b>212</b>
5.1	Cloning of the Human Rod NCKX1 cDNA	213
5.2	Chromosomal Localization and Role in Human Retinopathy	215
5.3	Genomic Organization and Implications	216
5.4	Alternate Splicing of NCKX1 Homologues in Mammals	218
5.5	Expression of OF Double Deletion Construct	220
5.6	Transmembrane Domain Mediates Na/Ca+K Exchange	221
5.7	Activity of the Cytosolic Domain	222
5.8	Activity of the Extracellular Domain	223
5.9	Inhibition of Heterologous Function Mediated by Cytoplasmic Domain	224
5.10	Future Experiments	226
<b>BIBLIOGRAPHY</b>		<b>229</b>
<b>APPENDIX I: Oligonucleotides</b>		<b>254</b>
<b>APPENDIX II: Cloned DNA Sequences</b>		<b>257</b>

## LIST OF TABLES

<b>Table 1</b>	<b>Causative Loci of Retinitis Pigmentosa . . . . .</b>	<b>44</b>
<b>Table 2</b>	<b>Digital Imaging Solution Buffers . . . . .</b>	<b>87</b>
<b>Table 3</b>	<b>Calculated and Published Values for <math>K_m</math> K, <math>K_m</math> Ca for OF (NCKX1) . .</b>	<b>208</b>

## LIST OF FIGURES

<b>Figure 1.1</b>	<b>Topological Models of NCX1. ....</b>	<b>7</b>
<b>Figure 1.2</b>	<b>The Topological Model of NCKX1. ....</b>	<b>9</b>
<b>Figure 1.3</b>	<b>Schematic Representation of the NCX1 and NCX3 Alternately Spliced Cytosolic Loops Alternate splicing in NCX1 and NCX3 .....</b>	<b>19</b>
<b>Figure 1.4</b>	<b>Rod and Cone Photoreceptor Physical Structure. ....</b>	<b>25</b>
<b>Figure 1.5</b>	<b>Excitation Cascade in the Rod Photoreceptor. ....</b>	<b>28</b>
<b>Figure 1.6</b>	<b>Recovery of the Rod Photoreceptor Following Excitation. ....</b>	<b>32</b>
<b>Figure 3.1</b>	<b>Chimeric and Deletion Constructs. ....</b>	<b>71</b>
<b>Figure 3.2</b>	<b>Digital Imaging Equipment. ....</b>	<b>89</b>
<b>Figure 4.1</b>	<b>Amino Acid Sequence Comparison. ....</b>	<b>98</b>
<b>Figure 4.2</b>	<b>The Bovine-Human Rod Na-Ca+K Exchanger. ....</b>	<b>101</b>
<b>Figure 4.3</b>	<b>Alignment of Acidic Repeats. ....</b>	<b>104</b>
<b>Figure 4.4</b>	<b>Genomic Organization of Human Rod NCKX1 Gene. ....</b>	<b>115</b>
<b>Figure 4.5</b>	<b>Human NCKX1 FISH. ....</b>	<b>118</b>
<b>Figure 4.6</b>	<b>Southern Blot of PAC 136E11. ....</b>	<b>122</b>
<b>Figure 4.7</b>	<b>PCR Digests. ....</b>	<b>124</b>
<b>Figure 4.8</b>	<b>Human NCKX1 Northern. ....</b>	<b>129</b>
<b>Figure 4.9</b>	<b>3'-RACE of Human NCKX1. ....</b>	<b>131</b>
<b>Figure 4.10</b>	<b>5'-RACE of Human NCKX1. ....</b>	<b>133</b>
<b>Figure 4.11</b>	<b>5' Flanking Sequence. ....</b>	<b>136</b>

<b>Figure 4.12</b>	<b>Sequence Alignment of Cytosolic Domains. ....</b>	<b>139</b>
<b>Figure 4.13</b>	<b>RT with No RT Control. ....</b>	<b>142</b>
<b>Figure 4.14</b>	<b>Exon Constituency of Human Alternately Spliced Bands. ....</b>	<b>144</b>
<b>Figure 4.15</b>	<b>Developmental Regulation of Human NCKX1 Alternate Splicing. ...</b>	<b>147</b>
<b>Figure 4.16</b>	<b>Mouse RT-PCRs of Cytosolic Region. ....</b>	<b>149</b>
<b>Figure 4.17</b>	<b>Amino Acid Sequence Alignment. ....</b>	<b>152</b>
<b>Figure 4.18</b>	<b>Human RPA. ....</b>	<b>156</b>
<b>Figure 4.19</b>	<b>Bovine RPA. ....</b>	<b>159</b>
<b>Figure 4.20</b>	<b>Domain Alignments of OF, EX, CR, Dolphin and Dbv. ....</b>	<b>162</b>
<b>Figure 4.21</b>	<b>Heterologously Expressed Human Splice Variant Western Blots. ....</b>	<b>165</b>
<b>Figure 4.22</b>	<b>Digital Imaging of HFD vs. ECH Transient Transfections. ....</b>	<b>167</b>
<b>Figure 4.23</b>	<b>CHO Stable Cell Lines. ....</b>	<b>173</b>
<b>Figure 4.24</b>	<b>Fura-2 Traces of Stable CHO Cell Lines. ....</b>	<b>176</b>
<b>Figure 4.25</b>	<b>Fluorescein-linked Immunohistochemistry of RCRII-CHO Cells. ....</b>	<b>179</b>
<b>Figure 4.26</b>	<b>Early p17, OF Digital Imaging Results. ....</b>	<b>182</b>
<b>Figure 4.27</b>	<b>Low Percentage of Cells Displaying K-dependent Na / Ca Exchange. .</b>	<b>185</b>
<b>Figure 4.28</b>	<b>Dependence K-dependent Na/Ca Exchange on Na-loading. ....</b>	<b>189</b>
<b>Figure 4.29</b>	<b>Thapsigargin / FCCP Addition Increases Percentage of Responding Cells. ....</b>	<b>192</b>
<b>Figure 4.30</b>	<b>340:380 ratios of Individual Cells Correlated with Screen Captures. ..</b>	<b>194</b>
<b>Figure 4.31</b>	<b>Multiple Exchange Cycles of OF. ....</b>	<b>197</b>
<b>Figure 4.32</b>	<b>Characteristic Kinetic Curve of Ca Influx: NCX vs OF. ....</b>	<b>199</b>

<b>Figure 4.33</b>	<b>Ca-dependence of Na/Ca+K Exchange Mediated by OF. ....</b>	<b>204</b>
<b>Figure 4.34</b>	<b>K-dependence of Na/Ca+K Exchange Mediated by OF. ....</b>	<b>206</b>

## LIST OF ABBREVIATIONS

$\alpha$	alpha
$\beta$	beta
$\gamma$	gamma
$\lambda$	lambda
$\mu$	micro
$\mu\text{g}$	microgram
$\mu\text{l}$	microlitre
$\mu\text{M}$	micromolar
A2-E	lipofuscin fluorophore component
ABCR	ATP binding cassette transporter - retina
AcMNPV	<i>Autographa californica</i> nucleopolyhedrovirus
AM	acetoxymethyl ester
AMD	age-related macular degeneration
arRP	autosomal recessive retinitis pigmentosa
ATP	adenosine 5'-triphosphate
BBS4	Bardet-Biedl Syndrome type 4
BES	N,N-bis(2-hydroxyethyl)-2-aminomethanesulfonic acid
bp	basepair
BSA	bovine serum albumin
C-terminal	carboxy-terminal
CaM	calmodulin
CCC	bovine NCX1 mutant with intracellular loop deleted and replaced by intracellular loop of NCKX1
cDNA	complementary deoxyribonucleic acid
CFTR	cystic fibrosis transmembrane conductance regulator
cGMP	cyclic guanosine monophosphate
CHO	chinese hamster ovary
cm	centimeter
CR	bovine NCKX1 deletion mutant lacking the extracellular hydrophilic loop.
CRD	cone rod dystrophy
CTP	cytosine 5'-triphosphate
dATP	2'-deoxyadenosine 5'-triphosphate
ddNTP	dideoxynucleoside triphosphate
DEPC	diethyl pyrocarbonate
DMEM	Dulbecco's modified Eagle's medium
DNA	deoxyribonucleic acid
dNTP	deoxynucleoside triphosphate
DTT	dithiothreitol
dUTP	deoxyuridine triphosphate
<i>E. coli</i>	<i>Escherichia coli</i>
ECH	human FLAG-tagged NCKX1 cDNA (exon III absent)
EDTA	ethylene-diamine tetraacetic acid

EGTA	ethylene glycol-bis (beta-aminoethyl ether) N,N,N',N'-tetraacetic acid
ERG	electroretinogram
EtOH	ethanol
EX	full length bovine Na/Ca+K exchanger (NCKX1)
FCCP	carbonylcyanide-p-(trifluoromethoxy)phenylhydrazone
FFM	fundus flavimaculatus
FISH	fluorescence <i>in situ</i> hybridization
g	gravity
GARP	glutamic acid rich protein
GC	guanylate cyclase
GCAP	guanylate cyclase activating protein
GDP	guanosine diphosphate
GTE	glucose / tris / EDTA
GTP	guanosine triphosphate
HEK	human embryonic kidney
HEPES	N-2-hydroxyethylpiperazine-N'-2-ethanesulfonic acid
HFD	human FLAG-tagged NCKX1 exon III-VI deletion mutant
hNCKX1	human NCKX1
HRP	horseradish peroxidase
i	internal
IFC	bovine NCKX1 mutant with extracellular and intracellular hydrophilic loops deleted, and the intracellular loop of the Na/Ca exchanger inserted.
IMDM	Iscoe's modified Dulbecco's medium
IP <sub>3</sub>	inositol trisphosphate
IPTG	isopropyl-β-D-thiogalactopyranoside
kb	kilobase
K <sub>m</sub>	Michaelis constant
L	litre
LB	Luria-Bertani broth
M	molar
mg	milligram
mM	millimolar
MOI	multiplicity of infection
mOsm	milliosmole
N-terminal	amino-terminal
NCBP	neuron-specific Ca-binding proteins
NEB	New England Biolabs
ng	nanogram
nM	nanomolar
o	external
OD	optical density
OF	bovine NCKX1 double deletion mutant with both the extracellular and intracellular hydrophilic loops deleted.

p17	full length bovine cardiac Na/Ca exchanger (NCX1)
PAC	P1-derived artificial chromosome
PBS-T	phosphate buffered saline - Tween-20
PBS	phosphate buffered saline
PCR	polymerase chain reaction
PDE	phosphodiesterase
PI	phosphatidylinositol
PIP <sub>2</sub>	phosphatidylinositol-4,5-bisphosphate
PKC	protein kinase C
poly-E	poly-glutamic acid
r.t.	room temperature
RACE	rapid amplification of cDNA ends
RK	rhodopsin kinase
RNA	ribonucleic acid
ROM1	retinal outer segment membrane protein-1
ROS	rod outer segment
RP	retinitis pigmentosa
RPA	RNase protection assay
RPGR	retinitis pigmentosa GTPase regulator
rpm	revolutions per minute
RT-PCR	reverse transcriptase-polymerase chain reaction
s.e.	standard error
SDS	sodium dodecyl sulphate
sec	seconds
SF9/SF21	<i>Spodoptera frugiperda</i> 9 / <i>Spodoptera frugiperda</i> 21
SSC	standard saline citrate
STGD	Stargardt's Disease
TAE	Tris / acetate / EDTA
TBE	Tris / borate / EDTA
TBS-T	Tris buffered saline - Tween-20
TBS	Tris buffered saline
TdT	terminal deoxynucleotide transferase
TEMED	N,N,N',N'-tetramethylethylenediamine
T <sub>m</sub>	melting temperature
tris	tris (hydroxymethyl) aminomethane
U	units
UTP	uridine 5'-triphosphate
UTR	untranslated region
UV	ultraviolet
V	volts
X-Gal	5-bromo-4-chloro-3-indolyl-beta-D-galactopyranoside
XIP	exchanger inhibitory peptide
°C	degrees celsius



## **EPIGRAPH**

**Believe those who are seeking the truth; doubt those who find it.**

**Andre Gide**

## **CHAPTER 1: INTRODUCTION**

## **1.1 Na/Ca Exchange**

Calcium is an important second messenger in most eukaryotic cells; Ca homeostasis therefore, is of central importance and is tightly regulated by multiple mechanisms. In higher eukaryotes, Ca entry into the cell is gated mainly by Ca channels. Extrusion of Ca out of the cell is often performed by ATP- dependent Ca pumps and Na/Ca exchangers. Free cytosolic Ca concentrations, ranging from 100 - 500 nM in most mammalian cells, generally represent only 1% of the total cellular Ca. Some of the cellular Ca is buffered by Ca binding proteins, while the majority is maintained in internal stores such as the sarco -endoplasmic reticulum. Internal Ca stores release Ca through the IP3 and Ryanodine sensitive channels, and are refilled by the sarco - endoplasmic calcium ATPase (SERCA).

Sodium / calcium (Na/Ca) exchangers, which couple the transport of Ca against its gradient to the transport of Na with its gradient, are among the key proteins involved in maintaining Ca homeostasis. Na/Ca exchangers are found in the heart, kidney, brain and retina among many other tissues, where they are fundamental to the proper physiological function of these tissues (for review see (Blaustein and Lederer, 1999)).

### **1.1.1 NCX and NCKX Gene Families**

Na/Ca exchangers have been cloned and were found to fall into two families, termed NCX and NCKX. The mammalian NCX family is composed of three thus far identified members, NCX1 (Nicoll et al, 1990), NCX2 (Li et al, 1994) and NCX3 (Nicoll et al, 1996a). NCX1 is the predominant exchanger, with high activity in cardiac muscle, brain and kidney. NCX2 and NCX3 are expressed in a more tissue-specific manner, primarily in brain and skeletal muscle.

The NCKX-type exchanger was originally detected as Na/Ca exchange activity in retinal rod photoreceptors (Schnetkamp, 1980) and was subsequently shown to be electrogenic (Yau and Nakatani, 1984a) and fundamentally different in the requirement for K (Schnetkamp, 1989). The NCKX cDNA has since been detected in neural tissue (Tsoi et al, 1998) and platelets (Kimura et al, 1993). Two members of the NCKX family have been cloned and described, NCKX1 (Reiländer et al, 1992) and NCKX2 (Tsoi et al, 1998). These membrane proteins are functionally similar to the NCX family of exchangers, but with important differences. While NCX exchangers mediate Na-dependent Ca transport, NCKX exchangers perform Na-dependent Ca transport that requires and transports K (Schnetkamp et al, 1989; Cervetto et al, 1989). The stoichiometry of exchange catalyzed by NCX exchangers is 3 Na for 1 Ca (Pitts, 1979); for NCKX exchangers 4 Na are transported in exchange for 1 Ca and 1 K (Schnetkamp et al, 1989; Cervetto et al, 1989). Both NCX and NCKX exchangers have been found to exhibit alternate splicing (Quednau et al, 1997; Tsoi et al, 1998), which, at least in the case of NCX, presumably adds to the complexity and subtlety of the Na/Ca exchange activities that may be exploited by the cell.

### **1.1.2 Comparisons of NCX and NCKX Exchangers**

#### *NCX, the Na/Ca Exchanger*

The Na/Ca exchanger is defined as mediating Na<sub>o</sub>-dependent Ca<sub>i</sub> transport across the plasma membrane. The NCX1 Na/Ca exchanger has widespread distribution, and is presumed to act primarily in the housekeeping function of maintenance of Ca homeostasis. The NCX1 turnover rate has been estimated at about 5000 cycles/sec for reverse exchange, correlating positive charge movement in giant membrane patches with the NCX1's

electrogenic transport of one net positive charge per cycle (Hilgemann et al, 1991; Hilgemann, 1996). NCX exchangers have been demonstrated experimentally to mediate exchange in both Ca influx and efflux modes (Reeves and Sutko, 1979). It has been argued that under certain physiologically relevant conditions in the heart, the Na/Ca exchanger may catalyze Ca influx to increase the strength of contraction (Leblanc and Hume, 1990; Kohomoto et al, 1994; Levi et al, 1994). Na/Ca exchange activity is modulated by cations at the internal and external transport sites as well as at internal sites which do not transport cations.  $K_m$  values for the Na/Ca exchanger, the concentrations of Ca and Na at which exchange is half-maximally activated, vary from the external to the internal transport sites for both ions. Na/Ca exchange current measurements found that the  $K_m$  for Ca at the internal site is approximately  $1\text{ }\mu\text{M}$  (Miura and Kimura, 1989), while the  $K_m$  for Ca at the external site is near 1 mM (Miura and Kimura, 1989; Lyu et al, 1992a). Similarly the  $K_m$  for Na at the external site ranges from 20 to 50 mM (Reeves and Sutko, 1983; Linck et al, 1998), while the  $K_m$  for Na at the internal site is close to 15 mM (Miura and Kimura, 1989; Lyu et al, 1992b). Two primary mechanisms of ionic regulation have been identified at the internal sites, termed Ca-dependent activation and Na-dependent inactivation (Hilgemann et al, 1992a; Hilgemann et al, 1992b).

#### *NCKX, the Na/Ca+K Exchanger*

The Na/Ca+K exchanger performs  $\text{Na}_o$ -dependent  $\text{Ca}_i$  transport out of the cell which requires and cotransports K with Ca (Schnetkamp, 1989; Cervetto et al, 1989). Na/Ca+K exchange activity was originally identified in retinal rod outer segments (Schnetkamp 1980) and has since been detected in platelets (Kimura et al, 1993). The NCKX cDNA was cloned

from bovine retina (Reiländer et al, 1992) and further clones have been isolated from cone outer segments (Prinsen et al, 2000) and neural tissue (Tsoi et al, 1998). In contrast to the asymmetric  $K_m$  values observed for NCX, with NCKX the symmetrical  $K_m$ s for Na, Ca and K are 35 mM (Schnetkamp et al, 1995; Schnetkamp, 1986), 1-3  $\mu$ M (Schnetkamp, 1991) and 1.5 mM (Schnetkamp et al, 1989; Schnetkamp et al, 1991a) respectively. These values may vary due to binding competition, identity and concentration of other cations, such as lithium or choline, present (Schnetkamp, 1991; Schnetkamp et al, 1991a). The turnover rate of the Na/Ca+K exchanger, measured via Na-dependent Ca efflux mediated by purified and reconstituted exchanger in proteoliposomes, is from 100-500/sec (Friedel et al, 1991), approximately 10-50 fold lower than that observed in the NCX1 Na/Ca exchanger. In addition, reverse exchange mediated by NCKX1 occurs at a 5-10 fold lower rate than does forward exchange (Schnetkamp, 1986; Schnetkamp and Szerencsei, 1991). This contrasts with NCX1, for which forward and reverse exchange rates are more similar to one another. In the extrusion mode, it appears that the NCKX1 exchanger fails to lower intracellular Ca to the predicted thermodynamic equilibrium (Schnetkamp et al, 1991a). Fluorescent Ca-indicator fluo-3 measurement of cytoplasmic Ca in dark-adapted and photosaturated rods found that during peak response after exposure to bright light, Ca concentrations did not fall below 30 nM (Sampath et al, 1998). Similarly, indo-dextran measurement of rod outer segment cytosolic Ca before and after photostimulation was unable to lower Ca below 25 nM (Gray-Keller and Detwiler, 1996). The inability to lower Ca to the equilibrium levels predicted by thermodynamics and the exchanger's stoichiometry is due to a regulatory mechanism which has been described as  $Ca_i$ -dependent or time-dependent inactivation

(Schnetkamp et al, 1991a; Sampath et al, 1998). However, the Na/Ca+K exchanger does not display Na<sub>i</sub>-dependent inactivation or Ca<sub>i</sub>-activation (Schnetkamp, 1989) that the Na/Ca exchanger does (Hilgemann, 1990).

### **1.1.3 Structural Similarities and Differences**

Hydropathy analysis suggested that the Na/Ca exchanger is composed of one hydrophilic and two hydrophobic domains (Nicoll et al, 1990). Following the cleaved signal peptide is a hydrophobic region composed of five membrane spanning alpha-helices and their associated connecting loops. This first hydrophobic region is succeeded by the large and acidic hydrophilic domain and then the second hydrophobic region. This second hydrophobic region was originally proposed to be composed of six alpha-helical membrane spanning domains (Nicoll et al, 1990), but the model has recently been amended to contain only four transmembrane helices and one incomplete helix (Figure 1.1) (Nicoll et al, 1999; Iwamoto et al, 1999a). In addition, the loop connecting the second and third membrane spanning domains in the first hydrophobic region has recently been suggested to form a re-entrant pore loop-like structure (Iwamoto et al, 1999a), due to the accessibility of H124, N125 and T127 from the cytoplasm. The amino terminus lies in the extracellular space and the carboxy terminus resides in the cytosol. A potential glycosylation site has been identified in the short extracellular stretch immediately following the signal cleavage site and N-linked glycosylation at N-9 has been demonstrated (Hryshko et al, 1993).

The Na/Ca+K exchanger is proposed to possess a similar topology to the Na/Ca exchanger (Figure 1.2) (Reiländer et al, 1992). Hydropathy plots reveal hydrophilic and hydrophobic regions, similar to those observed in NCX (Reiländer et al, 1992; Cooper et al,

### Figure 1.1

#### Topological Models of NCX1.

**a.** The initial dog heart NCX1 topological model. (after (Nicoll et al, 1990))

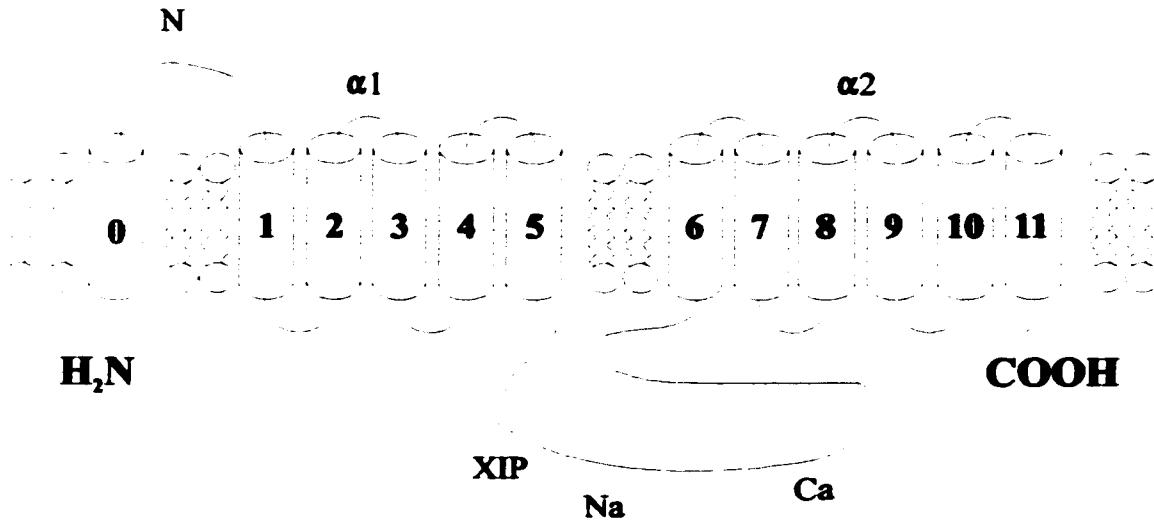
Based on hydropathy plot analysis, and knowledge of the location of the extracellular N-terminus and large cytosolic loop, a topological model was proposed. The model theorizes that the Na/Ca exchanger is composed of eleven membrane spanning helices (represented by cylinders) and an additional membrane-spanning helix in the cleaved signal peptide. A large hydrophilic cytosolic loop separates the fifth and sixth helices, and contains amino acid stretches implicated in the regulation of Na/Ca exchange. *N*, N9 N-linked glycosylation site.  $\alpha 1, \alpha 2$ , alpha repeats; *XIP*, exchanger inhibitory peptide; *Na*, domain associated with Na inactivation; *Ca*, domain associated with Ca activation.

**b.** The revised topological model of dog heart NCX1. (after (Nicoll et al, 1999))

Annotated as in **a**. Key differences between the original and revised models involve helices 6-9. Helix 6 is now proposed to lie in the cytosolic domain, causing helices 7 and 8 to be reversed in orientation to the original model. Helix 9 is proposed to form a pore-loop like structure, entering and leaving the membrane both on the cytosolic surface.



a.



b.

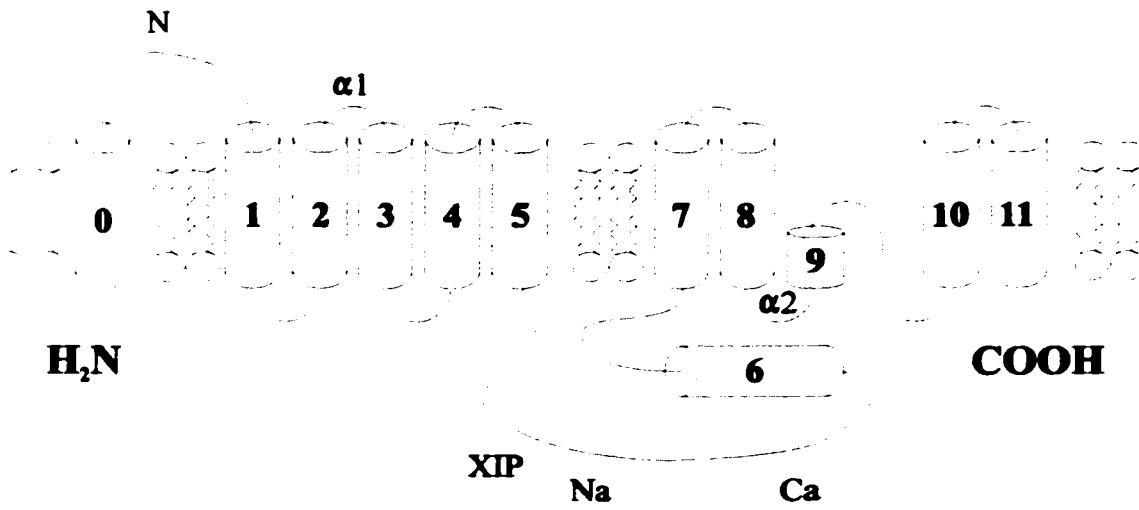
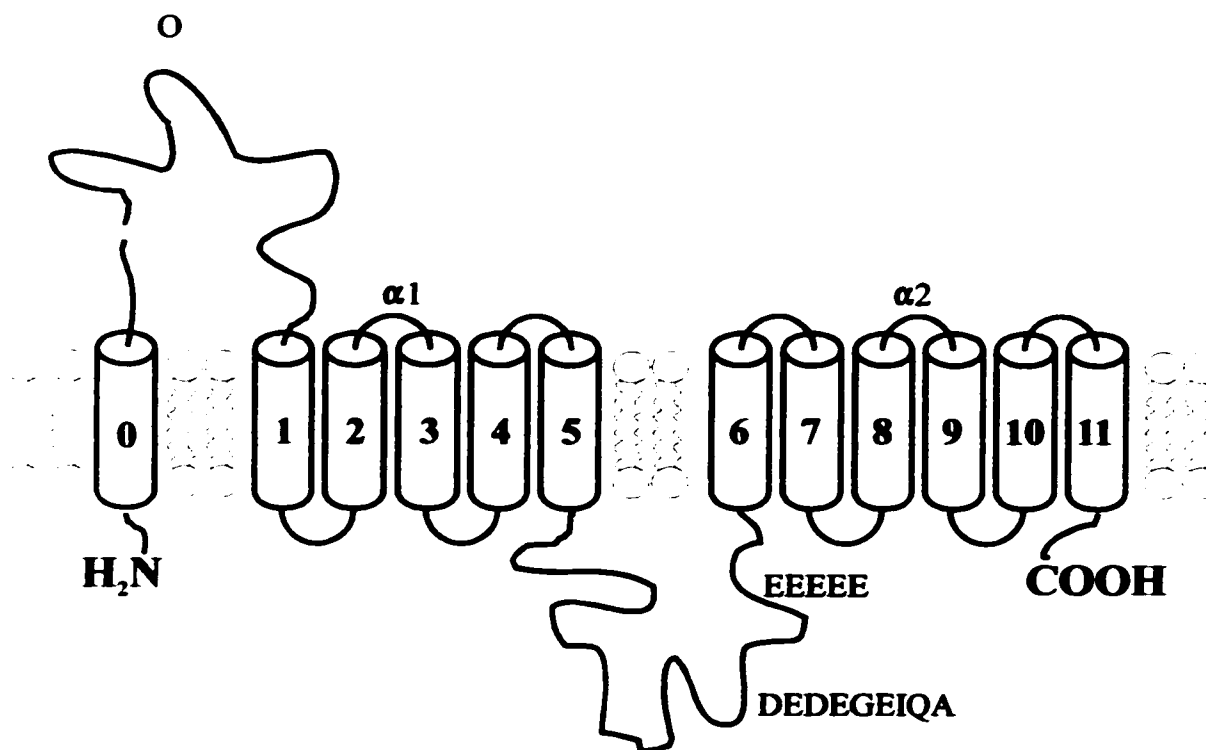


**Figure 1.2**

The Topological Model of NCKX1. (after (Reilander et al, 1992))

The bovine rod NCKX1 was assigned a topological model based on hydropathy plot analysis and comparison to the functionally related NCX1. The exchanger is proposed to be made up of 11 membrane-spanning helices in addition to another helix within the signal peptide. A large hydrophilic extracellular domain lies at the N-terminus of the mature protein. Subsequent to the first hydrophobic transmembrane domain, which consists of five membrane-spanning helices, falls the large hydrophilic cytosolic domain. The second hydrophobic transmembrane domain, composed of six membrane-spanning helices, completes the bovine rod Na/Ca+K exchanger. *O*, O-linked glycosylation site in the external domain; *EEEE*, poly-glutamic acid region of the cytosolic loop; *DEDEGEIQA*, repeat region of the bovine cytosolic loop;  $\alpha 1, \alpha 2$ , alpha repeats showing homology to those of NCX1.



1999a). Following the cleaved signal peptide is a large hydrophilic extracellular domain, quite unlike the shorter stretch of the Na/Ca exchanger. The extracellular region contains a number of putative O-linked glycosylation sites, and the apparent gel mobility suggests that the exchanger is heavily glycosylated (Kim et al, 1998). This region is succeeded by a hydrophobic domain modeled to contain five membrane spanning alpha-helices. Subsequently, a large acidic hydrophilic region, containing a poly-glutamic acid stretch is evident. In bovine (Reiländer et al, 1992) and rat NCKX1 (Poon et al, 2000) NCKX1 an acidic region is present, repeated multiple times. Finally, another hydrophobic transmembrane region follows, again modeled on the initial proposed topology of NCX and thus proposed to be composed of six alpha-helical membrane spanning domains and their associated connecting loops. The amino terminus lies outside the plasma membrane while the carboxy terminus resides in the cytosol.

#### **1.1.4 Similarities and Differences, at the Amino Acid Level**

The dog cardiac NCX1 cDNA (Nicoll et al, 1990) encoding a protein of 970 amino acids compared to the bovine rod NCKX1 cDNA (Reiländer et al, 1992) encoding 1199 amino acids. The difference in size is mainly due to the large extracellular domain of the Na/Ca+K exchanger, as the transmembrane and cytosolic regions of each exchanger respectively are similar in size. Sequence similarity is limited to two short stretches of about 30 amino acids in the membrane spanning alpha-helices (Reiländer et al, 1992). The two homologous stretches, termed the  $\alpha$  repeats, were first identified in the *Drosophila* Calx Na/Ca exchanger (Schwarz and Benzer, 1997). Site-directed mutagenesis studies found that amino acid residues in the  $\alpha$  repeats are critical to exchanger activity (Nicoll et al, 1996b).

Close inspection of the  $\alpha$ -repeats reveals homology to one another, suggesting that a duplication event within the original exchanger gene took place (Schwarz and Benzer, 1997) prior to the divergence of the NCX and NCKX families. However, revisions to the topological model of NCX1 (Nicoll et al, 1999; Iwamoto et al 1999a) that place the  $\alpha$ -repeats on opposite sides of the plasma membrane make the duplication hypothesis less attractive. Outside of the  $\alpha$ -repeats there is essentially no sequence homology, although highly acidic regions within the cytosolic domains are characteristic of both exchanger families. The NCX1 and NCX3 exchangers have been shown to undergo alternate splicing of the exons located in the C-terminal portion of the cytosolic region (Quednau et al, 1997; Lee et al, 1994; Kofuji et al, 1994), while NCKX1 has now been shown to undergo splicing of exons located in the N-terminal portion of the cytosolic region ((Tucker et al, 1998a) and this thesis).

### **1.1.5 Current Research on NCX**

#### **Regulatory and transport features**

The Na/Ca exchanger is regulated by several agents and mechanisms, including ATP (Hilgemann and Ball, 1996), protein kinase C (PKC) (Iwamoto et al, 1996), Na-dependent inactivation (Hilgemann, 1990) and Ca-dependent activation (Hilgemann, 1990). In giant cardiac membrane patches (see below), ATP effects appear to be mediated through the generation of phosphatidylinositol-4,5-bisphosphate (PIP<sub>2</sub>) and can be reversed by PI-specific phospholipase C (Hilgemann and Ball, 1996). Recent evidence suggests that the XIP region interacts with PIP<sub>2</sub>, as heterologously expressed exchangers with mutated XIP regions no longer respond to PIP<sub>2</sub> or PIP<sub>2</sub> antibodies (He et al, 2000). PKC up-regulated both forward

and reverse modes of exchange in cardiac myocytes and cells expressing NCX1 heterologously (Iwamoto et al, 1996). It is possible that the different regulatory mechanisms reported may be due to isoform-specific modulatory processes (He et al, 1998a; He et al, 1997; Smith et al, 1995; Iwamoto et al, 1996). In  $\text{Na}_i$ -dependent inactivation, application of Na to the cytosolic face of the Na/Ca exchanger results in a rapidly peaking outward current followed by a swift decay to a steady-state level. This regulation was first observed in cardiac sarcolemmal membranes using the giant excised patch technique (Hilgemann, 1990). In the giant excised patch variation of patch-clamping, a suction pipette with a very large diameter bore ( $\sim 30 \mu\text{M}$ ) is applied to exterior of the cell, and a large plasma membrane patch torn off. The patch is sealed to the opening of the suction pipette, exposing the cytosolic face of the membrane to the bathing solution. The previously difficult to control cytosolic side of the membrane is now readily accessible, permitting exchange current measurements activated from the cytosolic side of the Na/Ca exchanger.  $\text{Ca}_i$ -dependent activation requires Ca binding to a high affinity site which is distinct from the transport site, and is located on the cytosolic face of the exchanger (Hilgemann, 1990; Levitsky et al, 1994). Interestingly, in CALX, the *Drosophila* homologue of NCX1, the effect of  $\mu\text{molar}$   $\text{Ca}_i$  is to inhibit exchange activity rather than activate it (Hryshko et al, 1996).

### **Segregation of transport and regulatory features**

$\alpha$ -Chymotrypsin treatment of the cytosolic region in giant excised membrane patches removes the regulatory effects of  $\text{Na}_i$  and  $\text{Ca}_i$  on the exchanger and results in stimulation of activity (Hilgemann, 1990). Deletion mutagenesis can produce similar results (Matsuoka et al, 1993), and has demonstrated that the ion transport capabilities are mediated by sequences

contained within the membrane spanning domains while the regulatory properties are mediated by sequences contained within the cytosolic loop (Matsuoka et al, 1993). A domain involved in Ca regulation has been further characterized, and is discussed below.

### **Key sites for ion transport**

Comparisons of the amino acid sequences of NCX1 homologs from different species reveal considerable sequence similarity in the hydrophobic transmembrane domains, especially the  $\alpha$ -repeats (Schwarz and Benzer, 1997), where conservation extends even to the Na/Ca+K exchanger. The  $\alpha$ -1 repeat is modeled to include sections of membrane-spanning helices 2 and 3 and the loop which connects them (Figure 1.1). The  $\alpha$ -2 repeat is proposed to span from membrane-spanning helix 8 to 9 of the original topological model (Figure 1.1a but see Figure 1.1b), and include the connecting loop. Mutagenesis studies of amino acids located within the  $\alpha$ -repeats revealed that single amino acid substitutions (S109, S110, E113, S139, N143, T810, S811, D814, S818 or S838) abolished exchanger activity (Nicoll et al, 1996b). Mutation at residues T103, G108, P112, E120, G138, G809, G837 and N842 reduced exchanger activity (Nicoll et al, 1996b). A region which bears similarity to the Na/K ATPase (Nicoll et al, 1990) was also investigated. Here, two residues (E199 and T203) were found to be required for exchange activity while two others (E196 and G200) were not (Nicoll et al, 1996b). Similar single amino acid substitutions of other acidic and basic residues within the transmembrane segments but distinct from the  $\alpha$  repeats found only one functional mutant (D785) with altered exchange activity (Nicoll et al, 1996b).

### **Ca regulation and sites**

Upon the initial determination that the Ca regulatory activity was mediated by sequences with the large cytosolic loop (Hilgemann, 1990; Matsuoka et al, 1993), the specific localization was further investigated. Fusion proteins of portions of the cytosolic loop, in conjunction with  $^{45}\text{Ca}$  overlays and gel mobility studies narrowed the high affinity Ca binding domain to amino acids 371-508 of the cytosolic loop (Levitsky et al, 1994; Matsuoka et al, 1995). Two acidic sequences are observed within this region, each of which contain a triple aspartate motif. Mutations to these aspartates significantly reduce Ca binding affinity (Levitsky et al, 1994). Expression of exchangers mutated in the two acidic stretches, measured electrophysiologically with the inside-out giant membrane patch technique, also support this observation. Single-site mutations result in lowered affinity for regulatory Ca, as well as accelerated kinetics both for the stimulation by Ca application and for the decay of outward current upon Ca removal (Matsuoka et al, 1995). Gel mobility shifts and equilibrium dialysis of exchanger fusion proteins with single aspartate mutations have demonstrated a cooperative binding coefficient of  $\sim 2$ , with both acidic sequences being required for complete Ca binding (Levitsky et al, 1996). Interestingly, the *Drosophila* homologue CALX, is inhibited by Ca at the same concentrations at which Ca stimulates NCX1 and 2 (Hryshko et al, 1996). A chimeric exchanger with the cytoplasmic loop of CALX replaced by that of NCX1 produces an exchanger which is stimulated by Ca (Dyck et al, 1998), demonstrating that the NCX1 cytosolic loop contains the sequences required and sufficient for activation by internal Ca (Dyck et al, 1998). However, electrophysiological analysis of two CALX putative splice variants revealed distinct regulatory properties in



response to Ca (Omelchenko et al, 1998). Cytosolic Ca reduced inactivation of CALX 1.2 Na/Ca exchange mediated by cytosolic Na and increased the cytosolic Na-mediated inactivation of CALX 1.1 (Omelchenko et al, 1998). The five amino acid difference between these two variants occurs in the alternately spliced region and not the Ca binding site, demonstrating that sequences other than the Ca binding site contribute to the regulation of Na/Ca exchange.

### **Na Regulation, Sites and XIP**

Na-dependent inactivation is characterized as a rapid decay of outward current (ie. reverse exchange) to a steady state level upon application of Na to the cytosolic region. The exchanger inhibitory peptide, a putative autoregulatory domain, was originally identified on the basis of limited homology with calmodulin binding sites, and was found to non-competitively inhibit Na/Ca exchange when applied as a peptide to the cytoplasmic surface (Li et al, 1991). Reverse exchange current measurements from giant excised patches of XIP region mutants expressed in *Xenopus* oocytes, revealed that the endogenous XIP region is primarily involved in mediating Na-dependent inactivation (Matsuoka et al, 1997). Interestingly, mutants in this region fall into two classes, those that show accelerated kinetics of Na-dependent inactivation, and those for which inactivation was abolished (Matsuoka et al, 1997). Ca regulation is also altered by the XIP mutants, but to a relatively minor degree, demonstrating however that the two processes are interrelated (Matsuoka et al, 1997). Mutations in the putative XIP region of *Drosophila* CALX1.1, analogous to mutations made in the mammalian NCX1.1, demonstrated remarkable conservation in the resultant Na-dependent inactivation phenotypes observed, considering the homologues bear only 65%

amino acid sequence identity in these XIP regions (Dyck et al, 1998). Synthetic XIP peptide mutants were tested for their ability to inhibit Na/Ca exchange as measured by  $^{45}\text{Ca}$  uptake in cardiac sarcolemmal vesicles (He et al, 1997).  $^{45}\text{Ca}$  fluxes measure total cellular Ca movement, in contrast to indicator dyes such as fluo-3 which measure free cytosolic Ca. Two important residues in the 20 amino acid peptide were R12 and R14; A or E substitutions significantly reduced the exogenous XIP-mediated inhibition of reverse exchange (He et al, 1997). Aromatic residues were important in binding, and were suggested to be involved in hydrophobic interactions (He et al, 1997). The synthetic XIP peptide has been shown to crosslink to the exchanger (Kleiboeker et al, 1992), and a negatively charged putative interaction site has been identified (Hale et al, 1997). There is however no direct evidence that the exogenous XIP peptide is binding to the same site in the cytoplasmic loop that the endogenous XIP region does.

### **Topology**

Upon the original cloning of the dog heart Na/Ca exchanger (Nicoll et al, 1990), the topology of the mature polypeptide was proposed (based on hydropathy plots) to be composed of eleven membrane-spanning  $\alpha$ -helices separated between the fifth and sixth helix by a large hydrophilic cytosolic loop. Antibody mapping confirmed the cytoplasmic localization of the large hydrophilic loop (Porzig et al, 1993), the extracellular position of the N-terminus (Aceto et al, 1992) and the cytoplasmic location of the C-terminus (Cook et al, 1998). In addition, the loop connecting helices 1 and 2 has been demonstrated to reside on the cytosolic surface (Cook et al, 1998; Doering et al, 1998) Application of sulfhydryl reagents, which interact with cysteine residues, can affect the activity of the Na/Ca exchanger

(Pierce et al, 1986). Treatment of the extracellular or intracellular face of various Na/Ca exchanger cysteine mutants with membrane-impermeable sulfhydryl reagents (Nicoll et al, 1999) demonstrated the necessity of revisiting the topological model, as it revealed that the actual membrane-sidedness of the loops connecting helices 7-8 and 8-9 are opposite to the proposed model (see Figure 1.1a vs. Figure 1.1b). In addition, alanine insertion into helix six, which should disrupt the helical structure, fails to alter exchange activity, suggesting that helix six is not membrane-spanning but rather resides in the cytosol (Nicoll et al, 1999).

### **Tissue Specificity and Functional Differences of Alternately Spliced NCX1,2,3**

Of the three distinct NCX genes cloned, NCX1 (Kofuji et al, 1994; Lee et al, 1994) and NCX3 (Quednau et al, 1997) have been determined to possess multiple splice variants. Alternate splicing in NCX1 has been detected in a region of six exons located at the N-terminus of the large cytosolic loop (Kofuji et al, 1994), and also in the 5' UTR (Lee et al, 1994), where the variations are located in non-coding sequences. In the cytosolic loop, the exons A and B are mutually exclusive, while exons C through F are of the cassette type (Figure 1.3a). In NCX3, alternate splicing occurs in the A-C exons (Quednau et al, 1997) (Figure 1.3b). The splice variations have been suggested to underlie tissue specificity for both the NCX1 and NCX3 protein products, indicative of distinct roles or functions in specific environments (Quednau et al, 1997) (Lee et al, 1994).

Functional comparisons of paralogous and alternately spliced members of the mammalian NCX exchanger family reveal all to have similar properties, including cation affinities and activation due to chymotrypsin treatment (Linck et al, 1998). Some apparent regulatory differences have been noted between some NCX family members with respect to

**Figure 1.3**

Schematic Representation of the NCX1 and NCX3 Alternately Spliced Cytosolic Loops. Exons are shown as *rectangles* and intronic sequences as the *thin bar* which connects them. Exon identities are as indicated.

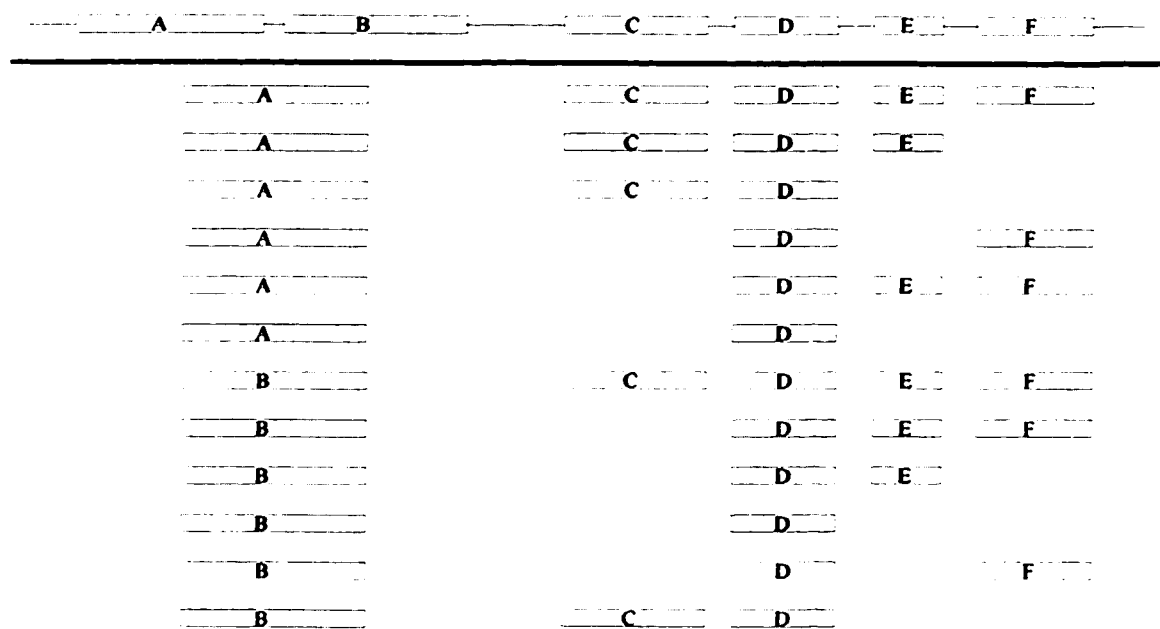
**a. Alternate splicing in NCX1**

For each splice variant, one of the mutually exclusive exons A or B is linked to a number of possible groupings of the cassette exons C, D, E and/or F.

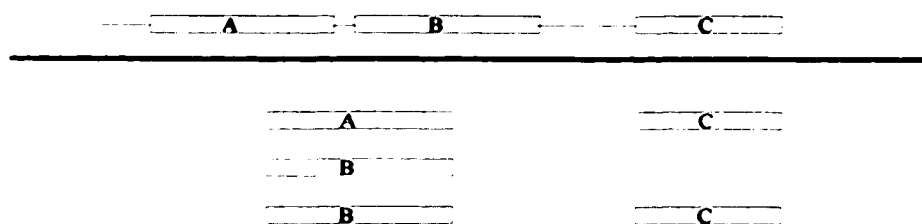
**b. Alternate splicing in NCX3**

Only three splice variants of NCX3 have been observed to date. NCX3 also has the mutually exclusive A and B exons, which are homologous to the NCX1 A and B exons.

a.



b.



ATP stimulation; outward exchange currents of NCX1 and NCX2 were inhibited by ATP depletion, while NCX3 was not affected (Linck et al, 1998). Stimulants of protein kinases A and C increased NCX1 and NCX3 activities, but not the activity of NCX2 (Linck et al, 1998). In addition,  $^{45}\text{Ca}$  uptakes have found that Ni competes with Ca for the external binding site with 10-fold greater affinity in NCX1 and NCX2 than it does with NCX3 (Iwamoto and Shigekawa, 1998; Iwamoto et al, 1999b). Whole-cell patch recordings of cultured cells expressing mutagenized NCX1 or NCX3 exchangers identified three amino acids in the  $\alpha$ -1 and  $\alpha$ -2 repeats which confer Ni sensitivity, and two amino acids in the  $\alpha$ -2 repeat which confer Li sensitivity (Iwamoto et al, 1999b). The Ca-influx inhibitor, isothioureia derivative KB-R7943, was 3-fold more potent against NCX3 than to either NCX1 or NCX2 (Iwamoto and Shigekawa, 1998). As stated above, splice variants of CALX demonstrate distinct regulatory properties (Omelchenko et al, 1998). Functional differences between NCX1 and NCX3 must therefore be carefully examined to determine if disparity results from exchanger dissimilarities or splice variant choice.

### **1.1.6 Current Research on NCKX**

#### **Regulatory and transport features**

Fluo-3 measurements (Schnetkamp et al, 1991b) of cytosolic free Ca and  $^{45}\text{Ca}$  uptake assays (Schnetkamp et al, 1991c) of total cell Ca have been used to explore the kinetics of the bovine Na/Ca+K exchanger in isolated rod outer segments. Unlike the Na/Ca exchanger, the Na/Ca+K exchanger has symmetrical cation affinities on either side of the membrane, supportive of the consecutive three site model proposed by Schnetkamp et al. (Schnetkamp and Szerencsei, 1991; Schnetkamp et al, 1995). The forward and reverse exchange rates,

however, are not symmetrical, as Ca efflux (forward exchange) is observed to occur at approximately 5-10 fold greater velocity than does Ca influx.

After initiation of Na<sub>o</sub>-dependent Ca extrusion, the Na/Ca+K exchanger is observed to operate at a maximal rate of exchange for approximately 30 seconds, following which it is inactivated approximately two orders of magnitude (Schnetkamp, 1995b). This inactivation feature prevents the lowering of cytosolic Ca levels below 25 nM (Sampath et al, 1998), even under conditions where thermodynamic considerations of the ion gradients coupled with the 4 Na : 1 Ca + 1 K stoichiometry would predict cytosolic free Ca concentrations below 1 nM. The predicted cytosolic free Ca concentration (Ca<sub>i</sub>) can be calculated from the equation:

$$Ca_i/Ca_o = (Na_i/Na_o)^4 \cdot (K_o/K_i) \cdot \exp(V_m z F / RT) \quad (\text{Schnetkamp et al, 1991d})$$

where V<sub>m</sub> is the membrane potential, z is net positive charge transported, F is Faraday's constant, R is the gas constant and T is temperature. Current measurements from photo-stimulated truncated rod outer segments were found to parallel the depletion in cytosolic Ca (Gray-Keller and Detwiler, 1994) which again failed to drop below 25 nM. Presumably, this mechanism functions to preclude the reduction of cytosolic free Ca to undesirably low levels during prolonged exposure to light.

### **Segregation of transport and regulatory features**

Based on the model of the Na/Ca exchanger, it could be hypothesized that the ion transport activities of the Na/Ca+K exchanger are localized to the transmembrane regions and the domain responsible for inactivation is contained within the cytosolic loop. Deletion of a portion of the cytosolic loop in the bovine rod NCKX1 exchanger expressed

heterologously did not prevent cation transport (Cooper et al, 1999a). Similarly, the observation of exchange activity in rod outer segment membranes with either the extracellular or cytoplasmic faces protease treated, supports the notion that exchange properties are segregated to the transmembrane loops (Kim et al, 1998). Results presented in this dissertation will further explore this issue.

### **Topology**

While the topological model of the Na/Ca+K exchanger is based heavily on the early model of the Na/Ca exchanger, very little evidence has in fact been gathered which demonstrates that this correlation can be correctly made. Antibody studies (Kim et al, 1998) have confirmed that the large hydrophilic domain at the N-terminus of the NCKX1 exchanger is extracellular, and that the large hydrophilic domain which separates the two hydrophobic regions is cytosolic (Figure 1.2) (Kim et al, 1998). The orientations of the putative membrane spanning alpha-helices and their connecting loops relative to the external or cytoplasmic face of the plasma membrane remain to be demonstrated.

### **Tissue Specificity**

Northern blots in bovine tissue reveal NCKX1 specificity for the retina (Reiländer et al, 1992). NCKX2 was cloned from rat brain (Tsoi et al, 1998), where the transcripts are detected in several regions, as well as weakly in the eye. *In situ* hybridization studies of human and chicken retinas reveal highly specific staining for transcripts of NCKX1 in rods and cone NCKX in cones (Prinsen et al, 2000). It seems likely, then, that the tissue specificity of the NCKX family is less complex than is found for the NCX family, with NCKX1 functioning primarily as a rod and platelet specific isoform, while cone NCKX /



NCKX2 acts as the cone and brain specific isoform.

### **Alternate Splicing in NCKX genes**

Like the NCX exchangers, NCKX1 and NCKX2 have been observed to undergo alternate splicing (Tsoi et al, 1998; Tucker et al, 1998a). The functional consequences of this are unclear, and no tissue specificities or distinct activities attributable to different isoforms have yet been described. The issue of alternate splicing in NCKX1 will be further examined in this dissertation.

## **1.2 The Role of Calcium in Phototransduction**

### *Summary*

The vertebrate rod photoreceptor is a specialized cell divided structurally and functionally into several regions (see Figure 1.4a). The outer segment is the cellular compartment which contains the phototransduction machinery. Structurally, it is cylindrical in shape and contains approximately 1000 disk-shaped lamellar membranes. The disks are essentially flattened spheres which are not fused to the plasma membrane. Each disk also contains a subcellular compartment termed the lumen which may store Ca (Schnetkamp, 1995a; Schnetkamp, 1995b; Schnetkamp et al, 1995). Embedded in or associated with the disk membranes are some of the key protein components of the phototransduction machinery, including rhodopsin (Nathans and Hogness, 1983), transducin (Lochrie et al, 1985), cGMP-phosphodiesterase (Ovchinnikov et al, 1987), as well as important structural proteins such as ABCR/rim protein (Illing et al, 1997), and rds/peripherin (Connell and Molday, 1990). In the plasma membrane are found the only two proteins known to mediate Ca transport into or out of the rod outer segment, the cGMP-gated channel (Yau, 1987) and

### **Figure 1.4**

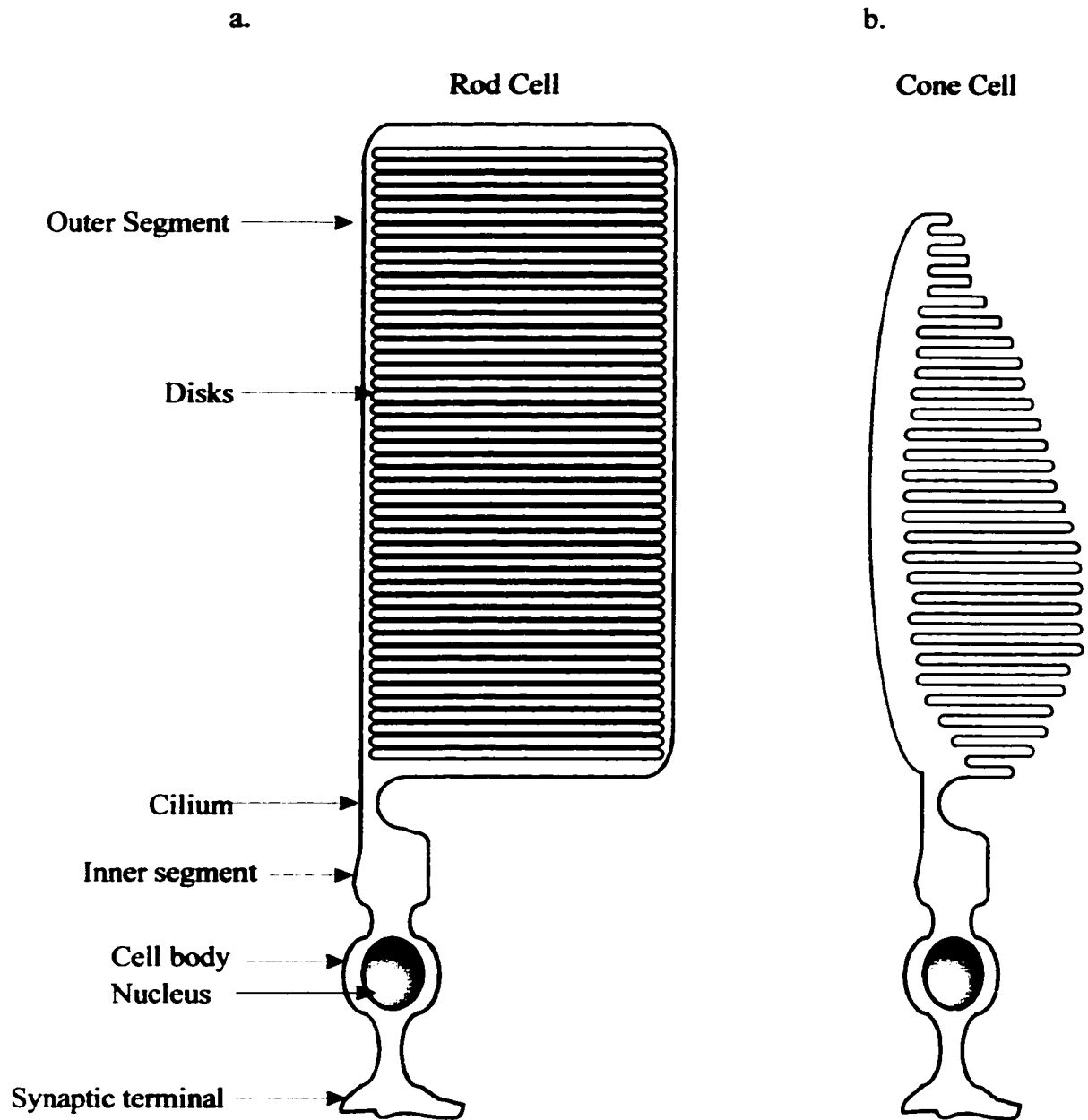
#### **Rod and Cone Photoreceptor Physical Structure.**

##### **a. Vertebrate rod photoreceptor**

The vertebrate rod photoreceptor is composed of three sections, the outer segment, the inner segment and the cell body. The outer segment is cylindrical in shape and contains approximately 1000 flattened lamellar membrane disks. Key proteins of the phototransduction cascade are embedded in or associated with the disk membranes, including rhodopsin, transducin, cGMP phosphodiesterase and ABCR. The disks are generated by invagination of the plasma membrane which occurs at the base of the outer segment. The rod outer segment plasma membrane is the location of the Na/Ca+K exchanger and the cGMP gated channel. The inner segment, connected to the outer segment by a thin cilium, contains mitochondria and other housekeeping cellular components. In the inner segment plasma membrane are embedded the Na / K ATPase and K channels. Beneath lies the cell body, containing the nucleus, and the synaptic terminals.

##### **b. Vertebrate cone photoreceptor**

The vertebrate cone photoreceptor is structurally very similar to the rod photoreceptor. Also composed of an outer segment, inner segment and cell body, the cone is specialized to detect colored light. Cone outer segments are shorter than rod outer segments, and are more conical in shape compared to the cylindrical rods. Cones also contain disks, but in this case the flat lamellar membranes are continuous with the plasma membrane, in contrast to the discrete rod disks. Some cone phototransduction proteins, homologous to the rod proteins, have been cloned. These include the cone cGMP gated channel, the cone Na/Ca+K exchanger and cone rhodopsins. It appears that the key phototransduction machinery proteins of the well studied rod photoreceptor are represented in the cone by distinct but homologous genes.



the Na/Ca+K exchanger (Schnetkamp, 1995a). The outer segment is connected via a thin ciliary strand of cytoplasm to the inner segment. Localized to the inner segment are the mitochondria, Na/K ATPase and K channels. Posteriorly lies the cell body, which contains the nucleus, and then the synaptic terminal, from which signals are transduced (for review see (Schwartz, 1981)) to bipolar and horizontal cells. Cone photoreceptor cells are structurally, and presumably functionally, similar to rods, with the exception that the outer segments are shorter and conical in shape, and the disks contained within are continuous with the plasma membrane (see Figure 1.4b.).

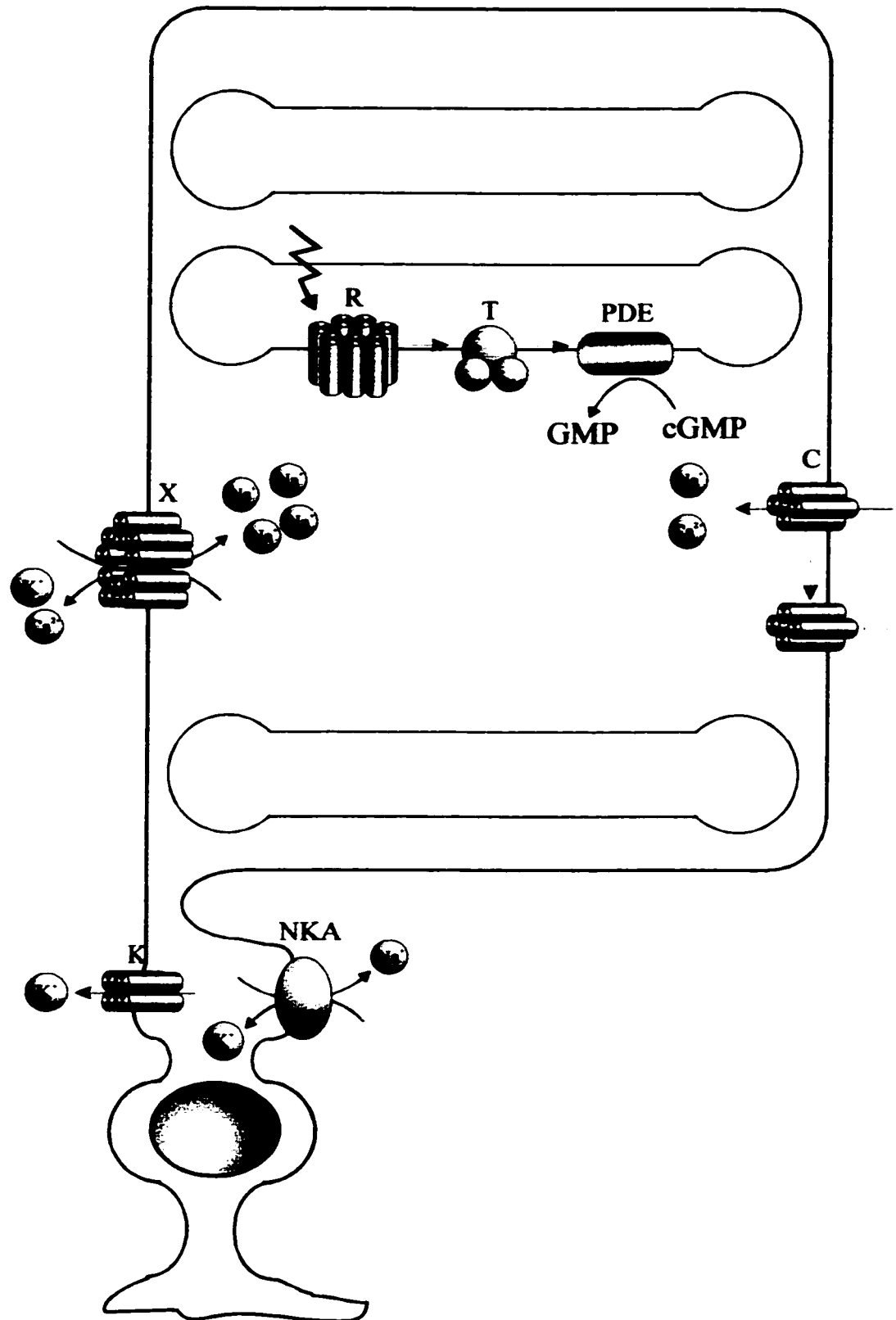
The phototransduction cascade of the retinal rod outer segment has been employed as an archetypical model for signal transduction in higher vertebrates, and consequently is well studied. The majority of the key proteins in phototransduction have now been identified, cloned and examined in detail. Remarkable discoveries that translate to many areas of signal transduction research have been uncovered; some of those pertaining to Ca homeostasis will be discussed below.

### **1.2.1 Phototransduction Excitation**

The phototransduction cascade is initiated by the absorption of a photon by a membrane-bound rhodopsin molecule (for review see (Mathies, 1999)) (Figure 1.5). This prototypical member of the 7-membrane spanning receptor family contains the chromophore retinal, whose conformation switches from 11-*cis* retinal to an all *trans* isomer upon absorption of a single photon. This structural change alters rhodopsin to an activated form, Metarhodopsin II, which binds to and activates the heterotrimeric G protein (Fung et al, 1981), thereby stimulating the exchange of GDP for GTP on the transducin  $\alpha$  subunit.

**Figure 1.5****Excitation Cascade in the Rod Photoreceptor.**

In the dark, high levels of cGMP ensure the cyclic nucleotide gated channel (*C*) remains open, allowing a constant influx of Na and Ca. The Na/Ca+K exchanger (*X*) uses the inward Na gradient and the outward K gradient to drive Ca out of the cell. In the inner segment, the Na / K ATPase hydrolyzes ATP to provide the energy to set the Na and K gradients of the photoreceptor cell. K channels (*K*) located in the inner segment set the membrane resting potential and complete the so-called dark current cycle. The reception of a single photon by the chromophore retinal in the rhodopsin (*R*) molecule transforms the inactive rhodopsin to the activated Meta II rhodopsin. This activates the heterotrimeric G protein transducin (*T*) which in turn stimulates the cGMP phosphodiesterase (*PDE*) to increase the hydrolysis of cGMP. As cytosolic cGMP levels fall, the cyclic nucleotide gated channels close, halting the influx of Na and Ca and interrupting the dark current cycle. The reduced influx of cations leads to hyperpolarization of the membrane and results in altered release of neurotransmitter.



Activated transducin in turn activates the cGMP-phosphodiesterase (PDE) (Morrison et al, 1989) through mediating the removal of the inhibitory  $\gamma$  subunit. The PDE then increases its hydrolysis of cGMP to GMP. The reduced concentration of this second messenger is detected by the cGMP-gated channel (Stryer, 1986; Lolley and Lee, 1990), a plasma membrane embedded cation channel which is open in the presence of cGMP. As cGMP levels decrease, the channel closes, preventing further influx of Na and Ca.

In dark adapted conditions, the rod outer segment exhibits a current loop, the so-called 'dark-current' (Hagins et al, 1970) in which Na and Ca ions continuously enter the rod outer segment and the charge is balanced by a constant efflux of K through the inner segment K channels. Under these conditions, the rod outer segment is maintained in a depolarized state, and the neurotransmitter glutamate is continuously released at the synaptic terminals.

In the dark, in mammalian rods, internal Ca is kept constant at  $\sim 500$  nM (Gray-Keller and Detwiler, 1996) by constant, light-insensitive Ca extrusion mediated by the plasma membrane Na/Ca+K exchanger (Schnetkamp, 1980; Schnetkamp et al, 1996). When the light stimulated phototransduction cascade leads to the hydrolysis of cGMP and the closure of the cGMP-gated channels, the current influx is halted, leading to hyperpolarization of the membrane. This in turn results in a reduction of neurotransmitter release at the synaptic terminals, thus transmitting the light-stimulated signal to the bipolar and horizontal cells. A simultaneous effect of the termination of the inward flux of Ca is the reduction of the cytosolic free Ca concentration, due to the light-insensitive extrusion of Ca by the Na/Ca+K exchanger. This lowered intracellular Ca level is the key secondary messenger which mediates the recovery of the photoreceptor to the ready state. The prevention of lowering

intracellular Ca by removal of extracellular Na or clamping of the intracellular Ca both result in the abolishment of recovery from the activated state (Matthews et al, 1988; Nakatani and Yau, 1988; Fain et al, 1989).

### **1.2.2 Recovery from Excitation**

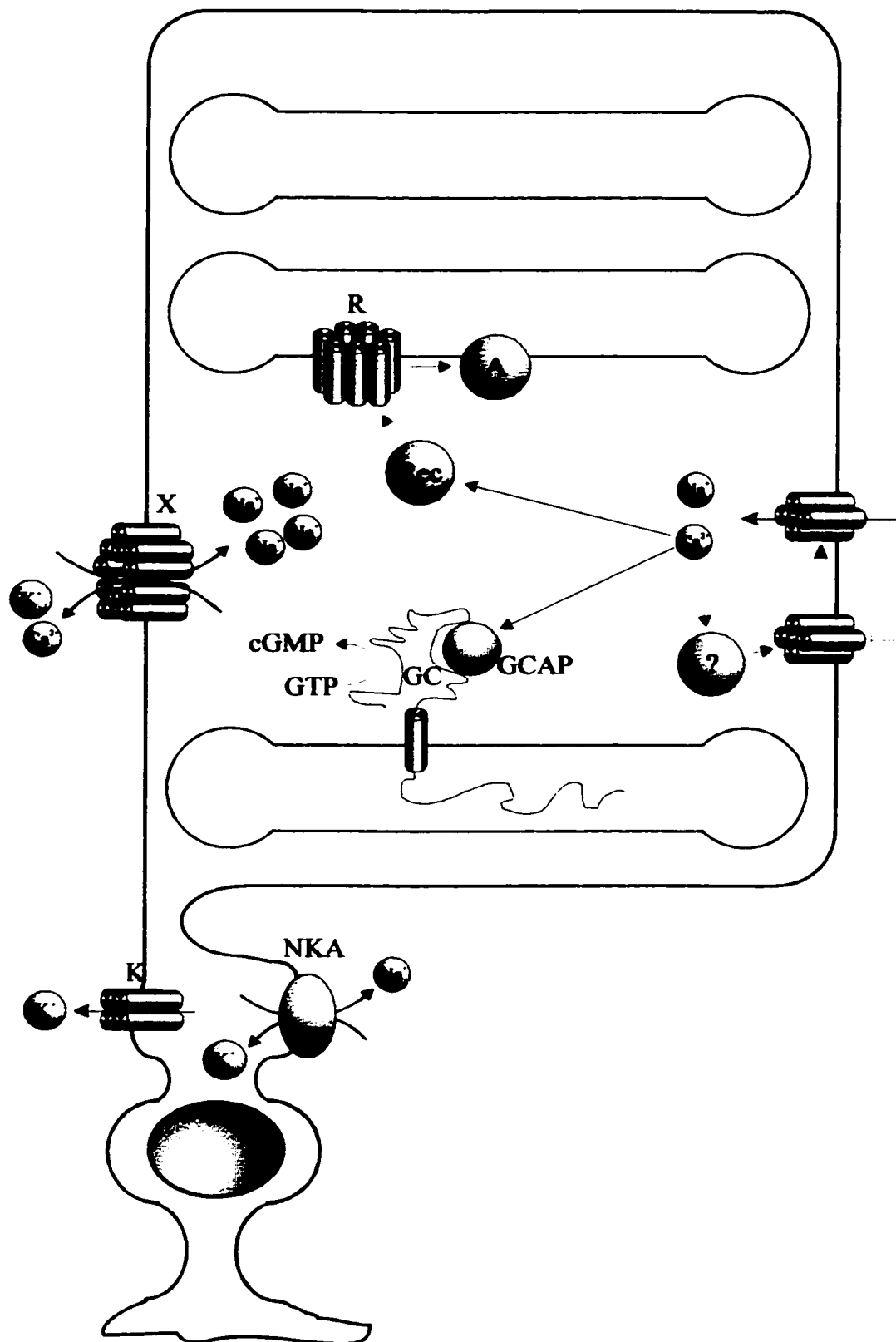
Recovery of the photoreceptor cell to the ready state is characterized generally as two processes, the inactivation of the activated components of the visual transduction cycle and recovery of the levels of cGMP (see Figure 1.6). In the dark, the constitutive level of phosphodiesterase activity exhibited by the cGMP-PDE is balanced by the guanylate cyclase (GC) (Thorpe and Garbers, 1989), which converts GTP to cGMP. After the activation of the visual cascade, the decreased level of intracellular Ca stimulates an increase in guanylate cyclase activity, mediated by the guanylate cyclase activating protein (GCAP) (Subbaraya et al, 1994).

Transducin and PDE are inactivated by hydrolysis of GTP to GDP on the  $\alpha$  subunit of transducin, via its intrinsic GTPase activity which is apparently stimulated by the RGS9 GTPase accelerating protein (GAP) (He et al, 1998b). Rhodopsin kinase (RK) phosphorylates the C-terminus of activated rhodopsin in an ATP-dependent manner (Palczewski et al, 1991). The phosphorylated rhodopsin is subsequently bound by arrestin (Krupnick et al, 1997) which sterically prevents transducin from binding to the phosphorylated rhodopsin. S-modulin (the frog homologue of recoverin) is bound to rhodopsin kinase in high Ca (dark adapted conditions) via its N-terminal region (Tachibanaki et al, 2000). Light-stimulated reduction in cytosolic Ca converts S-modulin to the Ca-free form which dissociates from rhodopsin kinase, thus releasing the block of RK activity. The



**Figure 1.6****Recovery of the Rod Photoreceptor Following Excitation.**

Closure of the cyclic nucleotide gated channels (*C*) results in a decrease in cytosolic Ca levels, as the Na/Ca+K exchanger (*X*) is not inactivated by the excitation cascade, and it continues to drive Ca out of the cell. Low cytosolic Ca causes the guanylate cyclase activating protein (*GCAP*) to bind to and activate guanylate cyclase (*GC*), stimulating increased synthesis of *cGMP*. Low Ca also causes a soluble factor (?), presumably calmodulin, to bind to the cyclic nucleotide gated channel and increase the activation affinity of the channel for cGMP. Recoverin (*Rec*), which binds rhodopsin kinase (*RK*) in a Ca-dependent manner, dissociates from *RK* in low Ca, derepressing the phosphorylation of rhodopsin by *RK*. Arrestin, *A* binds to phosphorylated rhodopsin which prevents further activation of transducin.



affinity of the cGMP-gated channel for cGMP increases as  $Ca_i$  is lowered, resulting in the channel opening at lower cGMP levels. This effect is suspected to be mediated by another soluble factor, putatively calmodulin (Grunwald et al, 1998; Hsu and Molday, 1993). Upon inactivation of activated components of the transduction machinery and recovery of the cGMP levels, the cGMP-channel reopens, allowing the return of the dark current. It is clear then that the reduction in  $Ca_i$  concentration, which mediates many of the aforementioned effects, is central to the recovery of the photoreceptor after signal transduction.

### **1.2.3 Calcium and the cGMP-gated Channel**

The cGMP-gated channel is composed of two subunits,  $\alpha$  (Kaupp et al, 1989) and  $\beta$  (Chen et al, 1994), which show considerable homology to one another. The subunits are believed to form a heterotetrameric complex, although this is not yet firmly established (Korschen et al, 1995; Liman and Buck, 1994; Gordon and Zagotta, 1995). Heterologous expression of the  $\alpha$  subunits form a functional homomeric channel which shows longer and more stable channel open times than the native channel, and is not subject to modulation by calmodulin (Kaupp et al, 1989; Dhallan et al, 1990).  $\beta$  subunits expressed in the absence of  $\alpha$  subunits, however, do not form a functional channel (Chen et al, 1993). Structurally and at the sequence level, the two subunits are very similar, each coding for a six  $\alpha$  helix membrane-spanning protein with a voltage sensor-like motif in helix four (S4) and a pore-forming loop between S5 and S6. Both subunits have a C-terminal cytosolic cGMP binding site, while the  $\beta$  subunit has, in addition, a cytosolic N-terminal region which is in large part identical to the glutamic acid rich protein (GARP) (Korschen et al, 1995). The GARP cDNA, which has been cloned separately (Sugimoto et al, 1991), appears to be the product of

alternate splicing. Immunoprecipitation studies have demonstrated that calmodulin binds to the  $\beta$  subunit in a Ca-dependent manner (Hsu and Molday, 1993; Grunwald et al, 1998). The Na/Ca+K exchanger has been observed to coprecipitate with the cGMP-gated channel (Bauer and Drechsler, 1992), and recent cross-linking data (Schwarzer and Bauer, 1999) are also suggestive of adjacent positioning of the two Ca transport proteins in the plasma membrane.

In truncated salamander rods, modulation of the cGMP-gated channel by Ca is observed. The decrease in Ca, which follows the signal cascade, results in an apparent two-fold increase of the  $K_m$  for activation of the channel by cGMP (Sagoo and Lagnado, 1996). This appears to be mediated by a soluble factor, because the activity can be dialyzed away. The Ca-dependent affinity modulation can be blocked by the addition of mastoparen, a calmodulin inhibitor (Hsu and Molday, 1994). Membrane vesicles purified from rod outer segments lose the activity of this factor, but the effect can be rescued by addition of exogenous calmodulin (Hsu and Molday, 1994). In cones, the recently developed electroporabilization technique (Rebrik and Korenbrot, 1998) has been used to measure currents through the inner segment still attached to the outer segment. Here, as in the previous studies, it is observed that the factor responsible for modulation of the cone cGMP gated channel, is Ca-dependent and soluble (Rebrik and Korenbrot, 1998). Moreover, the factor maintains its activity until free  $Ca_i$  is lowered, at which point it diffuses away. Although its identity has not yet been definitively established, the responsible factor in the cone outer segment does not appear to be calmodulin (Hackos and Korenbrot, 1997). In rods, the presumed calmodulin binding site on the cGMP gated channel has been localized to the C-terminal half of the  $\beta$  subunit by peptide analysis and heterologous expression studies

(Grunwald et al, 1998; Weitz et al, 1998). Deletion of this region results in channels which are free of CaM regulation yet retain high affinity for cGMP.

#### **1.2.4 Calcium and Guanylate Cyclase**

Guanylate cyclase (GC) catalyzes the synthesis of cGMP from GTP. The rod outer segment guanylate cyclase (ROS-GC), is a 115 kd membrane bound member of the GC family (Goraczniak et al, 1994). Structurally, ROS-GC has one membrane spanning  $\alpha$ -helix located near the center of the amino acid sequence, dividing the luminal and cytosolic domains. The cyclase maintains the levels of cGMP required to open the cGMP-gated channel. Modulation of ROS-GC activity therefore, has considerable effects on the recovery from light activation and reestablishment of the dark current. In truncated salamander rods the activity of the cyclase is inhibited by Ca with  $K_m$  inhibition of photocurrent response measured at  $\sim 100$  nM and a Hill coefficient of 2 (Nikonov et al, 1998). This modulation of cyclase activity is mediated by a diffusible factor, which has recently been identified as a calmodulin-like Ca binding protein, guanylate cyclase activating protein (GCAP) (Gorczyca et al, 1994). Additionally, the maximal rate of guanylate cyclase has been reported to be increased by PKC, using an optical assay in rod outer segments (Wolbring and Schnetkamp, 1995). Na and cGMP have been suggested to play a role in regulating the Ca sensitivity of guanylate cyclase, although the physiological implications of these effects are unclear (Wolbring and Schnetkamp, 1996).

The recent cloning of several guanylate cyclases has revealed a subfamily specific to photoreceptors. The two members, ROS-GC1 (Goraczniak et al, 1994) and ROS-GC2 (Lowe et al, 1995), are highly homologous, especially within the intracellular region, and

both show cyclase activity when expressed heterologously. In addition, two isoforms of guanylate cyclase activating protein, GCAP1 (Palczewski et al, 1994) and GCAP2 (Dizhoor et al, 1995), have recently been cloned. The guanylate cyclase activating proteins are 25 kd calmodulin family proteins containing four EF hand Ca binding motifs, three of which are capable of binding  $\text{Ca}^{2+}$  (Palczewski et al, 1994). Reconstitution studies of expressed cloned cyclases with GCAPs demonstrated Ca-dependent modulation of cyclase activity (Krishnan et al, 1998; Goraczniak et al, 1998). In addition, though both GCAPs can modulate either ROS-GC1 or ROS-GC2, mutagenesis and reconstitution has revealed that GCAP1 is specific for ROS-GC1 and GCAP2 is specific for ROS-GC2 (Krishnan et al, 1998; Goraczniak et al, 1998). Mutagenesis and proteolysis investigations of GCAP1 have revealed that Ca binds EF hands 3 and 4, inducing significant conformational changes which result in conversion of the protein from an activator to an inhibitor of ROS-GC1 (Rudnicka-Nawrot et al, 1998). Employment of the recently developed Multipin Peptide Synthesis (Chiron Technologies Inc.) allowed the wholesale screening of the entire cytosolic region of ROS-GC1 against GCAP1 and 2 and revealed that both bind to residues 968-982 of the ROS-GC1 catalytic domain (Sokal et al, 1999). This amino acid stretch is a potent inhibitor of GCAP modulation when added exogenously (Sokal et al, 1999). Immunocytochemistry has recently demonstrated that ROS-GC1 and GCAP1 are localized to rod and cone outer segments and in synaptic terminals, while GCAP2 appears to be localized not to outer segments, but rather to inner segments and synaptic terminals, especially in cones (Gorczyca et al, 1995; Frins et al, 1996; Otto-Bruc et al, 1997). Based on the subcellular localization, ROS-GC1 and GCAP1 seem likely to have a physiologically relevant role in the recovery phase of

phototransduction. Modulation of synaptic terminal function has been suggested as potential roles for ROS-GC2 and GCAP2.

### **1.2.5 Calcium and Phosphodiesterase**

Ca is believed to modulate the activity of the rod cGMP-phosphodiesterase (PDE) by two indirect mechanisms. First, Ca inhibits the deactivation of rhodopsin by recoverin (Kawamura, 1993). Second, Ca increases the rate of the rising phase of the photoresponse, in a process independent of recoverin (Gray-Keller and Detwiler, 1994). Both of these are believed to mediate effects prior to the stimulation of transducin, with the downstream effect being detected in the activity of the PDE.

Structurally, recoverin has a hydrophobic cleft and two functional Ca binding sites (Dizhoor et al, 1991). It belongs to a family of neuron-specific Ca-binding proteins (NCBPs) which include the subfamily of GCAPs. When recoverin was originally cloned, it was proposed to directly regulate ROS-GC activity (Dizhoor et al, 1991). However, when tested *in vitro*, this hypothesis turned out to be incorrect (Hurley et al, 1993). The nature of its activity was revealed when it was discovered that recoverin is the bovine ortholog of S-modulin (Kawamura et al, 1993), which was cloned from frog photoreceptors. S-modulin was originally reported as a soluble protein which associated with disk membranes at high Ca concentrations and attenuated the activity of the PDE (Kawamura and Murakami, 1991). Subsequently, S-modulin was demonstrated to inhibit the phosphorylation of rhodopsin in a Ca-dependent manner (Kawamura, 1994). Activated rhodopsin (Metarhodopsin II) is phosphorylated at several serines near the carboxy terminus by the G-protein coupled receptor, rhodopsin kinase (Ohguro et al, 1995). The phosphorylation of activated rhodopsin

reduces its ability to stimulate transducin and increases its affinity for arrestin (Krupnick et al, 1997). Binding of arrestin to rhodopsin prevents the activation by rhodopsin of transducin (Kuhn and Wilden, 1987). Arrestin binds tightly until the active chromophore all-*trans* retinal is released, which ends the stimulatory abilities of the opsin molecule. *In vitro* phosphorylation of rhodopsin by rhodopsin kinase is prevented by the addition of exogenous S-modulin or recoverin over physiological Ca ranges (Klenchin et al, 1995). Recoverin has been demonstrated to bind to rhodopsin kinase in a Ca-dependent manner (Klenchin et al, 1995). Recent data from recoverin knockout mice, reveal only moderate alteration of the photoresponse kinetics, suggesting other pathways functioning in the regulation of rhodopsin phosphorylation (Chen et al, 1995).

Peptide competition assays recently revealed that the cytoplasmic loops in rhodopsin between transmembrane segments V and VI, and also to a lesser extent between I and II, mediate binding to arrestin (Krupnick et al, 1997). Mutagenesis demonstrated that the loops between segments I and II and segments III and IV also are involved in binding to arrestin (Raman et al 1998). In addition, a strong rhodopsin binding domain of arrestin has been localized to amino acids 109-130 by synthetic peptide inhibition of PDE activity (Smith et al, 1999). Rhodopsin kinase mediated phosphorylation of rhodopsin leads to blockage of further activation of transducin, and the effective lifetime of the activated rhodopsin is reduced. Two different mutations have been identified in Oguchi disease, a congenital stationary form of night blindness. Each lacked either a functional arrestin or rhodopsin kinase, and displayed delayed dark adaptation (Yamamoto et al, 1997).



In contrast to the results presented above, permeabilization of bovine rods with  $\alpha$ -toxin and measurement of rhodopsin phosphorylation, found no detectable difference in the level of phosphorylation in high or low  $\text{Ca}_i$  conditions (Otto-Bruc et al, 1998). These results, while not denying the physiological effect of recoverin, call into question its presumed role as a modulator of rhodopsin kinase.

### *Physiological Effects*

In rods, background light reduces the sensitivity 100-1000 fold while the kinetics of the activation peak and recovery time are reduced only 2-3 fold (Detwiler and Gray-Keller, 1996). The gain of the activation after light adaptation is also observed to decrease (Detwiler and Gray-Keller, 1996). The effects of reduced Ca have been uncoupled from other post light stimulation effects, while soluble cytosolic proteins are retained. In one protocol, an improved Ca clamping method was employed to demonstrate that clamping Ca at the resting dark level increased the sensitivity to activation, but did not affect the time constant for recovery from saturation (Lyubarsky et al, 1996). Similarly, using saturating flash response kinetics calibrated to reduce Ca to its minimum and thereby stimulate guanylate cyclase to its maximum, it was observed that background illumination decreased the saturation period, indicating a reduction in the gain of activation (Pepperberg et al, 1992). Whole cell current recordings from truncated salamander rods revealed that Ca increases the gain of activation (Detwiler and Gray-Keller, 1996). While the falling phase of the activation current may be attributable to Ca modulated recovery mechanisms outlined previously, the increase in gain of the rising phase is not predicted by these recovery mechanisms. The observed effect of low Ca was attributed to the reduced formation of active rhodopsin, resulting in a lower PDE

activity, as if the light signal were dimmed (Detwiler and Gray-Keller, 1996). Significantly, dialysis removed the Ca-dependence of the activation gain response and neither exogenous calmodulin or recoverin was capable of rescuing the effect (Lagnado and Baylor, 1994), suggesting a completely different molecular basis for this activity.

The kinetics of internal Ca following exposure to saturating light has two components, a fast component and a slow component, suggested to be due to so-called “low” and “high” affinity buffers, respectively. At strong background illumination with low internal Ca levels, the fast component is absent, consistent with the low affinity buffers not binding Ca (Gray-Keller and Detwiler, 1994). In addition, Ca kinetics do not faithfully mimic current during flash response. During recovery from photostimulation, Ca reaches a peak and then falls for ~15 seconds to a sustained plateau; this occurs *after* the electrical response has fully recovered. The fact that the electrical response recovers before Ca levels suggests that some form of Ca homeostasis regulation is occurring, as the site of Ca influx (the cGMP-gated channel) has already recovered, as evidenced by the returned current.

Extensive investigations have ascribed to Ca a critical role in the recovery of photoreceptors following light stimulated signal transduction. The prevalence of Ca-dependence by the key regulatory proteins underscores the importance of Ca as a signaling molecule in phototransduction. Attempts have been made to quantify the relative contribution of these Ca-dependent mechanisms to photoresponse sensitivity modulation (Koutalos and Yau, 1996). Considering the central role of Ca in phototransduction, a closer examination of the mechanisms of Ca homeostasis is warranted.

### 1.3 Retinitis Pigmentosa

Retinitis pigmentosa (RP) is a common cause of blindness and the most common hereditary degenerative disease of the retina (for review see (Berson, 1993)). Approximately 1 person in 4000 is diagnosed with RP in the United States, and there are an estimated 1.5 million people worldwide who suffer from this affliction (Berson, 1996). Ophthalmologists have classified a number of symptomatically similar disorders as retinitis pigmentosa, on the basis of intraretinal pigment appearing around the region of the mid-peripheral retina (Berson, 1996). RP can be detected early in life by electroretinographic (ERG) testing, which in the diseased state reveals reduced amplitude and temporal delay in the kinetics of light response (Shady et al, 1995). Abnormal ERGs are detectable in afflicted patients as much as 10 years earlier than diagnosis is possible by ocular exam. If ERG results are normal for individuals six years of age or older, it has been found that RP will not develop later in life (Berson 1996). Clinically, retinitis pigmentosa is first apparent in adolescence, when impaired adaptation, night blindness and the loss of mid-peripheral vision is reported. RP is a slowly progressive disorder, with the majority of afflicted individuals being classified legally blind by the age of 60, although it can cause blindness as early as 30 years of age. Histopathological examination reveals the loss of vision is due to degeneration of both the rod and cone photoreceptors (Birch and Fish, 1987). The discovery of a recessive nonsense mutation in a *Drosophila* opsin gene that results in photoreceptor degeneration (Washburn and O'Tousa, 1989) sparked an international search for mutations in rhodopsin and other photoreceptor proteins as causative agents in retinitis pigmentosa families.

Retinitis Pigmentosa is a group of genotypically and phenotypically heterogeneous diseases caused by a large number of distinct genetic lesions (for review see (Inglehearn, 1998)). The clinical categorization is not always clear, and multiple hereditary retinal degenerative disorders, including retinitis pigmentosa have occasionally been linked to the same gene. As a further confounding factor, the clinical manifestations of the disease are heterogeneous between families with the same genetic mutation, and even within a family (Berson, 1996). The variety of clinical indications as well as the late onset, slow progression and associated cone degeneration from a disorder which originates in the rods suggests other genes or biological factors involved in the observed phenotypes.

RP has been genetically observed as autosomal dominant (Sullivan et al, 1999), autosomal recessive (Morimura et al, 1999), X-linked (Zito et al, 1999), mitochondrial (Mansergh et al, 1999) and digenic (Dryja et al, 1997) types. Clinically, there are three categories of retinitis pigmentosa; regional (Type I), diffuse (Type II) and sectorial (Type III). Type I RP demonstrates reduced rod ERG response while the cone ERG is not affected. Type II RP demonstrates severe loss of rod and cone function associated with diffuse pigmentary changes. Type III RP shows normal rod and cone function but detectable pigmentary changes, and is a non-progressive form of the disease. The three RP types have never been observed in the same family and so are considered distinct genetic entities. Currently, around 100 distinct genetic loci for hereditary retinal dystrophy have been identified, with over 30 mapped for RP, not counting the syndromic forms such as the Bardet-Biedl and Usher syndromes (Table 1). Mutations in over 19 genes have thus far been identified, including rhodopsin (Dryja et al, 1991), the  $\alpha$  (Dryja et al, 1999a) and  $\beta$

**Table 1****Causative Loci of Retinitis Pigmentosa.**

Table 1 shows a list of some of the genetic loci identified to date which are associated with Retinitis pigmentosa. The type of RP, dominant, recessive, digenic, X-linked or mitochondrial (*mito*), is indicated. In cases where the defective gene has been cloned, the protein name is given.

### Retinitis Pigmentosa Associated Loci

Symbol	Location	RP type	Protein	References
RP20	1p31	Recessive	RPE65	Morimura 98
RP19	1p21-p22	Recessive	ABCR	Cremers 98
RP18	1q13-q23	Dominant		Xu 96
RP12	1q31-32.1	Recessive	crumbs homolog 1	den Hollander 99
RP28	2p11-p16	Recessive		Gu 99
RP26	2q31-q33	Recessive		Bayes 98
SAG	2q37.1	Recessive	arrestin	Nakazawa 98
RP4	3q21-q24	Dominant	rhodopsin	Dryja 90
PDE6B	4p16.3	Recessive	rod PDE $\beta$	Bayes 95
CNGA1	4p12.cen	Recessive	rod cGMP channel $\alpha$	Dryja 95
PDE6A	5q31.2-q34	Recessive	rod PDE $\alpha$	Huang 95
RP14	6p21.3	Recessive	tubby-like 1	Hagstrom 98
RDS	6p21.2-cen	Dom/digenic	peripherin/rds	Kajiwara 91
RP25	6cen-q15	Recessive		Ruiz 98
RP9	7p15-p13	Dominant		Inglehearn 93
RP10	7q31.3	Dominant		Jordan 93
RP1	8q11-q13	Dominant	RP1 protein	Blanton 91
TTPA	8q13.1-q13.3	Recessive	TTPA	Yokota 96
ROM1	11q13	Digenic	ROM1(with rds)	Kajiwara 94
RP16	14	Recessive		Bruford 94
RP27	14q11.2	Dominant	NRL	Bessant 99
RLBP1	15q26	Recessive	CRALBP	Maw 97
RP22	16p12.1-12.3	Recessive		Finckh 98
RP13	17p13.3	Dominant		Greenberg 94
RP17	17q22	Dominant		Bardien 95
CRX	19q13.3	Dominant	CRX	Sohocki 98
RP11	19q13.4	Dominant		Al-Magthteh 94
RP23	Xp22	X-linked		Hardcastle 99a
RP15	Xp22.13-.11	X, Dom		McGuire 95a
RP6	Xp21.3-.2	X-linked		Ott 90
RP3	Xp21.1	X-linked	RPGR	Meindl 96
RP2	Xp11.3	X-linked	RP2	Hardcastle 99
RP24	Xq26-q27	X-linked		Gieser 98
RP21	MTTS2	Mito	serine tRNA 2	Mansergh 99

(McLaughlin et al, 1995) subunits of cGMP-PDE, the  $\alpha$  subunit of cGMP-channel (Dryja et al, 1995), peripherin/rds (Dryja et al, 1997), retinal outer segment membrane protein-1 (ROM1) (Bascom et al, 1995), ATP-binding cassette transporter-retinal (ABCR) (Cremers et al, 1998), retinitis pigmentosa GTPase regulator (RPGR) (Buraczynska et al, 1997) and myosin VIIA (Weil et al, 1997). This last has been identified as a genetic basis for Usher syndrome, in which RP cosegregates with profound congenital deafness. Despite the apparent wealth of knowledge concerning the genetic locus assignments of RP, about 70% of the loci remain to be identified. Most loci thus far assigned have been detected in single families. From that work, the rhodopsin gene has been identified as the single greatest cause of RP, recognized in approximately 10% of all cases. More than 70 distinct mutations in the rhodopsin gene have been characterized, most involving missense mutations altering only a single amino acid.

### **1.3.1 Rhodopsin Mutants**

Opsin is a prototypical member of the seven-membrane spanning receptor family, which are characteristically coupled to G-proteins. Opsin binds to the chromophore 11 *cis*-retinal via a Schiff base connection to form rhodopsin. The protein is 348 amino acids long and is inserted into the disk membrane. Structurally, rhodopsin is broken down into three domains; the intradiscal, transmembrane, and cytoplasmic. The intradiscal domain has been determined to be critical to ensuring proper folding and translocation to the disk membrane. A disulphide bridge between two cysteines in this region may be necessary for correct folding (Hwa et al, 1999). Mutants here typically are not efficiently transported to the disk membrane but rather fail to escape the endoplasmic reticulum (for review see (Shastry,

1994)). The transmembrane (or 'disc membrane') domain is composed of seven membrane spanning  $\alpha$ -helices, whose structure includes the chromophore pocket. The cytoplasmic domain contains charged amino acids which are believed to mediate interactions with transducin (Franke et al, 1992).

Mutants in the rhodopsin intradiscal domain are often, but not exclusively, associated with sectorial type RP disorders. Many of the intradiscal mutation associated phenotypes are less severe than those associated with mutations in the cytoplasmic domain, with patients reporting visual acuity and non-pathologic reduction in the peripheral field. Misfolding appears to be a major disruptive factor of the intradiscal domain, as mutations at the same codon which induce larger shifts in structure, such as Asp-190-Tyr compared to Asp-190-Asn, result in more severe functional consequences (Dryja et al, 1991). Apparently, misfolded rhodopsin molecules are inefficiently transported out of the endoplasmic reticulum, leading to the observed phenotypes.

Transmembrane domain mutants present more variable phenotypes. Two mutations within the first transmembrane helix, Leu-40-Arg and Thr-58-Arg, result in disease phenotypes of differing severity (Kim 1993, Fishman 1991). Further, a deletion mutant (codon 255) from the sixth transmembrane helix presents with variable pigmentation while a mutation in the seventh helix (Ala-292-Glu) causes stationary night blindness rather than retinitis pigmentosa (Dryja et al, 1993). Intriguingly, a 50 amino acid insertion caused by incorrect splicing leads to late onset night blindness in some patients and yet presents no abnormal symptoms in others (Dryja et al, 1993).



The cytoplasmic domain of rhodopsin is phosphorylated by rhodopsin kinase and is involved in the activation of transducin. Mutations in this region would therefore be expected to alter protein:protein interactions, activation and recovery from the phototransduction cascade. Somewhat surprisingly, a consistent mechanism for impairment is not observed however, as similar mutations result in heterogeneous phenotypes. Mutation at codon 347 causes early onset of night blindness and loss of visual field while mutation at codon 344 causes late onset night blindness (Berson 1991). Similarly, the Pro-347-Leu mutant shows severe pigment deposition while the Pro-347-Arg mutant does not. The reason behind the heterogeneity of presented symptoms remains to be clarified.

### **1.3.2 RIM/ABCR Mutants**

The ATP-binding cassettes transporter - retinal (ABCR) was recently cloned and found to be identical to the previously identified RIM protein. This protein is found on the rim region of the disk membranes in photoreceptor outer segments. The gene has been identified as the mutant locus for cases of Stargardt's disease (STGD) (Shroyer et al, 1999), fundus flavimaculatus (FFM) (Gerber et al, 1995), age-related macular degeneration (AMD) (Allikmets et al, 1997), RP (Martinez-Mir et al, 1998) and cone-rod dystrophy (CRD) (Cremers et al, 1998). The phenotypic heterogeneity is indicative of the range of retinal disorders that can originate from mutations in a single gene. Interestingly, in one study, the screening of 40 unrelated STGD families found that all of the ABCR mutations resulted in premature truncation of the protein (Rozet et al, 1998). Conversely, of 15 FFM families studied, all demonstrated missense mutations to uncharged amino acids (Rozet et al, 1998). Some correlation therefore exists between the severity of the retinopathy in the continuum

of retinal degenerative disease, and the degree of modification to the target protein.

The ATPase activity of immunoaffinity purified ABCR reconstituted into liposomes was found to be stimulated by all-trans-retinal (Sun et al, 1999), a photoexcitation end-product of the chromophore 11- *cis* retinal. ABCR knockout mice showed increased levels of all-trans-retinaldehyde, accumulation of N-retinylidene-phosphatidylethanolamine (an all-trans-retinaldehyde phosphatidylethanolamine complex) and deposition of A2-E, a component of cell lipofuscin fluorophore, in the retinal pigment epithelium (Weng et al, 1999). These data suggest that ABCR functions as a retinoid transporter, and that pathology of ABCR genetic lesions may be due to A2-E toxicity in the retinal pigment epithelium and subsequent loss of support activity, leading to photoreceptor degeneration.

### 1.3.3 *rds* / Peripherin Mutants

Peripherin/RDS (RDS) (Connell and Molday, 1990) is a 39 kd protein which is localized to the rim region of disk membranes. Structurally, the protein is divided into intradiscal, membrane and cytoplasmic regions, in which the membrane domain is proposed to contain four membrane-spanning  $\alpha$ -helices. Peripherin forms a heterotetrameric complex with ROM-1 in both rod and cone photoreceptor outer segments (Goldberg and Molday, 1996). Peripherin is the bovine ortholog of the mouse *rds* gene (Travis et al, 1989), which is responsible for the mouse retinal degeneration - slow phenotype. RDS mutations have been identified in retinitis punctata albescens (Shastri and Trese, 1997), macular dystrophy (Nakazawa et al, 1995), butterfly shaped pigment dystrophy (Daniele et al, 1996) and autosomal dominant RP (Ekstrom et al, 1998). The majority of RDS disease-causing mutations are found in the intradiscal region, and again the range of phenotypes displayed

is significant. Digenic RP is associated with heterozygous mutations in RDS and ROM1, with the RDS mutation consistently being the missense Leu185Pro change, while the ROM1 mutations may vary. ROM1 itself has not been implicated as the sole cause of any retinopathy.

#### **1.3.4 Retinal Rod cGMP Phosphodiesterase**

Mutations have been identified in both the  $\alpha$  and  $\beta$  subunits of the rod cGMP PDE (McLaughlin et al, 1995; Huang et al, 1995; Saga et al, 1998). These heterozygous mutations lead to autosomal recessive retinitis pigmentosa (arRP). Comparison of the mutations in both the  $\alpha$  (PDE6A) and  $\beta$  (PDE6B) subunits demonstrates that the catalytic domain and cGMP binding domain are the location of the mutations (Dryja et al, 1999b). Mutations in the PDE6B gene are the most common identified cause of autosomal recessive retinitis pigmentosa, accounting for 4% of all cases in North America (McLaughlin et al, 1995).

#### **1.3.5 Retinal Rod cGMP-gated Channel**

The cGMP-gated channel controls the flow of Na and Ca ions into the photoreceptor outer segment, and is regulated by the levels of cGMP in the cytosol. The channel is composed of the homologous  $\alpha$  and  $\beta$  subunits, which differ in the presence of the glutamic acid rich protein domain at the N-terminal of the  $\beta$  subunit. Both subunits have six putative membrane spanning helices, a cGMP-binding domain, a pore loop and a voltage sensor motif (Kaupp et al, 1989). Homozygous or heterozygous missense mutations have been found in the cone cGMP-gated channel  $\alpha$  subunit (CNGA3), in families with the autosomal recessive rod monochromacy (total colourblindness) phenotype (Kohl et al, 1998). Nonsense or frameshift mutations in the  $\alpha$  subunit of the rod cGMP-gated channel (CNGA1) have been

found to result in arRP (Dryja et al, 1995). *In vitro* expression of the frame shifted mutant, or a missense mutant also observed to cause arRP, found that the produced polypeptide failed to be transported to the plasma membrane (Dryja et al, 1995).

### **1.3.6 Genotypic and Phenotypic Diversity**

The genotypic and phenotypic heterogeneity of retinitis pigmentosa are as much distinguishing features as are the clinical manifestations for which it is named. One common thread, however, of many of the hypotheses for the diversity in disease progression and phenotype is incorrect protein folding and the subsequent transport to the disk membranes. Heterogeneous carriers of a rhodopsin null mutant were observed to display normal vision (McInnes and Bascom, 1992), suggesting a mechanism other than reduced function at work in the large number of autosomal dominant RP cases. The apparent inconsistency of rod-specific gene mutations leading to overall retinal deterioration may be due to structural degradation. It is known that the outer segment sheds and renews 10% of the disk membranes each day (Tamai et al, 1982). Mutations in photoreceptor specific proteins which affect the ordered disk structure or the protein:protein interactions may have deleterious effects on correct shedding of outer segment membranes. Excessive shedding of outer segment membranes would lead to rod degeneration over time, resulting in the loss of the majority of the physical structure of the outer segment layer. It is conceivable that toxic waste products could accumulate and contribute to the degeneration as well. The rate of such shedding and waste product build up may well be determined by other factors specific to the afflicted individual. Regardless, the genetic identities of the large number of RP-causative loci remaining to be elucidated necessitates the ongoing investigation into the role each

photoreceptor specific protein plays in the development of human inherited retinopathies.

### **1.3.7 Potential Role of NCKX1 in Degenerative Human Retinopathies**

Phototransduction is a system where key paradigms of intracellular signaling are explored. The role of Ca, a central regulator of cellular processes throughout evolution and across many systems, is vital to the mediation of recovery from photoexcitation. Principal proteins involved in Ca homeostasis and Ca-dependent proteins involved in signal transduction have historically received considerable attention. Perhaps one of the overlooked proteins involved in mediating the large Ca fluxes of the rod photoreceptor outer segment is the Na/Ca+K exchanger. Its role in Ca homeostasis is perhaps not as clear as generally assumed, evidenced by the identification of unexpected regulatory features and the lack of knowledge concerning its structure function relationships.

Identification and investigation of human retinal degenerative disease-causing genes has increased our knowledge of photoreceptor specific genes and also provided insight into their functions. Future studies of the many genes involved in retinitis pigmentosa that remain to be identified will undoubtedly further our understanding of this disease and the physiology of the photoreceptor. Additional investigation is required into the molecular biology of the Na/Ca+K exchanger, due to its key role in Ca homeostasis of the rod photoreceptor, both to identify structure function relationships, and to initiate research into the role it may play in human retinal diseases.

## **CHAPTER TWO: OBJECTIVES**

- 1. Clone human NCKX1 homologue.**
  - a. Define significance of certain domains based on conservation.**
  - b. Attempt to isolate a clone which is functional when heterologously expressed.**
- 2. Determine genomic organization and chromosomal localization.**
  - a. Investigate possibility of role in human disease.**
  - b. Gain insight into evolutionary relatedness to NCX1.**
- 3. Examine structure function relationships of the bovine rod Na/Ca+K exchanger using the bovine cardiac Na/Ca exchanger as a template.**

### **CHAPTER THREE: MATERIALS AND METHODS**



### **3.1 Molecular Techniques**

#### **3.1.1 DNA Preparation**

##### **Bacterial DNA purification**

Bacterial plasmid DNA was isolated and purified by several methods. Early on, DNA was isolated by a standard phenol/chloroform extraction (Sambrook et al, 1989). Briefly, a bacterial pellet from an overnight culture was resuspended in a glucose, tris, EDTA (GTE) buffer and then lysed with NaOH. Subsequently, the solution was neutralized with Na, K acetate and centrifuged to remove lipids and proteins. Extraction of the DNA was accomplished by three phenol / chloroform extractions followed by ethanol precipitation and resuspension in distilled deionized water or 10 mM Tris, pH 9.0. Residual RNA was removed by 30 minute treatment with RNaseA at 37°C. Alternatively, DNA was isolated using the Qiagen midi columns as per the manufacturer's instructions (Qiagen Inc.).

When cloning new constructs, single colonies were often screened via a miniprep approach. Originally, these were performed using the GeneClean system (Bio 101, La Jolla, CA) with some modifications to the protocol. 1 ml cultures from single colonies were grown in eppendorf tubes overnight at 37°C. These 1 ml cultures were spun down in a microfuge and the supernatant removed. The bacterial pellet was resuspended in GTE then NaOH lysed and Na,K Acetate neutralized. Rather than extracting with phenol / chloroform, 10 µl GeneClean glass milk was added to the centrifugation supernatant and the DNA purified as per the GeneClean manufacturer's instructions. Alternatively, the plasmid DNA from bacterial minipreps was also isolated using the Qiagen miniprep kit, as per the manufacturer's instructions.

### **P1-AC (PAC) DNA Purification**

A 50 ml overnight culture was grown in LB shaking at 37°C. The culture was then added to 450 ml fresh LB and returned to the shaking 37°C incubator. After growth until OD<sub>550</sub> of 0.15 was reached, at about 3 hours, 5 ml 0.1 M IPTG was added to the culture and allowed to grow until OD<sub>550</sub> of 1.5 was achieved. The cells were centrifuged at 5000 rpm for 20 minutes and the supernatant discarded. DNA was isolated using the Qiagen midi prep system (Qiagen Inc, ) with the exception that the resuspension, lysis, neutralization and wash solutions were doubled in volume. The PAC DNA was eluted and precipitated as per the manufacturer's instructions and resuspended in 500 µl 10 mM tris pH 9.

### **Lambda DNA Extraction**

10 µl DNase (5 mg/ml) and 25 µl RNase (10 mg/ml) was added to 50 ml liquid phage lysates. Following centrifugation for 1.5 hours at 132000g at 4°C, the pellet was resuspended in 200 µl 0.05 M Tris pH 8. 200 µl phenol was added and the lysates shaken a further 20 minutes. After a 2 minute spin in a microcentrifuge the upper aqueous layer was collected and phenol extracted twice followed by extraction with 200 µl chloroform. The DNA was pelleted by addition of 20 µl 3 M NaAc pH 4.8 and 440 µl 100% EtOH prior to spinning 10 minutes in a microcentrifuge. Pellets were washed with 70% EtOH and recentrifuged, followed by drying and resuspension in 100 mM Tris, pH 8.

#### **3.1.2 RNA**

Total RNA was prepared from both human and bovine retinal RNA. Bovine retinas were obtained from a local slaughterhouse. The retinas were frozen immediately after enucleation in liquid nitrogen and returned to the lab where the RNA was extracted using

Trizol reagent according to the manufacturer's directions. Human retinas were obtained from the Lions Eye Bank (Rockyview Hospital, CRHA) from recently deceased patients. Typically, the retina was removed from the enucleated eye two to three hours after death of the donor. The retina would then be frozen immediately on dry ice and the RNA extracted via the Trizol procedure at a later time.

For cells grown in culture, cells were removed from the plate or flask in PBS and pelleted in a centrifuge at 1500 rpm for 5 minutes. 1 ml Trizol™ was added to each 10 cm plate equivalence of cells. The remainder of the RNA isolation procedure was performed as per the Trizol manufacturer's directions. The RNA pellet was resuspended in DEPC-treated water and incubated for 10 minutes at 60°C to aid solubilization. RNA concentrations were determined spectrophotometrically and samples stored at -80°C. Residual DNA contamination was removed by the addition of 55 µl NEB buffer 2 (New England Biolabs), 2 µl RNasin, and 2 µl DNase (RNase free - RQ DNase) to 500 µl of total RNA. After 30 minute incubation at 37°C, 5 µl 5 mM EDTA was added to stop the reaction. Phenol / chloroform extraction was followed with precipitation via the addition of 50 µl 3 M NaAc pH 5 and 2.5 volumes 100% EtOH and centrifugation.

Poly A<sup>+</sup> RNA was purified from total RNA using the NEB oligo dT columns essentially as per the manufacturer's recommendations. Briefly, total RNA was precipitated with EtOH and resuspended in Elution buffer and NaCl. After denaturation the total RNA was applied to the oligo dT column, washed three times with Wash buffer and once with Low Salt buffer. Following elution in prewarmed Elution buffer, the isolated poly A<sup>+</sup> RNA was precipitated with NaOAc and EtOH, as described.

For synthesis of 1<sup>st</sup> strand DNA from an RNA template, 2 ug total RNA or 100 ng of poly A<sup>+</sup> RNA was added to 100 ng random primers in 10 µl total volume. This was denatured at 70°C for 10 minutes then quick chilled on ice. To this was added 500 uM dNTPs, 10 mM DTT, and First Strand Buffer. Incubation with Superscript enzyme (Gibco BRL) for 10 minutes at room temperature and 2 minutes at 42°C was followed by addition of RNasin, Reverse Transcriptase (GibcoBRL), incubation at 42°C for 1 hour and inactivation of the enzyme with a 15 minute incubation at 70°C. The resulting transcribed DNA was cleaned up by 15 minute RNaseH treatment followed by purification through QiaQuick columns using a post-PCR protocol (Qiagen Inc., ). When necessary, 2<sup>nd</sup> strand synthesis was accomplished by poly-A tailing the 1<sup>st</sup> strand using the terminal deoxynucleotide transferase (TdT) enzyme and initiating second strand synthesis with oligo dT primers. PCRs that followed the 1<sup>st</sup> strand synthesis were as described below, using ~40 ng of the 1<sup>st</sup> strand product as template.

### **3.1.3 Gel Electrophoresis**

#### **Agarose Gels**

Typically, DNA was assayed for fragment size, quantity and quality via agarose gel electrophoresis. Also, when necessary in isolating restriction fragments, or for Southern analysis, agarose gel electrophoresis was employed. Agarose gels were made from ultra pure agarose (Gibco BRL) in 1xTAE buffer (Sambrook et al, 1989). Gels were typically run at 100 volts for 30 minutes to 2 hours as required. DNA was visualized by exposure to ultraviolet light and photographed with a Polaroid Gelcam camera using Polapan film (Polaroid Corp., Cambridge, MA).

For RNA purposes, 1% agarose / formaldehyde gels would be melted and poured in dedicated RNA-only apparatus which was treated with RNaseZap before and after all handling. Gloves were always worn. When working with RNA, all solutions not obtained from commercial sources were made with diethyl pyrocarbonate (DEPC) treated water. All solutions and reagents except DEPC treated water, were obtained in the Northern Max kit from Ambion. Denaturing agarose gels were made by heating DEPC treated water in a microwave and adding RNase free agarose and formaldehyde. Only high quality RNA samples, ie. those showing no significant degradation of the 18S and 28S bands upon visual inspection, were used. For Northern hybridization, the RNA samples were run along with a marker lane containing ethidium bromide stained commercially available single stranded RNA fragments (NEB). After a 3 hour electrophoresis, the gel was photographed under ultraviolet light next to a phosphorescent ruler for later size determination.

### **Polyacrylamide Gels**

For sequencing applications, 65 ml of acrylamide mix (1 x TBE, 6% acrylamide, 50% w/v urea) was mixed with 650  $\mu$ l ammonium persulfate and 25  $\mu$ l TEMED. Sequencing gels were run at 2000 V for 3-9 hours, as required, at a constant temperature of 55°C.

Polyacrylamide gels for protein separation were prepared by polymerizing a 4% stacking / 7.5% resolving gel (Short Protocols, 1995) in a 1.5 mm thick BioRad gel apparatus. Protein samples were electrophoresed at 200 V in 1 x Running buffer (Short Protocols, 1995) for 1-2 hours, as necessary. Gels were either stained with Coomassie blue to determine protein loading, or transferred to membrane as described elsewhere.

### **3.1.4 DNA Manipulation**

#### **DNA Restriction Digestion, Purification and Ligation**

DNA to be digested was incubated with restriction endonuclease at the appropriate temperature, usually 37°C, for 1-2 hr in the recommended buffer. Digestion fragments were separated and visualized on an agarose gel. When DNA fragments were to be isolated, the DNA sample was run on the gel to separate the fragments. Upon visualization with UV light, the appropriate band was excised with a razor blade and the DNA purified by one of several protocols. Initially, DNA fragments were isolated using the Geneclean kit as per the manufacturer's instructions. Later, Qiagen QiaEx kits were employed as per the manufacturer's instructions (Qiagen Inc., Mississauga, ON). In some cases, where DNA isolated from a band was only to be used as template for a future polymerase chain reaction (PCR) procedure, the DNA was extracted using the 'freeze-squeeze' technique. In this method, the appropriate band was excised from the agarose gel with a razor blade, frozen at -20°C, and then squeezed in a piece of parafilm. The liquid squeezed out of the frozen gel slice was used as a template for PCR amplification. Ligation of DNA fragments was carried out with T4 DNA ligase (New England Biolabs, Beverly, MA) in the appropriate buffer at either room temperature (r.t.), 16°C or 4°C as required. Generally, it was found that ligation of low concentration DNA fragments or of blunt-ended species was most efficient when incubated at 4°C overnight.

### 3.1.5 PCR

#### Polymerase Chain Reaction

For amplification of DNA fragments via the polymerase chain reaction (PCR) 20, 50 or 100  $\mu$ l reactions were cycled in a Perkin-Elmer 2400 Thermocycler (Perkin-Elmer Corp., Foster City, CA). For PCR reactions where the expected product was 2-3 kb or less, *Taq* DNA polymerase in an appropriate buffer was used, primers were added to 200 nM final concentration, nucleotides were added to 200  $\mu$ M and magnesium was kept at 1.5 mM. Typical conditions required an initial 2 minute denaturation at 94°C followed by 25-35 cycles of: 30 second, 94°C denaturation; 30 second 60°C annealing, 30 second to 2 minute 72°C extension. The cycles were followed by a 7 minute extension at 72°C. Post PCR purification included one or more of the following: ethanol precipitation, QiaQuick purification (Qiagen Inc., Mississauga, ON), or separation by agarose gel electrophoresis followed by gel-excision and purification as described above.

For PCR products expected to be larger than 3 kb, the Expand Long Template PCR protocol (Boehringer Mannheim, Mannheim, Germany) was employed, generally as per the manufacturer's instructions. Efficiency was found to increase when using longer primers with higher melting temperatures ( $T_m$ ) and when the reaction conditions were modified to use a 15 second 94°C denaturation step; a 30 second 62°C annealing step and a 2 to 15 minute (as required) 68°C extension step.

For PCR reactions where fidelity was an issue, the High Fidelity PCR kit (Boehringer Mannheim, Mannheim, Germany) was used. Here the manufacturer's recommended protocols were found to give the best results.

### **Rapid Amplification of cDNA Ends (RACE)**

5'-RACE of the human NCKX1 transcript was accomplished with three individual oligonucleotide primers, JTG-35, JTG-21 and *back*. First strand cDNA was prepared from total human retinal RNA as described above, with the exception the above primers replaced the random oligonucleotide primers in individual reaction tubes. Poly-adenylation of the first strand DNA was achieved using TdT with 1 mM ATP. Second strand cDNA synthesis was initiated from dTAnchor-B1 (Appendix I), essentially as was performed for the first strand. First round PCR, with the (upstream) Anchor2 primer, which is complementary to unique regions on dTAnchor-B1, and the JTG-35, JTG-21 or *back* primers (downstream) was sufficient to amplify DNA fragments from the second strand cDNA template.

3'-RACE was employed to obtain the region from the stop codon to the 3' end of the human NCKX1 cDNA. Total RNA was purified to poly-A<sup>+</sup> RNA as described above. First strand cDNA was primed with dTAnchor-B1, and synthesized with Superscript enzyme. Second strand synthesis was initiated with oligonucleotide JTG-17 (Appendix I). PCR of the second strand cDNA template was as for typical PCR reactions, described above, and employed JTG-17 (upstream) and each of Anchor1, 2, 3 and 4 (downstream), which are all complementary to dTAnchor-B1, in individual reaction tubes. All four PCR reactions produced identical fragment banding patterns.

#### **3.1.6 Sequencing Reactions**

Primers were end-labeled with <sup>33</sup>P-γ dATP using T4 kinase via incubation at 37°C for 30 minutes, followed by heating to 70°C, chilling on ice for 10 minutes and a brief spin down. Template DNA was added to each primer, along with the appropriate terminator mix



(dXTP/ddXTP) and Taq polymerase. Extension in a thermocycler was followed by denaturation and electrophoresis on a 6% polyacrylamide / TBE / urea gel. When complete, the gel was fixed with 7% methanol / 7% acetic acid solution, dried, wrapped in Saran® wrap and exposed to Kodak MR film.

### **3.1.7 Probe Synthesis**

As template for probe preparation, DNA fragments from bovine NCKX1, NCX1 and the chimeric IF construct were utilized, where appropriate. For radiolabeled DNA probes, 100 ng template DNA was added to 10 µl primer and heated to 95°C for 7 minutes. A brief spin to collect the liquid in the bottom of the tube was followed by addition of buffer, dNTPs, <sup>32</sup>P-dATP and Superscript™ enzyme. After 5 minutes at 37°C, EDTA was added to stop the reaction and the mixture was heated to 95°C for 10 minutes. To remove contaminants from the radiolabeled DNA probes, they were applied in a volume of 50 µl to a vortexed G-50 column and spun through.

For riboprobes, template DNA cloned such that Sp6 or T<sub>7</sub> phage promoter sites were positioned appropriately upstream of the target of interest was linearized with a restriction site downstream of the homologous sequence and isolated by gel excision and QiaEx purification. This template was incubated at the appropriate temperature with Sp6 or T<sub>7</sub> DNA polymerase, ribonucleotides ATP, CTP and GTP and <sup>32</sup>P-γ UTP. For transcripts longer than 400 bases, cold UTP was also added to allow longer extension. Following transcription, the DNA template was removed by digestion with RNase-free RQ DNase. Finally, contaminants including salts and enzyme were removed by purification over a Sephadex G-50 column.

### **3.1.8 Sample Detection**

#### **Southern Blot Analysis**

For detection of DNA fragments by the Southern blot method, the sample to be assayed was digested with the appropriate enzymes and then run on a 1% agarose gel to achieve adequate separation of the bands of interest. A marker lane containing commercially available DNA fragments such as Hind III digested lambda or the NEB 1 kb ladder was always run alongside. After electrophoresis of the DNA samples, the gel was photographed with a luminescent ruler, to allow the later determination of hybridized band molecular weights. Denaturation of the DNA was performed while still in the gel, followed by neutralization and rinsing in 2xSSC. The DNA was transferred to Nylon or Nitrocellulose membranes by either upward fluid capillary transfer or the 'squash-blot' method (Short Protocols, 1995). Squash-blots were typically sufficient for most Southern applications. After overnight transfer, the DNA was fixed to the membrane by 2 hour incubation at 80°C.

Hybridization of the membrane with radiolabeled probe was performed in either a shaking water bath or a rotating oven. When hybridizing in a water bath, the membrane was gently shaken while submerged in the prehybridization buffer for 1 hour, followed by overnight incubation at 65°C in hybridization buffer containing radiolabeled probe synthesized as described above. The following day, the membrane was washed twice at room temperature in low stringency wash buffer (2XSSC, 0.1% SDS), followed by four washes in high stringency wash buffer (0.1XSSC, 0.1% SDS) at 65°C. When hybridizing in a rotating oven the QuickHyb protocol was used essentially as suggested by the manufacturer (Clontech). In all Southern hybridization reactions the hybridization temperature was kept

at 65°C. After washing, the membrane was wrapped in Saran® wrap and exposed to X-ray film (Kodak) from four hours to several days, as necessary.

### **Northern Blot Analysis**

For Northern blot analysis, RNA samples were collected, electrophoresed through an agarose-formaldehyde gel and purified essentially as described above. The RNA samples were then transferred overnight by upward capillary transfer using the Northern Max transfer protocol according to the manufacturer's instructions. The next day the membrane was baked at 80°C for two hours. Hybridization of the membrane was to either radiolabeled DNA probe or riboprobe, prepared as described. Hybridization occurred in a rotating oven at 42°C for DNA probes and 68°C for riboprobes. Hybridization was according to the Northern Max kit's recommended directions. Briefly, the membrane was prehybridized for 1 hour in hybridization buffer, the probe was added and the hybridization continued overnight. The membrane was washed the next day in two low stringency washes and two high stringency washes, all at the hybridization temperature. Exposure to X-ray film (MR film Kodak) was typically overnight, although some strongly hybridizing samples required only 1 to 2 hours.

### **Western Blot Analysis**

Cells were collected from culture and washed in PBS several times to remove serum. The cell pellet was resuspended in a PBS/protease inhibitor cocktail (Complete™, Boehringer Mannheim) in order to prevent proteolysis of the cellular proteins. Genomic DNA was removed via a RIPA buffer post-nuclear treatment. Briefly, the cell pellet was resuspended in RIPA buffer (1% Triton, 0.5% deoxycholate, 140 mM NaCl, 10 mM EDTA, 25 mM Tris pH 7.5 and protease inhibitors) and incubated 20 minutes on ice. Centrifugation

at 5000g for 5 minutes to pellet the nuclei was followed by collection of the supernatant. The cellular protein concentration in the supernatant was spectrophotometrically measured via the modified Bradford assay.

Typically, 30 µg of protein was diluted 1:2 in sample buffer (Sambrook et al, 1989) and run on a 1.5 mm thick 7.5% polyacrylamide gel. To ensure equal loading of protein, a duplicate gel was stained, after electrophoresis, with either Coomassie blue or colloidal gold (BioRad). For protein transfer, the original gel was electrotransferred to nitrocellulose in a glycine Tris 0.05% SDS transfer buffer. The percentage of SDS was found to be critical in ensuring good transfers, as balance must be struck between liberating the hydrophobic membrane proteins from the gel while preventing the transfer of protein completely through the membrane. After transfer the membranes were blocked for 1 hour at r.t. in either TBS-T (tris buffered saline - 0.1% Tween-20) or PBS-T (phosphate buffered saline - Tween-20) containing 5% w/v skim milk powder. Afterwards the membrane was washed four times, for 15 minutes each wash, in TBS-T (or PBS-T) and then incubated overnight at 4°C in primary antibody in 1% skim milk w/v TBS-T (or PBS-T) solution. For detection of proteins carrying the bovine rod Na/Ca+K exchanger cytosolic loop, that is EX, CR and CCC, the PME 1B3 monoclonal antibody, was employed as a 1/20 dilution of hybridoma supernatant. For detection of proteins carrying the external signal peptide of the bovine cardiac Na/Ca exchanger, namely CR, IF, OF, IFC, p17 and CCC, the 6H2 monoclonal antibody was employed. The C<sub>2</sub>C<sub>12</sub> monoclonal antibody binds to the cytosolic loop of the bovine NCX1 exchanger, and so was used to detect protein expression from the IFC and p17 constructs. For detection of proteins carrying the synthetic FLAG epitope, the commercial monoclonal

antibody M2 (Kodak IBI) was used at a concentration of 10 µg/ml. Following the overnight incubation in primary antibody, the membrane was washed four times, as before, in TBS-T and then incubated in secondary antibody for 1 hour at r.t.. Following four more washes in TBS-T, the membrane was washed in TBS to remove the Tween and then, optionally, in 50 mM Tris-Cl pH 7.5 to prepare the membrane for HRP detection. Detection of HRP was accomplished with the Phototope-HRP kit (NEB).

### **Immunohistochemistry Protocol for Coverslips**

Coverslips with cells attached were washed twice in PBS containing 0.1 mM CaCl<sub>2</sub> and 0.1 mM MgCl<sub>2</sub>. Cells were fixed in 3% formaldehyde, 15 minutes at room temperature, followed by solubilization in 0.1% triton. The cells were blocked in 0.2% fish gelatin / 1XPBS for 10 minutes at r.t. followed by addition of 100 µl primary antibody diluted in fish gelatin / PBS per coverslip and incubated at r.t. for 1 hour. Coverslips were washed as before, then incubated with secondary antibody linked to rhodamine for 1 hour at r.t.. Following a final wash, 1 drop coverslip mounting medium was added, each coverslip was placed on a glass slide face down and sealed with clear nail polish.

### **Ribonuclease Protection Assay (RPA)**

RPA was performed on human and bovine total retinal RNA using the RPA III kit (Ambion), essentially according to the manufacturers directions. 5 and 10 µg samples of total RNA were employed in each experiment as internal controls for one another, to demonstrate that complete degradation of non-homologous sequences was achieved. Two positive and one negative control were employed for both the bovine and human RPA assays. The full length probe control contained riboprobe and 10 µg of yeast RNA but was not subjected to

later degradation with RNase. The + strand control contained riboprobe and + strand single stranded RNA of the riboprobe template, transcribed with the Maxiscript kit. This positive control was later treated with RNase, resulting in the digestion of the ends of the riboprobe which were not identical to the + strand RNA. The negative control contained riboprobe and yeast RNA, and was later treated with RNase.

The RNA samples were co-precipitated with and hybridized to  $1.2 \times 10^5$  cpm bovine or human template specific riboprobe which had been prepared as described above. RNase digestion was effected by the addition of RNase A / RNase T1 mixture to each sample except the full-length riboprobe control, which was mock digested. Following precipitation, the protected fragments of each sample were separated on a 6 % denaturing polyacrylamide gel run at 200 V. The positive control samples were diluted prior to gel loading, in order to normalize the cpm with the much less radioactive retinal RNA samples. Unrelated riboprobes of known lengths were mixed together and run as a marker lane. When the gel electrophoresis was complete, the gel was fixed with 20% methanol, 5% acetic acid and vacuum dried on Whatman 3MM paper.

For accurate quantification of the protected fragments, a Molecular Dynamics phosphorimager was employed. The dried RPA gel was exposed to a phosphor screen overnight at r.t.. ImageQuant software was used to count the relative photon emissions from the screen upon scanning, and equal sized regions were counted for each fragment of interest. All data were analyzed and plotted with Microsoft Excel and Sigma Plot V.

### **Primers and Oligonucleotides**

All primers and oligonucleotides referred to in this thesis are listed in Appendix I.

## 3.2 Clone Construction

### 3.2.1 Cloning of Bovine NCKX1 / NCX1 Mutants

To construct deletion and chimeric mutants, the full length cDNAs of the bovine rod Na/Ca+K exchanger (*pEX*), and the bovine Na/Ca exchanger (*p17*) were obtained from Drs. H. Reiländer and J. Reeves, respectively. The pRc/CMV vector was used for expression in CHO and HEK cells, pVL1392 was for SF9/SF21 cells and pEIA was used for the HighFive cell system. Figure 3.1 illustrates schematically the various exchangers and derived mutants constructed and/or examined in this study.

#### EX (NCKX1)

The full length bovine NCKX1 was transferred to each of the different expression vectors. To make these clones, *pEX* was digested with Kpn I and Sal I and subcloned into pBluescript II (Pharmacia). The bovine NCKX1 cDNA coding sequence was then digested with Not I and EcoR I and subcloned into the baculovirus vector pVL1392, creating the *pVEX* construct. *pVEX* was then digested with Not I and Xba I and subcloned into pRc/CMV (Invitrogen), creating *pREX*. Finally, the EX construct was liberated from the *pREX* vector with Not I and Xba I and ligated into the pEIA insect expression vector (Farrell et al, 1998).

#### p17 (NCX1)

As a positive control, the NCX1 exchanger, which demonstrates robust Na/Ca exchange activity in a variety of expression systems, was also cloned into the pVL1392, pRc/CMV and pEIA expression vectors. Using the NCX1 p17 clone, obtained from Dr. J. Reeves, the coding region was liberated by digestion with EcoR I and Xba I and ligated into appropriately digested pRc/CMV. This construct was then subcloned into pEIA.

**Figure 3.1****Chimeric and Deletion Constructs.**

Full length constructs and mutants of the bovine NCKX1 and NCX1 cDNAs are shown. Putative membrane-spanning  $\alpha$ -helices are presented as embedded *cylinders*, NCKX1 domains are illustrated by *black lines*, NCX1 domains are represented by *gray lines*.

**a.** EX, full length rod bovine NCKX1

**b.** p17, full length cardiac bovine NCX1

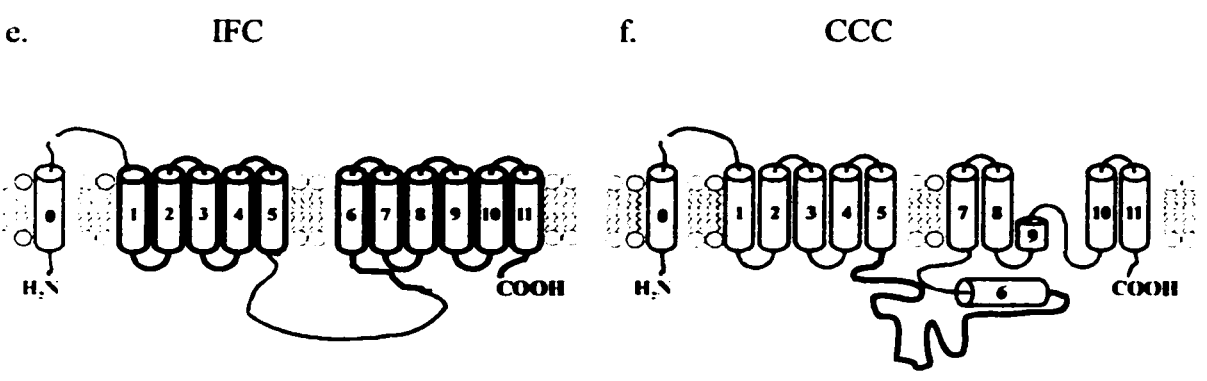
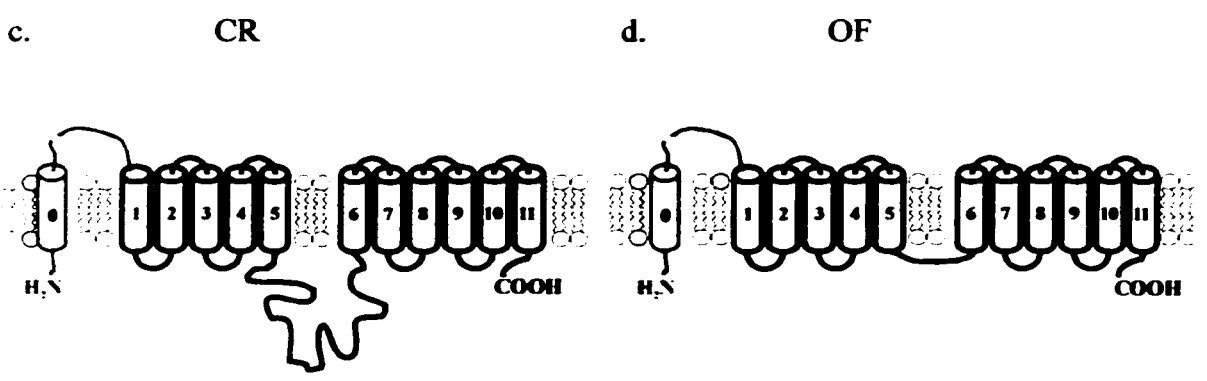
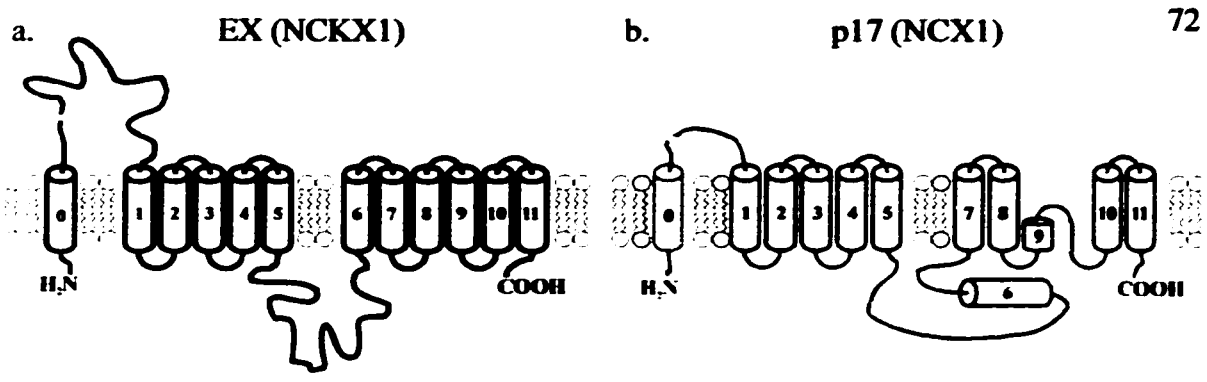
**c.** CR, NCKX1 with N-terminal extracellular region and signal peptide replaced by that of NCX1

**d.** OF, CR mutant with the additional modification of the deletion of the majority of the cytosolic domain

**e.** IFC, OF mutant with the cytosolic domain of the NCX1 cDNA replacing that removed from NCKX1

**f.** CCC, NCX1 cDNA with the cytosolic domain deleted and replaced by the cytosolic domain of NCKX1.





## CR

The first chimeric mutant, CR, was based on the bovine rod Na/Ca+K exchanger, but with the external loop removed and replaced with the signal sequence of the Na/Ca exchanger. The CR clone was created to examine what effect the lack of the extracellular domain would have on Na/Ca+K exchange. To make this construct, the signal sequence of the bovine NCX1 was amplified via PCR with the primers Bovcardsig1 and Bovcardsig2, which created a Not I site at the 5' end and Spe I site at the 3' end of the fragment. The fragment of the bovine NCKX1 gene corresponding to the first amino acid of transmembrane region 1 up to the Bgl II site was PCR amplified from pEX template using the primers Rod5' and Rod3', which created a novel Spe I site at the 5' end of the fragment. The NCKX1 PCR amplified fragment was digested with Spe I and Bgl II and subcloned into appropriately digested pBluescript-NCKX1 plasmid. The NCX1 PCR fragment was then subcloned into the pBluescript-NCKX1 plasmid at the Not I and Spe I sites, completing the construction of *pBS-CR*. The CR chimeric mutant was subcloned into pBluescript II, pVL1392, and pRc/CMV as described above for the EX construct.

## OF (and IF)

The next constructs were based on the CR chimera and were designed to test whether the transmembrane regions alone are capable of mediating Na/Ca+K exchange. Once the pBS-CR construct was completed, the cytosolic loop had to be removed. pBS-CR was digested with Avr II and Bsm I, removing the majority of the cytosolic domain. Small duplexes of DNA with overhanging ends corresponding to the overhangs of the Avr II and Bsm I were made by annealing the synthetic oligomers BandidTop and BandidBottom (for

IF) and Rodbandaid1 and Rodbandaid2 (for OF). The fragments for each construct were ligated, resulting in the *pBS-IF* and *pBS-OF* clones. This OF construct was then subcloned into pVL1392, pRc/CMV and pEIA as described for pBS-CR.

## IFC

In an attempt to ascertain whether the regulatory features of the cardiac Na/Ca exchanger could be imposed upon the rod Na/Ca+K exchanger, the NCX1 cytosolic loop, which has been shown to mediate those activities, was inserted into the IF construct. The IF clone contains a Bcl I recognition site in place of the region which coded for the cytosolic loop.

We obtained from Dr. J. Reeves the plasmid *p17m* which contains a bovine cardiac NCX1 clone, in which site-directed mutagenesis has produced a silent mutation which incorporates a Bcl I site to the 5' end of the region coding for the cytosolic domain. This alteration allowed the release of the cytosolic region from NCX1 by restriction digestion with Bcl I. The cytosolic region fragment was ligated into the Bcl I site engineered in the cytosolic region of pBS-IF during its construction. The resulting clone, *pBS-IFC*, was then subcloned into pVL1392, pRc/CMV and pEIA as described for the CR construct.

## CCC

To test whether the rod Na-Ca+K exchanger's regulatory features could be imposed upon the cardiac Na-Ca exchanger, the cytosolic domain of NCX1 was removed and the analogous region of NCKX1 was inserted. To do this, the NCX1 mutant, *p17m*, described above, was digested with Bcl I and the cytosolic fragment gel purified away. The construct was then religated and termed *p17m-c*. The DNA fragment corresponding to the rod

Na/Ca+K exchanger's cytosolic loop was synthesized in a multi-step process. The primers 1-5' and 1-3' were used to amplify the portion of the NCKX1 cytosolic domain from the Bsm I site to the first amino acid of membrane-spanning helix H6. Next, the Xho I - Bsm I fragment of the NCKX1 cytosolic coding region was isolated. Third, a synthetic duplex was created by annealing 3-sense and 3-antisense, to use as a linker. These three fragments were ligated together and, subsequently, into the Bcl I site of p17m-c; the resulting construct was termed *pCCC*. *pCCC* was next subcloned into pRc/CMV and pEIA as described for p17.

### **3.2.2 Construction of Human NCKX1 Derived Clones**

To clone the human NCKX1 exchanger,  $1 \times 10^6$  plaque forming units of a lambda gt10 human retinal cDNA library (gift of Dr. R. McInnes) were screened (Tucker et al, 1998b). The entire bovine rod exchanger cDNA was used as a template to synthesize radiolabeled probe, and of 42 plaques picked, one clone (p27) contained an insert of 579 bases corresponding to the bovine exchanger from amino acid 866 to 1059. The primers Primer2, get5', H1 and H5, derived from this sequence and that of the published bovine NCKX1 sequence (Reiländer et al, 1992) were applied to a less amplified version of the same human retinal library (gift of Dr. J. Nathans). The resulting PCR fragment of approximately 1450 bp was used to synthesize radiolabeled probe with which the newer human retinal library was screened. 48 partial clones were picked and 12 were sequenced with the  $\lambda$ gt10Forw and  $\lambda$ gt10Rev primers to determine the human NCKX1 cDNA sequence. Three of the partial clones were used to put the NCKX1 clone together. To create a full length cDNA, clone 5'10, which starts at position -193 and continues to nucleotide 2797 was ligated at the Aat II site to clone 16, which begins at position 2224 and terminates approximately 1 kb into the 3'

untranslated region (UTR). As no antibody presently exists which is able to detect the human NCKX1 protein, a construct with the FLAG epitope (DYKDDDK) was engineered (Eastman Kodak). The 5'10 clone was ligated at the Aat II site to clone 11, which starts at nucleotide 1104 and ends at 3290. Clone 11 fortuitously extends up to and including the last amino acid codon, but has the termination codon replaced by an Eco RI site. Into this Eco RI site was inserted a FLAG epitope synthetic duplex, which was formed by annealing the oligonucleotides FLAG-TOP and FLAG-BOTTOM. The resulting construct, when transcribed and translated, codes for the human NCKX1 cDNA with a carboxy-terminal FLAG epitope.

To remove the alternately spliced domain from the human NCKX1 cDNA, a three-step approach was required. First, a multiple cloning site was engineered by annealing the oligonucleotides EHApatch1 and EHApatch2 and ligating into pBluescript™. Second, the fragment of human NCKX1 from nucleotides 1442 to 1891 was PCR amplified using the primers JTG-4 and JTG-61. This fragment was cloned into the Ehe I and Hind III sites in the pBluescript-EHApatch multiple cloning site. Third, the fragment of human NCKX1 from nucleotides 2233 to 2978 was PCR amplified and cloned into the Hind III and Aat II sites of the pBluescript-EHApatch multiple cloning site. The resulting ligated fragment was released from pBluescript and cloned into the Ehe I and Aat II sites of the human NCKX1-FLAG cDNA. The resulting construct, verified by sequencing, codes for human NCKX1 protein which has had the alternately spliced region (ie. exons III, IV, V and VI) replaced by a single leucine. In addition, the construct may be immunohistochemically detected using commercial M2 antibodies (Eastman Kodak) directed at the FLAG epitope.

Both the human NCKX1-FLAG cDNA and the human NCKX1-FLAG-deletion cDNA were cloned into pEIA using the Not I and Xba I sites. The resulting plasmids were termed pECH and pHFD, respectively.

### **3.2.3 Construction of RNase Protection Assay (RPA) Probe Templates**

Human NCKX1 RPA probe template had to be PCR amplified from human retinal RNA as no full length cDNA (ie. containing exon III) has been cloned. 1<sup>st</sup> strand DNA synthesized from total human retinal RNA was PCRRed with the primers JTG-27E and JTG-8E and the resulting fragment cloned into the Eco RI site of pBluescript™. Clones were sequenced until one with no errors was found, as even a single base PCR error would lead to inappropriate RNA degradation during the RPA. Riboprobe was synthesized using T<sub>3</sub> polymerase from plasmid linearized with Xho I. The resulting probe was 780 nucleotides in length, including the multiple cloning site sequences at the 5' and 3' ends which together totaled 120 nucleotides. The remnant multiple cloning site sequences are not problematic for the RPA, as they are digested away during the experiment.

The bovine RPA probe template was PCR amplified from the full length cDNA obtained from Dr. H. Reiländer (Reiländer et al, 1992). The PCR fragment amplified with the primers BovB and BovK was cloned into the Bam HI and Kpn I sites of pBluescript and sequenced to ensure 100% fidelity. Riboprobe was synthesized from the T<sub>7</sub> viral promoter, using plasmid linearized with Not I. The resulting probe was 509 nucleotides in length, with 35 of the nucleotides coming from the 5' and 3' residual multiple cloning site sequences.

### **3.3 Cell Culture**

#### **3.3.1 Bacteria**

##### ***Escherichia coli (E. coli) Strains***

*E. coli* strains C600hf1 and Y1090 were used for human retinal library lambda gt10 clone maintenance and screening, respectively. DM1 competent cells (Gibco BRL) are dam<sup>-</sup> dcm<sup>-</sup> for use with the Bcl I methylase sensitive enzyme, while DH5  $\alpha$  bacteria were employed for general plasmid DNA propagation and subcloning.

##### **Bacterial culture**

Most DNA species of interest were kept on plasmids and grown in *E. coli*. Liquid cultures consisted of 50 ml of Luria Broth (LB) shaken overnight in a 37°C incubator. Occasionally, bacteria were grown in NZCYM media under the same conditions (Gibco BRL). For streaking to single colony purity, or in transforming bacteria with plasmids, LB-agar plates were used. For blue-white colony screening with pBluescript II, 100 mM IPTG and 4% X-Gal in dimethyl formamide was employed. 40  $\mu$ l IPTG was mixed with 40  $\mu$ l X-Gal and spread onto 10 cm hardened LB-agar plates and allow to dry.

To prepare competent bacteria, a 5 ml primer culture in LB broth of DM-1 or DH5- $\alpha$  bacterial cells was grown, shaking at 37°C overnight. The primer culture was added to 50 mL LB and grown until an OD 595 of 0.600 was reached, about 3-4 hours. Cells were chilled on ice 5 minutes, then washed twice in 5 ml ice-cold 0.1 M CaCl<sub>2</sub>. The cell pellet was resuspended in 2 ml ice-cold 0.1 M CaCl<sub>2</sub> / 300  $\mu$ l glycerol and aliquoted, frozen in liquid nitrogen and stored at -80°C.

For bacterial cell transformation, 10 - 200 ng of DNA in a volume of 10  $\mu$ l or less was inoculated into 100  $\mu$ l competent bacteria thawed on ice. After 30-45 minute incubation on ice, the cells were heat-shocked at 45°C for 90 seconds then chilled on ice prior to being spread onto LB-agar plates. Plates were inverted and grown overnight in a 37°C incubator and colonies picked the next day.

Plating bacteria for lambda phage were prepared by overnight growth in NZCYM or LB media supplemented with 0.2% maltose, followed the next day by centrifugation at 4000g for 10 minutes and resuspension in 0.01 M  $\text{MgSO}_4$  (Sambrook et al, 1989). To plate lambda phage, 0.1 mL phage diluted in SM was added to 0.1 mL plating bacteria, vortexed briefly and incubated at 37°C for 20 minutes. 3 ml 47°C 0.7% agarose was added, vortexed and the bacterial mixture poured onto 10 cm plates containing 30 ml hardened LB or NZCYM bottom agar. Plates were inverted and incubated at 42°C overnight, at which time plaques were lifted. For screening purposes, circular nylon membranes (Magna) were placed in contact with the agar plate for 1 minute, then denatured, neutralized and rinsed with 2 x SSC (Sambrook et al, 1989). Membranes were air-dried on 3MM paper and baked at 80°C for 2 hours to fix the DNA. Hybridization to radiolabeled probe was carried out as described for Southern analysis. Recombinant plaques were picked with 1 ml pipet tips cut with a razor blade and ejected into 1 ml SM with 50  $\mu$ l chloroform. They were then vortexed and incubated at 4°C overnight to allow the phage to diffuse out of the plug. These stocks were maintained at 4°C as temporary founder stocks until plate lysate stocks were generated.

Approximately 100  $\mu$ l of a 1 ml plug stock was incubated with plating bacteria as described above. Bacteria with adsorbed phage would be mixed with 3.5 ml 47°C top



agarose (0.7%) and poured onto 10 cm plates containing 25 ml hardened NZCYM 1.5% agarose. Following overnight growth at 42°C, 5 ml of lambda diluent (10 mM Tris pH 7.5, 10 mM MgSO<sub>4</sub>) was poured onto the plate and incubated at room temperature with gentle shaking to elute the phage. After 2 hours the lambda diluent was collected and centrifuged at 5000g for 10 minutes and the supernatant maintained at 4°C as a liquid stock.

### **3.3.2 CHO Cells**

A dihydrofolate reductase deficient chinese hamster ovary (CHO) cell line, DG44, was obtained from Dr. Randy Johnston and maintained in a modified Dulbecco's- minimum essential medium (DMEM) containing 10% heat-denatured fetal bovine serum, hypoxanthine / thymidine, 100 U/ml penicillin/ 100 µg/ml streptomycin, and fungizone. Cells were grown at 37°C, 5% CO<sub>2</sub> in T75 or T150 flasks, or in 10 cm plates for transfection procedures. Cells were split approximately 1:6, every three or four days, as necessary. To release CHO cells from their substrate for splitting required washing with PBS/5mM EDTA.

Transfections of CHO were carried out using CaPO<sub>4</sub> methods or Lipofectin type reagents (according to the manufacturer's directions). For CaPO<sub>4</sub> transfections, CHO cells were split onto 10 cm plates one day prior to transfection, so that the cells were 60-80 % confluent on the day of transfection. 1-10 µg DNA was diluted into 880 µl 0.1 X TE (1 mM Tris pH 7.4, 0.1 mM EDTA) then added to 120 µl 2 M CaCl<sub>2</sub> and mixed gently. Cells were rinsed gently twice with serum-free IMDM. The DNA/CaCl<sub>2</sub> mixture was added dropwise to 4 ml IMDM serum-free media. Cell culture media was removed and replaced with the DNA/CaCl<sub>2</sub>/IMDM mixture. After 5 hour incubation at 37°C, the mixture was replaced with IMDM containing 20% glycerol for 45 seconds then rinsed with serum-free IMDM and

replaced with complete culture media. Stable transfections were carried out essentially as with transients, with two important distinctions. First, the pRc/CMV-based plasmid DNA being transfected was linearized at the Xmn I (Asp700 I) site in the ampicillin resistance gene. This was done to prevent plasmid cleavage within the coding region, which can occur during crossover and incorporation into the host genome. Second, on the third day post transfection, the culture cells would be transferred to their normal media now supplemented with 800 ug / ml G-418 (Geneticin). Over the next two to four weeks the cells were subcultured and the dead cells removed, until stable lines, each derived from a single cell representing one insertion point in the genome, were obtained.

### **3.3.3 HEK Cells**

Human embryonic kidney (HEK) 293 cells were obtained from Dr. Wayne Chen and grown in Dulbecco's modified Eagle's Medium (Gibco) supplemented with 10% fetal bovine serum, 2 mM L-glutamine, 1% MEM non-essential amino acids, and 100 U/mL penicillin / 100 µg/mL streptomycin (Gibco). Cells were grown at 37°C, 5% CO<sub>2</sub> on 10 cm plates or in T75 flasks and split every three or four days, approximately 1:6.

For HEK CaPO<sub>4</sub> transfections, cells were split into 10 cm plates one day prior to transfection so that the cells were at 60-80% confluence on the day of the transfection. 10 µg pRc/CMV-based vector DNA was diluted into 450 µl water / 50 µl 2.5 M CaCl<sub>2</sub>. The DNA/CaCl<sub>2</sub> solution was added dropwise to 500 µl 2 X HEPES or BES buffer (280 mM NaCl, 25 mM HEPES or 25 mM BES (pH 7), 1.5 mM Na<sub>2</sub>HPO<sub>4</sub>). After incubation for 5 minutes, this solution was added dropwise to a plate containing HEK cells and 10 ml complete media. Cells were harvested or assayed 2-3 days later. For LipofectAMINE™

transfections, cells were seeded into a six-well (35 mm) plate one day prior to transfection so that they were 60-80% confluent on the day of transfection. In a 14 ml tube, 100  $\mu$ l of serum-free media was added to 1  $\mu$ g DNA. In another 14 ml tube, 100  $\mu$ l serum-free media was added to 10  $\mu$ l LipofectAMINE reagent. The two solutions were mixed gently and incubated at r.t. for 45 minutes. 800  $\mu$ l serum-free media was added and mixed, and the resultant solution poured onto cells that had been rinsed once with serum-free media. After 5 hours, the DNA / LipofectAMINE media was removed and replaced with fresh media containing 10% fetal bovine serum. Cells were assayed 2-3 days later.

#### **3.3.4 SF9/SF21 Cells**

Cells were grown at 27°C in roller bottles or flasks, in TNM-FH media containing 10% fetal bovine serum, yeastolate, and lactalbumin hydrolysate as well as penicillin, streptomycin and fungizone. For transfection of SF9 or SF21 cells, linear AcMNPV DNA was incubated with pVL1392-based plasmid DNA of the construct to be transfected and Insectin Liposomes (Invitrogen) in 5 ml Grace's media. This mixture was added to rinsed 10 cm plates with  $5 \times 10^6$  SF9 cells attached. After 4 hours 5 ml of TNM-FH media was added to the plates, and 48 hours later the media was collected as a viral stock. Dilutions of the stock were used to isolate individual recombinant virus carrying the construct of interest.

To assay plaques for recombinant baculovirus, SF9 or SF21 cells were seeded at  $2 \times 10^6$  cells per 10 cm plates. Diluted viral stocks were added for 1 hour and then overlaid with 1.5% low-melt agarose / TNM-FH equilibrated to 40°C. Plates were inverted and incubated at 27°C for 4-6 days at which time plaques were counted or picked. Recombinant plaques do not contain the occlusion bodies found in wild-type plaques and these were

discriminated from one another using strong side lighting. Individual plaques were picked as an agarose plug using a pipet tip and incubated in 1 ml Graces media. In most cases three rounds of purification were required to isolate pure recombinant viral stocks.

Prior to functional assays, SF9 suspension cultures were infected with previously titered recombinant AcMNPV viral particles at a multiplicity of infection (MOI) of 10. Cells were counted then pelleted by centrifugation at 1000g for 15 minutes. The pellet was resuspended in TNM-FH media at a density of  $10^7$  cells / ml, virus added and the cells incubated at 27°C for 1 hour. The cells were then diluted in TNM-FH media to  $5 \times 10^5$  cells / ml and returned to 150 ml flasks where they were incubated at 27°C for 2 days prior to collection for experimentation.

### **3.3.5 HighFive Cells**

For use of the proprietary pEIA system (Farrell et al 1998), the HighFive *bombyx* cell line was employed. These cells were maintained in IPL-41 media containing 2.6 g/L tryptose phosphate, 0.35 g/L NaHCO<sub>3</sub>, 0.069 mg/L ZnSO<sub>4</sub>•7H<sub>2</sub>O, 7.59 mg/L AlK(SO<sub>4</sub>)•12H<sub>2</sub>O and 10% fetal bovine serum. The pH was adjusted to 6.2 with 10 M NaOH and the osmotic pressure was adjusted to 370 mOsm with 9.0 g/L sucrose. Typically, these cells were grown in T150 or T75 flasks or in 2 L roller bottles at 27°C.

HighFive cells were transfected using Lipofectamine (according to the manufacturer's directions) and required the addition of the helper plasmid pBmA.HmB. This plasmid was used at a molar ratio 1:100 of the cotransfected pEIA-based construct. For selection of stable clones, HygromycinB was added to the media two to three days post transfection and the cells were maintained in the HygromycinB media for two to three weeks.

Generally, the rate of transfection was sufficiently high that HighFive cells grown in six well plates provided enough transfected clones to isolate more single colonies than required. In the case of transient expressions where the construct was to be tested rapidly, a T150 flask provided ample cells to carry out both  $^{45}\text{Ca}$  flux experiments and Western blots.

### **3.4 Functional Assays**

#### **Reverse Exchange**

Measurement of reverse exchange, that is the influx of Ca mediated by the exchanger, takes advantage of the reversibility of both the Na/Ca and Na/Ca+K exchangers. The direction of ion movement is dictated by the electrochemical gradients of Na, Ca and, in the case of NCKX1, K. At normal physiological conditions, free cytosolic Ca is in the 100 - 500 nM range. Preliminary experiments demonstrated that, in the HighFive insect cell expression system, it was difficult or impossible to detect the reduction of Ca below this physiological basement level. To measure forward exchange (Ca extrusion) would therefore require abnormally high initial free cytosolic Ca levels, in the  $\mu\text{M}$  to mM range. Loading HighFive cells with such levels of Ca causes abnormal cellular Ca handling or complete abolishment of responsiveness to external ionic gradient perturbation. As well, the endogenous Ca extrusion mechanism discovered in HighFive cells prevents the meaningful quantification of additional Ca extrusion mediated by an activated Na/Ca (or Na/Ca+K) exchanger.

#### **Na Loading**

Under physiological conditions the Na/Ca+K exchanger couples the strong inward Na gradient to the strong outward K gradient to drive Ca against its gradient and out of the cell. In the heterologous systems employed here, to efficiently promote reverse exchange a

large outwardly directed Na gradient must exist, that is the physiological Na gradient must be completely reversed. This requires the loading of much larger than physiological concentrations of Na into the cell, and Ca influx measurement under low external Na conditions.

Na loading can be accomplished in several ways. Ouabain interferes with the normal operation of the Na/K ATPase, preventing the constitutive Na efflux in exchange for K influx that it mediates. Monensin is an ionophore which permits Na to freely pass back and forth through the plasma membrane. Incubation in a high Na / monensin solution allows the cytosolic Na levels to match the external medium. However, monensin must be removed from the plasma membrane via washing with BSA, prior to switching the external solution to a low Na buffer. Alternatively, passive Na-loading can be accomplished by extended (ie. 2 hour) incubation in a high Na / 0 K buffer, which directly inhibits Na/K ATPase cycling and prevents it from removing from the cytosol that Na which constantly leaks in.

### **Calcium Flux Measurements**

Our lab has employed several protocols for measuring Ca fluxes into or out of the cell. The dynamic cellular changes of free cytoplasmic Ca were measured with Fluo-3, bearing in mind that free cytoplasmic Ca represents perhaps 1% of the cell's total Ca complement. Total cell Ca fluxes were measured using  $^{45}\text{Ca}$ . Reverse mode exchange was measured, with increases in total Ca being calculated from increases in radioactive Ca uptake upon alteration of the cells environmental conditions to those appropriate for reverse exchange. The dual excitation wavelength dye FURA-2 (Tsien et al, 1985) was employed in a single cell digital imaging system. The use of this ratiometric dye eliminated artifacts

that stemmed from unequal dye-loading in individual cells. This technique also allowed us to measure, at the single cell level, free intracellular Ca.

### **Single cell Digital Imaging**

Cells to be assayed were collected from stock flasks by gentle resuspension with a 10 ml pipet and transferred to a 13 mm coverslip in a single well of a 12 well plate. Cells were allowed to settle and attach for 1-2 days. The IPL-41 growth medium was replaced with a Na-medium (150 mM NaCl, 10 mM HEPES, 80 mM sucrose) and the cells loaded passively with Na via incubation for 2 to 3 hours. The Na-medium was then replaced by Na-medium containing 5  $\mu$ M FURA-2 AM. FCCP and thapsigargin were added to the well at a final concentration of 5  $\mu$ M each, and gently mixed. The cells were allowed to load with FURA-2 for 30 minutes at which time they were transferred to a PH3 perfusion chamber (Warner Instruments Corp., Hamden, CT), and a solution of Na/EDTA (150 mM NaCl, 10 mM HEPES, 80 mM Sucrose, 100  $\mu$ M EDTA) perfused over the coverslip. Solution changes were to those media described in Table 2. The solutions to be applied to the cells were pumped via a peristaltic pump (Pharmacia) and heated using a SH-27A in-line heater (Warner Instruments Corp.) (Figure 3.2). The combination of heated solution and heated stand were employed to keep the cells at 32°C. The cells were observed through a Axiovert 135 microscope (Zeiss) with a 20x/0.75 FLUAR objective. A DeltaRam High Speed Illuminator (PTI, Monmouth Junction, NJ) was used to elicit the FURA-2 fluorescence which was captured with an IC-200 camera (PTI). Images were acquired and analyzed under the control of the ImageMaster v1.4 imaging software (PTI). Fura-2 ratios were graphed and coefficients calculated using Microsoft Excel and SigmaPlot software.

**Table 2****Digital Imaging Solution Buffers.**

All solutions are isosmotic for HighFive cells at 390 mM. In addition to the contents shown in the table, all solutions contain 80 mM sucrose and 10 mM HEPES 7.4. Solutions were typically made fresh from stocks on the day of the experiment. Ca contamination of reverse osmosis water used to make the solutions was assumed to be 10  $\mu$ M. Final concentrations of LiCl, NaCl and KCl are given in mM, final concentrations of CaCl<sub>2</sub>, CaHEDTA, HEDTA and EDTA are given in  $\mu$ M. The default K concentration, ie. when [K] is not shown, is 20 mM. The default Ca concentration is 6  $\mu$ M.

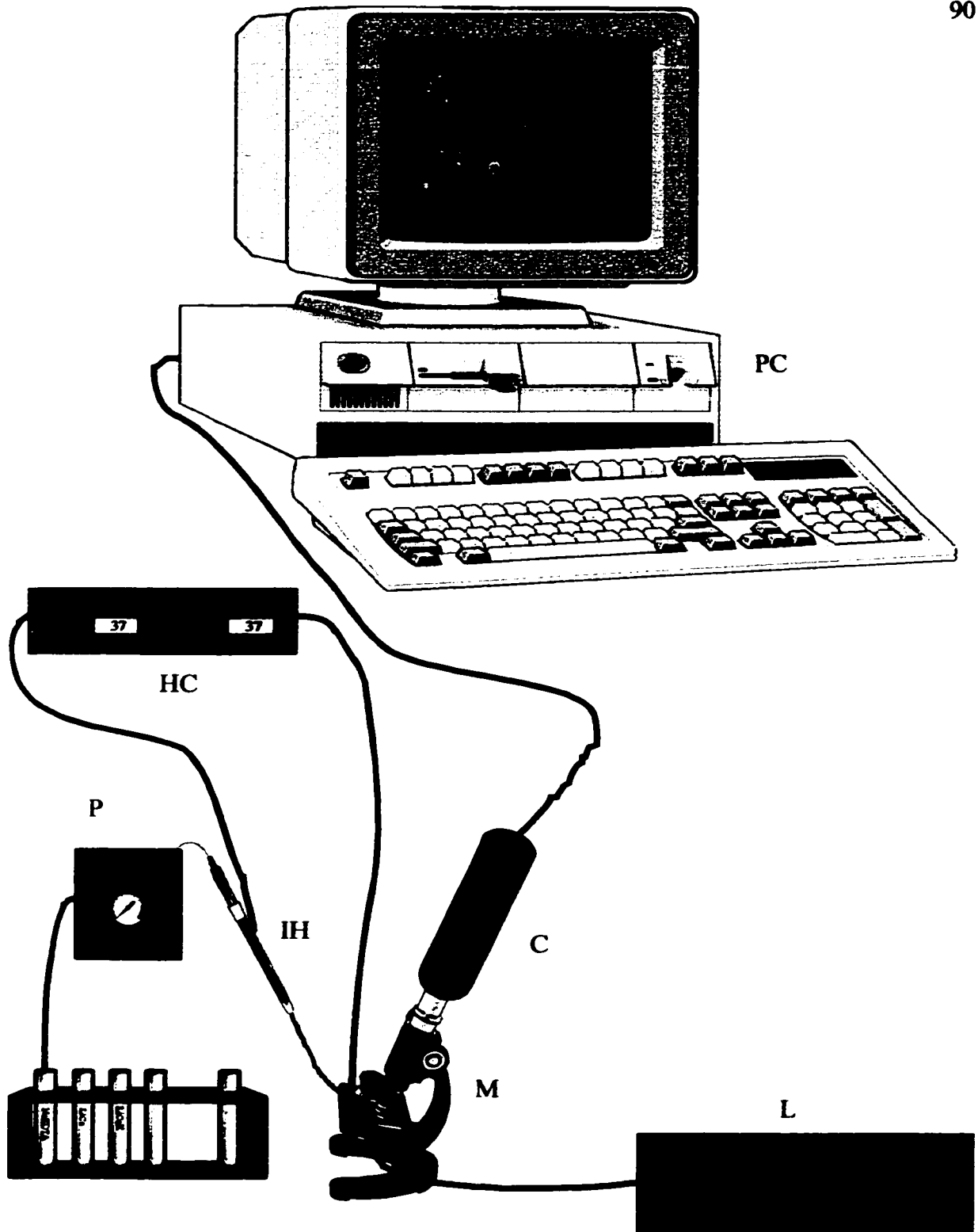


### Digital Imaging Buffers

Solution	LiCl	NaCl	KCl	CaCl <sub>2</sub>	CaHEDTA	HEDTA	EDTA
Na loading	0	150	0	0	0	0	0
Na/EDTA	0	150	0	0	0	0	100
Li/EDTA	150	0	0	0	0	0	100
LiKEDTA	130	0	20	0	0	0	100
LiCa(6)	150	0	0	0	400	100	0
<b>K dependence buffers</b>							
LiCaK(1)	149	0	1	0	400	100	0
LiCaK(2)	148	0	2	0	400	100	0
LiCaK(5)	145	0	5	0	400	100	0
LiCaK(10)	140	0	10	0	400	100	0
LiCaK(20)	130	0	20	0	400	100	0
LiCaK(35)	115	0	35	0	400	100	0
LiCaK(50)	100	0	50	0	400	100	0
<b>Ca dependence buffers</b>							
LiCa(0.5)	150	0	0	0	33	100	0
LiCa(0.5)K	130	0	20	0	33	100	0
LiCa(1)	150	0	0	0	67	100	0
LiCa(1)K	130	0	20	0	67	100	0
LiCa(3)	150	0	0	0	200	100	0
LiCa(3)K	130	0	20	0	200	100	0
LiCa(6)	150	0	0	0	400	100	0
LiCa(6)K	130	0	20	0	400	100	0
LiCa(10)	150	0	0	0	667	100	0
LiCa(10)K	130	0	20	0	667	100	0
LiCa(20)	150	0	0	0	1330	100	0
LiCa(20)K	130	0	20	0	1330	100	0
LiCa(50)	150	0	0	40	0	0	0
LiCa(50)K	130	0	20	40	0	0	0

**Figure 3.2****Digital Imaging Equipment.**

HighFive insect cells were grown on 13 mm round coverslips overnight to ensure sufficient attachment. Coverslips were mounted on a PH3 heated perfusion chamber and secured to the microscope stage. Solutions were delivered to the chamber at about 3 mL / minute by P-1 (Pharmacia) peristaltic pump (*P*), through an SH-27A in-line heater (*IH*). Both the in-line heater and the heated chamber, regulated by a TC-344A Dual Heater Controller (*HC*), were employed to maintain constant temperature at 32°C. The cells were illuminated with a DeltaRam High Speed Illuminator lamp (*L*) and viewed through an Axiovert 135 inverted microscope (*M*). Images were captured with an IC-200 CCD camera (*C*) and then stored and analyzed using ImageMaster v1.4 software on a personal computer (*PC*).



## **CHAPTER FOUR: RESULTS**

#### **4.1 cDNA Cloning of the Human Retinal Rod Na-Ca+K Exchanger; Comparison with a Revised Bovine Sequence**

- Preamble.** Chapter 4.1 has been published (Tucker et al, 1998b). Sequences employed in the generation of Figures 4.1, 4.2, and 4.3 were obtained by various authors. Human retinal rod NCKX1 sequence; J. Tucker, revised partial bovine rod NCKX1 sequence; R. Winkfein and C. Cooper, buffalo retinal rod NCKX1 partial sequence; R. Winkfein and C. Cooper, dolphin retinal NCKX1; C. Cooper.
- Purpose.** To clone the complementary DNA of the human retinal rod Na-Ca+K exchanger.
- Methods.** A human retinal cDNA library was screened initially with a radiolabeled probe representing the entire bovine rod Na-Ca+K exchanger cDNA and subsequently with probes from polymerase chain reaction fragments of the human retinal rod Na-Ca+K exchanger obtained after the initial screen. Twelve positive clones were used to obtain the entire coding sequence of the human retinal rod Na-Ca+K exchanger.
- Results.** The cDNA of the human retinal rod Na-Ca+K exchanger codes for a protein of 1081 amino acids, which shows 64.3% overall identity with the bovine retinal rod Na-Ca+K exchanger at the amino acid level. The two sets of putative transmembrane-spanning domains and their short connection loops showed the highest degree of identity (94%-95%), whereas the extracellular

loop at the N-terminus showed a 59% identity. The large cytosolic loop that bisects the two sets of transmembrane-spanning domains contained two large deletions in the human exchangers, the first deletion contains 18 amino acids, whereas the second deletion involved a series of repeats that are dominated by acidic amino acid residues observed in the bovine, but not in the human sequence. The authors observed that the bovine sequence contains a ninth repeat in addition to the eight repeats of the published sequence.

**Conclusions.** The authors cloned the cDNA of the human retinal rod Na-Ca+K exchanger as a first step in examining the possibility that this gene could be the locus of disease causing mutations.

The outer segment of a retinal rod outer segment (ROS) is a specialized organelle that contains the entire molecular machinery for visual transduction. In darkness, a significant percentage of the inward current using the light-regulated and cyclic guanosine monophosphate (cGMP) - gated channels is carried by Ca ions. The Na-Ca+K exchanger is a specialized protein in ROS that removes calcium from the cytosol and mediates a rapid light-induced lowering of cytosolic-free calcium that is responsible for the process of light adaptation (for a review on the role of calcium in the physiology of retinal photoreceptors, see (Kaupp and Koch, 1992)). The Na-Ca+K exchanger uses the inward sodium gradient and the outward potassium gradient to remove calcium from the cytosol (Cervetto et al, 1989; Schnetkamp et al, 1989; Schnetkamp, 1989) . The Na-Ca+K exchanger is functionally related to the Na-Ca exchangers, which only use the inward sodium gradient for calcium

extrusion (for a comprehensive series of reviews on Na-Ca(+K) exchangers, see (Hilgemann et al, 1996). To date, the Na-Ca+K exchanger has been cloned from bovine retinal rods (Reiländer et al, 1992), whereas three mammalian Na-Ca exchanger complementary deoxyribonucleic acid (cDNA) clones (NCX1 to 3) have been reported that share a 65% to 75% identity with each other at the amino acid level (Nicoll et al, 1996a; Zhaoping et al, 1994; Nicoll et al, 1990). The bovine ROS Na-Ca+K exchanger (NCKX) has been shown to have limited (<4%) sequence identity with the NCX Na-Ca exchanger clones (Reiländer et al, 1992). Despite the limited sequence identity, a similar membrane topology has been proposed for both the NCKX and the NCX genes (Reiländer et al, 1992; Nicoll et al, 1990). Here, we report cloning and sequencing of the cDNA of the human ROS Na-Ca+K exchanger. Sequence comparison between human and bovine NCKX sequences revealed considerable divergence, particularly in the repeat area observed in the large cytosolic loop of the bovine ROS NCKX cDNA. We compared this part of the bovine and human sequences with sequences obtained from buffalo and dolphin, and, in the process, we determined that the bovine rod NCKX gene contains nine repeats rather than the eight repeats reported by Reiländer et al. (Reiländer et al, 1992).

## **Experimental Procedures**

### **Screening and Sequencing of the Human Retinal Na-Ca+K Exchanger Clones**

To clone the human exchanger,  $1 \times 10^6$  plaque-forming units of a lambda gt10 human retinal cDNA library (gift of J. Nathans) were screened. The entire bovine rod-exchanger cDNA was used to make a radiolabeled probe for screening. Initially, one clone was sequenced and was shown to contain an insert of 579 bases corresponding to the bovine

exchanger amino acids 866-1059. From this sequence, two oligonucleotides were synthesized for use as antisense primers in polymerase chain reactions (PCRs), 5' A G G C C A G T C C A G G G A C A G A G G 3' and 5'TTGGTACCAAGGTGAAAACAAAAA ACTTCCTA3'. Additionally, two degenerate oligonucleotides, for use as sense primer, were synthesized from the published bovine Na-Ca+K exchanger sequences, (Reiländer et al, 1992) 5'CA[GT]AT[CTA]TT[TC]GG[ACGT]ATGATGTA[TC]GT3' and 5'TT[TC]AC[ACGT]ATGAA[AG]TGGA[CT]CA[AG]CA3'. PCR amplification of the library with the above primers produced a fragment of approximately 1450 bp, which was used to make a radiolabeled probe. Screening of the human retinal cDNA library produced 48 positive plaques. Twelve clones were isolated (none of which was full length) and were used to sequence the entire coding region, with each region sequenced at least twice from distinct clones. Inserts from each of the 12 isolated exchanger clones were amplified directly from lambda clones using standard lambda gt10 forward and reverse primers and were sequenced with those same primers. Further primers were based on the sequence thus obtained. Sequences were determined by standard automated (ABI 373A, Applied Biosystems, Foster City, CA) and manual (dsDNA Cycle, BRL, Burlington, Ontario) sequencing protocols.

#### **Construction and Sequencing of Buffalo and Bovine Retinal Na-Ca+K Exchanger cDNA**

Bovine and buffalo retinas were dissected from freshly obtained eyeballs and were frozen at -75°C for future use. Total RNA was isolated from frozen retinas with Trizol



Reagent (Gibco/BRL, Burlington, Ontario, Canada) according to the manufacturer's instructions. Poly A<sup>+</sup> RNA was isolated on New England Biolabs oligo(dT) cellulose spin columns (Mississauga, Ontario, Canada) according to the manufacturer's instructions. The forward primers, 5'CAGACGTCAAGGGAGATCAGGAGG3' and 5'CCATCCACACCTTCCTCGTCATC3', and the reverse primers, 5'CCNTC(T/C)TG(G/A)TGNGCACCA3' and 5'TCCCGGCAGAAAGGAGAGGAGATG3', were synthesized to flank the cytosolic region of the exchanger, based on the published bovine NCKX sequence. Single-stranded cDNAs were generated by using reverse transcription (Superscript II, Gibco/BRL) with the use of random hexamer primers according to the manufacturer's instruction. Using the above primers, PCR fragments from our buffalo and bovine cDNA clones, as well as from a previously cloned bovine cDNA (Reiländer et al, 1992), were synthesized, isolated, and used for generating overlapping nucleotide sequences from part of the cytosolic loop that includes the repeat region. Sequences were confirmed by correlating Alu I restriction maps with the number of nucleotides between Alu I sites read on the sequences obtained.

## **Results**

### **Cloning the Human Retinal Rod Na-Ca+K Exchanger**

We screened a human retinal cDNA library for clones that showed homology with the bovine retinal rod Na-Ca+K exchanger cDNA and from which the entire coding sequence was obtained. In all cases, overlapping sequences between different cDNA clones apparently represented a single cDNA species. The deduced amino acid sequence of the human rod Na-Ca+K exchanger resulted in a protein of 1081 amino acids, 135 amino acids shorter than our

revised sequence of the bovine rod Na-Ca+K exchanger. The comparison of the deduced amino acid sequence of the human Na-Ca+K exchanger as revised by us (see below) is illustrated in Figure 4.1. Sequence comparison suggests an identical topology for both exchangers, with four distinct domains within the entire Na-Ca+K exchanger sequence (Figure 4.2), and yields an overall identity of 64.3% at the amino acid level between the bovine and human rod Na-Ca+K exchangers. The greatest degree of identity is observed between the two sets of putative transmembrane-spanning domains and their short connecting loops: 94% for H1 through H5, and 95% for H6 through H11. Identity or, in one case, a conservative substitution was observed for all charged residues within the putative transmembrane-spanning domains. The extracellular loop was poorly conserved, with only 59% overall identity, although the length was similar in both sequences (the major exception is a six amino acid insertion observed in the human sequence after residue 423). H0 as well as the sequence around the proposed cleavage site at D66 were relatively well conserved. The native bovine Na-Ca+K exchanger is heavily glycosylated (Reid et al, 1990), and the extracellular loop of the bovine exchanger contains six possible glycosylation sites. Of the six glycosylation sites, two are conserved in the human rod exchanger (at positions 129 and 290, respectively) and four are lost, whereas one new site is observed (at residue 347). Finally, the large cytosolic loop between the transmembrane-spanning domains H5 and H6 shows only 45% identity between the human and bovine sequences, in part caused by two deletions. First, at amino acid 629 in the human exchanger sequence, a drop out of 18 amino acids was observed (as obtained from two separate clones). Second, the bovine exchanger sequence contains several repeats of a 17-amino acid motif that was not observed in the

**Figure 4.1****Amino Acid Sequence Comparison.**

Comparison between the deduced amino acid sequences of the human and bovine retinal rod Na-Ca+K exchangers. This is the revised sequence of the bovine cDNA that we obtained (see text and Figure 4.3). *Black-shaded* residues indicate identity, whereas *gray-shaded* residues indicate conservative substitutions.

## Start to H1

Human	1	[REDACTED] F W L R T [REDACTED] H R R S [REDACTED] H Q
Bovine	1	[REDACTED] A R S W F [REDACTED] Y T S Q F [REDACTED] Q H
Human	61	[REDACTED] S E [REDACTED] S E P [REDACTED] G G K M L V [REDACTED] M S E A T L S T V E I [REDACTED] R K
Bovine	61	[REDACTED] N K [REDACTED] E T S [REDACTED] E V E A W A E [REDACTED] A R G T P P G A R K T [REDACTED] T G S
Human	121	[REDACTED] I T T K [REDACTED] A A E R [REDACTED] F S R T T Y S S S Q K K [REDACTED] P P [REDACTED] Y S
Bovine	121	[REDACTED] T A I P [REDACTED] E T N G M T A E G V N H [REDACTED] Q [REDACTED] P N S R L A [REDACTED] S R
Human	179	[REDACTED] M E K V [REDACTED] R G M F [REDACTED] E T [REDACTED] S T Y E S L
Bovine	178	[REDACTED] S G K E E [REDACTED] L N A L [REDACTED] P R [REDACTED] R M K A P S
Human	238	[REDACTED] S [REDACTED] T F S [REDACTED] T H [REDACTED] A N V [REDACTED] S [REDACTED] N N F F [REDACTED] A H P W
Bovine	238	[REDACTED] K [REDACTED] P [REDACTED] T N [REDACTED] L S [REDACTED] T D T [REDACTED] N [REDACTED] K T T [REDACTED] T N H Q
Human	298	[REDACTED] S P K [REDACTED] T [REDACTED] P T [REDACTED] G A [REDACTED] F A S [REDACTED] S [REDACTED] V S A
Bovine	298	[REDACTED] N L T [REDACTED] E A M [REDACTED] R [REDACTED] T [REDACTED] S D K [REDACTED] L A P I
Human	358	[REDACTED] T A P I V W R [REDACTED] T [REDACTED] S T T [REDACTED] K L [REDACTED] K T A M L T [REDACTED] L
Bovine	358	[REDACTED] I S S T F R G L N [REDACTED] P A A R [REDACTED] N F [REDACTED] E A V A P A [REDACTED] A
Human	418	E E L [REDACTED] P S V L P P S L [REDACTED] H [REDACTED] P [REDACTED]
Bovine	418	G I P [REDACTED] ----- G Q [REDACTED] Y [REDACTED] R [REDACTED]

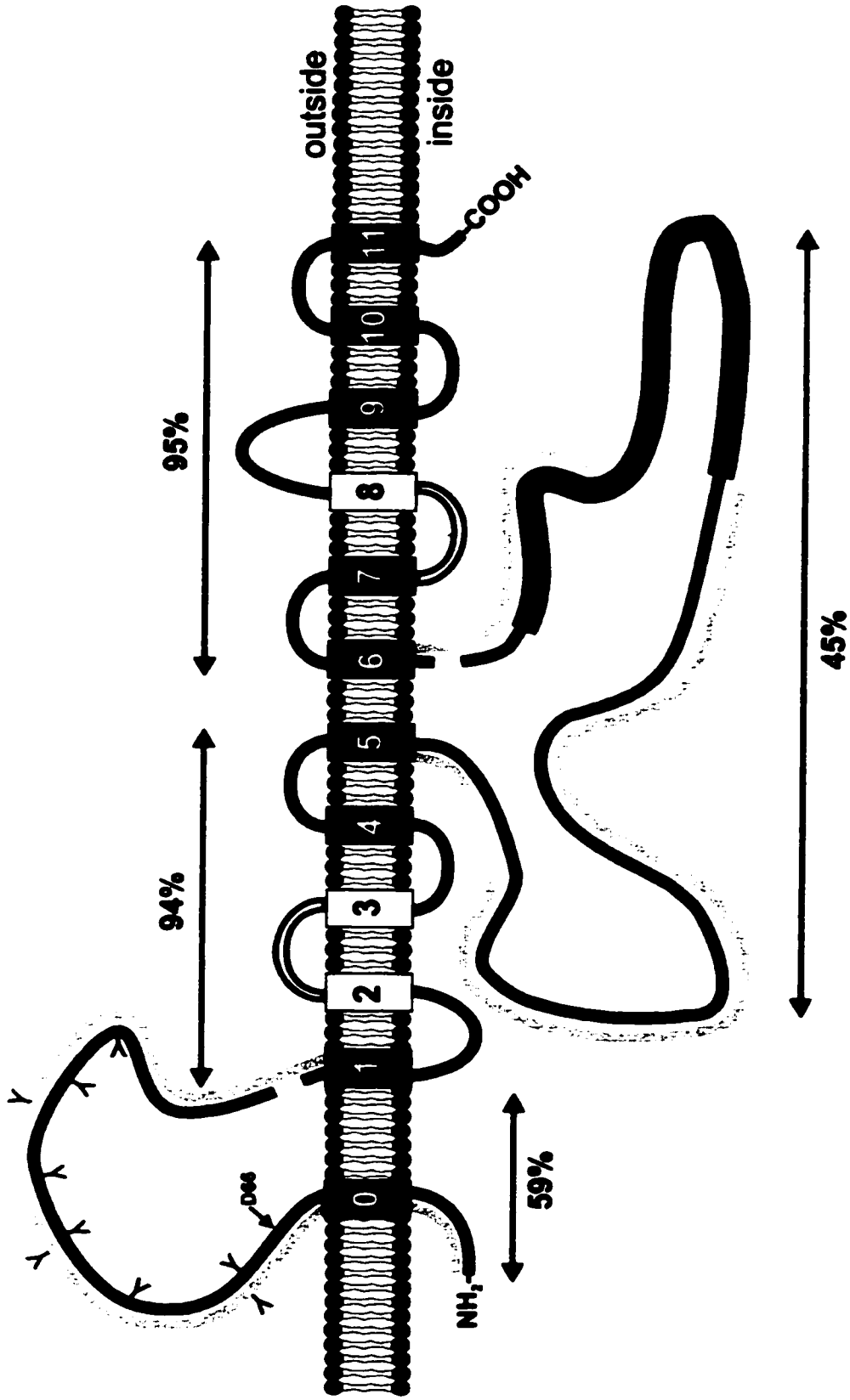
## H1 through H5

Human	454	[REDACTED]
Bovine	448	[REDACTED]
Human	478	[REDACTED]
Bovine	472	[REDACTED]
Human	538	[REDACTED] S [REDACTED] L [REDACTED]
Bovine	532	[REDACTED] A [REDACTED] F [REDACTED]
Human	598	[REDACTED] K H [REDACTED]
Bovine	592	[REDACTED] Q Q [REDACTED]



**Figure 4.2****The Bovine-Human Rod Na-Ca+K Exchanger.**

Diagram of the putative topology of the bovine (*black*) and human (*gray*) rod outer segment (ROS) Na-Ca+K exchangers. Possible glycosylation sites (*Y*) are indicated only in the extracellular loop. D66 represents the N terminus of the exchanger purified from bovine ROS. For cases in which one of the two sequences shows a deletion about the other, gaps are shown. The *open boxes* of transmembrane-spanning domains 2, 3, and 8 with their connecting loops (2-3, 7-8) represent the only areas with sequence similarity to the NCX1 clones. The *thickened portion* of the bovine cytosolic loop marks the position of the repeats dominated by acidic amino acid residues. Percentages indicate sequence identity in the respective domains.



human sequence (obtained from three separate clones; see also below and Figure 4.3). Both the human and the bovine rod Na-Ca+K exchangers have a long stretch of approximately 30 glutamic acid residues immediately adjacent to H6. In this case, the bovine sequence (at residue 1009) shows a dropout of seven amino acids compared to the human sequence.

### **Partial Cloning and Sequencing of Bovine and Buffalo Na-Ca+K Exchanger cDNA Clones**

Unlike the NCX cDNAs, the rod Na-Ca+K exchanger seems to have at least two large, poorly conserved domains, and we were particularly intrigued about the presence (bovine) or absence (human) of a series of repeats of a stretch of mostly acidic amino acids located in the putative large cytosolic loop. To address the issue of these repeats in more detail, we obtained a partial sequence from a buffalo retinal rod Na-Ca+K exchanger clone, and we examined the same stretch in the sequence of the bottle-nosed dolphin (*Tursiops*) retinal rod Na-Ca+K exchanger that we had cloned in our laboratory. The buffalo sequence was obtained from PCR fragments isolated by using primers that flank the area of interest on first-strand cDNA synthesized from buffalo retinal poly A<sup>+</sup> RNA. In this experiment, we ran, as a control, the same PCR fragment obtained from bovine retinal poly A<sup>+</sup> RNA, and we noted a significant difference in size between the bovine and buffalo sequences measuring approximately 100 nucleotides. The buffalo fragment was sequenced, and it was discovered to be 51 nucleotides shorter when compared with the published bovine sequence (Reiländer et al, 1992). Hence, we obtained the same PCR fragment using the published bovine rod Na-Ca+K exchanger clone as a template. The fragment proved to be identical in size to that fragment isolated from our bovine cDNA (synthesized from poly A<sup>+</sup> RNA), suggesting a

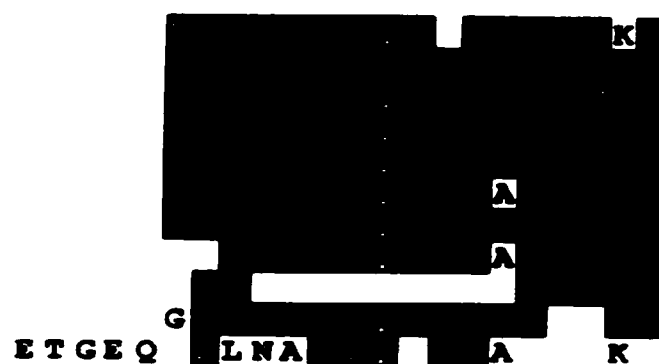


**Figure 4.3**

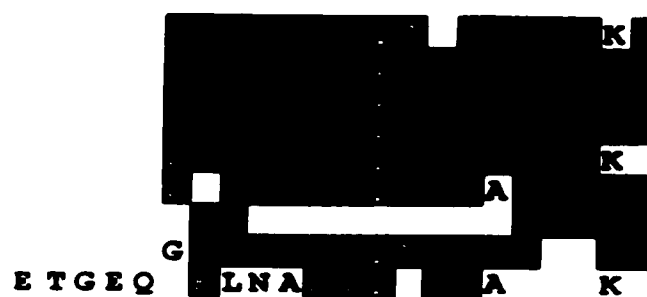
**Alignment of Acidic Repeats.**

Alignment of the repeats consisting of mostly acidic amino acid residues and observed most extensively in the bovine and buffalo sequences.

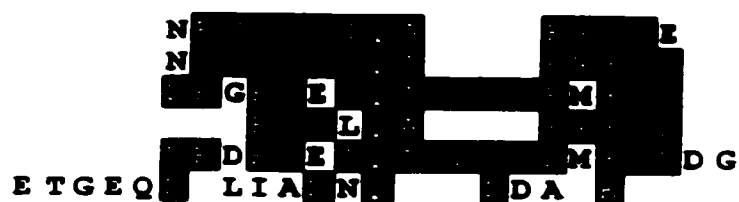
## BOVINE



## BUFFALO



## DOLPHIN



## HUMAN



discrepancy between the published cDNA sequence and the actual sequence of the bovine Na-Ca+K exchanger clones. Sequencing of the PCR fragments showed that the bovine sequence contains a glycine as residue 857 rather than the alanine residue in the published sequence and that it contains an additional full repeat. Thus, the cDNA of the bovine exchanger codes for 9 rather than 8 of the 17 amino acid repeats, resulting in an insert of DEDEGEIQAGEGGEVEG between residues 862 and 863 of the published sequence (Reiländer et al, 1992).

Figure 4.3 illustrates for the different species the alignment of the sequences that corresponds to the area of the acidic repeats found in the bovine sequence. The buffalo sequence showed that two repeats were deleted (as indicated here by the removal of repeats 6 and 7), and that, in addition, just a few individual amino acids were changed or deleted. Comparing the dolphin sequence with the bovine sequence showed that not a single one of the bovine repeats was observed in its entirety, although the EGE/DIQA motif was observed five times with only one substitution (L replaces I). Finally, no clear repeats were observed in the human sequence and not a single IQA motif was observed.

## **Discussion**

In this study, we present the cloning and sequencing of the cDNA of the human retinal rod Na-Ca+K exchanger. When comparing the human sequence obtained by us with the published sequence of the bovine rod Na-Ca+K exchanger (Reiländer et al, 1992), the most striking observation is of the poor conservation of the two large domains, which are thought not to be imbedded in the membrane, as judged by hydropathy analysis (Figures 4.1 and 4.2 ). This is in contrast to other sodium-coupled transporters, such as the NCX1 Na-Ca

exchanger, the NHE1 Na-H exchanger, or the  $\alpha$  subunit of the Na-K ATPase, for which greater than 95% identity has been observed at the amino acid level between clones from different mammalian species, both in putative transmembrane sequences or in putative cytosolic domains (the rod Na-Ca+K exchanger is unusual in that it possesses a large extracellular domain). Because a significant component of the low degree of identity was caused by a series of deletions or insertions, we were concerned that this might reflect artificial deletions or insertions in the cDNA clones in the retinal cDNA library. We have now verified the cDNA sequence with the genomic sequence we obtained while examining the genomic organization of the Na-Ca+K exchanger gene, and we confirmed that the cDNA sequence is correct.

Rods and cones in the retina express in most cases genetically related but different genes for outer segment proteins that are involved in phototransduction - that is, rods and cones express distinct gene products for the cGMP-gated channel (Bonigk et al, 1993). We do not think we obtained a cone Na-Ca+K exchanger because retinal rods greatly outnumber cones in most mammalian retinas, including those of humans and cows; hence, transcripts of rod proteins are expected to greatly outnumber transcripts originating from cones. Moreover, all 12 clones obtained and analyzed from the human retinal cDNA library seem to reflect a single cDNA species because overlapping sequences were identical in all cases. Because we used probes for screening that were based on the bovine rod Na-Ca+K exchanger, we consider it unlikely that we picked up human clones only of the cone exchanger and not of the rod exchanger.

### **Analysis of an Acidic Repeat Region in the Large Cytosolic Loop**

A peculiar example of the variability of domains in the rod Na-Ca+K exchanger sequence was obtained by analyzing the sequence of an acidic amino acid repeat motif observed in the bovine sequence and by comparing it with partial sequence from the dolphin and buffalo. Figure 4.3 illustrates that the acidic repeat sequence observed in the bovine clone is localized to a part of the sequence that is highly variable across species. Significant changes were already observed when comparing close relatives, such as the bovine and buffalo sequences, whereas most of the repeat sequence disappeared when we compared the bovine to the dolphin sequence (cetaceans are close relatives of hoofed animals), although some repeats of part of the IQA motif can still be observed. The human Na-Ca+K sequence did not show much evidence for any repeats and does not contain a single IQA motif.

### **A Revised Sequence for the Bovine Rod Na-Ca+K Exchanger**

When we analyzed PCR fragments of the repeat area from both buffalo and bovine cDNA, it seemed that the difference in size between the bovine and buffalo fragments was larger than predicted from a sequence comparison. We sequenced the bovine repeat area both from our own cDNA and from that obtained from Dr. Reiländer, and we discovered an additional ninth repeat that was missed in the original study on cloning and sequencing of the bovine retinal rod Na-Ca+K exchanger (Reiländer et al, 1992). The fidelity of the repeats in the bovine sequence combined with the lack of conservation of this repeat motif in other mammalian species suggests that the repeats observed in the bovine and buffalo sequences arose recently and have not had time to diverge. Poorly conserved acidic repeat motifs have also been observed in the large  $\beta$  subunit of the rod cGMP-gated channel, which contains a

large acidic domain in the N-terminal part of the sequence localized in the cytosol. The bovine sequence contains at least four repeats of the sequence EEGREKEEEG that are not observed in the human  $\beta$  subunit of the rod cGMP-gated channel (Colville and Molday, 1996), similar to the deletions of the bovine acidic repeats in the human sequences of the rod Na-Ca+K exchanger. The significance of the acidic stretches in the  $\beta$  subunit of both the cGMP-gated channel and the Na-Ca+K exchanger remains to be established, and why the repeats are observed in both bovine genes but not in the respective human genes must be clarified. Figure 4.3 suggests that few conservation constraints exist in this region of the protein sequence, as manifested by the rapid evolutionary divergence.

## 4.2 Chromosomal localization and genomic organization of the human retinal rod Na-Ca+K exchanger

- Preamble** Chapter 4.2 has been published (Tucker et al, 1998a). The FISH results illustrated in Figure 4.5 were performed by S. Murthy and D. Demetrick. Radiation hybrid screening was carried out by J. Friedman and M. Walter.
- Abstract** The retinal rod Na-Ca+K exchanger is a unique calcium extrusion protein found only in the outer segments of retinal rod photoreceptors. Rod Na-Ca+K exchanger cDNA (NCKX1) has been cloned from bovine and human retinas. Here, we have used fluorescent in situ hybridization and radiation hybrid mapping to localize the human NCKX1 gene to chromosome 15q22. We have determined the genomic organization of human rod NCKX1 and found one intron in the 5' untranslated region and eight introns within the coding region.

### Introduction

The retinal rod Na-Ca+K exchanger uses both the inward sodium gradient and the outward potassium gradient to extrude calcium that enters the outer segments of rod photoreceptors via light-sensitive and cGMP-gated channels (Schnetkamp et al, 1989). The retinal rod Na-Ca+K exchanger cDNA (NCKX) has been cloned from bovine (Reiländer et al, 1992) and human (Tucker et al, 1998b) retina and shows little sequence similarity with other proteins, including the functionally related family of NCX Na-Ca exchangers. Recently, a second NCKX2 cDNA has been cloned from rat brain and shown to have a wide

distribution in various regions of the brain (Tsoi et al, 1998). Sequence similarity between the two NCKX cDNAs is limited to the two sets of putative transmembrane domains.

Inhibition of the Na-Ca+K exchanger by replacing extracellular sodium by other cations results in a rapid abolition of the light-sensitive current (Yau and Nakatani, 1984b), and, hence, mutations that lead to impairment of the exchanger are expected to have significant consequences for vision. Retinitis pigmentosa (RP) is a heterogeneous group of inherited human diseases in which retinal degeneration leads to visual loss and eventually to blindness. Many disease-causing mutations have been identified as resulting in RP, and these mutations are mostly localized to genes coding for rod outer segment proteins (for a review, see (Dryja and Li, 1995)). However, many more RP loci and/or the responsible gene products have yet to be identified. We have recently cloned and sequenced the cDNA of the human retinal rod Na-Ca+K exchanger ((Tucker et al, 1998b); GenBank accession no. AF026132). Here, we report the structure of the human rod NCKX1 gene and its chromosomal localization.

### **Materials and methods**

To obtain the genomic organization and chromosomal localization of the human NCKX gene, a 1.5-kb fragment of the cDNA (nucleotides 152-1760) was amplified by the polymerase chain reaction (PCR) and purified. The above PCR fragment was provided to Dr. Lap-Chee Tsui who generously screened a P1-derived artificial chromosome (PAC) library and returned to us two distinct PAC constructs, viz., 136E11 and 25H12. PAC constructs consist of a 17-kb kanamycin-selectable vector containing an insert of 100-200 kb human genomic DNA (Ioannou et al, 1994) . Constructs 136E11 and 25H12 were analyzed via



restriction endonuclease digestion and agarose gel electrophoresis and found to display similar fragment banding pattern, suggesting that the two PAC constructs contain two overlapping genomic fragments. Clone 136E11 was further characterized by restriction digestion and Southern analysis. Probes from both the 5' and 3' regions of the cDNA hybridized to fragments of the PAC, indicating that it contained the entire human rod NCKX gene. PCR was used initially to amplify the 5' end of the gene, and the fragment from nucleotides 152-773 was sequenced entirely and found to be identical to the cDNA. Further characterization of 136E11 via PCR and sequence analysis demonstrated that the entire coding region of the human NCKX1 was contained within the PAC.

In order to ensure that the entire human NCKX1 gene was contained in PAC 136E11, the sequence of the hNCKX1 transcript was elucidated from the transcription initiation site through to the poly A tail and compared with the PAC sequences and PCR products. The 5' UTR was deduced via 5' rapid amplification of cDNA ends (RACE) PCR analysis; its 287-bp length was confirmed by primer extension, and the sequence was confirmed by resequencing directly from the PAC. The polyadenylation signal (AAUAAA) was found 1754-bp downstream of the stop codon, and 33bp upstream of the poly A tail. The full length transcript is therefore 5374 bp in length prior to addition of the poly A tail, which agrees with Northern blot analysis of human retinal poly A<sup>+</sup> RNA. An alternate polyadenylation signal, the product of which was identified by 3' RACE PCR, was found 906 bp downstream of the stop codon.

For fluorescent in situ hybridization (FISH), the entire PAC 136E11 was labeled with digoxigenin-dUTP, and Cy3 was used as a secondary stain. The metaphase preparations

were made following established methods on methotrexate/thymidine-synchronized phytohemagglutinin-stimulated normal peripheral blood lymphocytes (Demetrick 1995). To reduce the background, suppression for 30 min with a mixture of sonicated human DNA (Sigma) and human COT-1 DNA (Gibco/BRL) was employed. The Cy3-stained slides were counterstained with 4'-6-diamino-2-phenylindole (DAPI) and actinomycin D (for a DA-DAPI banding pattern), mounted in antifade medium, and visualized utilizing a Zeiss Axioplan 2 microscope. Approximately 50 metaphase spreads were examined for probe localization. Images of representative mitoses were captured by using a cooled charge-coupled device camera (Photometrics PXL 1400). Digital alignment of the images from each fluorescent marker was performed after registration calibration through a triple bandpass filter (fluorescein isothiocyanate/Texas Red/DAPI) to minimize registration error, by utilizing commercial software (Electronic Photography v1.4, Biological Detection, Pittsburgh, Pa.).

Human NCKX1 primers were also used to screen the Genebridge 4 radiation hybrid panel (Research Genetics). Sense primer ST1 (TTACTACACCTCAACTTCAAGCAG) and antisense primer Back (AGTTGGGGTGCTATCAAACATTCC) amplified a 318-bp fragment. PCRs were carried out under the following conditions: 94°C for 8 min, 30 cycles of 94°C for 30 s, 62°C for 30 s, and 68°C for 30 s, followed by an extension at 72°C for 7 min. The PCR products from all 93 radiation hybrid cell lines, HFL121 (human positive control), and A23 (hamster negative control) were separated on agarose gels and scored as positive, negative, or ambiguous. The results were electronically submitted to the Whitehead Institute for Biomedical Research to be analyzed.

## Results and discussion

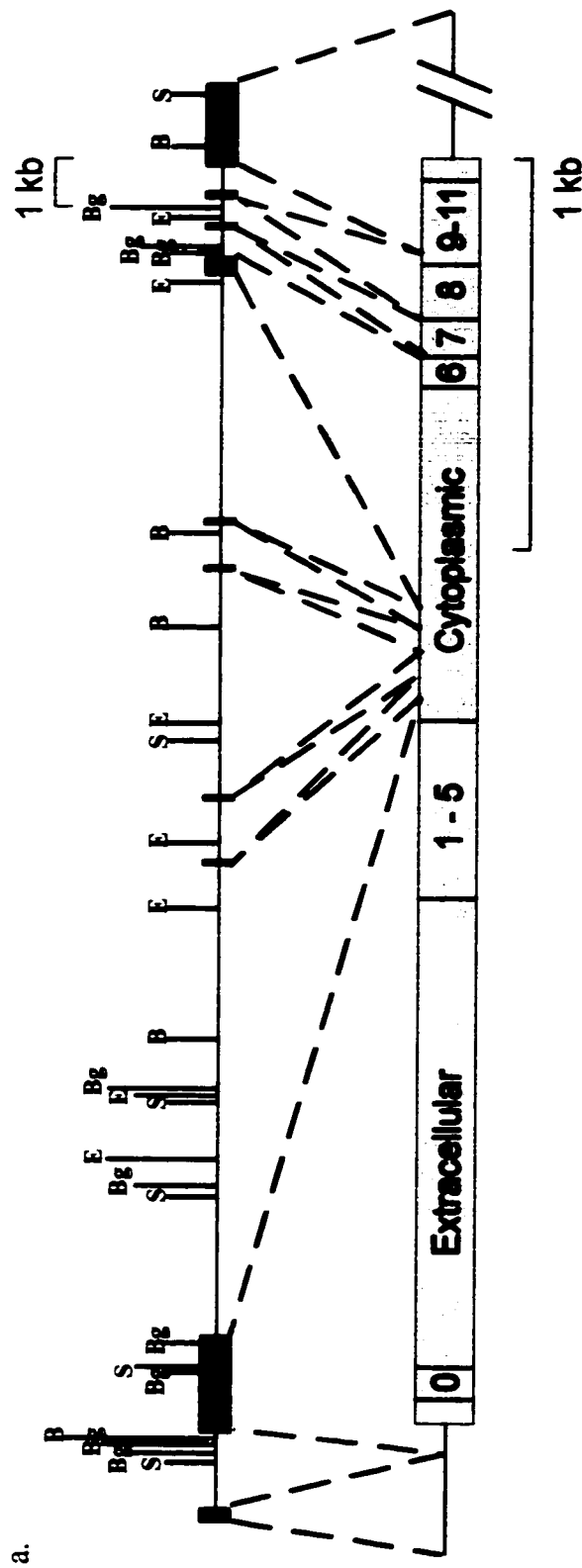
The genomic organization of the human NCKX1 gene was characterized from PAC 136E11. Primers were synthesized from the cloned cDNA sequence and used to amplify gene fragments via PCR. These fragments were then sequenced with standard manual sequencing protocols (Thermosequenase; Amersham, Oakville, Ontario). The sizes of observed introns were estimated by PCR amplification and agarose gel analysis. Restriction digestion of the PCR-amplified gene fragments allowed the construction of a genomic map (Figure 4.4a). One intron was identified in the 5' untranslated region, and eight introns were identified within the coding region of the human rod NCKX1 gene. All introns adhered to the 5'GU and 3' AG requirement the nucleotide sequences of the intron/exon junctions are shown in Figure 4.4b. Intronic sequences of human NCKX1 have been submitted to GenBank under accession numbers AF076932-AF076949. Southern analysis of agarose-gel-separated PAX 136E11 restriction fragments was performed by using four different probes from human NCKX1 sequences. The four probes encompassed, respectively, bases -171 to 1560 (Probe I), 2103 to 3211 (Probe II), 3028 to 3273 (Probe III), and 2779 to 3597 (Probe IV). All results confirmed the genomic map (data not shown).

The genomic sequence was found to be identical to our previously reported cDNA sequence obtained from lambda gt10 clones, with one exception. The human cDNA clones did not contain exon III (Figure 4.4a). The presence of exon III was suggested by a comparison between the published human and bovine NCKX1 cDNAs. Reverse transcription/PCR analysis of human retinal RNA revealed a splice variant of NCKX1 containing this exon; this was not found in our original lambda cDNA clones. Recently,

**Figure 4.4****Genomic Organization of Human Rod NCKX1 Gene.**

**a.** Genomic organization and intron-exon boundaries of the human rod NCKX1 gene. *Black bars* Exons, *B Bam*HI, *Bg Bgl*II, *E Eco*RI, *S Sca*I, *dashed lines* regions of the transcript encoded by genomic sequences. Putative polypeptide domains encoded for by the mRNA are as indicated.

**b.** The 10 bases flanking the junctions of introns 1-9 are shown. Introns 1-9 are estimated to be 1700, 12000, 1300, 4900, 900, 4165, 705, 700, and 865 bp in length, respectively. They are inserted at positions -127 of the 5' untranslated region and 1891, 1945, 2054, 2141, 2233, 2794, 2884, and 3051 of the coding sequence, respectively. The length of the complete transcript before addition of the poly A<sup>+</sup> tail is 5374 bp.



b.

Exon	Exon size	5' Exon/Intron Junction	Intron size	3' Intron/Exon Junction
I	161 bp	A GGT CTG AAG <sub>17</sub> gtaaatgagt	1.7 kb	accacacatagG <sub>12</sub> GT TGT GGA T
II	2016 bp	C CTC AGC AAG <sub>180</sub> gtaaaggaacaa	12 kb	cgttttgcagC <sub>1891</sub> CG GGC GAT G
III	54 bp	G AAG CTG AAG <sub>194</sub> gttgggtgccg	1.3 kb	tcctgcicagC <sub>1941</sub> TC CCG TCC T
IV	109 bp	CTG AGG GAA G <sub>205</sub> gttaagcaagg	4.9 kb	tcatttgcagT <sub>2051</sub> T CGC CTT GC
V	87 bp	AAA CCA GAA G <sub>214</sub> gttgcagaggat	0.9 kb	tccttaaaagA <sub>2141</sub> G GAG GAG CC
VI	92 bp	A GGC GGT CAG <sub>223</sub> gttgcagacc	4.2 kb	tggaattgcagG <sub>223</sub> AA GAT GTG G
VII	561 bp	C CGA AGG CAG <sub>230</sub> gttgcaggtgc	0.7 kb	ttcaaaacagG <sub>2301</sub> AG TCT AGG A
VIII	90 bp	G GCT CAC CAG <sub>238</sub> gttgcaggaac	0.7 kb	cgtttacacagG <sub>2381</sub> TT GGT GAA A
IX	167 bp	TC ACT GTG GG <sub>240</sub> gttgcaggtgca	0.9 kb	aaattgcagC <sub>2401</sub> TTG CCT GTT
X	2037bp			

alternate splice variants including this exon have been shown in rat NCKX1 (Poon et al, 2000). Inclusion of exon III in the human NCKX1 cDNA results in the “in frame” insertion of eighteen amino acids (**PGDGAI****AVDELQDNKKLK**) after position 630 of our published human deduced polypeptide sequence (Tucker et al, 1998b). The highly homologous stretch (**PGDGT****VVVDEQQDNKKLK**) is found in the published bovine NCKX1 sequence (conserved residues in bold; (Reiländer et al, 1992)).

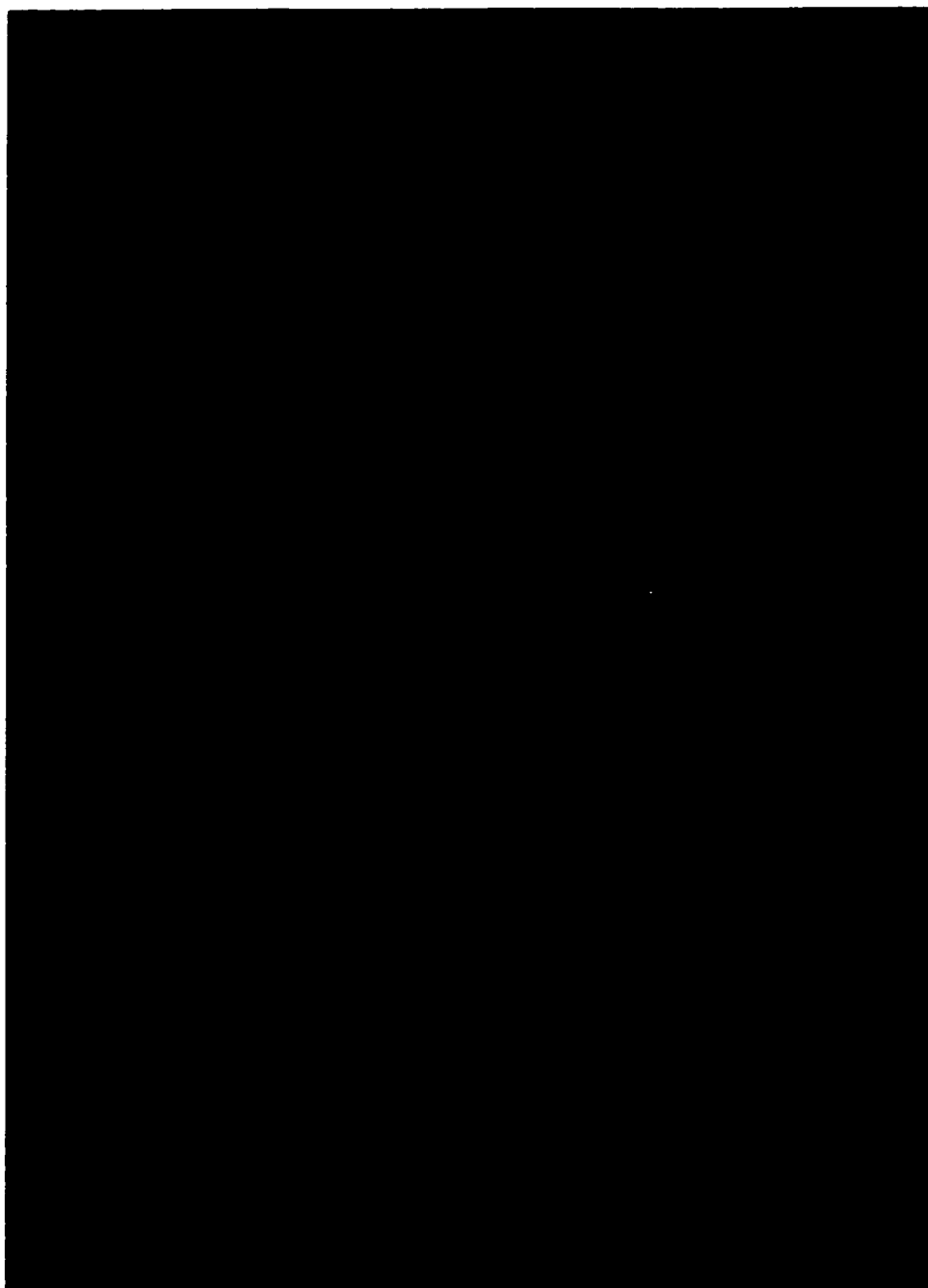
To complement the genomic restriction map, we sequenced 943 bp of the 5' flanking region, which presumably contains all or a portion of the human NCKX1 gene promoter. No canonical TATA box is present; however, 35 bp upstream of the transcript initiation site lies the sequence TATTA, which is adjacent to purine-rich sequences and may function as a promoter element. Similarly, two sequences, ACAAT and CCAAG, resembling the CAAT box consensus (CCAAT) are located 69 bp and, in reverse orientation, 101 bp upstream of the transcription start site, respectively. No sites bearing significant homology to SP1 (GC box) recognition sequences are apparent.

For FISH analysis, we used the entire PAC 136E11 labeled with digoxigenin-dUTP. More than 90% of the metaphase spreads showed localization of the probe to 15q22, with most metaphases showing specific signals on both chromatids of both chromosomes (Figure 4.5). We used human NCKX1 primers to screen the Genebridge 4 radiation hybrid panel and localized NCKX1 on distal chromosome 15 between framework markers D15S159 and AFM094YC1 with a lod score greater than nine. One congenital disease that may be linked to the human NCKX1 gene is Bardet-Biedl syndrome,. Bardet-Biedl is a clinically and genetically heterogeneous disorder characterized by mental retardation, obesity, renal

**Figure 4.5**

Human NCKX1 FISH.

Fluorescence in situ hybridization of the human NCKX1 gene (ROS Na-Ca+K exchanger) to a human chromosome spread. A combined image with DAPI and Cy3 staining is shown.





problems, and RP, and one of the loci (BBS4) has been identified on chromosome 15q22-23 between framework markers D15S131 and D15S114 (Carmi et al, 1995; Bruford et al, 1997). The NCKX1 gene appears to lie just proximal to the BBS4 locus. We are currently in the process of assessing whether mutations or deletions in the gene coding for the human retinal rod Na-Ca+K exchanger are found in patients suffering from severe and early onset retinal dystrophy.

### **Addendum to Chapter 4.2**

Some of the data generated during the elucidation of the genomic organization were omitted from Chapter 4.2 in order to facilitate the chapter's publication (Tucker et al, 1998a). The omitted data are presented here.

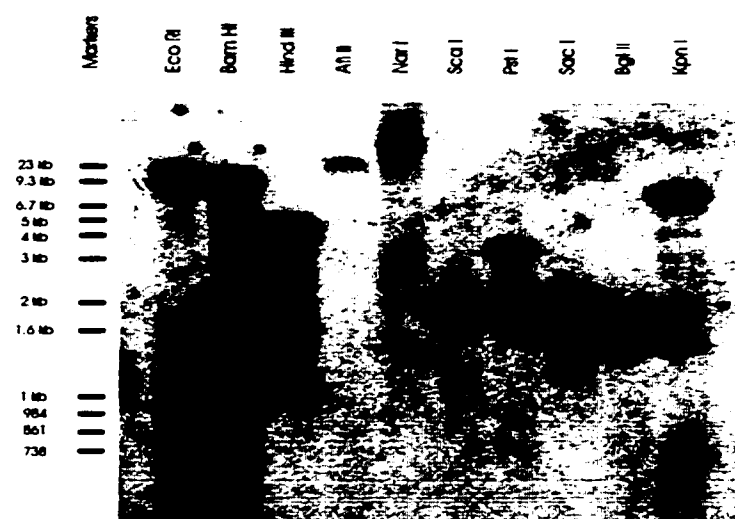
As reported (Tucker et al, 1998a), PAC 136E11 DNA was digested with a number of restriction enzymes and subjected to Southern analysis in order to establish a preliminary map of the human NCKX1 gene (Figure 4.6) (Tucker et al, 1998a). Using the PAC DNA as template, numerous PCR products were synthesized, covering all regions of the human NCKX1 gene and employing many of the oligonucleotides found in Appendix I. The PCR products were then digested with the same restriction enzymes employed in the earlier Southern analysis, and analyzed by agarose gel electrophoresis (Figure 4.7). Size analysis of the DNA restriction fragments allowed the construction of a more complete genomic map, and revealed the considerable number of introns clustered in the 5' end of the sequence coding for the cytosolic loop. It was not possible to ascertain from the Southern analysis and restriction mapping data, whether the 54 base pair deletion of the human cDNA sequence (Tucker et al, 1998b) observed relative to the bovine cDNA sequence (Reiländer et al, 1992) represented an evolutionary drop-out or a splice variant. Degenerate primers (Appendix I) based on the bovine 54 bp segment were synthesized and employed in PCR analysis of the PAC template. The resulting products were isolated and sequenced, and confirmed the presence, at the genomic level, of human NCKX1 exon III (data not shown). To identify precisely the intron / exon junctions (Figure 4.4b), PCR products of primer pairs surrounding each putative intron were sequenced and compared against the cDNA sequence.

**Figure 4.6****Southern Blot of PAC 136E11.**

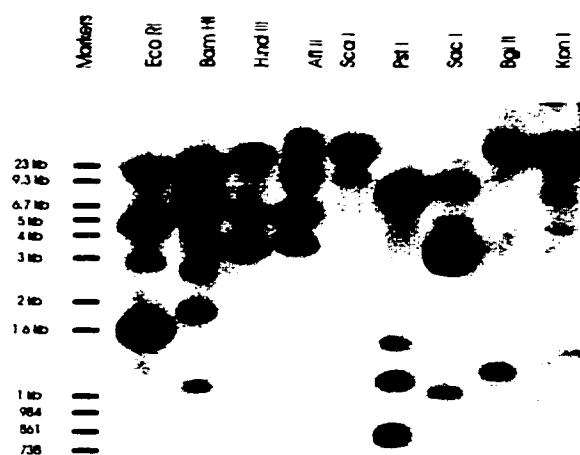
PAC 136E11 DNA was digested with several restriction endonuclease enzymes in separate reactions. The resulting fragments were electrophoresed through a 1% agarose gel and transferred to nitrocellulose for detection by Southern hybridization. Radiolabeled DNA probe was synthesized using random primers from a polymerase chain reaction fragment of the human cDNA. Hybridization to the nitrocellulose of this probe detected major fragments of the restriction digested PAC DNA bearing homology. Commercial 1 kb ladder DNA size markers are as indicated. Lanes contain the restriction fragments of single enzymes, as labeled.

- a. Probe synthesized with primers Front and JTG-13
- b. Probe synthesized with primers 3'Race and JTG-10
- c. Probe synthesized from primers JTG-9 and JTG-10.

a.



b.



c.

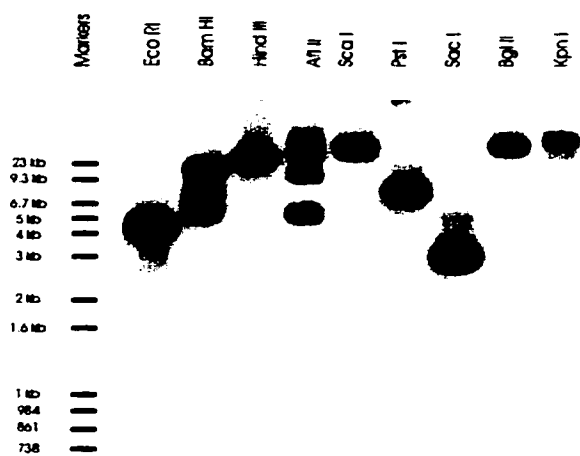
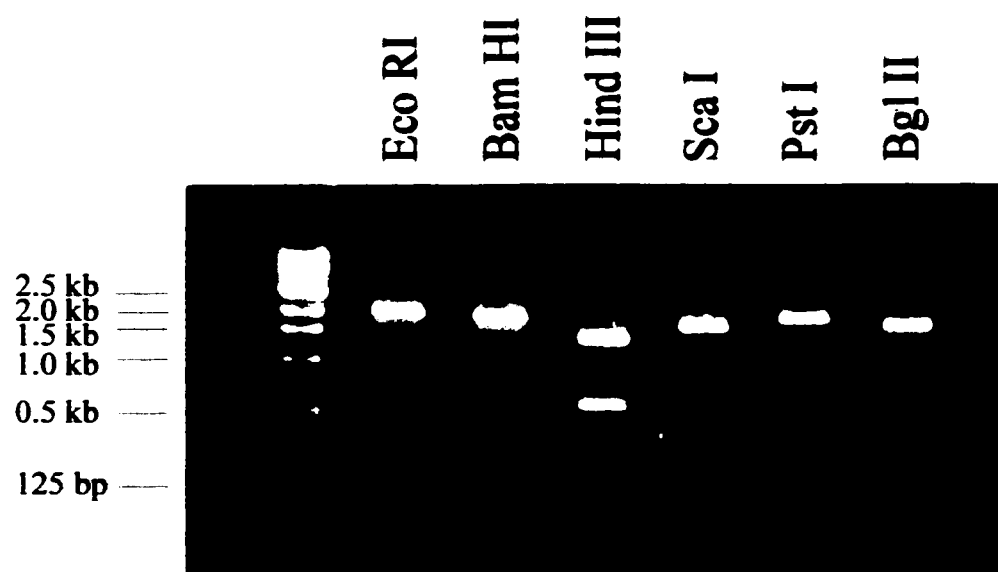


**Figure 4.7****PCR Digests.**

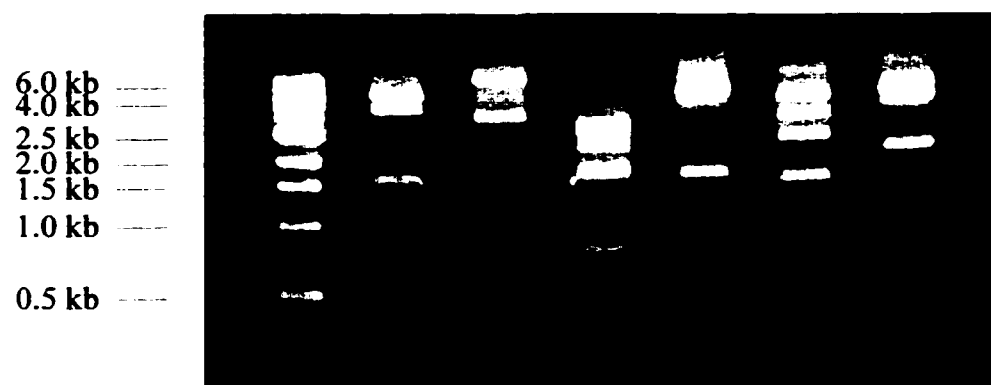
PAC 13E65 plasmid DNA was isolated and subjected to polymerase chain amplification using primers flanking each intron insertion point. Amplified fragments were restriction endonuclease digested and electrophoresed on 1% agarose gels. The observed bands were visually inspected to determine approximate sizes by comparison with commercial 1 kb marker. The seven restriction enzymes used to characterize each intron were *Eco RI*, *Bam HI*, *Hind III*, *Sca I*, *Pst I* and *Bgl II*.

- a. primers JTG-36 and JTG-35 flanking intron 1;
- b. primers JTG-27 and JTG-30 flanking intron 2;
- c. primers JTG-29 and JTG-25 flanking intron 3;
- d. primers JTG-6 and JTG-7 flanking intron 4;
- e. primers JTG-26 and JTG-1 flanking intron 5;
- f. primers BovBuf and JTG-20 flanking intron 6;
- g. primers get3' and get5' flanking intron 7;
- h. primers JTG-9 and JTG-18 flanking intron 8;
- i. primers JTG-17 and JTG-11 flanking intron 9.

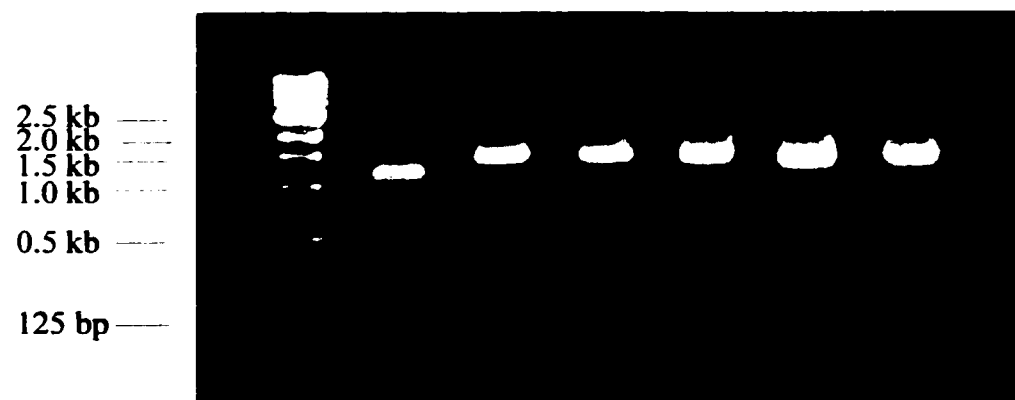
a.



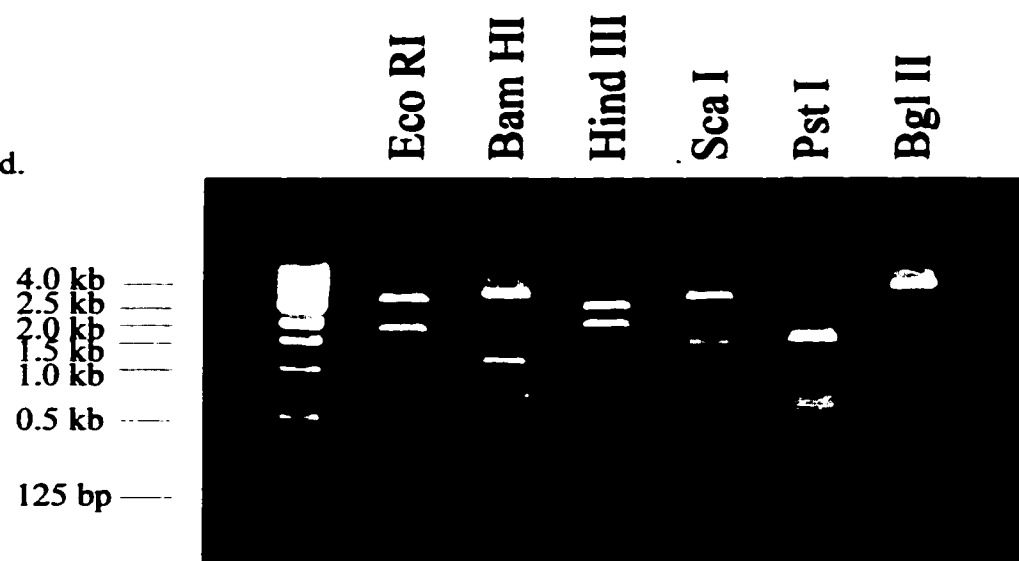
b.



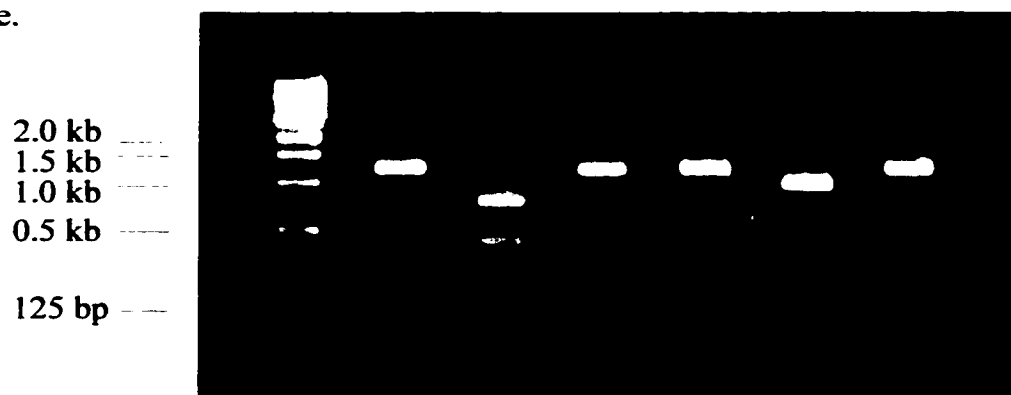
c.



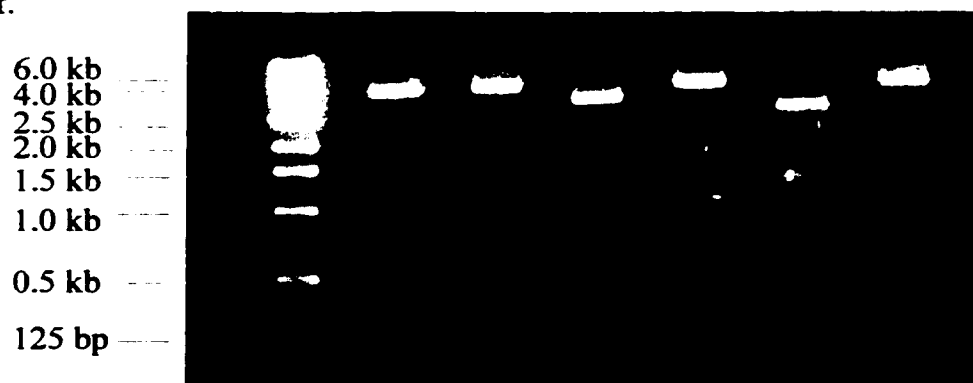
d.



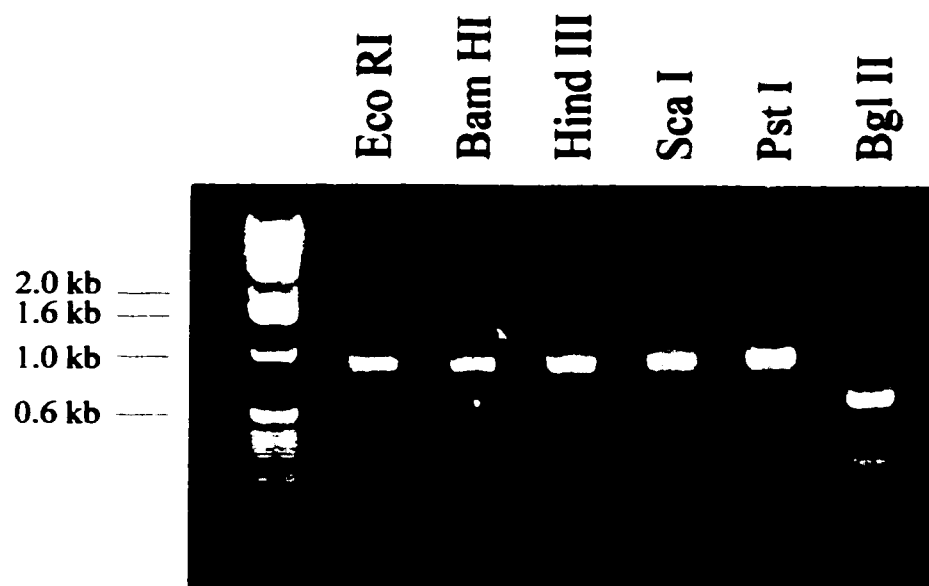
e.



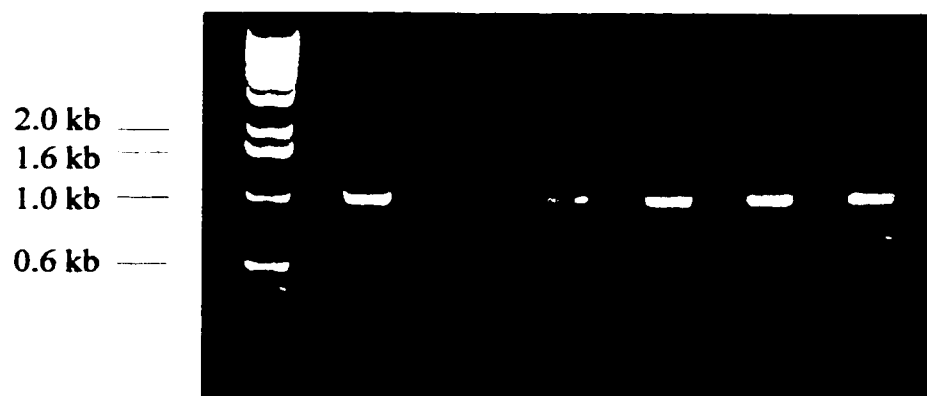
f.



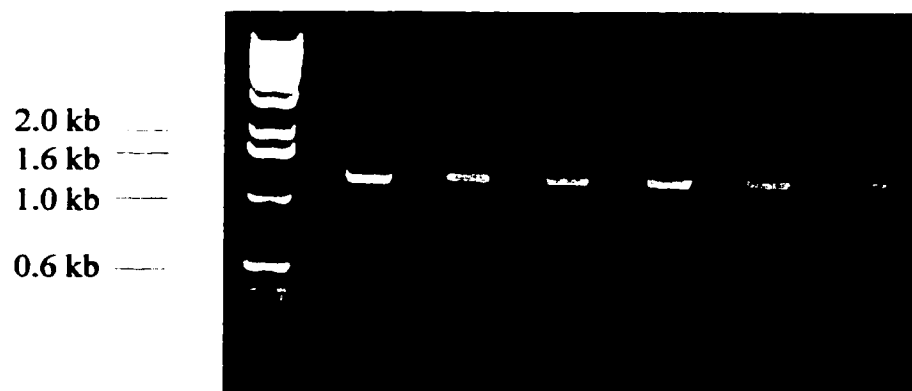
g.



h.



I.





To examine the retinal expression of NCKX1 mRNA, retinal human and bovine RNA was purified for use in transcript analysis with human NCKX1 specific probe. Northern hybridization demonstrated robust expression of human NCKX1 mRNA (Figure 4.8a). The probe specificity for human NCKX1 combined with high stringency conditions resulted in inefficient detection of bovine NCKX1 mRNA; indeed a weakly hybridizing band only became visible upon long exposure to X-ray film (Figure 4.8b). The length of the human transcript was observed to be approximately 6 kb, while the length of the bovine transcript was close to 6.5 kb, in agreement with results reported by others (Reiländer et al, 1992).

3'-RACE examination of human retinal RNA revealed transcripts of NCKX1 with two different sized 3'-untranslated regions (UTRs) (Figure 4.9). Sequence determination of the 3'-UTR from the two 3'-RACE PCR products and the PAC DNA found two polyadenylation signals, whose position within the sequence agreed with the 3'-UTR sizes and sequences observed.

5'-RACE was performed using three different downstream primers; all detected the same unique 5'-UTR (Figure 4.10), which was subsequently sequenced from both 5'-RACE products and the PAC template. S1 nuclease protection assay confirmed the length of the 5'-UTR, but was not sufficiently unambiguous to determine the exact nucleotide from which transcription initiates (data not shown). Unlike NCX1, which has been observed to have different 5'-UTRs originating from discrete promoters (Nicholas et al, 1998; Scheller et al, 1998), my results suggest that human NCKX1 does not undergo alternate splicing in the untranslated regions.

**Figure 4.8****Human NCKX1 Northern.**

Human total RNA isolated from the retinas of a recently deceased 73 year old male was electrophoresed on a 1% agarose gel. Total bovine retinal RNA was employed as a control. Hybridization was with a radiolabeled DNA probe specific for the human transcript, which additionally showed very weak cross-reactivity with the bovine transcript. Exposure to X-ray film was for 1 hour (*left panel*) and 48 hours (*right panel*). Sizes in kilobases are as indicated, as derived from a commercial RNA ladder.

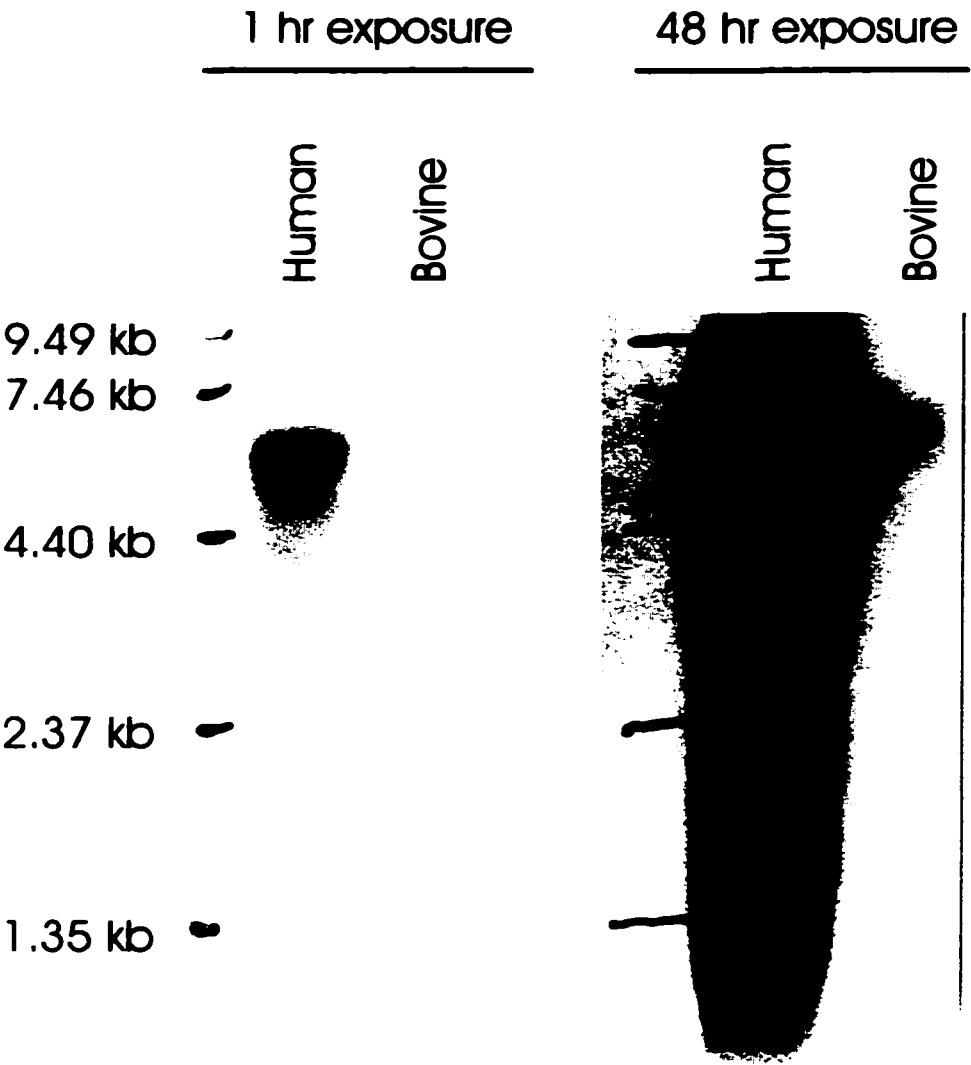
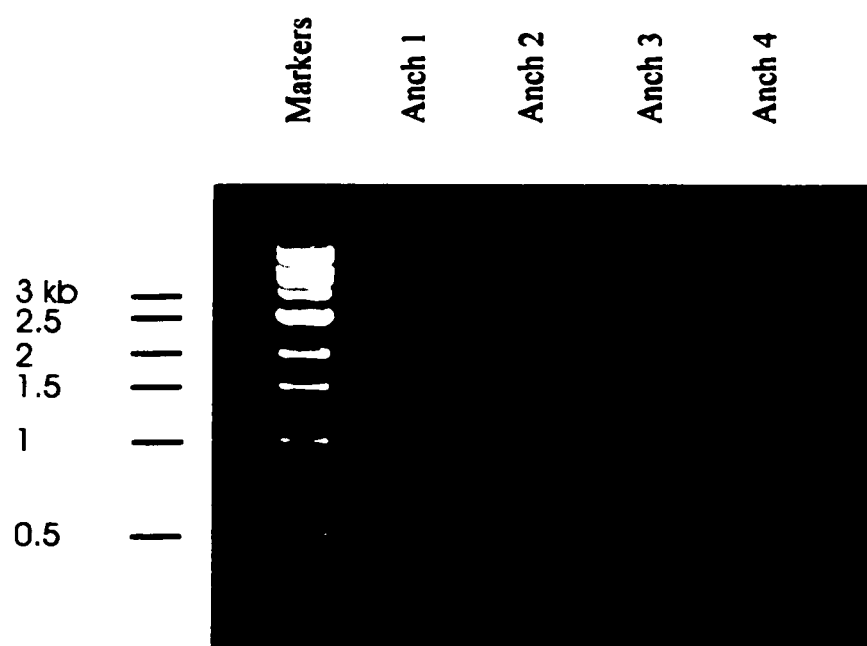


**Figure 4.9****3'-RACE of Human NCKX1.**

- a.** Anchor primed 3' RACE reverse transcriptions of the human rod NCKX1 gene were performed on human retinal RNA using four distinct anchors. Polymerase chain reaction amplification of the 1<sup>st</sup> strand cDNA with JTG-17 primer from the 3' end of the known human sequence was followed by electrophoretic separation of the resultant DNA products on a 1% agarose gel. All four anchors show the same pattern of fragments. Commercial DNA size markers are as indicated.
- b.** the same gel, transferred to nitrocellulose and hybridized to a radiolabeled random primed DNA probe specific for the 3' end of the human NCKX1 cDNA.

a.



b.

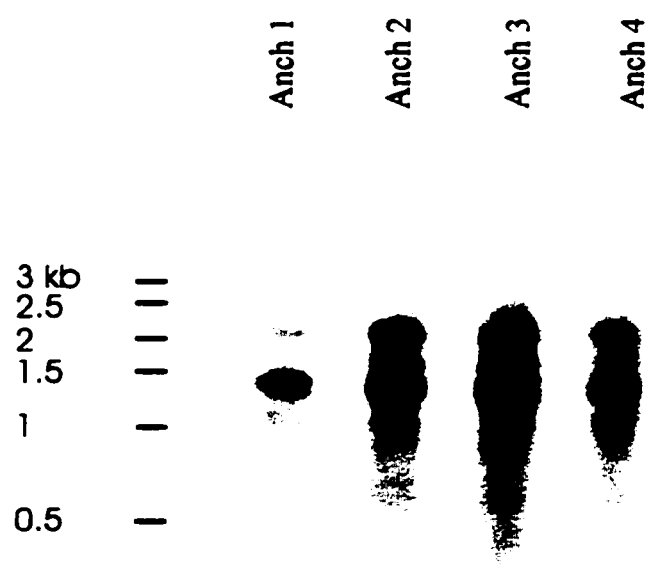
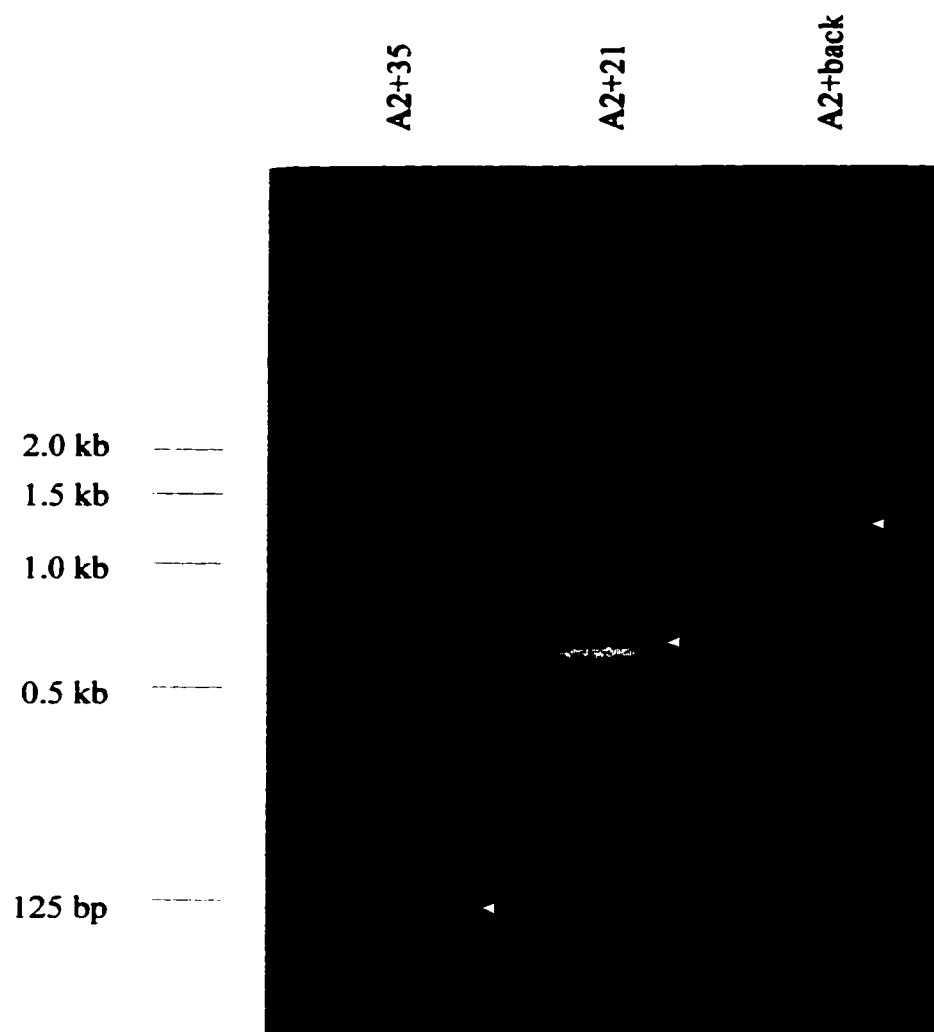


**Figure 4.10****5'-RACE of Human NCKX1.**

Human retinal RNA was reverse transcribed to 1<sup>st</sup> strand cDNA using TdT poly-A tailed RNA and a poly-T primer. Polymerase chain reaction amplification using Anchor2 and three different primers, JTG-35, JTG-21 and 'back' revealed major DNA products when electrophoretically separated on a 1% agarose gel, as indicated by *arrows*. All three major fragments, predict an identical sized 5' UTR, when their relative position in the sequence is considered. Commercial DNA size markers are as indicated, in kilobases, at the left of the gel.



To catalog the presumptive promoter region, PAC 136E11 DNA was sequenced for 943 bp upstream of the putative transcription start site. The sequence, along with consensus sites for potentially relevant promoter elements, is shown in Figure 4.11. Although perfect consensus matches were not found for the TATA box, CAAT box or cap initiation site (Tucker et al, 1998a), sites which scored highly according to Bucher (Bucher, 1990) were identified. A TATA-like site is apparent at nucleotides -35 to -30 (relative to the putative transcription initiation site); a CAAT-like site at -101 to -96 and a cap initiation site at -4 to -1 (Figure 4.11). The existence of a TATA-containing promoter is consistent with the cell-type specific expression expected for this gene (Reiländer et al, 1992; Kimura et al, 1999). The sequence of the cap site suggests that the actual transcription start site may lie one base 5' from where my 5'-RACE placed it (Tucker et al, 1998a), as initiation usually occurs at the T of the consensus CCT<sub>0</sub>G cap site (Bucher, 1990).



**Figure 4.11****5' Flanking Sequence.**

The 943 bases 5' of the presumed transcription start site are shown. CAAT-like sequences are located in the reverse orientation from position -101 to -97 and in the forward orientation from position -166 to -161. A TATA-like sequence is located spanning bases -35 to -31. A Cap consensus sequence, indicative of the transcription start site, is found at positions -4 to -1. Other promoter recognition sequences which may play a role in the transcriptional control of the human rod NCKX1 gene are as indicated.

-943 TCAGAGATGA AGCCAGCTCT TCACAGTGGT GGCCTTCTGT GGCTTCAGCA  
 -893 GAGGGAGCTC GTGACCTTCT TACTGTTCCA GGCCACTCAA GGTGAAGCAG  
 -843 GGTAGAGGTG AGGCTGTGAG GATTAAGTGC TATTTTCAGAT GAAAGTAACC  
 -793 CAAAGCATCA TGCACCCAGG TACTCTGGAG GAAACAGGAA AGGGAGAAAG  
 -743 GGGCAGTCAG TAAATGTCAG GCCGAGTTAG CTGAATGATT GAAAGGGCTT  
 -693 CCAGATCAAT GGTAGGATC ACAAGATCCC CACTACCTTA CCCTACTCCC  
 SPl AP-2  
 -643 ACTTTGATCA GCTCCAAGTC ATGGGCTGGA GCGCGGGGG GCTCAGGGCA  
 SPl SPl AP-2  
 -593 CCAACTCCTC AGGTATCTTG GGATGTCCCA GCCTGCTCTG GGGAGATCCA  
 -543 TTAGTGCCCT CTACACCAAG GATTTCCTTT AGGCCTAATA AAATAGATTT  
 CP-2  
 -493 CAGGTATGAA TGCTTTGAAG TTTGCTTGGT GTTTTCTCTA TAATCTTTGT  
 CAP/CRP  
 -443 TTTTTATTTT GATTCTCACA TTCACCTTAC AAATAGGAAG GACAGGTATT  
 AP-2 NF-1  
 -393 ATTATCCCCA CATTACTTTA GATTACATAG AATCACACAG TAGCCAAGTC  
 CP-2/CAP/CRP/NF-1  
 -343 GAGCCTAATG GCTAACTGAG GTCTTCTGAT CTCTTAAGCC CCAGTCACTT  
 C/EBP C/EBP $\alpha$ /AP-3/NF-1  
 -293 TCCCTTCGTT TTCTCAGAGC GCCTTCTGAA TCTTTTCAAA ACTTTCCACC  
 SPl  
 -243 ATCTAAGCAT GGAAACCCTA GACCACCTCT CAATTCTCAT AGCTTAGAAA  
 C/EBP $\beta$  CP-2 SPl/CCAAT-like  
 -193 CAAGTTGAGA AATCTCCCCC AGTTCCTCCA TTGACTTTGT GGGCCACAG  
 CP-2 CAAT-like  
 -143 TGAGCCCCTC TGTGTCCCTG GTGGAAGGCC CACTCTCTCA GGCTTGGTCA  
 SPl CP-2 GATA-1  
 -93 GGTGTACCGG GACCCAGAAC TTGTACAATG CCCTGATAAG CTTCTTAGAG  
 SPl TATA-like GATA-2 Cap  
 -43 GAGGTGGGTA TTAGCCACGA TCGGATATTC TTCCCCTGAG CAG

### **4.3 Alternate Splicing of the Human NCKX1 Exchanger**

#### **4.3.1 Introduction**

The elucidation of the genomic organization of the human Na/Ca+K exchanger revealed the presence of multiple introns (Tucker et al, 1998a). When the cloned human cDNA (lacking exon III) is aligned to the putative full length human cDNA (containing exon III) as well as to the bovine and dolphin cDNAs, correlation to the human NCKX1 exon/intron junctions is observed (Figure 4.12). This suggests that alternate splicing may occur in human NCKX1 and might in fact be a common feature of the NCKX1 gene among mammalian species (Poon et al, 2000; Tucker et al, 1998b).

#### *RT-PCR Analysis of Alternate Splicing in NCKX1*

It was reported that the rat NCKX1 gene undergoes alternate splicing, as detected by RT-PCR (Poon et al, 2000). Here, RT-PCR evidence of alternate splicing in the human and bovine NCKX1 genes will be presented.

#### *Ribonuclease Protection Assay of NCKX1*

Ribonuclease protection assay (RPA) analysis provides quantitative evidence for the existence and relative abundance of alternately spliced transcripts. In the absence of the ability to distinguish protein isoforms, RPA analysis is suggestive as to the identity and relative abundance of such protein isoforms. Ribonuclease protection assay results for human and bovine retinal RNA are presented here.

#### *Heterologous Expression of Human NCKX1 Splice Variants*

Of the human retinal NCKX1 alternately spliced transcripts revealed by RPA analysis in this study, two variants were further investigated for potential functional differences. The

**Figure 4.12****Sequence Alignment of Cytosolic Domains.**

The cytosolic domains of full length human, bovine, dolphin and cDNA cloned human NCKX1 exchangers are aligned. *Thick black line* indicates the exon not present in the human cloned NCKX1 cDNA, but present in the full length human NCKX1 transcript. *Dashed line* indicates the region missing from the cloned dolphin NCKX1 cDNA. *Dotted line* indicates the repeat region present in bovine NCKX1 but not in human or dolphin NCKX1.

.....

• • • • •






[illegible]

\_\_\_\_\_

-----

Human	247
Bovine	360
Dolphin	172
Hum cDNA	229

two clones were constructed using standard molecular techniques, expressed heterologously and examined via a modified single cell digital imaging protocol for K-dependent Na/Ca exchange activity. The results of that study are also presented here.

#### **4.3.2 Results**

##### **4.3.2.1 RT-PCR of Alternately Spliced Transcripts**

RT-PCR of human retinal RNA, employing primers surrounding the exon cluster in the N-terminus of the NCKX1 cytosolic loop, revealed transcripts of five different apparent weights (Figure 4.13a). Gel purification and re-PCR of the observed bands allowed the isolation of six discrete splice products which were then sequenced. Comparison with the genomic organization confirmed that all transcripts detected were representative of possible alternate splice combinations of the exons located in the region coding for the cytosolic domain. The exon constituency of the individual transcripts is shown in Figure 4.14. Interestingly, the largest transcript detected corresponds to the full length NCKX1 exchanger, inclusive of exon III (which was absent from the sequence of the initially reported human NCKX1 cDNA) (Tucker et al, 1998b). While most of the sequenced transcripts maintain the coding frame, the -exonIII,V,VI variant does not. This variant is frameshifted and would terminate prematurely if translated. There is at present no indication that such a protein would be capable of Na/Ca exchange; it is possible that this splice variant, and perhaps some of the others, are in fact incompletely spliced transcripts detected by the considerable amplifying power of PCR. In fact, incompletely spliced NCX1 transcripts have been detected in RNA from tissues allowed to remain at room temperature for several hours (Scheller et al, 1998). The human retinas from which the RNA samples were obtained in this study were

**Figure 4.13**

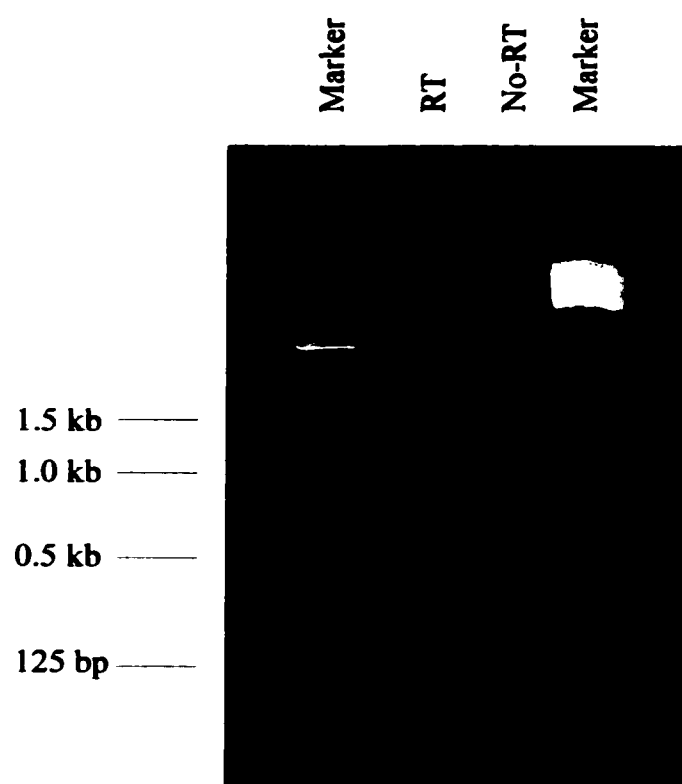
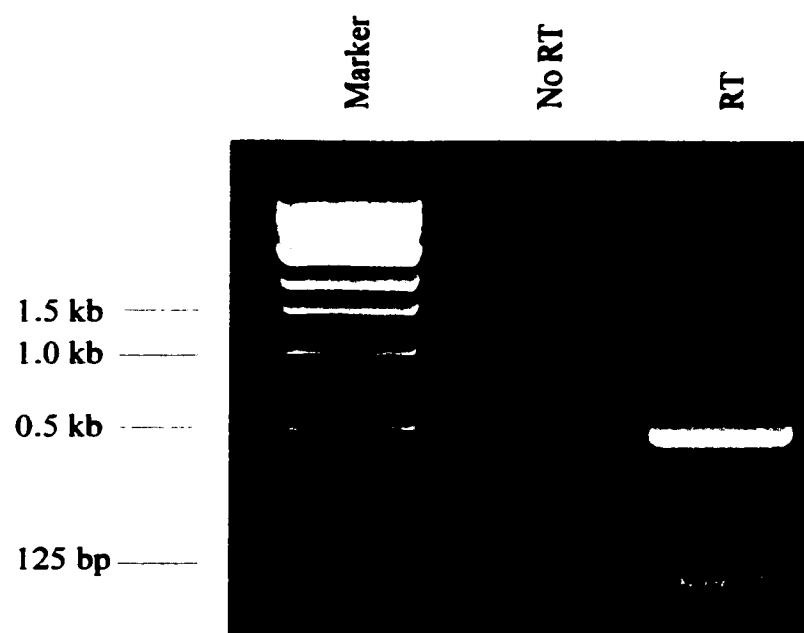
RT with No RT Control.

**a. Human**

Retinal human RNA was reverse transcribed and subjected to polymerase chain reaction amplification using primers specific for the region encompassing the putative alternately spliced domain. Resulting fragments were electrophoresed through a 1% agarose gel. *Marker*, 1 kb ladder; *No RT*, reverse transcriptase not present; *RT*, reverse transcriptase present; *Marker*, 123 bp ladder.

**b. Bovine**

Retinal bovine RNA was reverse transcribed and subjected to polymerase chain reaction amplification using primers specific for the region encompassing the putative alternately spliced domain. Resulting fragments were run on a 1% agarose gel and electrophoresed. *Marker*, 1 kb ladder; *No RT*, no reverse transcriptase negative control; *RT*, reverse transcriptase present.

**a.****b.**



**Figure 4.14****Exon Constituency of Human Alternately Spliced Bands.**

Linear block representation of presumed splice variants observed via RT-PCR and confirmed by sequencing. To save room exon I is omitted and exons II and X are not shown in their entirety. The polypeptide domain for which each region codes are indicated in the upper most blocks. Exon numbering as per (Tucker et al, 1998a) is specified at the bottom of the figure. Each exon present is symbolized by a block in the appropriate location, locations from which introns are removed are represented by gaps. The terminology for each variant, originally identified only on the basis of agarose gel separation, is as indicated at the left of the figure.

H0	EXTRACELLULAR	H1-5	CYTOPLASMIC	EEEE	H6-11
----	---------------	------	-------------	------	-------

<b>Full length</b>	[]
- Exon III	[]
- Exon III, IV, VI	[]
- Exon III, V, VI	[]
- Exon IV-VI	[]
- Exon III-VI	[]

Partial Exon II III IV V VI VII VIII IX Partial X

subject to similar conditions post mortem.

To test whether bovine NCKX1 also undergoes alternate splicing, bovine retinal RNA was RT-PCR'd with primers analogous to those used for the human RT-PCRs. Agarose gel electrophoresis demonstrated the presence of multiple splice variants; the number and sizes of the transcripts however, differed from those of human NCKX1 (Figure 4.13b). It seems then, that while alternate splicing of NCKX1 transcripts occurs in bovine, human and rat, the splice variants present differ in a species specific manner.

Alternate splicing has been observed to play a role in the regulation of developmental stage specific expression of protein isoforms. To test this possibility in NCKX1, human retinal RNA was acquired from a deceased elderly man, a newborn child that died shortly after birth, a stillborn baby, and the pooled retinal RNA of ten deceased adults. RT-PCR did not show any clear differences in relative splice products represented between the prenatal, postnatal or adult tissues (Figure 4.15).

Alternate splicing may constitute a characteristic feature of NCKX1 across species. The observed splicing in rat NCKX1 (Poon et al, 2000), the variants detected in human and bovine retinal RNA, and the apparent fit of the dolphin cDNA (Cooper et al, 1999a) with this paradigm are in agreement with this hypothesis. To test this theory against a previously uncloned NCKX1 homologue, a number of bovine and human specific primers flanking the alternately spliced region were applied in PCR reactions to 1<sup>st</sup> strand DNA reverse transcribed from mouse retinal RNA (Figure 4.16a). A number of the primers bore sufficient homology to support PCR, and agarose gel analysis of the resultant products revealed transcripts of at least two discrete sizes (Figure 4.16b). The apparent length of the two

**Figure 4.15****Developmental Regulation of Human NCKX1 Alternate Splicing.**

Human retinal RNA isolated from distinct individuals was reverse transcribed using random primers. 1<sup>st</sup> strand cDNA was subjected to PCR with primers specific for the alternately spliced region of the cytosolic domain. Resulting fragments were electrophoresed on a 1% agarose gel. *Marker*, 1 kb marker; *Old Man*, RNA from an 80 year old male; *Stillborn*, RNA from a stillborn child; *Newborn*, RNA from a child that died shortly after birth; *Pooled*, RNA pooled from ten adult individuals older than 40.

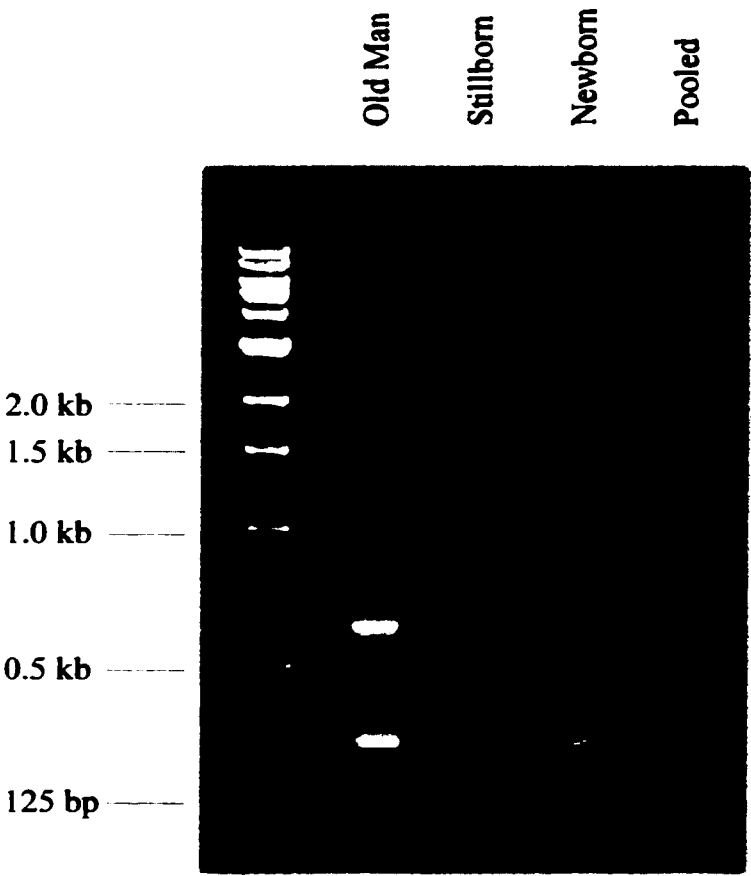


**Figure 4.16****Mouse RT-PCRs of Cytosolic Region.**

Mouse RNA isolated from fresh whole mouse eyes was reverse transcribed using random primers. The resulting 1<sup>st</sup> strand cDNA was employed as template in subsequent polymerase chain reactions using various human, bovine and degenerate primers flanking the putative alternately spliced cytosolic domain.

a. linear representation of the approximate position of the primers employed in this study, assuming representative sequence conservation across species. The region from JTG-4 to JTG-19 was previously PCR amplified and sequenced.

b. The PCR reaction products were electrophoresed on a 1% agarose gel and compared visually to the 1 kb / 100 bp marker. Primer identities are as indicated.



different transcripts, as judged by agarose gel electrophoresis, correlated with the lengths expected for the mouse homologues of the full length and - exons III - VI transcripts. To confirm the NCKX1 origin of these PCR products, sequences from several primers were obtained and putative polypeptide translations aligned with dolphin, bovine, human and rat NCKX1 amino acid sequences (Figure 4.17 and Appendix II).

#### **4.3.2.2 RNase Protection Assay**

While RT-PCR is a simple, fast and powerful method of examining the alternately spliced transcripts present in the retina, the extreme sensitivity of the amplification process precludes accurate quantitative analysis. Ribonuclease protection assay, however, provides reasonably faithful values for the relative abundance of splice variants. In an attempt at semi-quantification of the transcripts present, which admittedly does not necessarily translate directly to a quantification of the protein levels present in the rod outer segment, RNase Protection Assays were performed on retinal RNA from both human and bovine retinas.

Riboprobe templates were constructed for the human and bovine alternately spliced regions downstream of appropriate viral promoters. The riboprobe synthesized was mainly full length, although enough was shorter than full length to require gel purification. Once isolated and purified, the full length riboprobe ran as a discrete band on a polyacrylamide gel.

The human RPA is shown in Figure 4.18a. The results suggest that there are three major splice variants of the human Na/Ca+K exchanger at the RNA level. Three clear bands are observed, corresponding to the full length, the -exonIII and the -exonIII-VI splice variants, in agreement with the RT-PCR results. Phosphoimaging quantitation of equal sized regions enclosing each band and normalization for the number of UTP residues present,



**Figure 4.17****Amino Acid Sequence Alignment.**

Alignment of the deduced amino acid sequences of the full length dolphin, bovine, human and rat NCKX1 sequences compared to the translated partial sequences from RT-PCR of mouse total eye RNA. *Black boxes* indicate homologous residues. *Grey boxes* indicate conserved residues.

Dolphin 1 [REDACTED] V [REDACTED] W [REDACTED] R [REDACTED] Y [REDACTED] S [REDACTED] R [REDACTED] C [REDACTED] H [REDACTED]  
 Bovine 1 [REDACTED] A [REDACTED] S [REDACTED] W [REDACTED] E [REDACTED] Y [REDACTED] T [REDACTED] S [REDACTED] Q [REDACTED] H [REDACTED]  
 Human 1 [REDACTED] P [REDACTED] W [REDACTED] R [REDACTED] T [REDACTED] H [REDACTED] R [REDACTED] R [REDACTED] S [REDACTED] H [REDACTED] Q [REDACTED]  
 Mouse 1 [REDACTED]  
 Rat 1 [REDACTED] T [REDACTED] R [REDACTED] F [REDACTED] H [REDACTED] R [REDACTED] Q [REDACTED] N [REDACTED] P [REDACTED] T [REDACTED] K [REDACTED] Q [REDACTED] E [REDACTED]

Dolphin 61 [REDACTED] R [REDACTED] N [REDACTED] P [REDACTED] S [REDACTED] P [REDACTED] V [REDACTED] T [REDACTED] W [REDACTED] R [REDACTED] G [REDACTED] T [REDACTED] T [REDACTED] G [REDACTED] T [REDACTED] I [REDACTED] R [REDACTED] I [REDACTED] N [REDACTED]  
 Bovine 61 [REDACTED] S [REDACTED] K [REDACTED] K [REDACTED] T [REDACTED] S [REDACTED] S [REDACTED] V [REDACTED] A [REDACTED] W [REDACTED] A [REDACTED] R [REDACTED] G [REDACTED] T [REDACTED] P [REDACTED] G [REDACTED] A [REDACTED] R [REDACTED] K [REDACTED] T [REDACTED] G [REDACTED] S [REDACTED]  
 Human 61 [REDACTED] S [REDACTED] S [REDACTED] E [REDACTED] S [REDACTED] S [REDACTED] P [REDACTED] G [REDACTED] G [REDACTED] K [REDACTED] L [REDACTED] V [REDACTED] S [REDACTED] E [REDACTED] A [REDACTED] T [REDACTED] L [REDACTED] S [REDACTED] T [REDACTED] T [REDACTED] I [REDACTED] M [REDACTED] T [REDACTED] R [REDACTED] K [REDACTED]  
 Mouse 1 [REDACTED]  
 Rat 61 [REDACTED] I [REDACTED] L [REDACTED] P [REDACTED] D [REDACTED] E [REDACTED] T [REDACTED] T [REDACTED] D [REDACTED] K [REDACTED] E [REDACTED] P [REDACTED] E [REDACTED] A [REDACTED] G [REDACTED] M [REDACTED] L [REDACTED] D [REDACTED] I [REDACTED] I [REDACTED] G [REDACTED] E [REDACTED] A [REDACTED] S [REDACTED] A [REDACTED] N [REDACTED] P [REDACTED] I [REDACTED] T [REDACTED] K [REDACTED]

Dolphin 121 [REDACTED] V [REDACTED] I [REDACTED] A [REDACTED] P [REDACTED] S [REDACTED] S [REDACTED] D [REDACTED] A [REDACTED] A [REDACTED] R [REDACTED] E [REDACTED] E [REDACTED] V [REDACTED] A [REDACTED] A [REDACTED] G [REDACTED] A [REDACTED] N [REDACTED] P [REDACTED] P [REDACTED] G [REDACTED] P [REDACTED] T [REDACTED] N [REDACTED] N [REDACTED] A [REDACTED] T [REDACTED] R [REDACTED] Y [REDACTED] R [REDACTED]  
 Bovine 121 [REDACTED] I [REDACTED] T [REDACTED] A [REDACTED] I [REDACTED] P [REDACTED] N [REDACTED] P [REDACTED] T [REDACTED] G [REDACTED] V [REDACTED] S [REDACTED] A [REDACTED] G [REDACTED] V [REDACTED] N [REDACTED] T [REDACTED] Q [REDACTED] P [REDACTED] P [REDACTED] N [REDACTED] S [REDACTED] R [REDACTED] L [REDACTED] T [REDACTED] A [REDACTED] S [REDACTED] R [REDACTED]  
 Human 121 [REDACTED] M [REDACTED] I [REDACTED] T [REDACTED] T [REDACTED] N [REDACTED] A [REDACTED] A [REDACTED] E [REDACTED] E [REDACTED] R [REDACTED] T [REDACTED] T [REDACTED] R [REDACTED] T [REDACTED] Y [REDACTED] T [REDACTED] S [REDACTED] S [REDACTED] Q [REDACTED] K [REDACTED] K [REDACTED] T [REDACTED] P [REDACTED] Y [REDACTED] S [REDACTED]  
 Mouse 1 [REDACTED]  
 Rat 120 [REDACTED] I [REDACTED] T [REDACTED] T [REDACTED] S [REDACTED] L [REDACTED] N [REDACTED] T [REDACTED] R [REDACTED] E [REDACTED] Q [REDACTED] I [REDACTED] P [REDACTED] R [REDACTED] A [REDACTED] P [REDACTED] S [REDACTED] E [REDACTED] I [REDACTED] S [REDACTED] G [REDACTED] Q [REDACTED] R [REDACTED] K [REDACTED] S [REDACTED] K [REDACTED] P [REDACTED] G [REDACTED] R [REDACTED] S [REDACTED] S [REDACTED]

Dolphin 181 [REDACTED] A [REDACTED] G [REDACTED] K [REDACTED] V [REDACTED] R [REDACTED] L [REDACTED] M [REDACTED] N [REDACTED] A [REDACTED] F [REDACTED] T [REDACTED] R [REDACTED] A [REDACTED] A [REDACTED] M [REDACTED] T [REDACTED] N [REDACTED] P [REDACTED] S [REDACTED]  
 Bovine 178 [REDACTED] S [REDACTED] G [REDACTED] K [REDACTED] E [REDACTED] L [REDACTED] M [REDACTED] N [REDACTED] A [REDACTED] L [REDACTED] P [REDACTED] R [REDACTED] M [REDACTED] K [REDACTED] A [REDACTED] P [REDACTED] S [REDACTED]  
 Human 179 [REDACTED] V [REDACTED] E [REDACTED] K [REDACTED] V [REDACTED] R [REDACTED] R [REDACTED] G [REDACTED] V [REDACTED] E [REDACTED] T [REDACTED] Y [REDACTED] S [REDACTED] L [REDACTED]  
 Mouse 1 [REDACTED]  
 Rat 179 [REDACTED] H [REDACTED] T [REDACTED] E [REDACTED] E [REDACTED] G [REDACTED] R [REDACTED] M [REDACTED] H [REDACTED] A [REDACTED] A [REDACTED] P [REDACTED] R [REDACTED] T [REDACTED] E [REDACTED] T [REDACTED] T [REDACTED] Y [REDACTED] E [REDACTED] M [REDACTED] P [REDACTED] R [REDACTED] S [REDACTED] E [REDACTED]

Dolphin 241 [REDACTED] L [REDACTED] G [REDACTED] E [REDACTED] P [REDACTED] T [REDACTED] V [REDACTED] L [REDACTED] P [REDACTED] I [REDACTED] N [REDACTED] A [REDACTED] G [REDACTED] K [REDACTED] T [REDACTED] T [REDACTED] E [REDACTED] N [REDACTED] T [REDACTED] N [REDACTED] H [REDACTED] R [REDACTED]  
 Bovine 238 [REDACTED] L [REDACTED] M [REDACTED] E [REDACTED] K [REDACTED] P [REDACTED] T [REDACTED] P [REDACTED] L [REDACTED] S [REDACTED] T [REDACTED] N [REDACTED] K [REDACTED] T [REDACTED] T [REDACTED] S [REDACTED] T [REDACTED] N [REDACTED] H [REDACTED] Q [REDACTED]  
 Human 238 [REDACTED] I [REDACTED] M [REDACTED] E [REDACTED] E [REDACTED] T [REDACTED] M [REDACTED] F [REDACTED] S [REDACTED] P [REDACTED] T [REDACTED] H [REDACTED] E [REDACTED] A [REDACTED] S [REDACTED] Y [REDACTED] N [REDACTED] N [REDACTED] F [REDACTED] P [REDACTED] S [REDACTED] A [REDACTED] H [REDACTED] P [REDACTED] W [REDACTED]  
 Mouse 1 [REDACTED]  
 Rat 224 [REDACTED] R [REDACTED] T [REDACTED] A [REDACTED] G [REDACTED] S [REDACTED] R [REDACTED] V [REDACTED] P [REDACTED] R [REDACTED] T [REDACTED] R [REDACTED] E [REDACTED] V [REDACTED] S [REDACTED] E [REDACTED] V [REDACTED] G [REDACTED] N [REDACTED] G [REDACTED] E [REDACTED] R [REDACTED] G [REDACTED] E [REDACTED] R [REDACTED]

Dolphin 301 [REDACTED] N [REDACTED] S [REDACTED] L [REDACTED] T [REDACTED] E [REDACTED] A [REDACTED] A [REDACTED] I [REDACTED] T [REDACTED] A [REDACTED] S [REDACTED] S [REDACTED] A [REDACTED] T [REDACTED] V [REDACTED]  
 Bovine 298 [REDACTED] N [REDACTED] N [REDACTED] L [REDACTED] M [REDACTED] E [REDACTED] A [REDACTED] V [REDACTED] T [REDACTED] M [REDACTED] R [REDACTED] T [REDACTED] D [REDACTED] E [REDACTED] P [REDACTED] L [REDACTED] P [REDACTED] A [REDACTED] I [REDACTED]  
 Human 298 [REDACTED] S [REDACTED] N [REDACTED] P [REDACTED] K [REDACTED] T [REDACTED] L [REDACTED] P [REDACTED] T [REDACTED] M [REDACTED] G [REDACTED] A [REDACTED] F [REDACTED] S [REDACTED] S [REDACTED] P [REDACTED] V [REDACTED] S [REDACTED] A [REDACTED]  
 Mouse 1 [REDACTED]  
 Rat 273 [REDACTED] S [REDACTED] L [REDACTED] R [REDACTED] A [REDACTED] Q [REDACTED] P [REDACTED] E [REDACTED] A [REDACTED] I [REDACTED] R [REDACTED] M [REDACTED] G [REDACTED] A [REDACTED] T [REDACTED] E [REDACTED] G [REDACTED] O [REDACTED] F [REDACTED] G [REDACTED] L [REDACTED] S [REDACTED] G [REDACTED] T [REDACTED] A [REDACTED]

Dolphin 356 [REDACTED] G [REDACTED] S [REDACTED] F [REDACTED] W [REDACTED] G [REDACTED] V [REDACTED] N [REDACTED] P [REDACTED] P [REDACTED] A [REDACTED] R [REDACTED] S [REDACTED] P [REDACTED] T [REDACTED] E [REDACTED] V [REDACTED] V [REDACTED] S [REDACTED] S [REDACTED] D [REDACTED] G [REDACTED]  
 Bovine 358 [REDACTED] F [REDACTED] S [REDACTED] F [REDACTED] R [REDACTED] G [REDACTED] L [REDACTED] N [REDACTED] K [REDACTED] P [REDACTED] A [REDACTED] A [REDACTED] R [REDACTED] N [REDACTED] P [REDACTED] I [REDACTED] E [REDACTED] A [REDACTED] V [REDACTED] A [REDACTED] A [REDACTED]  
 Human 358 [REDACTED] K [REDACTED] T [REDACTED] A [REDACTED] P [REDACTED] I [REDACTED] V [REDACTED] W [REDACTED] R [REDACTED] A [REDACTED] K [REDACTED] T [REDACTED] S [REDACTED] T [REDACTED] T [REDACTED] K [REDACTED] L [REDACTED] M [REDACTED] K [REDACTED] T [REDACTED] A [REDACTED] M [REDACTED] L [REDACTED] T [REDACTED]  
 Mouse 1 [REDACTED]  
 Rat 327 [REDACTED] F [REDACTED] A [REDACTED] V [REDACTED] I [REDACTED] D [REDACTED] R [REDACTED] E [REDACTED] R [REDACTED] T [REDACTED] H [REDACTED] G [REDACTED] L [REDACTED] V [REDACTED] Q [REDACTED] P [REDACTED] V [REDACTED] L [REDACTED] T [REDACTED] K [REDACTED] A [REDACTED] V [REDACTED] P [REDACTED] M [REDACTED] T [REDACTED] A [REDACTED] I [REDACTED] F [REDACTED]

Dolphin 416 [REDACTED] T [REDACTED] S [REDACTED] V [REDACTED] S [REDACTED] O [REDACTED] R [REDACTED] K [REDACTED]  
 Bovine 418 [REDACTED] G [REDACTED] I [REDACTED] S [REDACTED] O [REDACTED] Y [REDACTED]  
 Human 418 [REDACTED] E [REDACTED] L [REDACTED] S [REDACTED] P [REDACTED] S [REDACTED] V [REDACTED] P [REDACTED] S [REDACTED] L [REDACTED]  
 Mouse 1 [REDACTED]  
 Rat 385 [REDACTED] A [REDACTED] S [REDACTED] G [REDACTED] P [REDACTED] S [REDACTED] A [REDACTED] P [REDACTED] W [REDACTED] E [REDACTED] P [REDACTED] T [REDACTED]

Dolphin	474
Bovine	472
Human	478
Mouse	1
Rat	445

Dolphin	534
Bovine	532
Human	538
Mouse	50
Rat	505

Dolphin	594
Bovine	592
Human	598
Mouse	108
Rat	565

Dolphin	627
Bovine	652
Human	658
Mouse	149
Rat	625

Dolphin	627
Bovine	711
Human	718
Mouse	149
Rat	684

Dolphin	646
Bovine	757
Human	764
Mouse	162
Rat	744

Dolphin	683
Bovine	794
Human	791
Mouse	184
Rat	804

Dolphin	711
Bovine	841
Human	806
Mouse	209
Rat	864

\_\_\_\_\_

\_\_\_\_\_

\_\_\_\_\_

100-443887-100

10  
 11  
 12  
 13  
 14  
 15  
 16  
 17  
 18  
 19  
 20  
 21  
 22  
 23  
 24  
 25  
 26  
 27  
 28  
 29  
 30  
 31  
 32  
 33  
 34  
 35  
 36  
 37  
 38  
 39  
 40  
 41  
 42  
 43  
 44  
 45  
 46  
 47  
 48  
 49  
 50  
 51  
 52  
 53  
 54  
 55  
 56  
 57  
 58  
 59  
 60  
 61  
 62  
 63  
 64  
 65  
 66  
 67  
 68  
 69  
 70  
 71  
 72  
 73  
 74  
 75  
 76  
 77  
 78  
 79  
 80  
 81  
 82  
 83  
 84  
 85  
 86  
 87  
 88  
 89  
 90  
 91  
 92  
 93  
 94  
 95  
 96  
 97  
 98  
 99  
 100  
 101  
 102  
 103  
 104  
 105  
 106  
 107  
 108  
 109  
 110  
 111  
 112  
 113  
 114  
 115  
 116  
 117  
 118  
 119  
 120  
 121  
 122  
 123  
 124  
 125  
 126  
 127  
 128  
 129  
 130  
 131  
 132  
 133  
 134  
 135  
 136  
 137  
 138  
 139  
 140  
 141  
 142  
 143  
 144  
 145  
 146  
 147  
 148  
 149  
 150  
 151  
 152  
 153  
 154  
 155  
 156  
 157  
 158  
 159  
 160  
 161  
 162  
 163  
 164  
 165  
 166  
 167  
 168  
 169  
 170  
 171  
 172  
 173  
 174  
 175  
 176  
 177  
 178  
 179  
 180  
 181  
 182  
 183  
 184  
 185  
 186  
 187  
 188  
 189  
 190  
 191  
 192  
 193  
 194  
 195  
 196  
 197  
 198  
 199  
 200  
 201  
 202  
 203  
 204  
 205  
 206  
 207  
 208  
 209  
 210  
 211  
 212  
 213  
 214  
 215  
 216  
 217  
 218  
 219  
 220  
 221  
 222  
 223  
 224  
 225  
 226  
 227  
 228  
 229  
 230  
 231  
 232  
 233  
 234  
 235  
 236  
 237  
 238  
 239  
 240  
 241  
 242  
 243  
 244  
 245  
 246  
 247  
 248  
 249  
 250  
 251  
 252  
 253  
 254  
 255  
 256  
 257  
 258  
 259  
 260  
 261  
 262  
 263  
 264  
 265  
 266  
 267  
 268  
 269  
 270  
 271  
 272  
 273  
 274  
 275  
 276  
 277  
 278  
 279  
 280  
 281  
 282  
 283  
 284  
 285  
 286  
 287  
 288  
 289  
 290  
 291  
 292  
 293  
 294  
 295  
 296  
 297  
 298  
 299  
 300  
 301  
 302  
 303  
 304  
 305  
 306  
 307  
 308  
 309  
 310  
 311  
 312  
 313  
 314  
 315  
 316  
 317  
 318  
 319  
 320  
 321  
 322  
 323  
 324  
 325  
 326  
 327  
 328  
 329  
 330  
 331  
 332  
 333  
 334  
 335  
 336  
 337  
 338  
 339  
 340  
 341  
 342  
 343  
 344  
 345  
 346  
 347  
 348  
 349  
 350  
 351  
 352  
 353  
 354  
 355  
 356  
 357  
 358  
 359  
 360  
 361  
 362  
 363  
 364  
 365  
 366  
 367  
 368  
 369  
 370  
 371  
 372  
 373  
 374  
 375  
 376  
 377  
 378  
 379  
 380  
 381  
 382  
 383  
 384  
 385  
 386  
 387  
 388  
 389  
 390  
 391  
 392  
 393  
 394  
 395  
 396  
 397  
 398  
 399  
 400  
 401  
 402  
 403  
 404  
 405  
 406  
 407  
 408  
 409  
 410  
 411  
 412  
 413  
 414  
 415  
 416  
 417  
 418  
 419  
 420  
 421  
 422  
 423  
 424  
 425  
 426  
 427  
 428  
 429  
 430  
 431  
 432  
 433  
 434  
 435  
 436  
 437  
 438  
 439  
 440  
 441  
 442  
 443  
 444  
 445  
 446  
 447  
 448  
 449  
 450  
 451  
 452  
 453  
 454  
 455  
 456  
 457  
 458  
 459  
 460  
 461  
 462  
 463  
 464  
 465  
 466  
 467  
 468  
 469  
 470  
 471  
 472  
 473  
 474  
 475  
 476  
 477  
 478  
 479  
 480  
 481  
 482  
 483  
 484  
 485  
 486  
 487  
 488  
 489  
 490  
 491  
 492  
 493  
 494  
 495  
 496  
 497  
 498  
 499  
 500  
 501  
 502  
 503  
 504  
 505  
 506  
 507  
 508  
 509  
 510  
 511  
 512  
 513  
 514  
 515  
 516  
 517  
 518  
 519  
 520  
 521  
 522  
 523  
 524  
 525  
 526  
 527  
 528  
 529  
 530  
 531  
 532

A T Q G A P S E E E I P E M A T A K P S  
 T T Q R V L A E E E N Q G H A Q A K P S E  
 A I H G A P S E E E I P E M A T A K P S

-----G-----S-----RD-----N-----VK-----  
 K-----A-----V-----E-----D-----S-----G-----V-----G-----N-----R-----  
 K-----A-----V-----I-----K-----N-----G-----E-----S-----M-----P-----E-----  
 -----ER-----ATGQOET-----AF-----  
 E-----A-----A-----D-----E-----D-----C-----E-----D-----H-----R-----M-----E-----E-----G-----E-----R-----E-----T-----A-----E-----G-----K-----K-----D-----E-----

```

PC-----G-----AQP-----G-----N-----DI-----QA-----EK
PA-----G-----AALG-----S-----GK-----N-----DI-----PA-----PR
AG-----T-----E-----TQP-----K-----
RRLLRC-----K-----E-----D-----QE-----PA-----K-----
E-----RKEDGQEEETETKGG-----Q-----TES-----KD-----Q-----A-----KEADHEGETEAEGKEV-----HE

```

N S F I R D G I Q G E D  
 D D I G E E G E I Q A G E G G E V D E D I Q G E G  
 E Q N S K E Q E R E T A E G K  
 T E A E G T E D Q T K E O E T E A E G K E V E H E V E T A E R K E T N H T E E G K

GEMKGD---GELAAERKED---E-----GGD-----D  
GEVEGDDEGEIQAGEA---V---DEDEGEIQAAGEAGEVGDD---DEGG-----DE  
--N-----D-----H-----N  
EADHEGTEAGGVVEHO---TAEQKVEHEGETEAGEKEEHGOSITETTDG

Dolphin 748 -----G-----I-----N-----D-----E-----E-----E-----E-----  
Bovine 901 IQAGEAGEVEGEDGEVEGGEGDEGEIQAGEGGEG-----G-----I-----G-----D-----E-----E-----  
Human 827 -----ES-----S-----NHG-----P-----P-----D-----  
Mouse 230 -----T-----A-----D-----C-----T-----G-----P-----P-----  
Rat 922 -----T-----A-----D-----C-----T-----A-----G-----P-----P-----

Dolphin	775	G		G		E	
Bovine	961	G					R
Human	854			C		EEEEKG	
Mouse	254						
Rat	946					S	

Dolphin	829	[REDACTED]	[REDACTED]	[REDACTED]	[REDACTED]
Bovine	1014	[REDACTED]	[REDACTED]	[REDACTED]	[REDACTED]
Human	914	[REDACTED]	[REDACTED]	[REDACTED]	[REDACTED]
Mouse		[REDACTED]	[REDACTED]	[REDACTED]	[REDACTED]
Rat	996	[REDACTED]	[REDACTED]	[REDACTED]	[REDACTED]

Dolphin	889	
Bovine	1074	
Human	974	
Mouse		
Rat	1056	

Dolphin	949		L	
Bovine	1134	A	L	
Human	1034		S	
Mouse				
Rat	1116	I	F S	

Dolphin	1009	
Bovine	1194	
Human	1094	
Mouse		-----
Rat	1176	

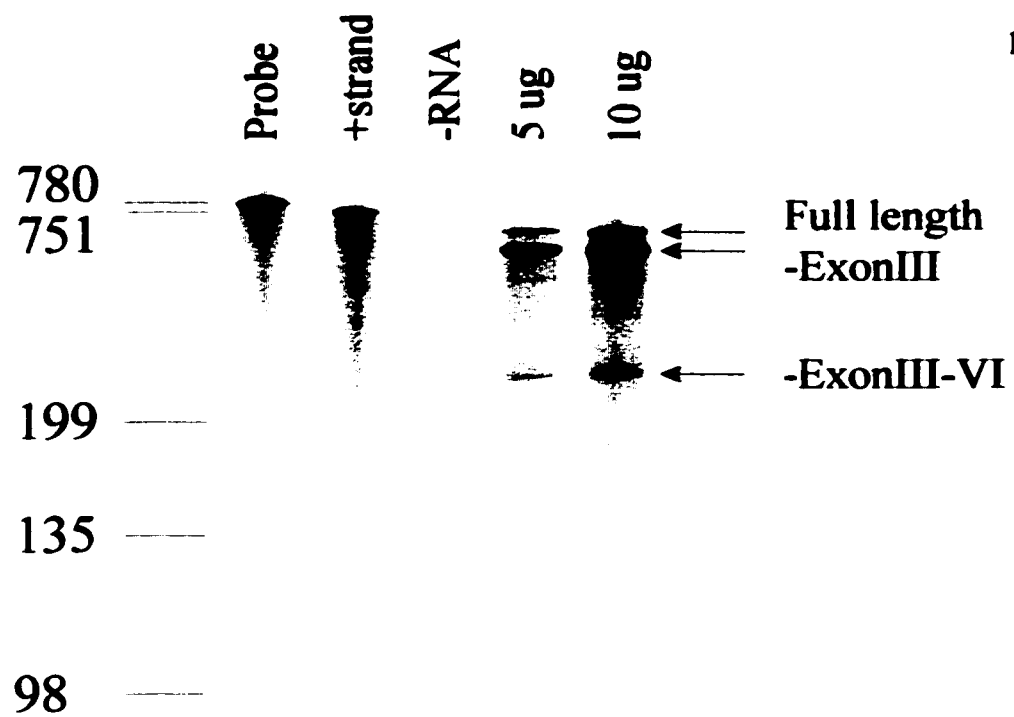
**Figure 4.18****Human RPA.****a. Protected Fragments**

RNase protection assay of human retinal RNA. Total RNA was hybridized to riboprobe homologous to the antisense strand spanning the alternately spliced domain. Following nuclease digestion, the protected fragments were electrophoresed on a 6% formaldehyde / polyacrylamide gel. Riboprobes of known length were employed as markers to determine sequence length of each fragment in bases, as indicated. *Probe*, full length undigested riboprobe; *+strand*, full length riboprobe hybridized to + strand and digested; *-RNA*, riboprobe nuclease digested with no RNA added; *5  $\mu$ g*, 5  $\mu$ g human retinal total RNA hybridized to riboprobe and digested; *10  $\mu$ g*, 10  $\mu$ g human retinal total RNA hybridized to riboprobe and digested. Major protected bands are as labeled and indicated with *arrows*. Several less abundant protected fragments are discernible between the 2<sup>nd</sup> and 3<sup>rd</sup> major protected fragments, but were judged to be of lesser significance and possibly artifactual, and so were not included in the tabulation and calculation of major splice variants.

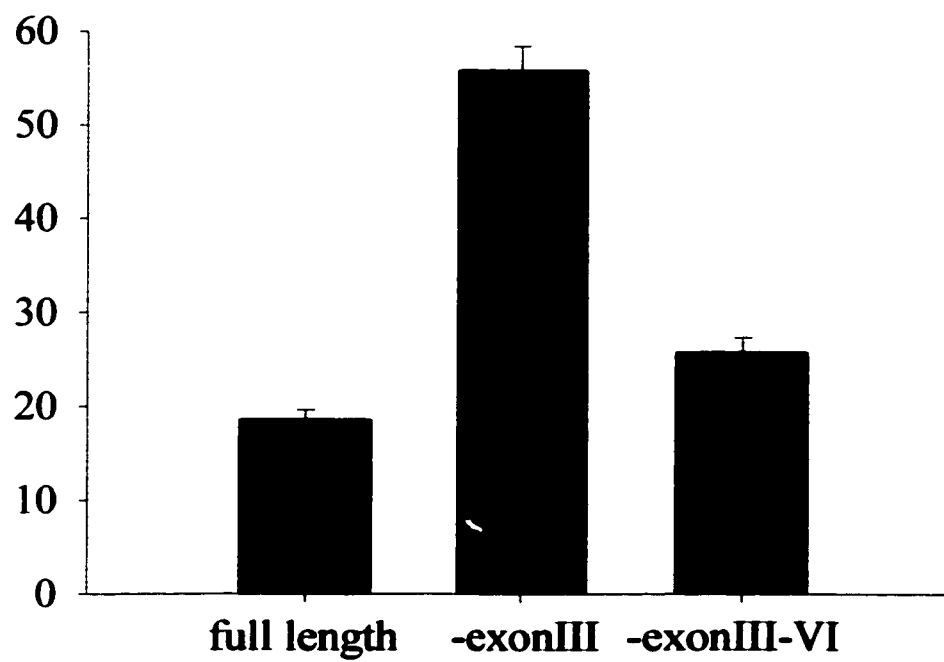
**b. Bar Graph**

The radiolabeled RPA filter was exposed to a phosphoimager for accurate quantitation of the protected fragments of interest. Equal sized regions were counted and relative abundance calculated based on the number of labelled UTP residues in that sequence. The 5  $\mu$ g and 10  $\mu$ g samples were employed as internal controls to ensure probe saturation did not affect the results. A bar graph of the three protected fragments above background levels and their associated standard deviations is shown (from the 5  $\mu$ g, 10  $\mu$ g comparison, ie. n=2).

a.



b.



allows determination of the relative abundances of the three major transcripts. The splice variant which corresponds to the original cDNA cloned (Tucker et al, 1998b), -exonIII, is predominant, followed closely by the variant with exons III-VI removed (Figure 4.18b). It is worth noting that during the original cloning of the human NCKX1 cDNA, when multiple clones were screened, only the larger clones were sequenced, in an attempt to avoid sequencing deletion or truncation artifacts. The full length transcript, analogous to the cDNA originally cloned for the bovine NCKX1, is also present in lesser amounts. Interestingly, the minor bands detected by RT-PCR are virtually unrepresented in the RPA, suggesting that these bands may simply be artifacts of the powerful amplification process of PCR coupled with the degradation of the human retinal tissue prior to RNA isolation.

The bovine RPA also revealed three significant bands (Figure 4.19a). The predominant transcript, as quantified by phosphoimaging corrected for the number of UTP residues present, is the full length transcript, corresponding to the original cDNA clone (Reiländer et al, 1992). Following very closely is the variant lacking the region analogous to exon III in the human NCKX1. Finally, a less abundant transcript is apparent which corresponds to a frame shifted splice variant that if translated is not expected to mediate Na/Ca exchange. This transcript is idiosyncratic in that its presence was not predicted by the assemblage of splice variants observed thus far in human and rat NCKX1. The fact that it codes for a prematurely terminating polypeptide suggests that this transcript may also represent an artifact of the RNA preparation process; perhaps the inadvertent capture of an intermediate splicing step. The calculated relative abundances of these three transcripts are shown in Figure 4.19b.

**Figure 4.19****Bovine RPA.****a. Protected Fragments**

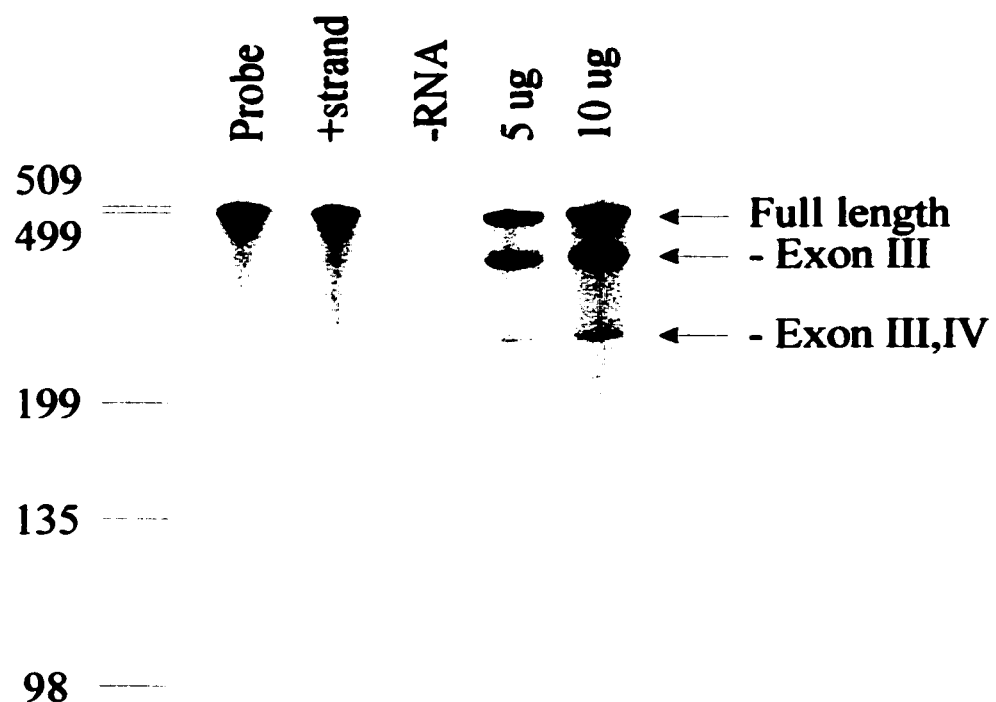
RNase protection assay of bovine retinal RNA. Total RNA was hybridized to riboprobe homologous to the antisense strand covering the presumed alternately spliced domain. Following nuclease digestion, the protected fragments were electrophoresed on a 6% formaldehyde / polyacrylamide gel. Riboprobes of known length were employed as markers to determine sequence length of each fragment in bases, as indicated. *Probe*, full length undigested riboprobe; *+strand*, full length riboprobe hybridized to + strand and digested; *-RNA*, riboprobe nuclease digested with no RNA added; *5 µg*, 5 µg bovine retinal total RNA hybridized to riboprobe and digested; *10 µg*, 10 µg bovine retinal total RNA hybridized to riboprobe and digested. Major protected bands are as labeled and indicated with *arrows*.

**b. Bar Graph**

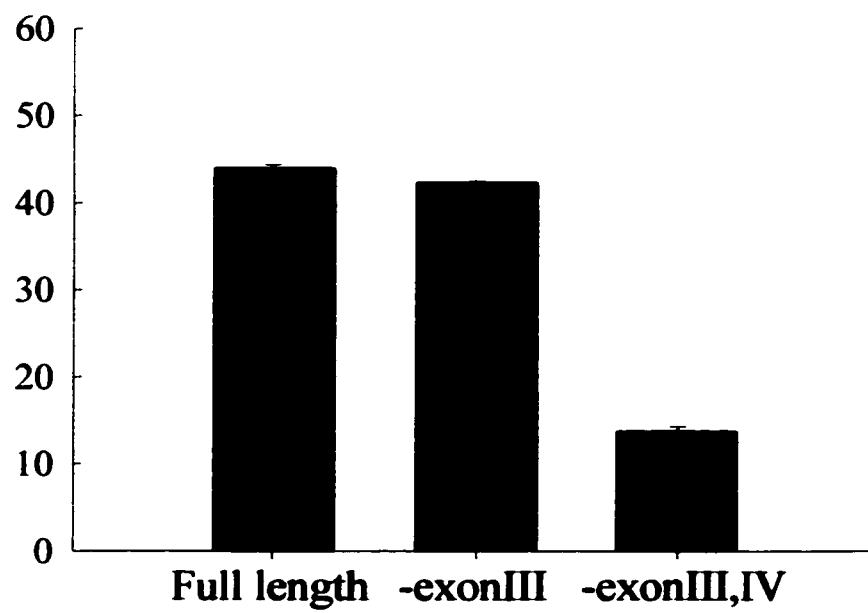
The radiolabeled RPA filter was exposed to a phosphoimager for accurate quantitation of the protected fragments of interest. Equal sized regions were counted and relative abundance calculated based on the number of labeled UTP residues in that sequence. The 5 µg and 10 µg samples were employed as internal controls to ensure probe saturation did not affect the results. A bar graph of the three protected fragments above background levels and their associated standard deviations is shown (from the 5 µg, 10 µg comparison, ie. n=2).



a.



b.



It seems, then, that human and bovine NCKX1 genes display three and two major splice variants respectively, that the two major bovine transcripts are represented in the three human variants, and that the relative abundances between the two species are not conserved. As there are presently no antibodies capable of distinguishing between any of the translated splice variants, there is no obvious way to determine how the relative abundance of transcripts correlates to the abundance of protein products *in vivo*. Certainly though, the results of the RPA provide a starting point for the future examination of NCKX1 splice variants.




















#### **4.3.2.3 Human Deletion Constructs**

Domain comparison of native and mutant NCKX1 cDNAs whose products have been demonstrated to express Na/Ca+K exchange activity heterologously, with those whose products do not, suggests a negative correlation (see Figure 4.20) (Cooper et al, 1999a; Tucker et al, 1998b; Szerencsei et al, 2000) (and Chapter 4.4). Insertion of the bovine cytosolic loop into the functional dolphin cDNA (which had lacked an analogous domain) resulted in the complete abolition of Na/Ca+K exchange (Cooper et al, 1999a). Removal of the cytosolic loop from the non-functional bovine full length exchanger, permitted Na/Ca+K exchange to occur ((Szerencsei et al, 2000) and Chapter 4.4). This suggests that some form of functional inhibition takes place in heterologous systems, perhaps mediated by one or more of exons III-VI of the alternately spliced domain. For this reason, the alternately spliced region and the role it plays in determining heterologous functional expression, was further explored.

**Figure 4.20**

Domain Alignments of OF, EX, CR, Dolphin and Dbv.

Schematic representation of domain-type alignment of several NCKX1 full-length, deletion and chimeric constructs. Each putative mature polypeptide is represented by a linear box arrangement. *Rectangles* denote domains. Bovine NCKX1 domains are in *black*, dolphin NCKX1 domains in *grey*. *X*, extracellular domain; *TM1*, transmembrane domain 1; *C1*, alternately spliced portion of cytosolic domain; *C2*, remainder of cytosolic domain; *TM2*, transmembrane domain 2. *EX*, bovine rod NCKX1 full length cDNA; *CR*, CR chimeric deletion clone; *OF*, OF double deletion chimeric clone; *Dolphin*, Dolphin NCKX1 cDNA (Cooper et al, 1999); *Dbv*, Dolphin/bovine chimeric construct (Cooper, Winkfein, Szerencsei, and Schnetkamp, 1999); +, Na/Ca+K exchange activity reported; -, inability to mediate Na/Ca+K exchange activity reported.

Clone	X	TM1	C1	C2	TM2	Activity
EX						-
CR						-
OF						+
Dolphin					 	+
Dbv						-

The human NCKX1 cDNA originally cloned, -exonIII, is the most abundant human NCKX1 splice variant according to the RPA. This transcript, termed ECH, (with a C-terminal FLAG tag) was tested in the HighFive expression system. In addition, a clone was constructed by PCR which closely resembles the -exonIII-VI variant. This construct, termed HFD, was also FLAG tagged at the C-terminus, to allow detection with the commercial M2 antibody (Kodak). These two clones were expressed in the pEIA / HighFive system which we have also employed (Chapter 4.4 and (Szerencsei et al, 2000)) to measure the Na/Ca+K exchange activity of the OF bovine deletion mutant.

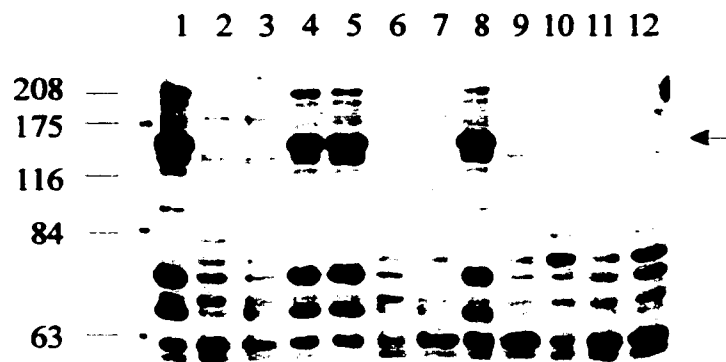
Expression of the human splice variant constructs in the HighFive cells resulted in clearly detectable levels of protein from some of the stable cell lines derived from these clones and in the transiently transfected heterogeneous population (Figure 4.21). The highly expressing cell lines and transient transfectants were further characterized by  $^{45}\text{Ca}$  uptakes and FURA-2 digital imaging.  $^{45}\text{Ca}$  uptakes consistently showed very low to undetectable K-dependent Na/Ca exchange for both constructs (data not shown). For the clone lacking exon III (ECH), single cell digital imaging was also invariably negative for Na/Ca exchange. Perhaps 5-10% of the cells from the HFD stable lines (the -exonIII-VI mutant) displayed some form of Ca homeostasis perturbation which did not appear to be unequivocal Na/Ca exchange. These cells increased their levels of cytosolic Ca, but at a rate slower than the typical exchange observed for the bovine OF deletion mutant under the same conditions, and did not extrude the Ca when the external solution was switched to high Na (data not shown). However, digital imaging of HighFive cells transiently transfected with HFD was intriguing, as single cells occasionally appeared to undergo K-dependent Na/Ca exchange (Figure 4.22).

**Figure 4.21****Heterologously Expressed Human Splice Variant Western Blots.**

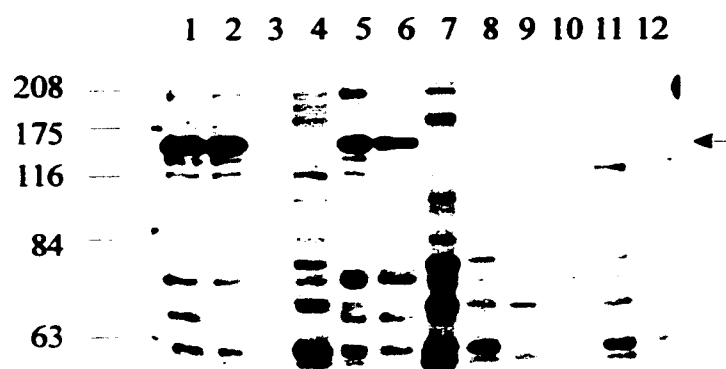
Twelve HighFive derived cell lines stably transfected for each the human NCKX1-FLAG cDNA and the human NCKX1-FLAG deletion mutant were assayed for protein expression by the Western blot method. Cells were collected from 75 ml flasks and total protein isolated with the RIPA post-nuclear protocol. 30 µg of protein, as assayed by the BioRad modified Bradford assay, was loaded into each well of a 7.5% polyacrylamide gel and electrophoresed. The separated proteins were transferred to nitrocellulose and detected with the commercial M2 anti-FLAG antibody. Commercial molecular weight markers are as indicated. The position of the heterologously expressed exchanger mutant is indicated by an arrow to the right of the nitrocellulose.

- a.** ECH cell lines western. Cell lines 1, 4, 5 and 8, as indicated by those same lanes, demonstrate significantly higher protein expression than do the other eight cell lines. These four highly expressing lines were further characterized by functional analyses.
- b.** HFD cell lines western. Lines 1, 2, 5 and 6, corresponding to the same numbered lanes, express higher quantities of protein than do the other eight HFD cell lines. Those four highly expressing lines were further subjected to exchanger functional analysis.
- c.** ECH and HFD constructs were transiently transfected into HighFive cells. *Marker*, commercial molecular weight marker; *Control*, OF HighFive cell line (negative for FLAG-epitope detection); *ECH*, transiently transfected ECH; *HFD*, transiently transfected HFD.

a.



b.



c.

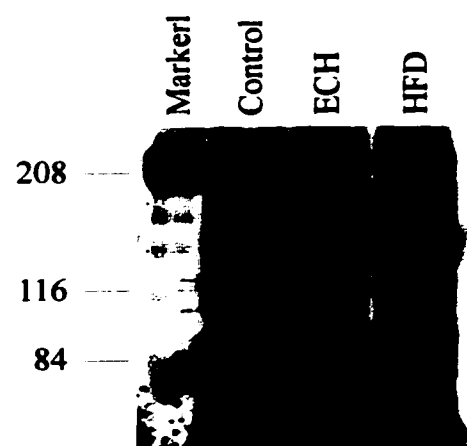


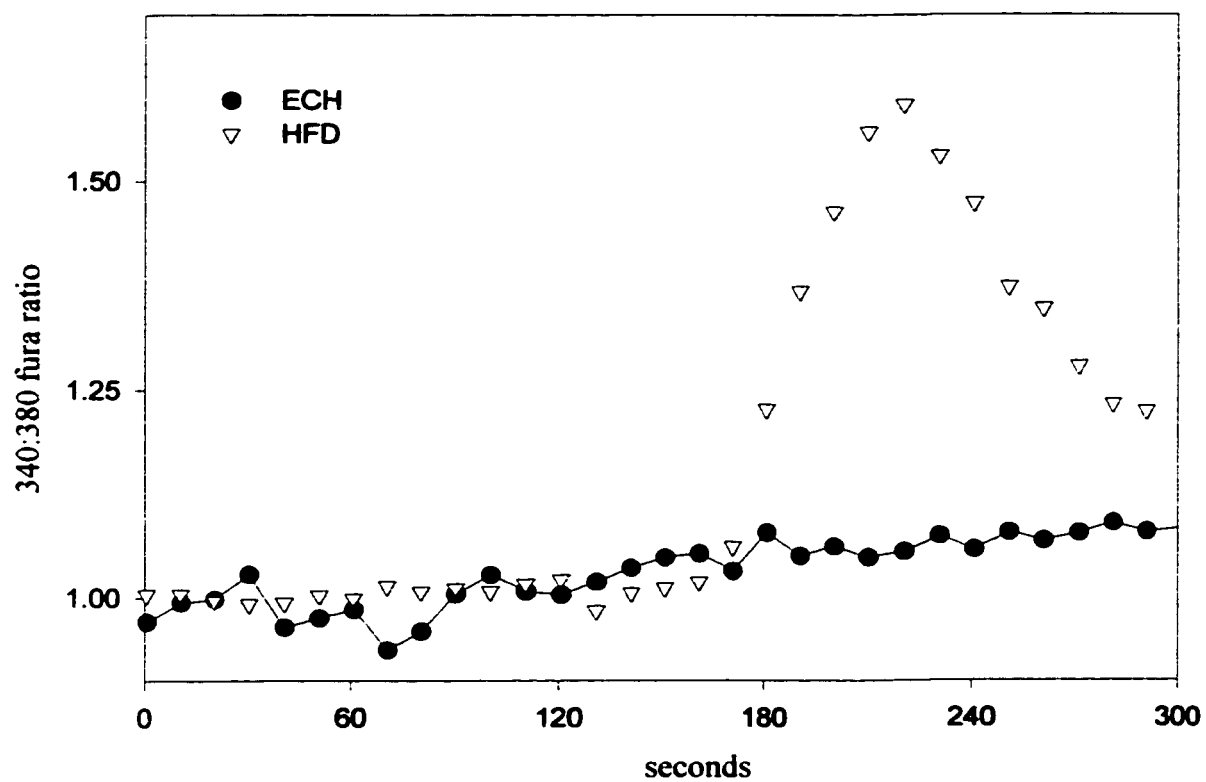
**Figure 4.22**

Digital Imaging of HFD vs. ECH Transient Transfections.

HighFive cells transiently transfected with the HFD or ECH constructs were assayed by FURA-2 ratio digital imaging. Cells on coverslips were Na-loaded and then 340/380 FURA-2 ratio measurements made while the bathing solution was switched. The initial bathing solution was NaEDTA and the solution was switched to LiCa and then LiCaK. Note the K-dependence and the characteristic shape of the Ca influx curve of the HFD transfectants. Traces represent the averages of twelve individual cells (*HFD*) and nine individual cells (*ECH*).



## Digital Imaging - Human Transients in HighFive Cells



0 20 40 60 80 100 120 140 160 180 200 220 240 260 280 300

The frequency of these cells within the total population was less than 5% (personal observation), calling into question the reproducibility of these results.

#### **4.3.3 Discussion**

Until the recent finding that the rat NCKX1 exchanger apparently undergoes alternate splicing, there was no indication that distinct isoforms of the Na/Ca+K exchanger existed within the rod outer segment. Functional data have not historically been interpreted to reflect the possibility that more than one type of functional K-dependent Na/Ca exchanger might be present. Here, RT-PCR has shown that both bovine and human retinas contain multiple splice variants of the exchanger at the transcript level, in agreement with a recent report of alternate splicing in the rat (Poon et al, 2000). Sequence analysis of human splice variants confirmed that all observed transcripts correlated to the published intron / exon structure laid out in the genomic organization (Tucker et al, 1998a).

The existence of, and purpose for, alternately spliced transcripts, and presumably distinct protein products, is intriguing. The supposition of multiple isoforms hints at functions or characteristics of the Na/Ca+K exchanger not yet revealed, and perhaps not readily measured. The conservation of the identity of some of the splice variants, from rat to bovine and human, is in apparent contradiction to the low sequence homology between these same species. Whatever functions these exons might mediate, they appear to be conserved among several mammalian species.

The discovery of human NCKX1 splice variants that appeared to correlate both with functional (ie. dolphin) and non-functional (ie. bovine) when heterologously expressed Na/Ca+K exchangers, presented an opportunity to test the prediction that the exon IV-VI

portion of the cytosolic loop would inhibit the Na/Ca+K exchange activity of heterologously expressed human NCKX1. The data presented here support this hypothesis, but the lack of reproducibility tempers the conviction with which the results may be held. Future efforts to resolve this question will be interesting to observe.

#### **4.4 Chimeric / Deletion Mutants of Bovine NCX and NCKX Exchangers**

##### **4.4.1 Introduction**

Studies of the Na/Ca exchanger have established that ion transport functions are relegated to the transmembrane regions, (Matsuoka et al, 1993) and the observed regulatory features of the Na/Ca exchanger are found in the cytosolic loop (Hilgemann, 1990). Removal of the cytosolic domain eliminates the regulation, but does not abolish the Na/Ca exchange capability (Matsuoka et al, 1993). An interesting and plausible hypothesis is that the Na/Ca+K exchanger might segregate transport and regulatory activities in a manner similar to the Na/Ca exchanger. Protease removal of bovine Na/Ca+K exchanger epitopes (Kim et al, 1998) suggests that the cytosolic domain is not required for Na/Ca exchange.

To investigate the structure function relationships of the Na/Ca+K exchanger, a series of deletion and chimeric mutants of the Na/Ca+K exchanger was constructed, drawing on the structural and functional similarity between the two exchangers. The effect of removal of the N-terminal extracellular region on K-dependent Na/Ca exchange was also examined.

Mutant exchanger proteins were heterologously expressed and examined in a number of cell types until a suitable system, the pELA:HighFive insect cell system, (Farrell et al, 1998) was found. Measurement of Na/Ca+K exchange activity proved challenging, necessitating modifications to our previously reported (Cooper et al, 1999b) single cell digital imaging protocol. Heterologous expression of reverse Na/Ca+K exchange activity, dependent on external Ca and K concentrations and mediated by a deletion mutant which lacks both the extracellular and cytosolic hydrophilic loops, is demonstrated. Our results prove that the two hydrophobic domains of the bovine Na/Ca+K exchanger are sufficient to

mediate K-dependent Na/Ca exchange. Calculation in the heterologous expression system of  $K_m$  activation constants for Ca and K revealed values comparable to those reported for the native exchanger *in situ*.

#### **4.4.2 Results**

##### **Selection of Heterologous Expression System**

Initially, the CR, EX, IF, IFC, p17 and CCC constructs in the pRc/CMV mammalian expression vector were stably transfected into DG44 CHO cells. Northern blots demonstrate the transcript expression of NCX1, CR and IF (Figure 4.23 a). To detect transcripts from both the bovine Na/Ca and Na/Ca+K exchangers, riboprobe was transcribed from the chimeric 5' portion of the IF construct, including the region coding for the short Na/Ca extracellular domain and the region coding for the Na/Ca+K exchanger transmembrane domains. The negative control, total RNA isolated from the DG44 parental cell line, showed no hybridization to this riboprobe in contrast to the IF, CR and NCX1 expressing cell lines, each of which revealed a hybridizing band of the appropriate lengths. Interestingly, total RNA from a CHO cell line expressing the human NCKX1 cDNA (see chapter 4.3) also hybridized to the riboprobe, apparently reflecting the high sequence homology between the human and bovine NCKX1 genes in the region coding for the transmembrane domains. Western blotting illustrated the expression of the protein products from the CR and EX constructs (Figure 4.23 b). The monoclonal antibody specific for the cytosolic domain of the bovine Na/Ca+K exchanger successfully detected the full length, EX, and extracellular deletion mutant, CR, while not detecting any protein in the DG44 parental control cell line. It was not possible with this antibody to detect the double deletion mutant of the Na/Ca+K

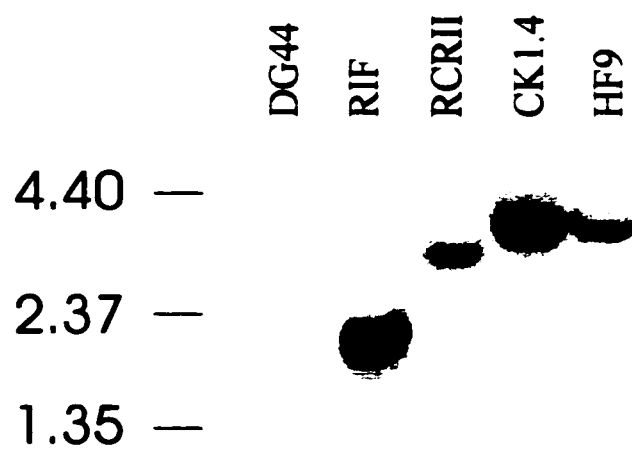
**Figure 4.23****CHO Stable Cell Lines.****a. Northern Analysis**

Total RNA from CHO stable cell lines was isolated and electrophoresed through a 1% agarose gel, blotted to nitrocellulose and riboprobed. Commercial marker sizes are as indicated in kilobases. *DG44*, control DG44 cell line; *RIF*, IF cell line; *RCR11*, CR cell line; *CK1.4*, NCX1 cell line; *HF9*, human NCKX1-FLAG tagged cDNA cell line.

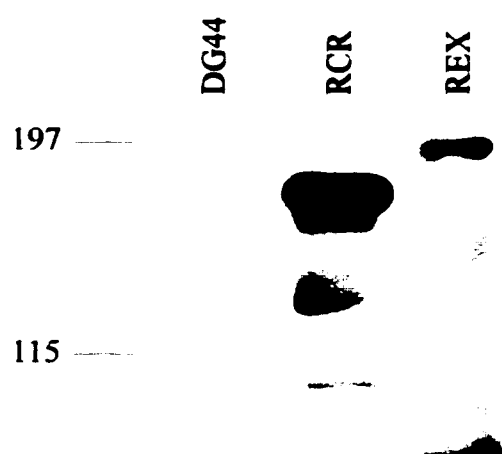
**b. Western blot**

Total protein was isolated from stable CHO cell lines growing on T75 flasks using the RIPA post-nuclear method. 30 µg protein was loaded per lane and electrophoresed through a 7.5% polyacrylamide gel. The separated proteins were transferred to nitrocellulose and detected with the PME 1B3 antibody, which is specific for the bovine rod Na/Ca+K exchanger cytosolic domain. The parental DG44 cell line, from which the stable cell lines were derived, is employed as a negative control. Commercial protein size markers are as indicated. *DG44*, control DG44 cell line; *RCR*, CR cell line; *REX*, EX (bovine NCKX1) cell line.

a.



b.



exchanger, as it lacked the cytosolic region containing the recognized epitope.

<sup>45</sup>Ca uptake experiments of the stable CHO cell lines, performed exhaustively by others in our laboratory (Szerencsei et al, 2000), detected Na/Ca exchange only in the NCX1 cell line. Fluo-3 spectrofluorometric assays (data not shown) and FURA-2 single cell digital imaging (Figure 4.24), also found no detectable functional activity in any of the constructs except the cardiac Na/Ca exchanger NCX1 (CK1.4) cell line. The NCX1-expressing CHO cell line demonstrated K-independent reverse Na/Ca exchange, with relatively constant cytosolic Ca levels under conditions that promote Ca entry. That is, upon modification of the Na gradient from inward directed to outward directed, there was a rapid influx of Ca into the cell until a plateau was reached. This Ca equilibrium condition was maintained until the Na gradient was altered to inward directed (ie. favoring Ca extrusion) (Figure 4.24 e). The Ca concentration plateau does not appear to be an artifact of FURA-2 quenching, as its peak magnitude can occur within the operational range of 340:380 ratios, ie. from 1-2. This 'square-waveform' of Ca influx, plateau and efflux, was also observed (described below) via FURA-2 digital imaging in the HighFive insect cell expression system, again mediated by the Na/Ca exchanger.

Occasionally with membrane-embedded proteins, incorrect targeting results in functionally active protein not being successfully transported to the plasma membrane. The most common cause of cystic fibrosis, the phenylalanine deletion mutant ( $\Delta$ F508) of CFTR, results in the CFTR protein product being unable to escape the endoplasmic reticulum (Fuller and Benos, 1992). If the heterologously expressed exchanger mutants are not successfully transported to the plasma membrane, it could result in the observed phenomenon of protein



**Figure 4.24****Fura-2 Traces of Stable CHO Cell Lines.**

Fura-2 single cell imaging was performed as described. Cell bathing solutions are indicated by the bars beneath each trace. Traces of several individual cells are shown for each stable cell line. The delay of  $\text{Ca}_i$  increase following switching to LiCa in **e.** is due to the time required for solution passage through the perfusion system. All concentrations are in mM.

**a.** *DG44*, control DG44 cell line

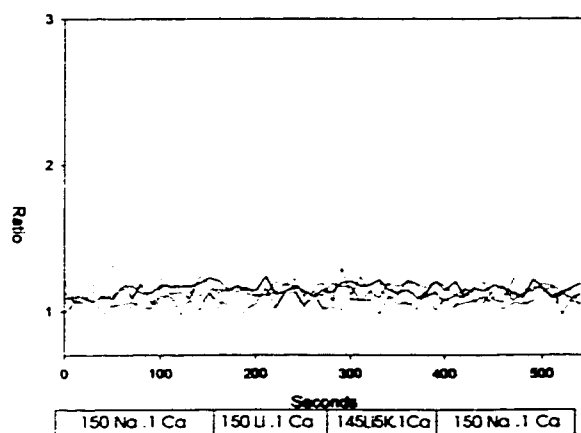
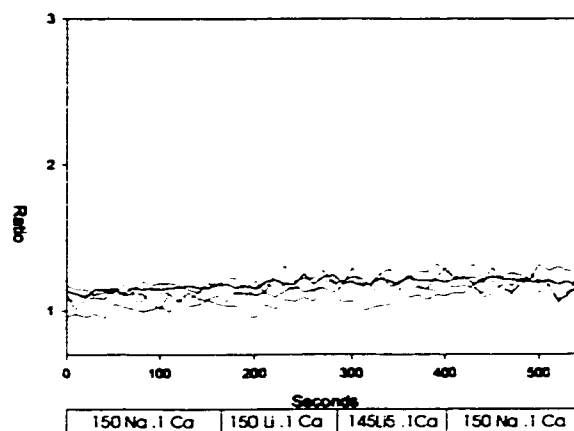
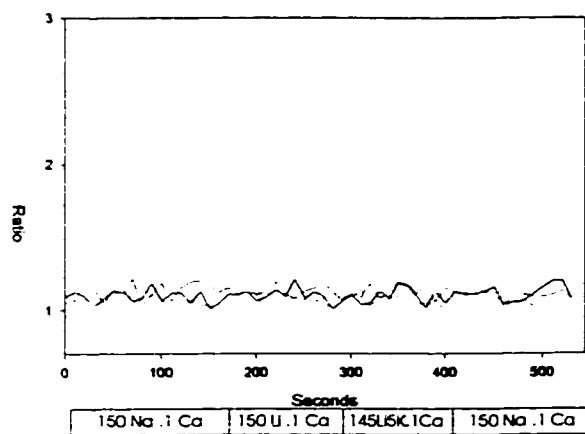
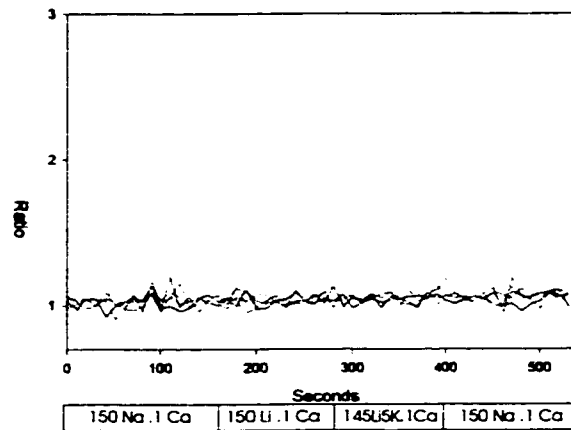
**b.** *RCRII*<sub>2</sub>, CR cell line

**c.** *RIF*<sub>2</sub>, IF cell line

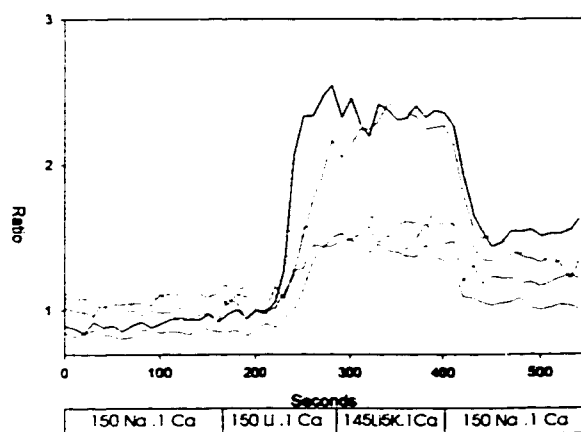
**d.** *RIFC*<sub>2</sub>, IFC cell line

**e.** *CK1.4*, NCX1 cell line.

a. DG44

b. RCR11<sub>2</sub>c. RIF<sub>2</sub>d. RIFC<sub>2</sub>

e. CK 1.4



expression while lacking detectable functional activity. Immunohistochemical observation of the stable CHO cell line expressing the CR external loop deletion mutant was performed with fluorescein-linked monoclonal antibody specific for the cytosolic loop of the Na/Ca+K exchanger (Figure 4.25). Staining is seen throughout the cell and, while detection of the epitope is strong, it was not possible to conclusively determine whether or not some of the heterologously expressed exchanger mutant protein was transported to the plasma membrane.

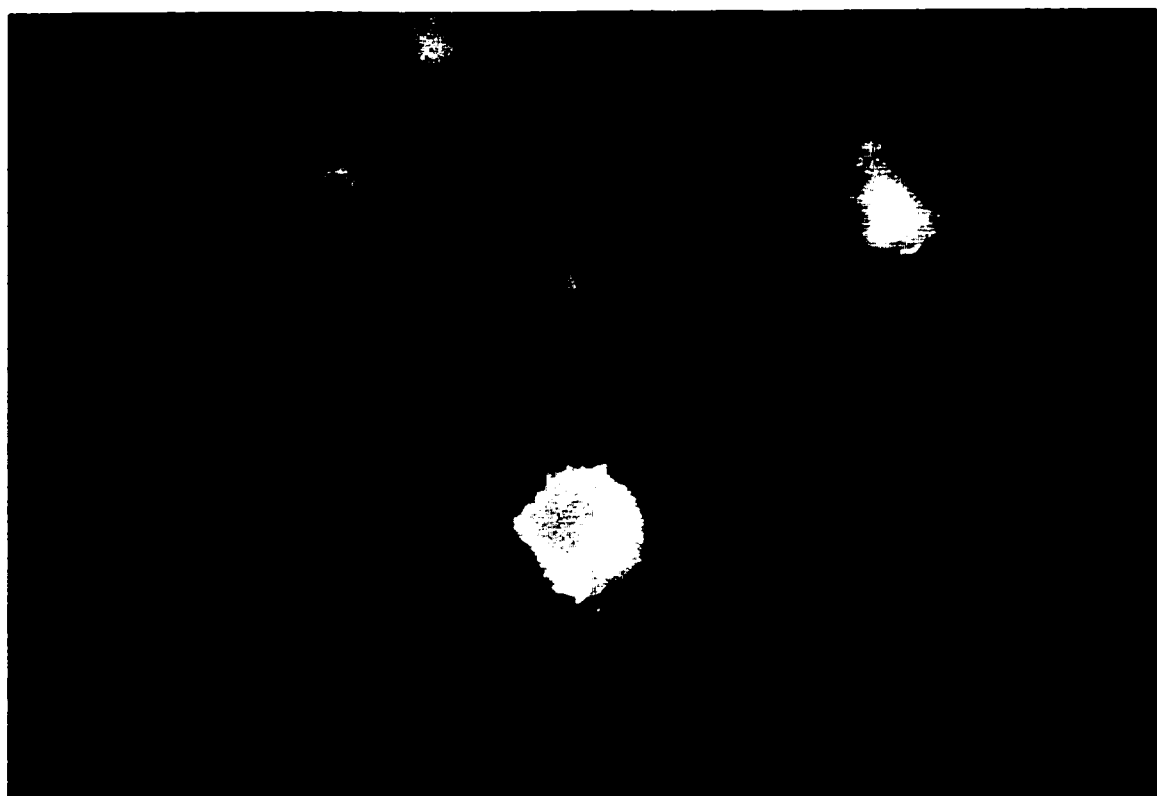
HEK cells were examined for expression system suitability. Unambiguous detection of K-dependent Na/Ca exchange was found to be difficult. The use of ouabain, an inhibitor of the Na/K ATPase, to Na load HEK cells appeared to stimulate an inherent K-independent Na/Ca exchange activity, as vector transfected cells imported calcium after sodium loading (data not shown). It is worth noting that the Na/Ca exchanger NCX1 cDNA has been RT-PCR cloned from the HEK cell line (Loo and Clarke, 1994). Alteration of the Na-loading procedure to a two hour incubation in a high Na solution, reduced the apparent Na/Ca exchange activity in control cells, yet did not result in the detection of K-dependent Na/Ca exchange for any of the mutant constructs.

The baculovirus constructs were found to express large quantities of protein in SF9 and SF21 insect cells. However, <sup>45</sup>Ca uptake experiments detected Na/Ca exchange activity only from the full length Na/Ca exchanger and not from any of the chimeric / deletion mutants (data not shown). It has been the experience in our lab, that if <sup>45</sup>Ca flux experiment fail to reveal Na/Ca exchange, single cell digital imaging experiments will fare no better.

Upon selection of stable HighFive insect cell lines, using the pEIA-vector heterologous expression system, respectable protein expression of each mutant exchanger

**Figure 4.25****Fluorescein-linked Immunohistochemistry of RCR11-CHO Cells.**

A stable CHO cell line carrying the RCR11 construct was grown on coverslips and permeabilized as described. Incubation with the bovine NCKX1 specific monoclonal antibody was followed by fluorescein-linked secondary antibody and visualization with the appropriate filtered light. The antibody clearly detects the bovine NCKX1 epitope but fails to unequivocally label the plasma membrane.



construct examined was detected (data not shown, but see (Szerencsei et al, 2000)).  $^{45}\text{Ca}$  uptake experiments, performed by others in our laboratory and published elsewhere (Szerencsei et al, 2000), demonstrated Na/Ca exchange from both the NCX1 and, for the first time, from the OF Na/Ca+K exchanger double deletion mutant. Significantly, the Ca uptakes for the OF construct were K-dependent, as is the native rod Na/Ca+K exchanger from which the mutant was derived. Fluo-3 free cytosolic Ca measurements, were attempted as a companion to the  $^{45}\text{Ca}$  total calcium fluxes assays. Unfortunately, the HighFive cells, in which the exchanger mutant constructs were expressed, rapidly removed the internalized dye, possibly through an anionic transporter, and thus precluded Fluo-3 spectrofluorometric detection of cytosolic free Ca.

Single cell digital imaging of the stable HighFive insect cell lines expressing NCX1 and OF constructs was then performed, using the dual wavelength indicator FURA-2. Modification of the external cationic conditions, accomplished by solution switching as described, demonstrated K-independent reverse Na/Ca exchange from the NCX1-expressing cell line (Figure 4.26 b). As was observed for the digital imaging experiment of the Na/Ca exchanger expressed in a stable CHO cell line (Figure 4.24 e), cytosolic Ca concentrations rapidly plateaued and remained relatively steady until conditions were altered to those favoring Ca extrusion whereupon cytosolic Ca swiftly returned to its original level. When the experiment was repeated with the Na/Ca+K exchanger OF double deletion mutant (Figure 4.26 a), reverse Na/Ca exchange was found to be K-dependent, as it was in the  $^{45}\text{Ca}$  experiments (Szerencsei et al, 2000). Ca influx occurred less rapidly when mediated by the OF construct than for the NCX1 exchanger, and decayed from the peak cytosolic Ca level,

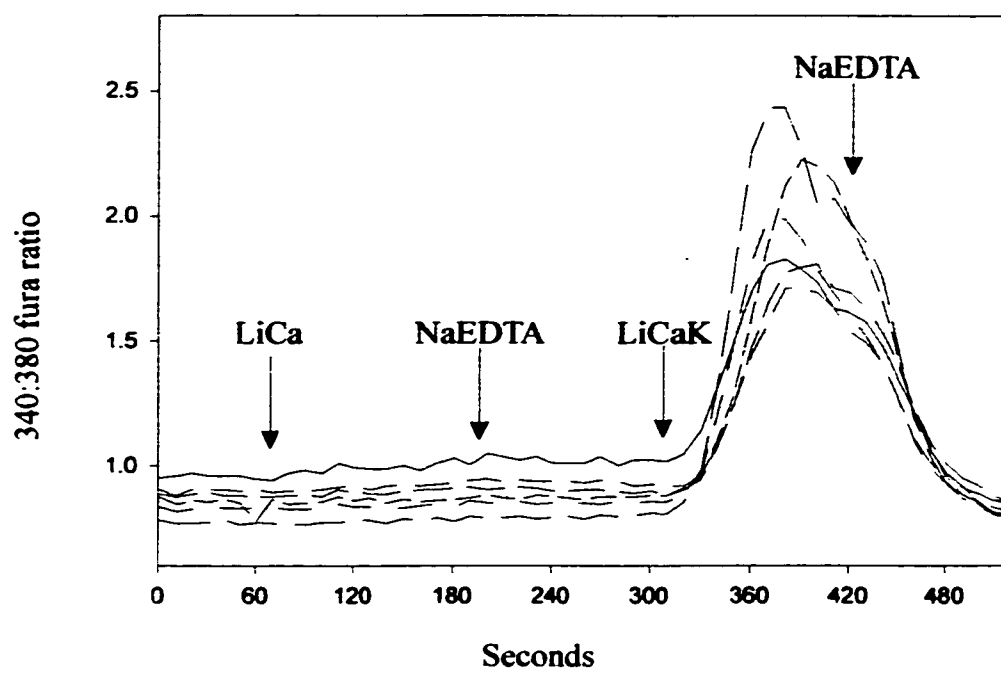
**Figure 4.26**

Early p17, OF Digital Imaging Results.

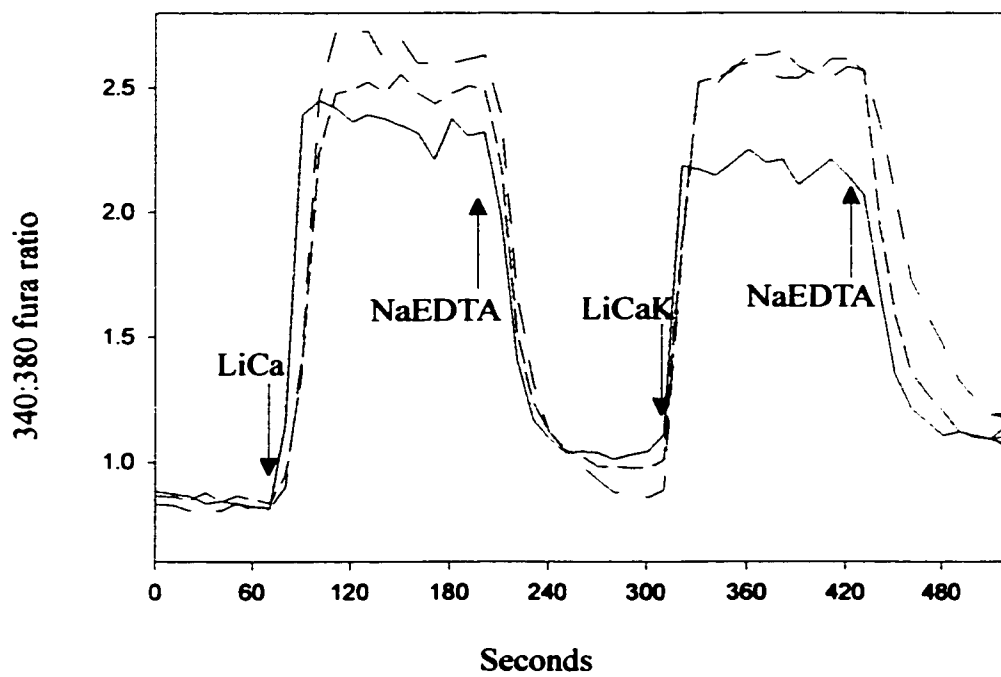
**a.** 340/380 Fura-2 fluorescence ratios for individual cells from the stable OF HighFive line vs. time (seconds). Bathing solutions were changed as indicated. LiCa solution fails to initiate Ca influx whereas LiCaK solution triggers a rise in cytosolic Ca. NaEDTA is expected to drive Ca out of the cell via forward exchange. Solutions: LiCa, 150 mM LiCl, 6  $\mu$ M  $\text{CaCl}_2$ ; LiCaK, 130 mM LiCl, 6  $\mu$ M  $\text{CaCl}_2$ , 20 mM KCl; NaEDTA, 150 mM NaCl, 100  $\mu$ M EDTA.

**b.** Fura-2 fluorescence ratios for individual cells from the stable NCX1 HighFive line vs. time (seconds). Unlike the OF line, the NCX1 stable line undergoes Ca influx upon addition of either LiCa or LiCaK solution. The bathing solutions and switches thereof are as for **a**.

a.



b.





rather than maintaining a plateau. Ratio imaging traces in Figure 4.26 are of individual cells. The promising results demonstrated by the OF NCKX1 double deletion mutant in the HighFive insect cell system led to further characterization of the Na/Ca exchange activity it mediated.  $^{45}\text{Ca}$  uptakes, which measure total Ca fluxes, were performed by others in our lab (Szerencsei et al, 2000). Here are detailed the results of FURA-2 single cell digital imaging studies which measured free cytosolic Ca.

### **Digital Imaging Protocol Modification**

$^{45}\text{Ca}$  fluxes consistently demonstrated reverse Na/Ca exchange mediated by the OF construct as K-dependent Ca uptake (Szerencsei et al, 2000). However, single cell digital imaging experiments of the OF cell line were often unreliable; whether or not Na/Ca+K exchange was observed varied from day to day and from one coverslip (on which the cells were grown) to the next. Often, in a field of view only 5 - 10 showed K-dependent Na/Ca exchange (Figure 4.27). This is not consistent with the fact that each cell of the stable line should have been genetically identical. Several refinements to the protocol were employed to improve the reproducibility of the digital imaging results.

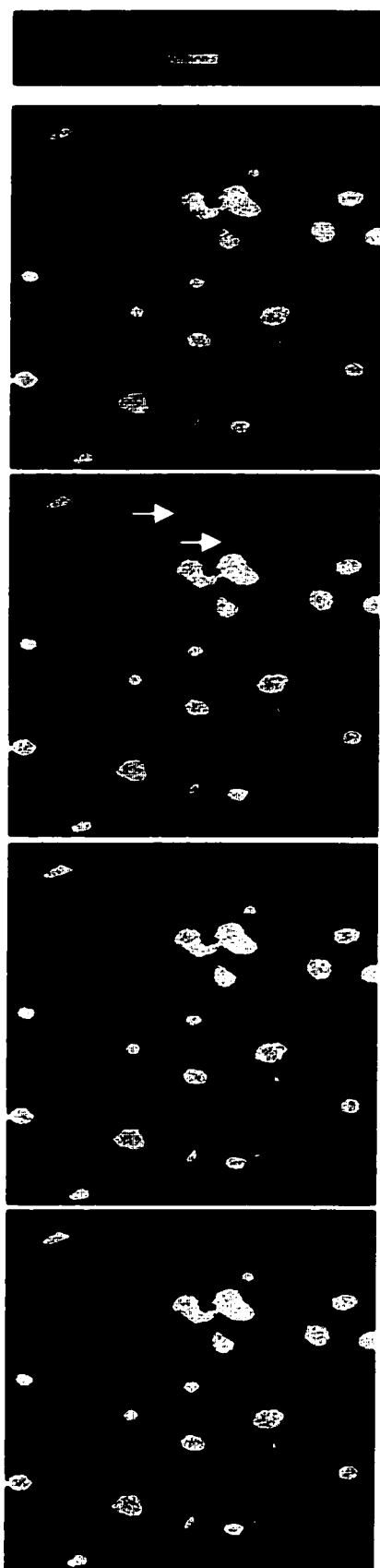
### *Isotonicity of External Medium*

Rod outer segments are compliant with a large dynamic range of tonicity. However, the insect culture cells we employed were apparently much less plastic. Significant heterogeneity in cytosolic Ca was observed both prior to and during digital imaging experiments, possibly due to perturbation of the transmembrane cationic gradients, resulting from hypertonicity-induced turgor pressure leading to membrane compromise. Sucrose was added to digital imaging solutions as a non-charged solute to increase osmolarity to be

**Figure 4.27**

**Low Percentage of Cells Displaying K-dependent Na / Ca Exchange.**

Screen captures of a field of view show the HighFive OF cell line subjected to bathing solutions as indicated. In LiCaK (third panel) two of the cells, indicated by white arrows, display increased 340:380 FURA-2 fluorescence ratios. Upon return to NaEDTA (fourth panel) the cytosolic Ca (as measured by 340:380 ratio) has returned to the original level. *NaEDTA*; *LiCa*; *LiCaK* solutions are as indicated in Table 2 (Chapter 3: Materials and Methods)



isotonic with HighFive cell culture media (GibcoBRL, 1997). This alteration to the protocol resulted in the reduction of the number of cells spontaneously uptaking Ca and an increase in the number displaying K-dependent Na/Ca exchange. However, the majority of cells on each coverslip still did not demonstrate Na/Ca+K exchange, despite their presumed homogenous genetic identity.

### *Na Loading*

Detection of reverse Na/Ca exchange in cells that were not Na-loaded prior to the experiment was consistently very difficult. Under physiological conditions of the rod outer segment, the Na/Ca+K exchanger mediates forward exchange (ie. Ca extrusion) exclusively. In order to reverse the direction of ion translocation, it is necessary to move one or more of the Na, Ca and K ion gradients far from the physiological norm.

Digital imaging found that elevating external K to 100 mM or greater resulted in apparent positive results from negative control cells; many would show an increase in cytosolic Ca. Raising the external Ca above 1 mM caused some of the cells examined to permanently elevate cytosolic Ca levels prior to changing the LiCa external solution to LiCaK; these cells were thereafter unresponsive to further perturbations of the ionic environment (data not shown).

Elevation of cytosolic Na has been observed to accelerate the rate of reverse Na/Ca+K exchange, in rod outer segments (Schnetkamp et al, 1995). When the HighFive cells were used in <sup>45</sup>Ca experiments, Na-loading was efficiently accomplished with monensin, as the cells were easily resuspended and the monensin removed via multiple washes with 1% BSA. For digital imaging experiments, where the cells had to remain

attached to the glass coverslip during washing, 1% BSA rinses were apparently incapable of removing all of the monensin. Residual ionophore then equilibrated the Na gradient, and precluded the measurement of Na/Ca exchange. Two hour incubation in NaCl solution was employed as an alternative, passive Na-loading method. While the resultant cytosolic Na concentrations were not measured, this procedure did allow sufficient Na-loading to drive exchange activity, which was qualitatively dependent on the Na concentration of the loading solution (Figure 4.28) as well as on the length of time for which the Na-loading had occurred (data not shown). Figure 4.28 shows the average of a number of cells that responded to altering the external cation solution from one which promoted Ca efflux (LiCa) to one which promoted Ca influx (LiCaK).

#### *Temperature Modulation*

It was reported (Szerencsei et al, 2000) that temperature affects the activity of heterologously expressed Na/Ca exchangers, possibly by altering the fluidity of the plasma membrane. The significant rigidity of the tissue culture cell plasma membrane could impede conformational changes necessary for ion translocation. Insect cells in which the OF construct was expressed were moved from room temperature to the more physiologically relevant (for the native exchanger) 32°C, for the duration of the experiment. This protocol modification resulted in an increase in the number of cells in the average field of view in which Na/Ca exchange activity was detected.

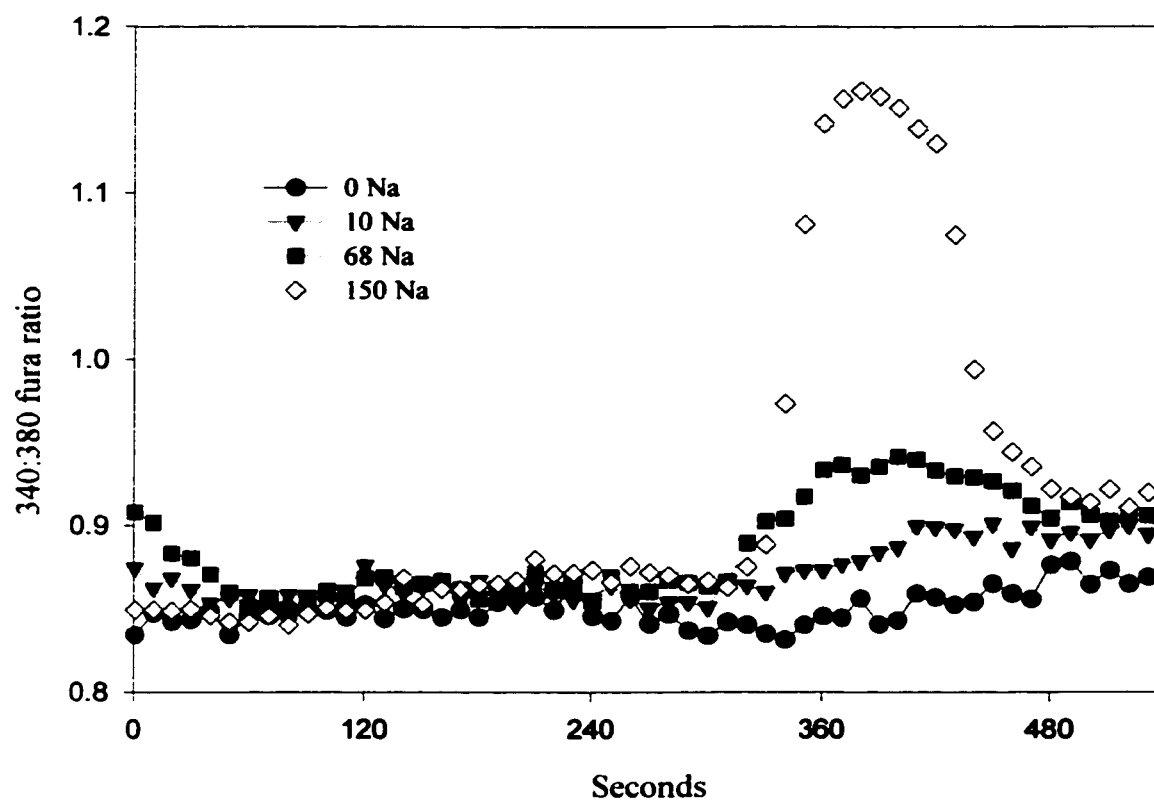
#### *Prevention of Sequestration*

<sup>45</sup>Ca uptake experiments continued to demonstrate strong exchange activity compared to the still somewhat inconsistent digital imaging results. This apparent contradiction might

**Figure 4.28**

Dependence K-dependent Na/Ca Exchange on Na-loading.

340:380 fura-2 fluorescence ratios of HighFive OF stable cells bathed in external solutions as indicated below the graph. One hour preincubation of the cells in sucrose-balanced isotonic solutions that contained 0, 10, 68 or 150 mM NaCl. The readings of 10-20 cells, taken at 10 second time points, are averaged for each Na preincubation concentration as indicated (*inset*).



be explained if Ca influxes were being masked due to internal sequestration by endogenous Ca homeostasis mechanisms. To curtail Ca sequestration, the Na-loading solution was modified to include 5  $\mu$ M FCCP (a protonophore that prevents Ca buffering in the mitochondria) and 5  $\mu$ M thapsigargin (which interferes with the SERCA pump and inhibits Ca storage in the endoplasmic reticulum). Figure 4.29 demonstrates that, with this protocol, K-dependent Na/Ca exchange activity was at last observed for as much as 50% of the cells in a field of view. Note that despite the increased homogeneity of the individual cells responses to cationic gradient alterations, the peak cytosolic Ca concentrations, indicated by the 340:380 FURA-2 ratio, were not identical from one cell to the next. Therefore, there may likely exist other variables which contribute to each individual cells ability to import, export and otherwise handle Ca.

In Figure 4.30 the 340:380 FURA-2 fluorescence ratios of individual cells are graphed versus time. Screen captures of the field of view correlate with measured changes to the fluorescence ratios and hence to the cytosolic Ca concentration. Note that cytosolic Ca levels decline and reach a plateau prior to the switching of the bathing solution to NaEDTA.

### **Qualitative Observations**

In rod outer segments, the Na/Ca+K exchanger is the only protein known to mediate Ca extrusion. Therefore, Na<sub>o</sub>-dependent Ca efflux is easily measured *in situ* following Ca loading, as cytosolic Ca levels remain high until forward exchange mediated by the Na/Ca+K exchanger is stimulated. In the HighFive insect cells, cytosolic Ca levels drop rapidly to resting concentrations once the cationic conditions no longer promote continuous Ca influx. Replacement of external LiCaK solution with any of LiEDTA, NaEDTA, LiCa, NaCa or



**Figure 4.29**

**Thapsigargin / FCCP Addition Increases Percentage of Responding Cells.**

340:380 fura-2 fluorescence ratios clearly shows K-dependence (eg. cell indicated by purple arrow) for close to 50% of all OF expressing HighFive cells within the field of view. Nevertheless, some cells still do not respond to external Ca and K, (eg. cell indicated by white arrow). Solution switches are as indicated by the colored bars beneath the screen captures.

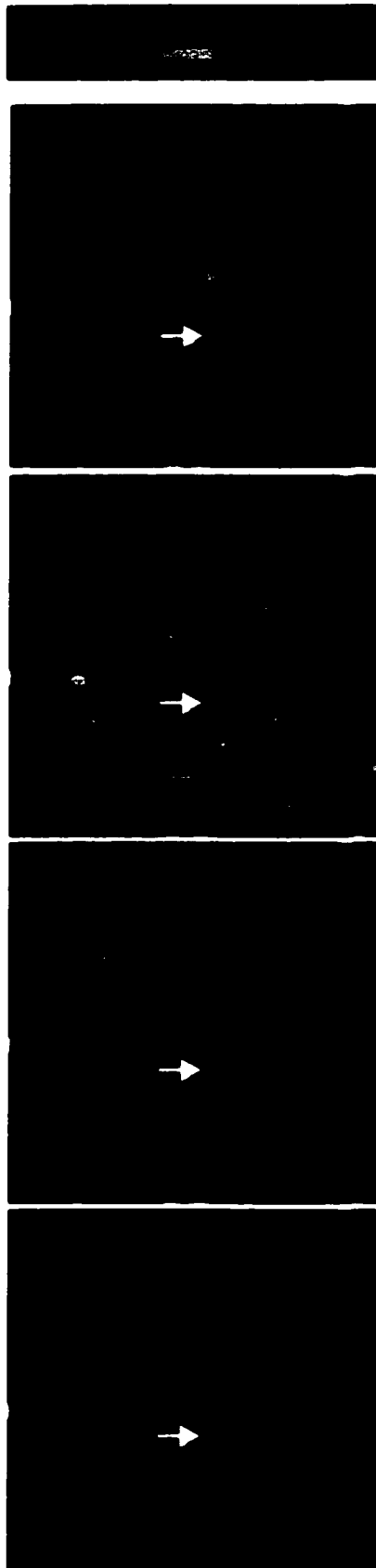
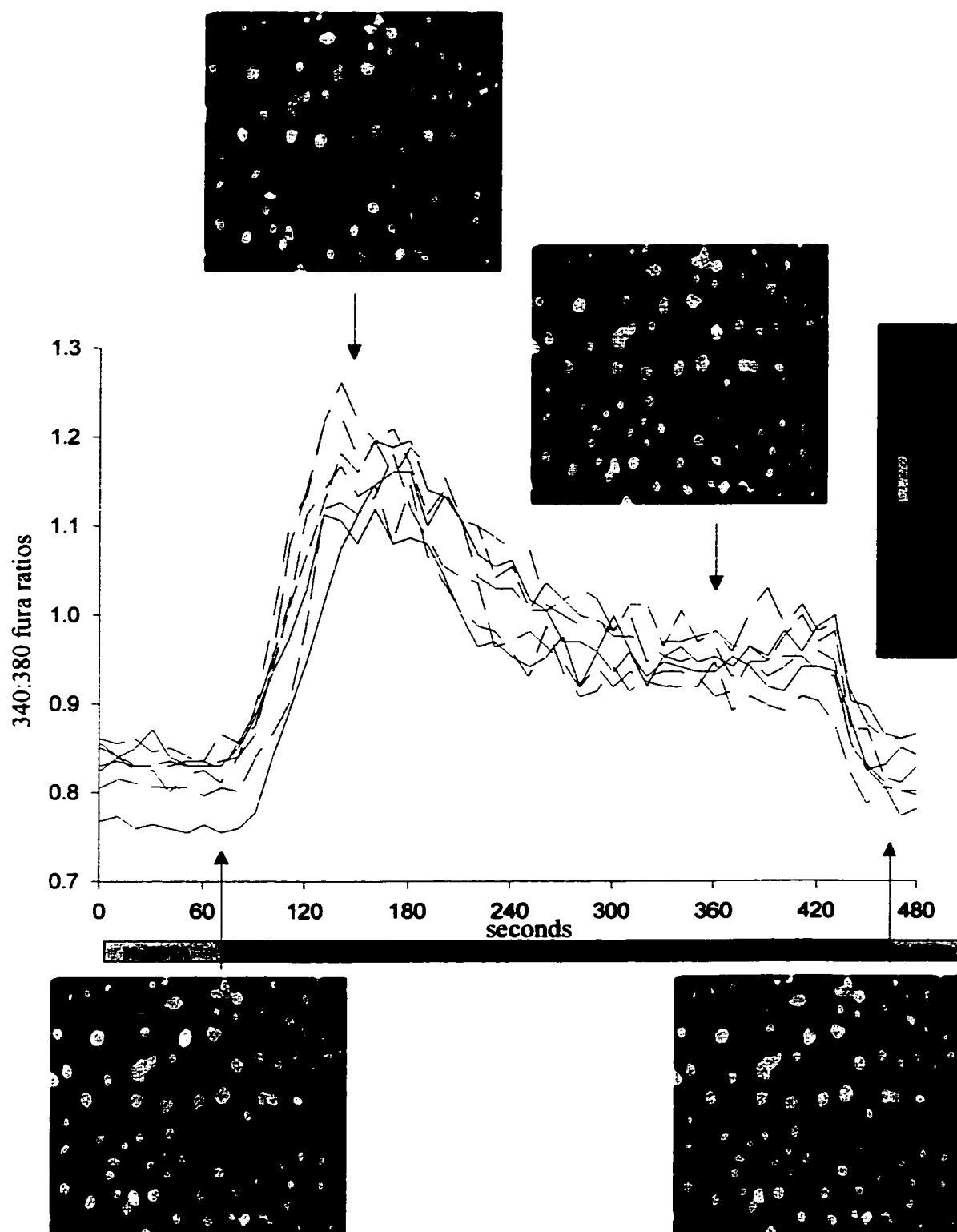


**Figure 4.30**

**340:380 ratios of Individual Cells Correlated with Screen Captures.**

Fura-2 digital imaging was performed as described. Individual cells were selected and the ratio of 340:380 fluorescence was plotted against time. Sample frames of the visual window are shown, *insets*, at different times, as indicated by the *arrows*. 340:380 fura-2 fluorescence ratios are represented by pseudocolors. Time is in seconds.



CholineCa resulted in the rapid decline of the cytosolic Ca concentration (Figure 4.31 and data not shown).

Intriguingly, comparison of the activity of the Na/Ca exchanger and the OF Na/Ca+K exchanger double deletion mutant reveals differences in the maintenance of an elevated steady state Ca level in the HighFive cells. The stable cell line expressing NCX1 consistently showed a K-independent rapid rise of cytosolic Ca upon replacement of the external media with a Na-free media containing Ca (eg. Figure 4.26b).  $^{45}\text{Ca}$  uptake experiments showed continued, although decelerating, Ca influx during the same time period that cytosolic Ca apparently remained at an elevated steady state according to the digital imaging results (Figure 4.32b and data not shown, see also (Szerencsei et al, 2000)). This suggested that an apparent equilibrium was reached between Ca influx mediated by the heterologously expressed Na/Ca exchanger and cytosolic Ca depletion mediated by an endogenous Ca extrusion or buffering mechanism. Removal of Ca from the external media resulted in the very rapid reduction of cytosolic Ca levels, to the original resting concentration.

The OF stable line invariably showed a rapid rise in cytosolic Ca upon incubation in Na-free media containing Ca and K, which was then followed by a relatively slow decline of cytosolic Ca to a lower, steady state concentration (Figure 4.32a). This 'falling-phase' suggests that, in contrast to the Na/Ca exchanger, the Na/Ca+K exchanger is unable to maintain Ca flux equilibrium with the endogenous Ca homeostasis mechanism, perhaps due to a decrease in the rate of exchange it mediates from the initial high activity. Subsequent removal of K or Ca from the external media, then caused the rapid decline of cytosolic Ca concentration, as was observed for the NCX1 Na/Ca exchanger, to the original resting level.

**Figure 4.31****Multiple Exchange Cycles for OF Clones.**

Averaged fura-2 340:380 fluorescence ratios measured from eight individual HighFive cells from the stable HighFive OF cell line. Three cycles of rising and falling of cytosolic  $\text{Ca}_i$  levels are shown. Each cycle is initiated by the bathing solution switch to LiCaK (130 mM Li, 20 mM K, 6  $\mu\text{M}$  Ca). The first cycle is terminated by the bathing solution switch to LiCa (150 mM Li, 6  $\mu\text{M}$  Ca). The second cycle is terminated by the switch of the bathing solution to LiEDTA (150 mM Li, 100  $\mu\text{M}$  EDTA). The third cycle is terminated by the addition of NaEDTA (150 mM Na, 100  $\mu\text{M}$  EDTA). Time is as indicated in seconds.

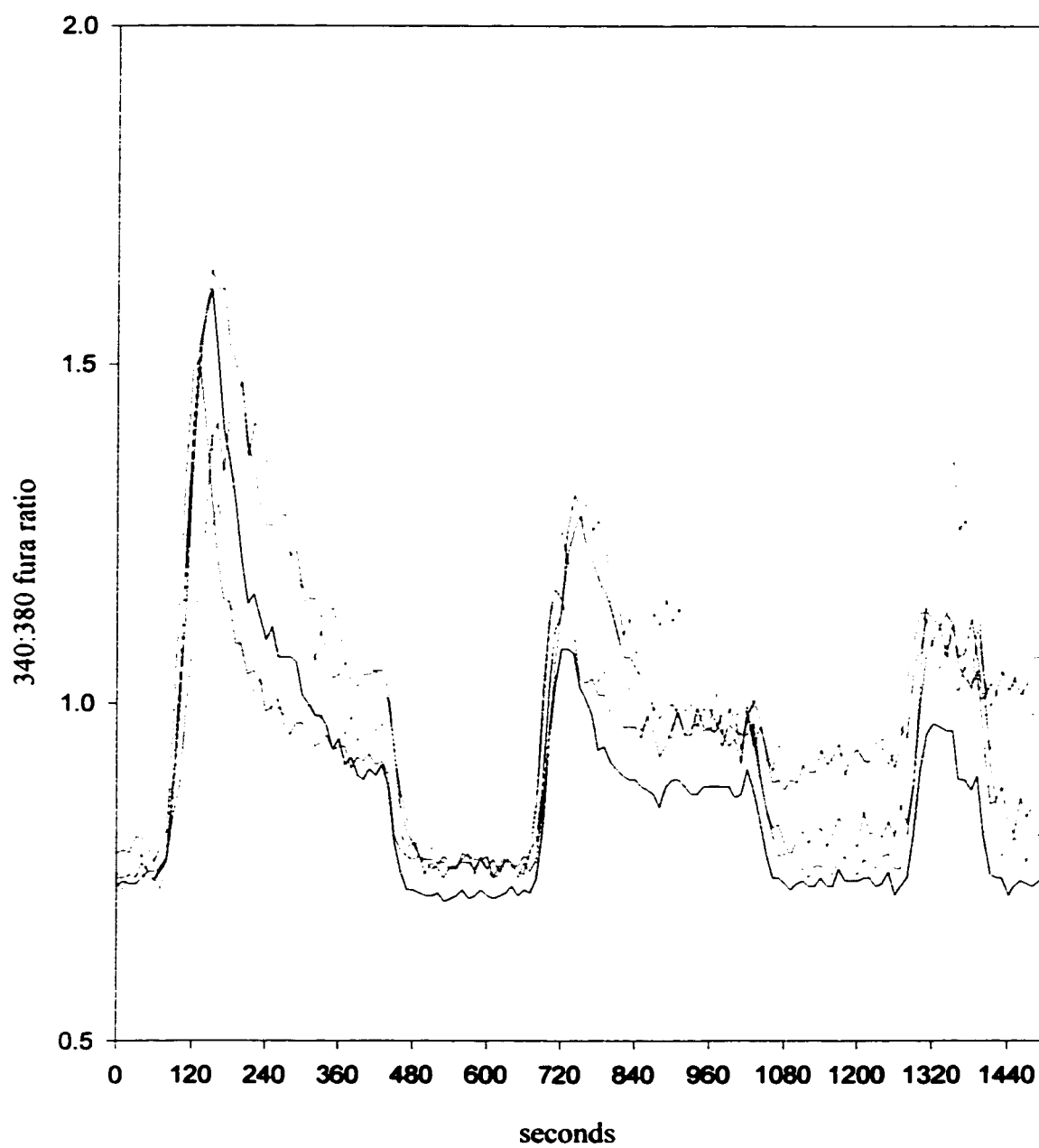


**Figure 4.32**

Characteristic Kinetic Curve of Ca Influx: NCX vs OF.

**a. OF mediates K-dependent Ca transport.**

Once peak  $Ca_i$  levels are reached, usually in 30 to 60 seconds, a secondary phase is observed. Internal free Ca levels decline over several minutes until a plateau is reached.  $Ca_i$  remains relatively constant at this level, until external Ca or K is removed. Cytosolic Ca levels then drop precipitously to the initial resting concentration.

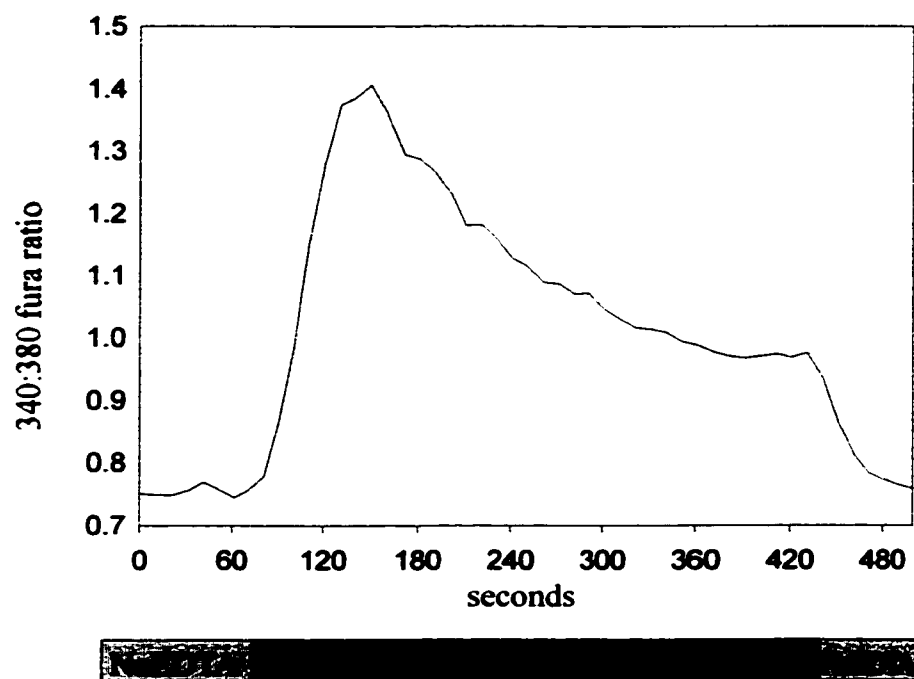
**b. NCX mediates Ca transport.**

Upon reaching equilibrium with the endogenous Ca extrusion mechanism of the HighFive cells, cytosolic Ca levels remain relatively constant. Following removal of external Ca, the cytosolic Ca levels plummet very rapidly to the initial resting concentration.



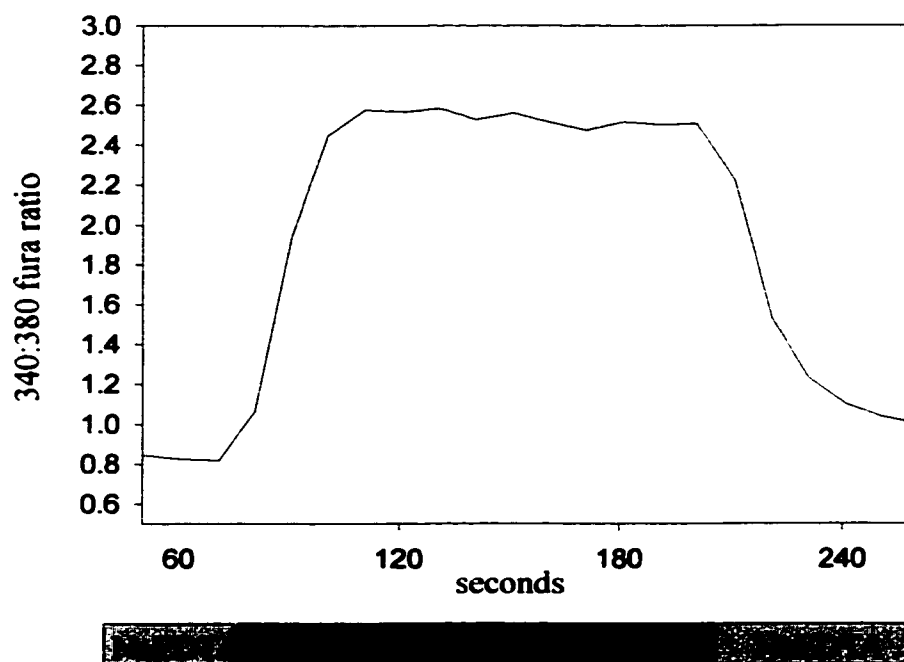
a.

## OF - HighFive Cells



b.

## NCX1 - HighFive Cells



The distinct kinetics of the two falling steps in Ca removal for the heterologously expressed OF double deletion mutant suggest that two discrete mechanisms operate. The first mechanism, the endogenous Ca extrusion/buffering phenomenon, appeared to be inherent to the expression system cells, and the second mechanism, possibly an exchanger inactivation phenomenon, was specific to the OF Na/Ca+K exchanger double deletion mutant. Quantification in the HighFive insect cells of Na/Ca exchange from both the OF and NCX1 constructs was hampered by the apparent endogenous Ca extrusion mechanism. While modification of the digital imaging protocol as described above revealed Ca influx, the insect cells were unable to maintain elevated cytosolic Ca levels in the absence of external Ca (and K in the case of OF), i.e. when the exchanger clone present wasn't actively transporting Ca into the cell. This precluded the possibility of measuring forward Na/Ca exchange, as the endogenous Ca extrusion/buffering mechanism was too rapid to allow any meaningful measurement of superimposed Ca extrusion mediated by the heterologously expressed exchanger mutants.

#### **Determination of $K_m$ Ca and $K_m$ K**

The qualitative reproducibility of the FURA-2 measurement of Ca fluxes mediated by the heterologously expressed mutant OF exchanger justified an attempt to measure  $K_m$  values in order to further characterize the OF mutant and compare it to the native exchanger. In light of the rapid endogenous apparent Ca extrusion/buffering mechanism observed to operate in the HighFive cells, measurement of forward exchange, in which Ca and K are transported out of the cell in exchange for Na, is untenable employing the digital imaging protocol. Using reverse exchange to quantify activity mediated by the OF mutant is also

problematic, considering that an endogenous apparent Ca extrusion/buffering mechanism of unknown activity is operating in the HighFive cells. However, the relative initial reverse exchange rates, i.e. those for the first 30 seconds or so of Ca influx, were found to be dependent on external Ca and K concentrations in pilot experiments (data not shown). It follows that, although the *absolute* rates of exchange would be difficult to measure in a system with an unknown cytosolic Ca homeostasis mechanism, the *relative* rates would still reflect the  $K_m$  values of the underlying exchange activity. It was undertaken, therefore, to compare the relative rates of the initial exchange activity, varying the external Ca or K concentrations, and thus arrive at representative  $K_m$  values for Ca and K.

Due to the observed heterogeneity from cell to cell in terms of the absolute Ca levels reached during reverse exchange, it would have been most accurate to examine each cell individually at various concentrations of K or Ca to investigate the cation dependence. As can be observed in Figure 4.31, in our system the exchange activity displayed significant run-down during repeated cycles of exchange, precluding the use of a single cell for multiple measurements. Therefore, the average of fura-2 ratios (representing the free cytosolic Ca) from many cells was used instead. The assumption was made that changes in free cytosolic Ca equated to changes in total cellular Ca. One second timepoints were employed to measure the initial rise in Ca for 30-60 seconds. It was observed that relative rates were most consistent within the experiments conducted on a single day, rather than between different days. To generate  $K_m$  values, the apparent initial rates were therefore compared directly only with experiments conducted on the same day. Calculated  $K_m$  values from different days were subsequently compared to one another.

Each initial rate calculated generally represents the average of 20-25 cells, although occasionally as many as 50 are represented. Figure 4.33a shows a typical Ca-dependence, with the fluorescence ratios normalized to a basal level for illustration purposes. Initial rates were determined from best fit slopes of the first 30-60 seconds of each trace. As seen for one of the 10  $\mu\text{M}$  concentration data points in Figure 4.33a, some scatter is apparent. Plotting of the rates on a Lineweaver-Burke plot and calculation of the linear function by regression methods allowed the determination of  $K_m$  for Ca (Figure 4.33b). Initial rates and  $K_m$  calculation for five separate complete experiments resulted in an averaged  $K_m$  Ca value of 9  $\mu\text{M}$  s.e. 3  $\mu\text{M}$ .

An illustrative K-dependence experiment is presented in Figure 4.34. Rate plotting and  $K_m$  calculation were performed as for Ca. As was observed in the Ca-dependence experiments, some scattering in the data is evident. When the  $K_m$  K values calculated for individual days were compared to one another, they were found (like the  $K_m$  Ca values) to be reasonably consistent. Initial rates and  $K_m$  calculation for three separate experiments resulted in an average  $K_m$  K value of 8 mM s.e. 0.9 mM.

$K_m$  Ca and  $K_m$  K have been determined for the native rod Na/Ca+K exchanger *in situ* at 1  $\mu\text{M}$  (Schnetkamp, 1991) and 1.5 mM (Schnetkamp et al 1989; Schnetkamp et al, 1991a) respectively. These values are similar to the results presented here, and also comparable to results from our laboratory reported elsewhere employing the OF deletion construct while measuring  $K_m$  with  $^{45}\text{Ca}$  flux experiments (Table 3). Competition with Li at the cation binding sites was suggested to result in  $K_m$  determinations that are lower in affinity than those observed in the absence of Li (Szerencsei et al, 2000). As presaged for the high Li

**Figure 4.33**

Ca-dependence of Na/Ca+K Exchange Mediated by OF.

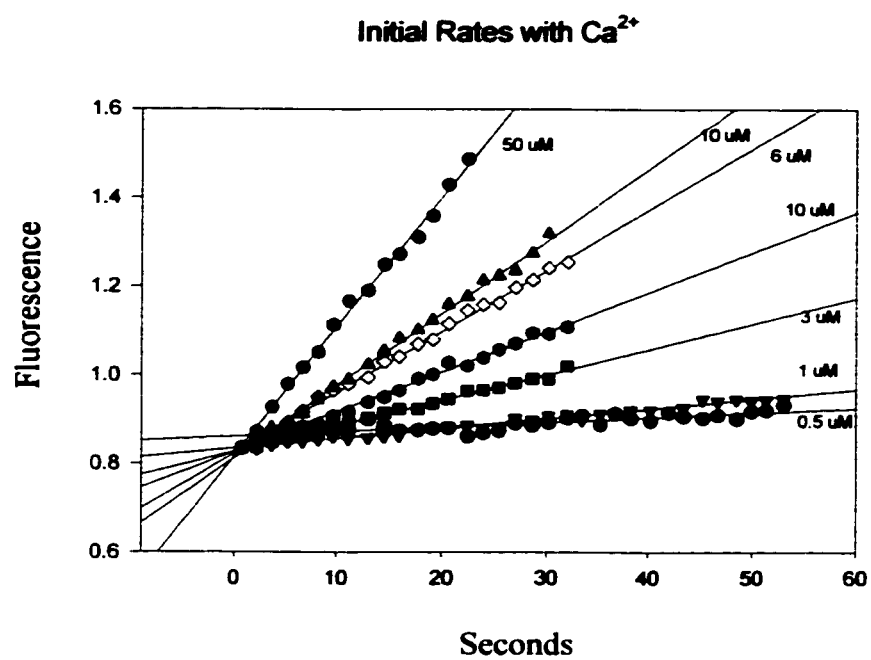
**a. Initial rates.**

The 340:380 fura-2 fluorescence ratios for 20 to 50 cells were averaged for each 1 second time point. The 20 to 55 seconds of relatively linear fluorescence increase following the application of LiCaK bath solution was considered valid to determine the initial rate. All traces were normalized to the 0.5  $\mu\text{M}$  plot, so that each had the same origin. In all cases K concentration was maintained at 20 mM and Li at 130 mM. Ca concentrations for each trace are as indicated. Initial rates were calculated by linear regression and are shown as a black line for each trace.

**b. Lineweaver-Burke plot.**

The reciprocals of each initial rate were plotted against the reciprocal of the associated Ca concentration, in  $\mu\text{M}$ . The best fit line connecting the points was determined by linear regression. The negative reciprocal of the best fit line is the calculated  $K_m$ .

a.



b.

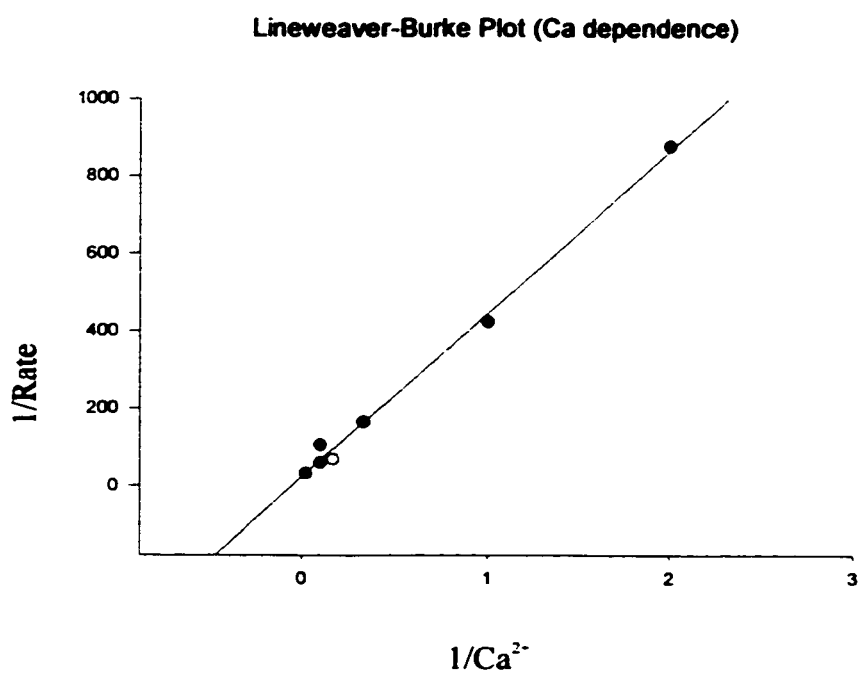


**Figure 4.34**

K-dependence of Na/Ca+K Exchange Mediated by OF.

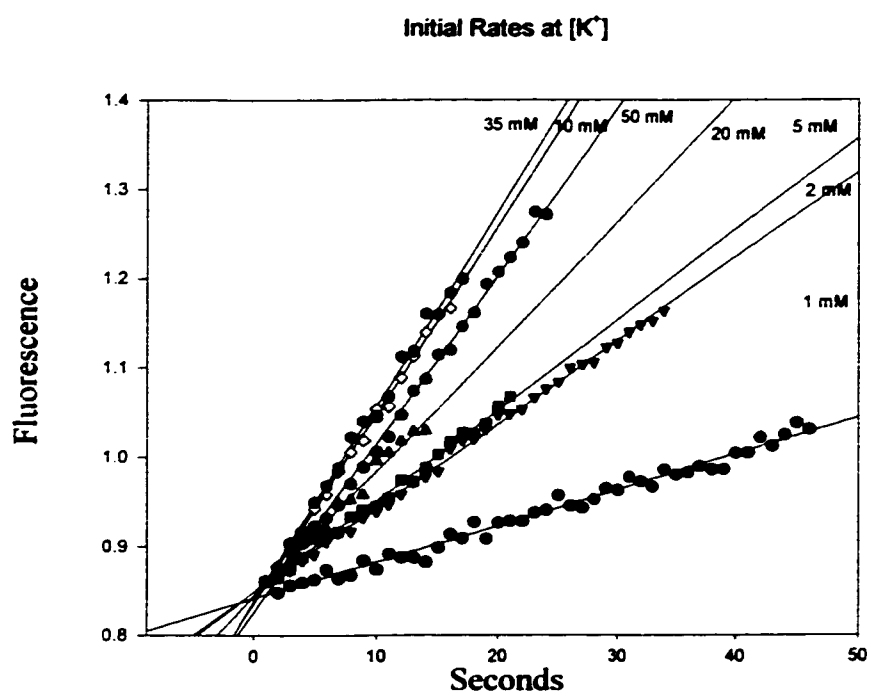
**a. Initial rates.**

The 340:380 fura-2 fluorescence ratios for 20 to 50 cells were averaged for each 1 second time point. The 15 to 45 seconds of relatively linear fluorescence increase following the application of LiCaK bath solution was considered valid to determine the initial rate. All traces were normalized to the 1 mM plot, so that each had the same origin. In all cases Ca concentration was maintained at 20  $\mu$ M while Li was balanced with K such that their total concentration was always 150 mM. K concentrations for each trace are as indicated. Initial rates were calculated by linear regression and are shown as a black line for each trace.

**b. Lineweaver-Burke plot.**

The reciprocals of each initial rate were plotted against the reciprocal of the associated K concentration, in mM. The best fit line connecting the points was determined by linear regression. The negative reciprocal of the best fit line is the calculated  $K_m$ .

a.



b.

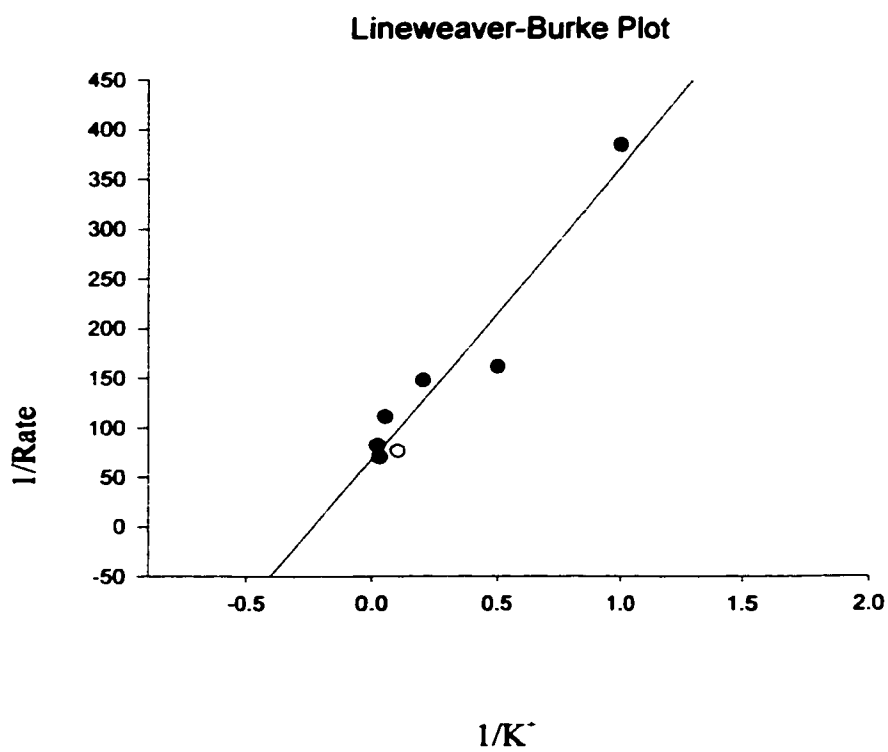




**Table 3**

Calculated and Published Values for  $K_m$  K and  $K_m$  Ca for OF (NCKX1) Reverse Na/Ca+K Exchange.

Published concentration values representing half-maximal activation ( $K_m$ ) of reverse exchange mediated by the bovine rod NCKX1 exchanger are presented. *DI*, digital imaging data;  $^{45}\text{Ca}$ ,  $^{45}\text{Ca}$  influx experimental data;  $\dagger \text{Li}$ , experiments carried out in the presence of high Li concentrations.

**References:**

1. (Schnetkamp et al, 1991)
2. (Schnetkamp et al, 1989)
3. (Schnetkamp, 1991)
4. (Szerencsei et al, 2000)

**Table 3**      Calculated and published  $K_m$  activation values for K and Ca  
(OF vs. NCKX1) Reverse Na/Ca+K exchange.

Cation	OF (bNCKX1dd)		ROS	
	$K_m$ (DI) $\uparrow$ Li	$K_m$ ( $^{45}$ Ca) $\uparrow$ Li	$K_m$ act.	$K_m$ act. $\uparrow$ Li
Ca	9 $\mu$ M s.e. 3	n/a	1 $\mu$ M <sup>3</sup>	n/a
K	6 mM s.e. 0.9	10-20 mM <sup>4</sup>	1.5 mM <sup>1,2</sup>	8 mM <sup>4</sup>

perfusion system employed in these experiments, the  $K_m$  values calculated are of somewhat lower affinities than that of the native rod exchanger in the absence of high Li, and are quite comparable to native rod exchanger in the presence of high Li (Table 3).

#### **4.4.3 Discussion**

##### *Expression of the OF Double Deletion Mutant in HighFive Cells*

Expression in the pEIA system allowed the remediation of several impediments to the detection of Na/Ca exchange activity from heterologously expressed mutant exchangers. Single cell digital imaging experiments convincingly demonstrated the potassium requirement and dependence of the OF construct, and corroborated the results of  $^{45}\text{Ca}$  flux experiments performed by others in our laboratory and reported elsewhere (Szerencsei et al, 2000).

##### *Domain Structure Function Analysis*

The mediation of Na/Ca exchange by the OF construct demonstrated that neither the extracellular domain nor the cytoplasmic loop are required for Na/Ca exchange activity. As hypothesized, and in agreement with results previously reported for the Na/Ca exchanger, (Matsuoka et al, 1993) deletion of the cytosolic domain did not abolish Na/Ca exchange activity. Deletion of the extracellular domain also did not preclude exchange activity; an interesting finding, as there is no similar domain in the NCX1 Na/Ca exchanger. From the results presented here, and results by others in our laboratory published elsewhere, the domains responsible for Na/Ca exchange activity can therefore be relegated to the two large hydrophobic transmembrane regions, which together constitute only about 1/3 of the entire NCKX1 protein's mass. This suggests that the extracellular domain may function in a role

separate from Na/Ca+K exchange. Certainly, these results have demonstrated that the extracellular loop is not required for exchange activity.

K-dependence was observed for the OF double deletion mutant. This finding demonstrates that heterologously expressed NCKX1-derived exchangers still display a requirement for K. In addition, the OF double deletion mutant established that K-dependence is mediated by sequences within the two hydrophobic membrane-spanning domains.

*K<sub>m</sub> Agreement of OF Double Deletion Mutant with the Native Rod Exchanger*

The K<sub>m</sub> values calculated for the OF deletion mutant are in reasonable agreement with those measured for the bovine rod Na/Ca+K exchanger in rod outer segments (Schnetkamp, 1991; Schnetkamp et al, 1989; Schnetkamp et al, 1991a; Szerencsei et al, 2000). It seems then, that the presence or absence of the hydrophilic extracellular and cytosolic loops does not greatly affect the affinities of the binding sites for Ca and K on the extracellular face of the exchanger.

The competitive effect of high concentrations of lithium on the native exchanger has been found to decrease the apparent K<sub>m</sub> affinity for K (Szerencsei et al, 2000). The single cell digital imaging data of the OF double deletion mutant assayed in high Li generated K<sub>m</sub> values in agreement with those reported elsewhere (Szerencsei et al, 2000). High external Li appears to have a similar inhibitory effect on the heterologously expressed double deletion mutant exchanger as it does on the full length native exchanger assayed *in situ* in the rod outer segment.

## **CHAPTER FIVE: DISCUSSION**

## **5.1 Cloning of the Human Rod NCKX1 cDNA**

In 1993, when this project was started, only the bovine rod NCKX1 cDNA sequence had been cloned and sequenced (Reiländer et al, 1992). Based on comparison to the functionally similar NCX1 cardiac exchanger, it seemed likely that sequence homology among mammalian species would be high. Considering the functional similarity and proposed topological resemblance of the NCX1 and NCKX1 exchangers, it was hypothesized that, as for NCX1, the NCKX1 transmembrane sequences would be responsible for the ion translocation events. Sequence homology was also expected to be highest in these hydrophobic domains. There was however, no reason to expect that the extracellular and cytosolic regions would not also retain strong homology between the human and bovine homologues.

The original sequencing of the prototypical bovine NCKX1 cytosolic domain had revealed an acidic region that was repeated eight (later shown to be nine (Tucker et al, 1998b)) times. This repeat domain appeared to hold remarkable promise as an important region for the function of the exchanger, possibly as a Ca binding domain, a cytoskeletal attachment point, a protein:protein interaction domain, or in mediating an unknown function related to the inactivation feature. Just C-terminal to the repeat region is found the poly-glutamic acid (poly-E) stretch. This region, which in the bovine homologue bears 23 glutamic acid and 3 aspartic acid residues in one uninterrupted stretch, might also mediate Ca binding, protein:protein interactions or cytoskeletal attachment. The N-terminal portion of the cytoplasmic region on first inspection was the most inscrutable. No obvious, primary amino acid sequence characteristics, like the poly-E stretch or the 'repeat' region of the C-

terminal portion, presented themselves. This region was later revealed to be the site of alternate splicing, thus perhaps the most intriguing portion of the cytosolic domain.

The extracellular domain was also enigmatic in terms of determining its role in Na/Ca+K exchange. Earlier extracellular protease work suggested that the extracellular domain was not required for Na/Ca+K exchange as measured in rod outer segment preparations. In addition, the Na/Ca exchanger had been shown to mediate Na/Ca exchange through the hydrophobic transmembrane domains (Matsuoka et al, 1993), suggesting that the extracellular region of the Na/Ca+K exchanger also might not be required for this activity.

Elucidation of the human rod NCKX1 cDNA sequence (Tucker et al, 1998b) revealed interesting and unexpected sequence results. While comparison to the NCX1 cDNA predicted high homology conservation across mammalian species, our results demonstrated high homology only in the two transmembrane domains, where the amino acid sequence identities are 94% and 95%, respectively. The putative extracellular domain of the bovine and human NCKX1 cDNAs are only 59% identical, and the cytosolic domain sequences are only 45% identical.

The cytoplasmic domain contains amino acid stretch dropouts in addition to lower overall identity. The bovine acidic repeat region was absent in the human, with only one partial match at the amino acid sequence level. The poly-glutamic acid stretch was still present, and contained 29 glutamic acid and 2 glutamine residues. Due mainly to the lack of the nine repeats, and an 18 amino acid dropout (later revealed to be a splice variant splice-out) near the N-terminal portion, the cytosolic domain of the human NCKX1 cDNA was significantly shorter than that of the bovine.

At the primary amino acid sequence level, comparison of the NCKX1 clones isolated to date show strong homology in the transmembrane domains, but remarkably little homology in the large extracellular and intracellular hydrophilic loops. While the high homology of the membrane spanning segments correlates to the high conservation of function when expressed heterologously, the sequence divergence of the hydrophilic loops suggests other evolutionary forces are in effect for these regions (Szerencsei et al, 2000).

The so-called 'repeat' region of the cytoplasmic loop, first identified in the bovine NCKX1 cDNA, has not yet been associated with a function. Repeats are found in several, but not all species, and differ in their primary amino acid sequence and iteration. This is suggestive of a domain whose structure, size and ionic charge may be more important than the identity of individual residues. Like the human cGMP-gated channel  $\beta$  subunit, the human Na/Ca+K exchanger contains no repeats while bovine homologues of each contain multiple repeats. Speculations as to the role of the repeat regions include involvement in protein : protein interaction, mediation of outer segment targeting, Ca binding or regulatory activities not yet uncovered.

## **5.2 Chromosomal Localization and Role in Human Retinopathy**

Retinitis pigmentosa is a heterogeneous disease characterized by a large number of genetic lesions responsible for the observed phenotypes. Many of the retina specific proteins identified to date have also been implicated as causative agents for RP. While the human NCKX1 has not yet been linked to retinopathy, the large number of genetic lesions expected to be revealed, and the fact that the majority of observed causative genotypes are found in single isolated cases, suggest that it is only a matter of time until a family is found whose RP



genotype is linked to NCKX1. As the Na/Ca+K exchanger performs a critical function in the continuous removal of Ca from the cytosol of the rod outer segment, it is highly likely that mutation- or deletion-induced abrogation of its activity would be pathogenic to the retina.

### **5.3 Genomic Organization and Implications**

The human NCKX1 gene was the first Na/Ca+K exchanger for which the genomic organization was investigated. Educated predictions of the promoter structure and the intron/exon organization were therefore precluded. The limited sequence homology of NCKX1 and NCX1, confined to the  $\alpha$ -repeats, allowed for the possibility that the two gene families have a common origin, and therefore might be similar at the genomic organization level. The repeat region of bovine NCKX1, which has not quite one iteration in the human cDNA, might have been predicted to be flanked by introns, to explain the acidic stretch duplication events. Conversely, the sequence coding for the inscrutable N-terminal portion of the cytosolic domain might have been predicted to contain no introns, as no obvious primary amino acid sequence features were apparent.

#### *Promoter Region*

The 5'flanking region of the human NCKX1 contains sequences which are very much TATA-like, and probably represent a non-canonical TATA / CAAT / Cap transcription initiation region. This is consistent with its apparent tissue specific distribution in retinal rod outer segments. For comparison, consider NCX1, the transcripts of which have been found to originate from three distinct promoters, only one of which is a typical TATA-driven promoter (Scheller et al, 1998; Nicholas et al, 1998).

*Intron / Exon Organization*

Elucidation of the genomic organization revealed greater analogy to the NCX1 gene than would have been predicted by the almost complete lack of sequence homology. Like the NCX1 gene, the 5' portion of the NCKX1 gene from base 161 of the 5' UTR to the end of the coding sequence of the first hydrophobic transmembrane domain, is contained in the long second exon. Several of the  $\alpha$  helices of the second hydrophobic transmembrane domain are separated by introns, and the 3' UTR is contained in one long exon. Most interestingly, the NCKX1 bears a region in the cytoplasmic domain which contains numerous introns in a short stretch. These introns do not flank the sequences coding for the 'repeat' (not repeated in human NCKX1) or poly-E regions, but rather are located in the region coding for the N-terminal end of the cytoplasmic loop. The NCX1 gene also contains numerous introns in the coding sequence of its cytoplasmic loop. In NCX1, the introns are located at the 3' end of the cytoplasmic loop, where they flank the alternately spliced region of the NCX1 cytoplasmic domain. NCX2, the genomic organization of which has been partially revealed, also has a highly analogous arrangement of its introns and exons (Kraev et al, 1996). In contrast, the genomic organization of the rat Na / H exchanger (Nhe3) has been uncovered and found to differ markedly (Kandasamy and Orłowski, 1996). The 16 introns in Nhe3 are distributed uniformly, and the exons range from 71 to 300 bp in size, with the exception of the last exon which contains the 3'UTR and is 1700 bp in length.

The work presented here demonstrates that the clustered introns of the NCKX1 cytoplasmic loop coding sequence, like those of NCX1, flank alternately spliced exons. The significant similarity in genomic organization between NCX1 and NCKX1, despite the lack

of primary sequence homology, is remarkable, and contributes to the contention that an evolutionary link exists between the two distinct types of Na/Ca exchangers.

#### **5.4 Alternate Splicing of NCKX1 Homologues in Mammals**

At the outset of this research project, alternate splicing of the NCKX1 gene had neither been observed nor was it predicted. *In situ* work on the bovine and salamander NCKX1 exchangers did not imply the existence of more than one functionally distinct Na/Ca+K exchanger protein. Northern analysis had not demonstrated obvious multiple transcripts, and RT-PCR and RNase protection assays had not been performed.

The report of the RT-PCR cloning of the rat NCKX1 cDNA was the first report of the discovery of NCKX1 transcript splice variants (Poon et al, 2000). These variants had exons alternately spliced in the cytosolic domain corresponding to the locations where introns were observed in the human NCKX1 gene. The dolphin Na/Ca+K cDNA, cloned in our lab (Cooper et al, 1999a), also appeared to be the result of alternate splicing, as its sequence aligns well with one of the reported rat splice variants. Comparison of the human cloned NCKX1 cDNA with that of the bovine revealed an 18 amino acid dropout that corresponded to known intron sites. Although it was not known at the time, publication of the human NCKX1 cDNA sequence was the first report of a less-than full length Na/Ca+K exchanger splice product.

The RT-PCR and RPA work presented in this thesis confirmed the presence of the alternately spliced NCKX1 gene products in the human and bovine retinas, and determined relative abundances of the major variants, respectively. Additionally, incomplete RT-PCR analysis revealed alternate splicing in the cytosolic domain of the mouse Na/Ca+K exchanger

as well, even though the mouse cDNA has not yet been cloned or sequenced in its entirety.

Alternate splicing of NCKX1 homologues has now been observed in human, bovine, rat and mouse transcripts. The cDNA cloned from the dolphin is also in agreement with major splice isoforms identified in human and rat NCKX1. Assuming that the splice variants identified at the transcript level are translated, the necessity for alternately spliced isoforms of the Na/Ca+K exchanger is intriguing, as there have been no reports suggesting protein products of different functional characteristics. Perhaps the existing data need to be reevaluated for indications of discrete functions attributable to distinct isoforms. It is conceivable that alternately spliced domains may play a role in sub-cellular localization of the exchanger or in protein : protein interactions. Alternatively, various characteristic activities, such as the observed inactivation feature, (Schnetkamp et al, 1991a) may in fact be specific to distinct Na/Ca+K exchanger isoforms. Interestingly, the relative abundance of the different splice variants at the transcript level varies between human and bovine. The splice variant species specificity, if it exists at the protein level, will likely be related to both the function of those exons and the cytosolic environment.

Some of the splice products identified in the human NCKX1 by RT-PCR may represent erratic splice events due to the degradation of the tissue from which the RNA was derived. As evident in the RT-PCRs and even faintly in the RNase Protection Assay, a small percentage of the splice products sequenced coded for presumably non-functional frame-shifted polypeptides. A recent report investigating the alternate splicing in NCX1 (Scheller et al, 1998) found that erratic splice products were observed in a time-dependent fashion following death of the donor tissue, and that these products did not represent the *in vivo*

complement of splice variants.

### **5.5 Expression of OF Double Deletion Construct**

The previously published work of others (Reiländer et al, 1992; Navangione et al, 1997) suggested that heterologous expression of the bovine Na/Ca+K exchanger would produce measurable functional activity. Despite the examination of a number of expression systems, the full length bovine NCKX1 cDNA cloned by Reiländer was not found to mediate heterologous Na-dependent Ca exchange in our hands.

The construction of a number of NCKX deletion mutants and NCKX/NCX chimeras, however, led to the successful identification of a mutant capable of K-dependent Na/Ca exchange. Selection of the most appropriate cell expression system was important in this endeavour, as functional assays required several key conditions be met. These included high levels of protein expression, correct targeting to the plasma membrane, and uncompromised membrane integrity. While CHO cells provided a system with low background Ca homeostasis mechanisms, the relatively low levels of protein produced may have interfered with the measurement of functional activity. HEK cells provided similar circumstances and in addition were discovered to possess an endogenous Na/Ca exchange activity which could be activated under some conditions. The SF9/AcMNPV insect cell system produced high levels of protein, but appeared to have reduced membrane integrity and likely, highly perturbed Ca homeostasis activities. Although the pEIA/HighFive system was unable to retain the Fluo-3 indicator dye, it was found to be the best system in which to examine function. Strong protein expression and intact membranes allowed consistent measurement with fura-2 of K-dependent Na/Ca exchange from the double deletion (OF) clone.

Significant effort went into the modification of the single cell digital imaging protocol to improve its utility in the measurement of cytosolic Ca in the HighFive stable cell lines. Osmolarity, temperature, Na-loading conditions and internal Ca sequestration posed significant challenges which had to be resolved. Once these impediments were overcome, consistent K-dependent Na/Ca exchange was readily observed from the bovine NCKX1 exchanger derived double deletion mutant (OF). The requirement for K was consistent with that found in the native rod exchanger. Work published by others has purported to show K-independent exchange mediated by the full-length bovine NCKX1 exchanger in HEK cells (Navangione et al, 1997), suggesting that K-dependence is a function of the rod outer segment environment and not an intrinsic attribute of the NCKX1 exchanger itself. Our lab has consistently been unable to measure full-length bovine NCKX1 mediated exchange in any heterologous system, but my work did uncover an inducible K-independent Na/Ca exchange artifact of HEK cells.

The reproducibility of the modified digital imaging protocol allowed the quantification of  $K_m$  values for the external Ca and K concentrations for reverse exchange. These values were found to compare favorably with values determined for the native rod exchanger *in situ* (Szerencsei et al, 2000), suggesting that at least the Ca and K concentration dependent activation attributes of the Na/Ca+K exchanger are maintained in heterologous systems.

## **5.6 Transmembrane Domain Mediates Na/Ca+K Exchange**

As reported in this thesis,  $K_m$  values measured by fura-2 single cell digital imaging are comparable to those determined for the native bovine exchanger *in situ*.  $^{45}\text{Ca}$  uptake

results from our lab, reported elsewhere (Szerencsei et al, 2000), extend these results and demonstrate clearly that the bovine double deletion mutant displays characteristic K-dependent Na/Ca exchange with very similar properties to native exchange activity (Szerencsei et al, 2000). This validates the hypothesis that the NCKX1 amino acid sequences which mediate both K-dependence and Na/Ca exchange are contained within the hydrophobic transmembrane domains. Sequence comparison of experimentally verified functional NCKX exchangers from bovine, dolphin and *C. elegans* reveals that significant homology is limited to TM1-5 and TM6-11, suggesting that the binding sites for Na, Ca and K are located in those regions.

### **5.7 Activity of the Cytosolic Domain**

Similar to NCX1, rod NCKX1 could be hypothesized to segregate its regulatory feature, time-dependent inactivation, to the cytoplasmic loop. If the decline in Ca influx activity observed for the OF clone, using digital imaging methods, is a manifestation of this inactivation activity when heterologously expressed, then this regulatory feature would be integral to the transmembrane domains. This contrasts with the hypothesis that the cytoplasmic loop contains the regulatory region. Unfortunately, the measurement of Ca efflux (the condition at which inactivation is observed for the native exchanger *in situ*) was not feasible in the HighFive system described here, due to the significant endogenous Ca clearance mechanism relative to the rate of exchange mediated by our exchanger mutant.

#### *Acidic Regions of the Cytosolic Domain*

A recent report investigated the role of retinal glutamic-acid rich proteins, GARPs, in protein:protein interactions, where they function in organizing key cGMP signaling

proteins in a complex localized to the rim region and incisures of rod outer segment disks (Korschen et al, 1999). This concurs with the hypothesis that one or both of the highly acidic regions of the Na/Ca+K exchanger's cytosolic loop may play a role in mediating protein:protein interactions. Indeed, crosslinking experiments have suggested that the Na/Ca+K exchanger forms a complex with the cGMP-gated channel *in vivo* (Schwarzer and Bauer, 1999). The fact that bovine NCKX1 and bovine cGMP-gated channel  $\beta$ -subunit amino acid sequences both contain an acidic stretch repeated several times while their human homologues contain only a single iteration of the corresponding acidic region is intriguing. It is possible that this correlation reveals an underlying mechanism for retinal rod protein complex organization, which differs from the human to the bovine retina.

### **5.8 Activity of the Extracellular Domain**

The N-terminal extracellular hydrophilic loop was not investigated in this project, other than in the determination that the loop is not required for Na/Ca exchange activity. The role *in vivo* remains unclear, and the lack of sequence conservation between the thus far cloned orthologs further clouds the issue. Conceivably, the extracellular loop may perform a feature unrelated to the Na/Ca exchange activity, in which the observed heavy glycosylation plays a role. The retinal rod cGMP-gated channel  $\beta$  subunit contains an N-terminal GARP domain, a member of the retinal GARPs that mediate protein complex formation (Korschen et al, 1999). Thus, the cGMP-gated channel  $\beta$  subunit provides a precedent where distinct domains from a single retinal rod protein have discrete activities.



### 5.9 Inhibition of Heterologous Function Mediated by Cytoplasmic Domain

Our lab has tested full length bovine NCKX1 in HEK cells (Cooper et al, 1999a) and in the stable and highly expressing HighFive system (Szerencsei et al, 2000; and this thesis), but it was only upon deletion of both the extracellular and intracellular domains, coupled with expression in the HighFive expression cell system, that we were able to demonstrate heterologous K-dependent Na/Ca exchange activity from a bovine NCKX1-derived exchanger.

The inability of the full length bovine NCKX1 clone to produce Na/Ca exchange activity in this system, suggested that either this protein is not correctly delivered to the plasma membrane or that once there is non-functional. The bovine double deletion mutant (OF), however, showed activity in this system when assayed by  $^{45}\text{Ca}$  uptake (Szerencsei et al, 2000) or single cell digital imaging methods (this thesis). Sequence comparison of the OF construct with the other mutants, led to the hypothesis that the cytosolic domain somehow blocked heterologous Na/Ca exchange activity. Recent work from our lab appears to confirm this observation, as the addition of the bovine cytosolic domain to the highly active (when heterologously expressed) dolphin NCKX1 cDNA resulted in the complete abolition of function (Cooper et al, 1999a).

Sequences contained within the cytosolic region might mediate protein : protein interactions or be required for correct targeting to the plasma membrane. Recent evidence has indicated that the rod Na/Ca+K exchanger and the cGMP-gated channel may form a complex *in vivo* (Bauer, 1998). If the cytoplasmic loop region contains amino acid stretches to which the cGMP-gated channel or cytoskeletal scaffolding proteins dock, the loop's

presence in a heterologous system might lead to misfolding, incorrect targeting or aggregation into non-functional complexes. Incorrect folding can result in the inability to escape from the endoplasmic reticulum, such as occurs in the phenylalanine deletion mutant of the cystic fibrosis transmembrane regulator (CFTR) protein (Dalemans et al, 1992).

An alternative explanation might be that the exchange activity measured in heterologous systems is intrinsic to the species homologue being expressed. It seems unlikely, however, that the primary sequence is the sole root of the discrepancy in function, as the full length bovine NCKX1 shows no activity at all in the pEIA system, while the double deletion mutant (OF) displays significant Na/Ca exchange. From the robust activity displayed by the dolphin cDNA, the extracellular loop is unlikely to be the cause of the inhibition, as it is present in the dolphin exchanger. As the molecular addition of the bovine cytosolic loop was inhibitory to heterologous functional expression of the dolphin, this domain remains the most likely candidate of the cause of the inhibition of activity in expression systems.

The observations from the bovine and dolphin NCKX1-derived mutants differ from the K-dependent Na/Ca exchange activity described from the cloned rat NCKX1 cDNAs, where splice variants containing the entire cytosolic regions are reported to function at the highest activity (Poon et al, 2000). Perhaps the low sequence conservation observed between the rat and bovine clones in the cytosolic loop region may in part explain the lack of functional conservation.

### 5.10 Future Experiments

The domains required for K-dependent Na/Ca exchange have now been localized to the transmembrane loops. Appropriate future experiments might focus on identifying the key residues within these stretches which are responsible for the ion translocation event. Using the NCX1 exchanger as a model, charged residues, conserved across the species for which cDNAs have now been cloned, make attractive targets for mutagenesis studies. In addition, the proposed K site, responsible for both the K-dependence and K transport of the Na/Ca+K exchanger, must be contained within the hydrophobic domains. As the activity of the K site distinguishes the NCKX1 exchanger functionally from NCX1, its identification, through domain swapping or mutagenesis studies, would be of significant interest.

Future studies need also be directed at elucidating the function of the highly acidic cytosolic loop, including the poly-glutamic acid stretch and the motif first identified in the bovine NCKX1 cDNA as a repeat. Sequence comparisons reveal acidic motifs in the bovine cGMP-gated channel  $\beta$ -subunit and the retinal GARPs. Sequence correlations between NCKX1 and other retinal proteins may suggest hypotheses from which these questions could be addressed. Concurrently, the inhibition of function from heterologously expressed NCKX1 cDNAs or mutant derivatives should be addressed. Although the observed exchange inhibition may be an artifact, the determination of the cause could provide insights into the *in vivo* role(s) of the cytosolic loop.

The function(s) of the alternately spliced exons should be explored. An approach which might shed some light on this question would be the swapping of cytosolic domains with the rat exchanger, which apparently functions with little regard to the absence or

inclusion of cytosolic exons (Poon et al, 2000). Other possible approaches include the subcloning of exons III - VI into fusion protein expression systems and the determination of which proteins, if any, found in either rod outer segments or heterologous expression systems, bind specifically to these domains. Until the problem of the inhibition of heterologous function by the cytosolic domain of the human and bovine Na/Ca+K exchangers is solved, it will likely prove difficult to allocate functions to the exons of the cytosolic domain.

Key investigations of the rod Na/Ca+K exchanger will need to examine the relative abundance of alternate splice products at the protein level as well as the functional differences between each isoform, and thus determine the role each plays in the outer segment. At the present time, detection of the protein isoforms in either human or bovine retinas, both in terms of quantification and subcellular localization, is not possible. However, the identification of the predominant species and quantification of RNA levels of those variants, reported in this thesis, provides a good starting point for future endeavors in this matter.

Not to be forgotten is the large extracellular loop whose role in the retina is not obvious, though presumably necessary, as the domain is present in thus far cloned NCKX1 cDNAs from mammalian species. Clearly, the results of this work have segregated the function of the extracellular region from the ion translocation events.

It is likely that the ongoing research into the role of the Na/Ca+K exchanger in human retinopathy will reveal mutations in the NCKX1 gene as an RP causative genetic locus. Further elucidation of the activity of the exchanger, and its structure-function

relationships, will provide a solid basis from which therapeutic intervention for a genetically identified cohort of patients may be designed. Also, the research presented here will lay the foundation for future testing of the functional effects of mutations found in human retinopathy in an *in vitro* system.

## Reference List

- Aceto, J.F., Condrescu, M., Kroupis, C., Nelson, H., Nelson, N., Nicoll, D., Philipson, K.D., and Reeves, J.P. (1992) Cloning and expression of the bovine cardiac sodium-calcium exchanger. *Arch. Biochem. Biophys.*, 298:553-560.
- Allikmets, R., Shroyer, N.F., Singh, N., Seddon, J.M., Lewis, R.A., Bernstein, P.S., Peiffer, A., Zabriskie, N.A., Li, Y., Hutchinson, A., Dean, M., Lupski, J.R., and Leppert, M. (1997) Mutation of the Stargardt disease gene (ABCR) in age-related macular degeneration [see comments]. *Science*, 277:1805-1807.
- Bascom, R.A., Liu, L., Heckenlively, J.R., Stone, E.M., and McInnes, R.R. (1995) Mutation analysis of the ROM1 gene in retinitis pigmentosa. *Hum. Mol. Genet.*, 4:1895-1902.
- Bauer, P.J. (1988) Evidence for two functionally different membrane fractions in bovine retinal rod outer segments. *J. Physiol (Lond)*, 401:309-327.
- Bauer, P.J. and Drechsler, M. (1992) Association of cyclic GMP-gated channels and Na(+)-Ca(2+)-K+ exchangers in bovine retinal rod outer segment plasma membranes. *J. Physiol (Lond)*, 451:109-131.
- Birch, D.G. and Fish, G.E. (1987) Rod ERGs in retinitis pigmentosa and cone-rod degeneration. *Invest Ophthalmol. Vis. Sci.*, 28:140-150.
- Blaustein, M.P. and Lederer, W.J. (1999) Sodium/calcium exchange: its physiological implications. *Physiol Rev.*, 79:763-854.
- Bonigk, W., Altenhofen, W., Muller, F., Dose, A., Illing, M., Molday, R.S., and Kaupp, U.B. (1993) Rod and cone photoreceptor cells express distinct genes for cGMP-gated channels. *Neuron*, 10:865-877.

Bruford, E.A., Riise, R., Teague, P.W., Porter, K., Thomson, K.L., Moore, A.T., Jay, M., Warburg, M., Schinzel, A., Tommerup, N., Tornqvist, K., Rosenberg, T., Patton, M., Mansfield, D.C., and Wright, A.F. (1997) Linkage mapping in 29 Bardet-Biedl syndrome families confirms loci in chromosomal regions 11q13, 15q22.3-q23, and 16q21. *Genomics*, 41:93-99.

Bucher, P. (1990) Weight matrix descriptions of four eukaryotic RNA polymerase II promoter elements derived from 502 unrelated promoter sequences. *J.Mol.Biol.*, 212:563-578.

Buraczynska, M., Wu, W., Fujita, R., Buraczynska, K., Phelps, E., Andreasson, S., Bennett, J., Birch, D.G., Fishman, G.A., Hoffman, D.R., Inana, G., Jacobson, S.G., Musarella, M.A., Sieving, P.A., and Swaroop, A. (1997) Spectrum of mutations in the RPGR gene that are identified in 20% of families with X-linked retinitis pigmentosa. *Am.J.Hum.Genet.*, 61:1287-1292.

Carmi, R., Rokhlina, T., Kwitek-Black, A., Elbedour, K., Nishimura, D., Stone, E.M., and Sheffield, V.C. (1995) Use of a DNA pooling strategy to identify a human obesity syndrome locus on chromosome 15. *Hum.Mol.Genet.*, 4:9-13.

Cervetto, L., Lagnado, L., Perry, R.J., Robinson, D.W., and McNaughton, P.A. (1989) Extrusion of calcium from rod outer segments is driven by both sodium and potassium gradients. *Nature*, 337:740-743.

Chen, J., Makino, C.L., Peachey, N.S., Baylor, D.A., and Simon, M.I. (1995) Mechanisms of rhodopsin inactivation in vivo as revealed by a COOH- terminal truncation mutant. *Science*, 267:374-377.

Chen, T.Y., Illing, M., Molday, L.L., Hsu, Y.T., Yau, K.W., and Molday, R.S. (1994) Subunit 2 (or beta) of retinal rod cGMP-gated cation channel is a component of the 240-kDa channel-associated protein and mediates  $\text{Ca}^{2+}$ -calmodulin modulation. *Proc.Natl.Acad.Sci.U.S.A.*, 91:11757-11761.

Chen, T.Y., Peng, Y.W., Dhallan, R.S., Ahamed, B., Reed, R.R., and Yau, K.W. (1993) A new subunit of

the cyclic nucleotide-gated cation channel in retinal rods. *Nature*, 362:764-767.

Colville, C.A. and Molday, R.S. (1996) Primary Structure and Expression of the human *B*-Subunit and Related Proteins of the Rod Photoreceptor cGMP-gated Channel. *J. Biol. Chem.*, 271:32968-32974.

Connell, G.J. and Molday, R.S. (1990) Molecular cloning, primary structure, and orientation of the vertebrate photoreceptor cell protein peripherin in the rod outer segment disk membrane. *Biochemistry*, 29:4691-4698.

Cook, O., Low, W., and Rahamimoff, H. (1998) Membrane topology of the rat brain Na<sup>+</sup>-Ca<sup>2+</sup> exchanger. *Biochim. Biophys. Acta*, 1371:40-52.

Cooper, C.B., Szerencsei, R.T., and Schnetkamp, P.P.M. (1999b) Spectrofluorometric detection of Na-Ca+K exchange. *Methods Enzymol.*, in press.

Cooper, C.B., Winkfein, R.J., Szerencsei, R.T., and Schnetkamp, P.P. (1999a) cDNA cloning and functional expression of the dolphin retinal rod Na-Ca+K exchanger NCKX1: comparison with the functionally silent bovine NCKX1. *Biochemistry*, 38:6276-6283.

Cremers, F.P., van de Pol, D.J., van Driel, M., den Hollander, A.I., van Haren, F.J., Knoers, N.V., Tijmes, N., Bergen, A.A., Rohrschneider, K., Blankenagel, A., Pinckers, A.J., Deutman, A.F., and Hoyng, C.B. (1998) Autosomal recessive retinitis pigmentosa and cone-rod dystrophy caused by splice site mutations in the Stargardt's disease gene ABCR. *Hum. Mol. Genet.*, 7:355-362.

Dalemans, W., Hinnrasky, J., Slos, P., Dreyer, D., Fuchey, C., Pavirani, A., and Puchelle, E. (1992) Immunocytochemical analysis reveals differences between the subcellular localization of normal and delta Phe508 recombinant cystic fibrosis transmembrane conductance regulator. *Exp. Cell Res.*, 201:235-240.

Daniele, S., Restagno, G., Daniele, C., Nardacchione, A., Danese, P., and Carbonara, A. (1996) Analysis of the rhodopsin and peripherin/RDS gene in two families with pattern dystrophy of the retinal pigment



epithelium. *Eur.J.Ophthalmol.*, 6:197-200.

Detwiler,P.B. and Gray-Keller,M.P. (1996) The mechanisms of vertebrate light adaptation: speeded recovery versus slowed activation. *Curr.Opin.Neurobiol.*, 6:440-444.

Dhallan,R.S., Yau,K.W., Schrader,K.A., and Reed,R.R. (1990) Primary structure and functional expression of a cyclic nucleotide- activated channel from olfactory neurons. *Nature*, 347:184-187.

Dizhoor,A.M., Ray,S., Kumar,S., Niemi,G., Spencer,M., Brolley,D., Walsh,K.A., Philipov,P.P., Hurley,J.B., and Stryer,L. (1991) Recoverin: A calcium sensitive activator of retinal rod guanylate cyclase. *Science*, 251:915-918.

Doering,A.E., Nicoll,D.A., Lu,Y., Lu,L., Weiss,J.N., and Philipson,K.D. (1998) Topology of a functionally important region of the cardiac  $\text{Na}^+/\text{Ca}^{2+}$  exchanger. *J.Biol.Chem.*, 273:778-783.

Dryja,T.P., Berson,E.L., Rao,V.R., and Oprian,D.D. (1993) Heterozygous missense mutation in the rhodopsin gene as a cause of congenital stationary night blindness. *Nat.Genet.*, 4:280-283.

Dryja,T.P., Finn,J.T., Peng,Y.W., McGee,T.L., Berson,E.L., and Yau,K.W. (1995) Mutations in the gene encoding the alpha subunit of the rod cGMP-gated channel in autosomal recessive retinitis pigmentosa. *Proc.Natl.Acad.Sci.U.S.A.*, 92:10177-10181.

Dryja,T.P., Hahn,L.B., Cowley,G.S., McGee,T.L., and Berson,E.L. (1991) Mutation spectrum of the rhodopsin gene among patients with autosomal dominant retinitis pigmentosa. *Proc.Natl.Acad.Sci.U.S.A.*, 88:9370-9374.

Dryja,T.P., Hahn,L.B., Kajiwar,K., and Berson,E.L. (1997) Dominant and digenic mutations in the peripherin/RDS and ROM1 genes in retinitis pigmentosa. *Invest Ophthalmol.Vis.Sci.*, 38:1972-1982.

Dryja,T.P. and Li,T. (1995) Molecular genetics of retinitis pigmentosa. *Hum.Mol.Genet.*, 4:1739-1743.

- Dryja, T.P., Rucinski, D.E., Chen, S.H., and Berson, E.L. (1999b) Frequency of mutations in the gene encoding the alpha subunit of rod cGMP-phosphodiesterase in autosomal recessive retinitis pigmentosa. *Invest Ophthalmol. Vis. Sci.*, 40:1859-1865.
- Dryja, T.P., Rucinski, D.E., Chen, S.H., and Berson, E.L. (1999a) Frequency of mutations in the gene encoding the alpha subunit of rod cGMP-phosphodiesterase in autosomal recessive retinitis pigmentosa. *Invest Ophthalmol. Vis. Sci.*, 40:1859-1865.
- Dyck, C., Maxwell, K., Buchko, J., Trac, M., Omelchenko, A., Hnatowich, M., and Hryshko, L.V. (1998) Structure-function analysis of CALX1.1, a  $\text{Na}^+$ - $\text{Ca}^{2+}$  exchanger from *Drosophila*. Mutagenesis of ionic regulatory sites. *J. Biol. Chem.*, 273:12981-12987.
- Ekstrom, U., Ponjavic, V., Abrahamson, M., Nilsson-Ehle, P., Andreasson, S., Stenstrom, I., and Ehinger, B. (1998) Phenotypic expression of autosomal dominant retinitis pigmentosa in a Swedish family expressing a Phe-211-Leu variant of peripherin/RDS. *Ophthalmic Genet.*, 19:27-37.
- Fain, G.L., Lamb, T.D., Matthews, H.R., and Murphy, R.L. (1989) Cytoplasmic calcium as the messenger for light adaptation in salamander rods. *J. Physiol (Lond)*, 416:215-243.
- Farrell, P.J., Lu, M.L., Prevost, J., Brown, C., Behie, L., and Iatrou, K. (1998) High-level expression of secreted glycoproteins in transformed lepidopteran insect cells using a novel expression vector. *Biotechnology and bioengineering*, 60:656-663.
- Franke, R.R., Sakmar, T.P., Graham, R.M., and Khorana, H.G. (1992) Structure and function in rhodopsin. Studies of the interaction between the rhodopsin cytoplasmic domain and transducin. *J. Biol. Chem.*, 267:14767-14774.
- Frins, S., Bonigk, W., Muller, F., Kellner, R., and Koch, K.W. (1996) Functional characterization of a guanylyl cyclase-activating protein from vertebrate rods. Cloning, heterologous expression, and

localization. *J.Biol.Chem.*, 271:8022-8027.

Fuller,C.M. and Benos,D.J. (1992) CFTR! *Am.J.Physiol*, 263:C267-C286.

Fung,B.K., Hurley,J.B., and Stryer,L. (1981) Flow of information in the light-triggered cyclic nucleotide cascade of vision. *Proc.Natl.Acad.Sci.U.S.A*, 78:152-156.

Gerber,S., Rozet,J.M., Bonneau,D., Souied,E., Camuzat,A., Dufier,J.L., Amalric,P., Weissenbach,J., Munnich,A., and Kaplan,J. (1995) A gene for late-onset fundus flavimaculatus with macular dystrophy maps to chromosome 1p13. *Am.J.Hum.Genet.*, 56:396-399.

GibcoBRL (1997) *GibcoBRL Products & Reference Guide*. Life Technologies, Burlington, ON.

Goldberg,A.F. and Molday,R.S. (1996) Defective subunit assembly underlies a digenic form of retinitis pigmentosa linked to mutations in peripherin/rds and rom-1. *Proc.Natl.Acad.Sci.U.S.A*, 93:13726-13730.

Goracznik,R.M., Duda,T., and Sharma,R.K. (1998) Calcium modulated signaling site in type 2 rod outer segment membrane guanylate cyclase (ROS-GC2). *Biochem.Biophys.Res.Comm.*, 245:447-453.

Goracznik,R.M., Duda,T., Sitaramayya,A., and Sharma,R.K. (1994) Structural and functional characterisation of the rod outer segment membrane guanylate cyclase. *Biochem.J.*, 302:455-461.

Gorczyca,W.A., Gray-Keller,M.P., Detwiler,P.B., and Palczewski,K. (1994) Purification and physiological evaluation of a guanylate cyclase activating protein from retinal rods. *Proc.Natl.Acad.Sci.U.S.A*, 91:4014-4018.

Gorczyca,W.A., Polans,A.S., Surgucheva,I.G., Subbaraya,I., Baehr,W., and Palczewski,K. (1995) Guanylyl cyclase activating protein. A calcium-sensitive regulator of phototransduction. *J.Biol.Chem.*, 270:22029-22036.

- Gordon, S.E. and Zagotta, W.N. (1995) Subunit interactions in coordination of  $\text{Ni}^{2+}$  in cyclic nucleotide-gated channels. *Proc. Natl. Acad. Sci. U.S.A.*, 92:10222-10226.
- Gray-Keller, M.P. and Detwiler, P.B. (1994) The calcium feedback signal in the phototransduction cascade of vertebrate rods. *Neuron*, 13:849-861.
- Gray-Keller, M.P. and Detwiler, P.B. (1996)  $\text{Ca}^{2+}$  dependence of. *Neuron*, 17:323-331.
- Grunwald, M.E., Yu, W.P., Yu, H.H., and Yau, K.W. (1998) Identification of a domain on the beta-subunit of the rod cGMP-gated cation channel that mediates inhibition by calcium-calmodulin. *J. Biol. Chem.*, 273:9148-9157.
- Hackos, D.H. and Korenbrot, J.I. (1997) Calcium modulation of ligand affinity in the cyclic GMP-gated ion channels of cone photoreceptors. *J. Gen. Physiol.*, 110:515-528.
- Hagins, W.A., Penn, R.D., and Yoshikami, S. (1970) Dark current and photocurrent in retinal rods. *Biophys. J.*, 10:380-412.
- He, S., Ruknudin, A., Bambrick, L.L., Lederer, W.J., and Schulze, D.H. (1998a) Isoform-specific regulation of the  $\text{Na}^{+}/\text{Ca}^{2+}$  exchanger in rat astrocytes and neurons by PKA. *J. Neurosci.*, 18:4833-4841.
- He, W., Cowan, C.W., and Wensel, T.G. (1998b) RGS9, a GTPase accelerator for phototransduction. *Neuron*, 20:95-102.
- He, Z., Feng, S., Tong, Q., Hilgemann, D.W., and Philipson, K.D. (2000) Interaction of  $\text{PIP}_2$  with the XIP region of the cardiac  $\text{Na}/\text{Ca}$  exchanger. *Am J. Physiol Cell Physiol.*, 278(4):C661-666.
- He, Z., Petesch, N., Voges, K., Roben, W., and Philipson, K.D. (1997) Identification of important amino acid residues of the  $\text{Na}^{+}$ - $\text{Ca}^{2+}$  exchanger inhibitory peptide, XIP. *J. Membr. Biol.*, 156:149-156.

Hilgemann,D.W. (1990) Regulation and deregulation of cardiac  $\text{Na}^{+}$ - $\text{Ca}^{2+}$  exchange in giant excised sarcolemmal membrane patches. *Nature*, 344:242-245.

Hilgemann,D.W. (1996) Unitary cardiac  $\text{Na}^{+}$ ,  $\text{Ca}^{2+}$  exchange current magnitudes determined from channel-like noise and charge movements of ion transport. *Biophys.J.*, 71:759-768.

Hilgemann,D.W. and Ball,R. (1996) Regulation of cardiac  $\text{Na}^{+}$ , $\text{Ca}^{2+}$  exchange and KATP potassium channels by PIP<sub>2</sub>. *Science*, 273:956-959.

Hilgemann,D.W., Collins,A., and Matsuoka,S. (1992b) Steady-state and dynamic properties of cardiac sodium-calcium exchange. Secondary modulation by cytoplasmic calcium and ATP. *J.Gen.Physiol*, 100:933-961.

Hilgemann,D.W., Matsuoka,S., Nagel,G.A., and Collins,A. (1992a) Steady-state and dynamic properties of cardiac sodium-calcium exchange. Sodium-dependent inactivation. *J.Gen.Physiol*, 100:905-932.

Hilgemann,D.W., Nicoll,D.A., and Philipson,K.D. (1991) Charge movement during  $\text{Na}^{+}$  translocation by native and cloned cardiac  $\text{Na}^{+}$ / $\text{Ca}^{2+}$  exchanger. *Nature*, 352:715-718.

Hilgemann,D.W., Philipson,K.D., and Vassort,G. (1996) Sodium-calcium Exchange. The New York Academy of Sciences, New York.

Hryshko,L.V., Matsuoka,S., Nicoll,D.A., Weiss,J.N., Schwarz,E.M., Benzer,S., and Philipson,K.D. (1996) Anomalous regulation of the *Drosophila*  $\text{Na}^{+}$ - $\text{Ca}^{2+}$  exchanger by  $\text{Ca}^{2+}$ . *J.Gen.Physiol*, 108:67-74.

Hryshko,L.V., Nicoll,D.A., Weiss,J.N., and Philipson,K.D. (1993) Biosynthesis and initial processing of the cardiac sarcolemmal  $\text{Na}^{+}$ -  $\text{Ca}^{2+}$  exchanger. *Biochim.Biophys.Acta*, 1151:35-42.

Hsu, Y.T. and Molday, R.S. (1993) Modulation of the cGMP-gated channel of rod photoreceptor cells by calmodulin [published erratum appears in *Nature* 1993 Sep 16;365(6443):279] [see comments]. *Nature*, 361:76-79.

Hsu, Y.T. and Molday, R.S. (1994) Interaction of calmodulin with the cyclic GMP-gated channel of rod photoreceptor cells. Modulation of activity, affinity purification, and localization. *J. Biol. Chem.*, 269:29765-29770.

Huang, S.H., Pittler, S.J., Huang, X., Oliveira, L., Berson, E.L., and Dryja, T.P. (1995) Autosomal recessive retinitis pigmentosa caused by mutations in the alpha subunit of rod cGMP phosphodiesterase. *Nat. Genet.*, 11:468-471.

Hurley, J.B., Dizhoor, A.M., Ray, S., and Stryer, L. (1993) Recoverin's role: conclusion withdrawn [letter: comment]. *Science*, 260:740.

Hwa, J., Reeves, P.J., Klein-Seetharaman, J., Davidson, F., and Khorana, H.G. (1999) Structure and function in rhodopsin: further elucidation of the role of the intradiscal cysteines, Cys-110, -185, and -187, in rhodopsin folding and function. *Proc. Natl. Acad. Sci. U.S.A.*, 96:1932-1935.

Illing, M., Molday, L.L., and Molday, R.S. (1997) The 220-kDa rim protein of retinal rod outer segments is a member of the ABC transporter superfamily. *J. Biol. Chem.*, 272:10303-10310.

Inglehearn, C.F. (1998) Molecular genetics of human retinal dystrophies. *Eye*, 12 ( Pt 3b):571-579.

Ioannou, P.A., Amemiya, C.T., Garnes, J., Kroisel, P.M., Shizuya, H., Chen, C., Batzer, M.A., and de Jong, P. (1994) A new bacteriophage P1-derived vector for the propagation of large human DNA fragments. *Nature Gen.*, 6:84-89.

Iwamoto, T., Nakamura, T.Y., Pan, Y., Uehara, A., Imanaga, I., and Shigekawa, M. (1999a) Unique topology of the internal repeats in the cardiac Na<sup>+</sup>/Ca<sup>2+</sup> exchanger. *FEBS Lett.*, 446:264-268.

Iwamoto, T., Pan, Y., Wakabayashi, S., Imagawa, T., Yamanaka, H.I., and Shigekawa, M. (1996)

Phosphorylation-dependent regulation of cardiac  $\text{Na}^+/\text{Ca}^{2+}$  exchanger via protein kinase C.

J.Biol.Chem., 271:13609-13615.

Iwamoto, T. and Shigekawa, M. (1998) Differential inhibition of  $\text{Na}^+/\text{Ca}^{2+}$  exchanger isoforms by

divalent cations and isothiurea derivative. Am.J.Physiol, 275:C423-C430.

Iwamoto, T., Uehara, A., Nakamura, T.Y., Imanaga, I., and Shigekawa, M. (1999b) Chimeric analysis of

$\text{Na}^+/\text{Ca}^{2+}$  exchangers NCX1 and NCX3 reveals structural domains important for differential

sensitivity to external  $\text{Ni}^{2+}$  or  $\text{Li}^+$ . J.Biol.Chem., 274:23094-23102.

Kandasamy, R.A. and Orłowski, J. (1996) Genomic organization and glucocorticoid transcriptional

activation of the rat  $\text{Na}^+/\text{H}^+$  exchanger Nhe3 gene. J.Biol.Chem., 271:10551-10559.

Kaupp, U.B. and Koch, K.W. (1992) Role of cGMP and  $\text{Ca}^{2+}$  in vertebrate photoreceptor excitation and

adaptation. Annu.Rev.Physiol, 54:153-175.

Kaupp, U.B., Niidome, T., Tanabe, T., Terada, S., Bonigk, W., Stühmer, W., Cook, N.J., Kangawa, K.,

Matsuo, H., and Hirose, T. (1989) Primary structure and functional expression from complementary DNA

of the rod photoreceptor cyclic GMP-gated channel. Nature, 342:762-766.

Kawamura, S. (1993) Rhodopsin phosphorylation as a mechanism of cyclic GMP phosphodiesterase

regulation by S-modulin. Nature, 362:855-857.

Kawamura, S. (1994) Photoreceptor light-adaptation mediated by S-modulin, a member of a possible

regulatory protein family of protein phosphorylation in signal transduction. Neurosci.Res., 20:293-298.

Kawamura, S., Hisatomi, O., Kayada, S., Tokunaga, F., and Kuo, C.H. (1993) Recoverin has S-modulin

activity in frog rods. J.Biol.Chem., 268:14579-14582.

- Kawamura, S. and Murakami, M. (1991) Calcium-dependent regulation of cyclic GMP phosphodiesterase by a protein from frog retinal rods. *Nature*, 349:420-423.
- Kim, T.S., Reid, D.M., and Molday, R.S. (1998) Structure-function relationships and localization of the Na/Ca-K exchanger in rod photoreceptors. *J.Biol.Chem.*, 273:16561-16567.
- Kimura, M., Aviv, A., and Reeves, J.P. (1993) K(+)-dependent Na<sup>+</sup>/Ca<sup>2+</sup> exchange in human platelets. *J.Biol.Chem.*, 268:6874-6877.
- Klenchin, V.A., Calvert, P.D., and Bownds, M.D. (1995) Inhibition of rhodopsin kinase by recoverin. Further evidence for a negative feedback system in phototransduction. *J.Biol.Chem.*, 270:16147-16152.
- Kofuji, P., Lederer, W.J., and Schulze, D.H. (1994) Mutually exclusive and cassette exons underlie alternatively spliced isoforms of the Na/Ca exchanger. *J.Biol.Chem.*, 269:5145-5149.
- Kohl, S., Marx, T., Giddings, I., Jagle, H., Jacobson, S.G., Apfelstedt-Sylla, E., Zrenner, E., Sharpe, L.T., and Wissinger, B. (1998) Total colourblindness is caused by mutations in the gene encoding the alpha-subunit of the cone photoreceptor cGMP-gated cation channel. *Nat.Genet.*, 19:257-259.
- Kohomoto, O., Levi, A.J., and Bridge, J.H. (1994) Relation between reverse sodium-calcium exchange and sarcoplasmic reticulum calcium release in guinea pig ventricular cells. *Circ.Res.*, 74:550-554.
- Korschen, H.G., Beyermann, M., Muller, F., Heck, M., Vantler, M., Koch, K.W., Kellner, R., Wolfrum, U., Bode, C., Hofmann, K.P., and Kaupp, U.B. (1999) Interaction of glutamic-acid-rich proteins with the cGMP signalling pathway in rod photoreceptors. *Nature*, 400:761-766.
- Korschen, H.G., Illing, M., Seifert, R., Sesti, F., Williams, A., Gotzes, S., Colville, C., Muller, F., Dose, A., and Godde, M. (1995) A 240 kDa protein represents the complete beta subunit of the cyclic nucleotide-gated channel from rod photoreceptor. *Neuron*, 15:627-636.



- Koutalos, Y. and Yau, K.W. (1996) Regulation of sensitivity in vertebrate rod photoreceptors by calcium. *Trends Neurosci.*, 19:73-81.
- Kraev, A., Chumakov, I., and Carafoli, E. (1996) The organization of the human gene NCX1 encoding the sodium-calcium exchanger. *Genomics*, 37:105-112.
- Krishnan, A., Goraczniak, R.M., Duda, T., and Sharma, R.K. (1998) Third calcium-modulated rod outer segment membrane guanylate cyclase transduction mechanism. *Mol. Cell Biochem.*, 178:251-259.
- Krupnick, J.G., Gurevich, V.V., and Benovic, J.L. (1997) Mechanism of quenching of phototransduction. Binding competition between arrestin and transducin for phosphorhodopsin. *J. Biol. Chem.*, 272:18125-18131.
- Kuhn, H. and Wilden, U. (1987) Deactivation of photoactivated rhodopsin by rhodopsin-kinase and arrestin. *J. Recept. Res.*, 7:283-298.
- Lagnado, L. and Baylor, D.A. (1994) Calcium controls light-triggered formation of catalytically active rhodopsin. *Nature*, 367:273-277.
- Leblanc, N. and Hume, J.R. (1990) Sodium current-induced release of calcium from cardiac sarcoplasmic reticulum [see comments]. *Science*, 248:372-376.
- Lee, S.L., Yu, A.S., and Lytton, J. (1994) Tissue-specific expression of Na(+)-Ca<sup>2+</sup> exchanger isoforms. *J. Biol. Chem.*, 269:14849-14852.
- Levi, A.J., Spitzer, K.W., Kohmoto, O., and Bridge, J.H. (1994) Depolarization-induced Ca entry via Na-Ca exchange triggers SR release in guinea pig cardiac myocytes. *Am. J. Physiol.*, 266:H1422-H1433.
- Levitsky, D.O., Fraysse, B., Leoty, C., Nicoll, D.A., and Philipson, K.D. (1996) Cooperative interaction between Ca<sup>2+</sup> binding sites in the hydrophilic loop of the Na(+)-Ca<sup>2+</sup> exchanger. *Mol. Cell Biochem.*,

160-161:27-32.

Levitsky,D.O., Nicoll,D.A., and Philipson,K.D. (1994) Identification of the high affinity  $\text{Ca}^{2+}$ -binding domain of the cardiac  $\text{Na}^{+}$ - $\text{Ca}^{2+}$  exchanger. *J.Biol.Chem.*, 269:22847-22852.

Li,Z., Nicoll,D.A., Collins,A., Hilgemann,D.W., Filoteo,A.G., Penniston,J.T., Weiss,J.N., Tomich,J.M., and Philipson,K.D. (1991) Identification of a peptide inhibitor of the cardiac sarcolemmal  $\text{Na}^{+}$ - $\text{Ca}^{2+}$  exchanger. *J.Biol.Chem.*, 266:1014-1020.

Liman,E.R. and Buck,L.B. (1994) A second subunit of the olfactory cyclic nucleotide-gated channel confers high sensitivity to cAMP. *Neuron*, 13:611-621.

Linck,B., Qiu,Z., He,Z., Tong,Q., Hilgemann,D.W., and Philipson,K.D. (1998) Functional comparison of the three isoforms of the  $\text{Na}^{+}$ / $\text{Ca}^{2+}$  exchanger (NCX1, NCX2, NCX3). *Am.J.Physiol*, 274:C415-C423.

Lochrie,M.A., Hurley,J.B., and Simon,M.I. (1985) Sequence of the alpha subunit of photoreceptor G protein: homologies between transducin, ras, and elongation factors. *Science*, 228:96-99.

Lolley,R.N. and Lee,R.H. (1990) Cyclic GMP and photoreceptor function. *FASEB J.*, 4:3001-3008.

Loo,T.W., and Clarke,D.M. (1994) Functional expression of human renal  $\text{Na}^{+}$ / $\text{Ca}^{2+}$  exchanger in insect cells. *Am. J. Physiol.*, 267(1 Pt 2):F70-4.

Lyu,R.M., Smith,L., and Smith,J.B. (1992b)  $\text{Ca}^{2+}$  influx via  $\text{Na}^{+}$ - $\text{Ca}^{2+}$  exchange in immortalized aortic myocytes. I. Dependence on  $[\text{Na}^{+}]_i$  and inhibition by external  $\text{Na}^{+}$ . *Am.J.Physiol*, 263:C628-C634.

Lyu,R.M., Smith,L., and Smith,J.B. (1992a)  $\text{Ca}^{2+}$  influx via  $\text{Na}^{+}$ - $\text{Ca}^{2+}$  exchange in immortalized aortic myocytes. II. Feedback inhibition by  $[\text{Ca}^{2+}]_i$ . *Am.J.Physiol*, 263:C635-C641.

- Lyubarsky,A., Nikonov,S., and Pugh,E.N., Jr. (1996) The kinetics of inactivation of the rod phototransduction cascade with constant  $\text{Ca}^{2+}$ . *J.Gen.Physiol*, 107:19-34.
- Mansergh,F.C., Millington-Ward,S., Kennan,A., Kiang,A.S., Humphries,M., Farrar,G.J., Humphries,P., and Kenna,P.F. (1999) Retinitis Pigmentosa and Progressive Sensorineural Hearing Loss Caused by a C12258A Mutation in the Mitochondrial MTTS2 Gene. *Am.J.Hum.Genet.*, 64:971-985.
- Martinez-Mir,A., Paloma,E., Allikmets,R., Ayuso,C., del Rio,T., Dean,M., Vilageliu,L., Gonzalez-Duarte,R., and Balcells,S. (1998) Retinitis pigmentosa caused by a homozygous mutation in the Stargardt disease gene ABCR [letter; comment]. *Nat.Genet.*, 18:11-12.
- Mathies,R.A. (1999) Photons, femtoseconds and dipolar interactions: a molecular picture of the primary events in vision. *Novartis.Found.Symp.*, 224:70-84.
- Matsuoka,S., Nicoll,D.A., He,Z., and Philipson,K.D. (1997) Regulation of cardiac  $\text{Na}^{+}$ - $\text{Ca}^{2+}$  exchanger by the endogenous XIP region. *J.Gen.Physiol*, 109:273-286.
- Matsuoka,S., Nicoll,D.A., Hryshko,L.V., Levitsky,D.O., Weiss,J.N., and Philipson,K.D. (1995) Regulation of the cardiac  $\text{Na}^{+}$ - $\text{Ca}^{2+}$  exchanger by  $\text{Ca}^{2+}$ . Mutational analysis of the  $\text{Ca}^{2+}$ -binding domain. *J.Gen.Physiol*, 105:403-420.
- Matsuoka,S., Nicoll,D.A., Reilly,R.F., Hilgemann,D.W., and Philipson,K.D. (1993) Initial localization of regulatory regions of the cardiac sarcolemmal  $\text{Na}^{+}$ - $\text{Ca}^{2+}$  exchanger. *Proc.Natl.Acad.Sci.U.S.A.*, 90:3870-3874.
- Matthews,H.R., Murphy,R.L., Fain,G.L., and Lamb,T.D. (1988) Photoreceptor light adaptation is mediated by cytoplasmic calcium concentration. *Nature*, 334:67-69.
- McInnes,R.R. and Bascom,R.A. (1992) Retinal genetics: a nullifying effect for rhodopsin [news]. *Nat.Genet.*, 1:155-157.

- McLaughlin, M.E., Ehrhart, T.L., Berson, E.L., and Dryja, T.P. (1995) Mutation spectrum of the gene encoding the beta subunit of rod phosphodiesterase among patients with autosomal recessive retinitis pigmentosa. *Proc. Natl. Acad. Sci. U.S.A.*, 92:3249-3253.
- Miura, Y. and Kimura, J. (1989) Dependence on Internal Ca and Na and Competitive Binding of External Na and Ca. *J. Gen. Physiol.*, 93:1129-1145.
- Morimura, H., Saindelle-Ribeaudeau, F., Berson, E.L., and Dryja, T.P. (1999) Mutations in RGR, encoding a light-sensitive opsin homologue, in patients with retinitis pigmentosa. *Nat. Genet.*, 23:393-394.
- Morrison, D.F., Cunnick, J.M., Oppert, B., and Takemoto, D.J. (1989) Interaction of the gamma-subunit of retinal rod outer segment phosphodiesterase with transducin. Use of synthetic peptides as functional probes. *J. Biol. Chem.*, 264:11671-11681.
- Nakatani, K. and Yau, K.W. (1988) Calcium and light adaptation in retinal rods and cones. *Nature*, 334:69-71.
- Nakazawa, M., Wada, Y., and Tamai, M. (1995) Macular dystrophy associated with monogenic Arg172Trp mutation of the peripherin/RDS gene in a Japanese family. *Retina*, 15:518-523.
- Navangione, A., Rispoli, G., Gabellini, N., and Carafoli, E., (1997) Electrophysiological Characterization of Ionic Transport by the Retinal Exchanger Expressed in Human Embryonic Kidney Cells. *Biophysical Journal*, 73:45-51.
- Nathans, J. and Hogness, D.S. (1983) Isolation, sequence analysis, and intron-exon arrangement of the gene encoding bovine rhodopsin. *Cell*, 34:807-814.
- Nicholas, S.B., Yang, W., Lee, S.L., Zhu, H., Philipson, K.D., and Lytton, J. (1998) Alternative promoters and cardiac muscle cell-specific expression of the Na<sup>+</sup>/Ca<sup>2+</sup> exchanger gene. *Am. J. Physiol.*, 274:H217-

H232.

Nicoll,D.A., Hryshko,L.V., Matsuoka,S., Frank,J.S., and Philipson,K.D. (1996c) Mutagenesis studies of the cardiac  $\text{Na}(+)\text{-Ca}^{2+}$  exchanger. *Ann.N.Y.Acad.Sci.*, 779:86-92.

Nicoll,D.A., Hryshko,L.V., Matsuoka,S., Frank,J.S., and Philipson,K.D. (1996b) Mutation of amino acid residues in the putative transmembrane segments of the cardiac sarcolemmal  $\text{Na}^{+}\text{-Ca}^{2+}$  exchanger. *J.Biol.Chem.*, 271:13385-13391.

Nicoll,D.A., Longoni,S., and Philipson,K.D. (1990) Molecular cloning and functional expression of the cardiac sarcolemmal  $\text{Na}(+)\text{-Ca}^{2+}$  exchanger. *Science*, 250:562-565.

Nicoll,D.A., Ottolia,M., Lu,L., Lu,Y., and Philipson,K.D. (1999) A new topological model of the cardiac sarcolemmal  $\text{Na}^{+}\text{-Ca}^{2+}$  exchanger. *J.Biol.Chem.*, 274:910-917.

Nicoll,D.A., Quednau,B.D., Qui,Z., Xia,Y.R., Lusi,A.J., and Philipson,K.D. (1996a) Cloning of a third mammalian  $\text{Na}^{+}\text{-Ca}^{2+}$  exchanger, NCX3. *J.Biol.Chem.*, 271:24914-24921.

Nikonov,S., Engheta,N., and Pugh,E.N., Jr. (1998) Kinetics of recovery of the dark-adapted salamander rod photoresponse. *J.Gen.Physiol*, 111:7-37.

Ohguro,H., Van Hooser,J.P., Milam,A.H., and Palczewski,K. (1995) Rhodopsin phosphorylation and dephosphorylation in vivo. *J.Biol.Chem.*, 270:14259-14262.

Omelchenko,A., Dyck,C., Hnatowich,M., Buchko,J., Nicoll,D.A., Philipson,K.D., and Hryshko,L.V. (1998) Functional differences in ionic regulation between alternatively spliced isoforms of the  $\text{Na}^{+}\text{-Ca}^{2+}$  exchanger from *Drosophila melanogaster*. *J.Gen.Physiol*, 111:691-702.

Otto-Bruc,A., Fariss,R.N., Haeseleer,F., Huang,J., Buczylo,J., Surgucheva,I., Baehr,W., Milam,A.H., and Palczewski,K. (1997) Localization of guanylate cyclase-activating protein 2 in

mammalian retinas. *Proc.Natl.Acad.Sci.U.S.A.*, 94:4727-4732.

Otto-Bruc,A.E., Fariss,R.N., Van Hooser,J.P., and Palczewski,K. (1998) Phosphorylation of photolyzed rhodopsin is calcium-insensitive in retina permeabilized by alpha-toxin. *Proc.Natl.Acad.Sci.U.S.A.*, 95:15014-15019.

Ovchinnikov,Y., Gubanov,V.V., Khramtsov,N.V., Ischenko,K.A., Zagranichny,V.E., Muradov,K.G., Shuvaeva,T.M., and Lipkin,V.M. (1987) Cyclic GMP phosphodiesterase from bovine retina. Amino acid sequence of the alpha-subunit and nucleotide sequence of the corresponding cDNA. *FEBS Lett.*, 223:169-173.

Palczewski,K., Buczylo,J., Kaplan,M.W., Polans,A.S., and Crabb,J.W. (1991) Mechanism of rhodopsin kinase activation. *J.Biol.Chem.*, 266:12949-12955.

Pepperberg,D.R., Cornwall,M.C., Kahlert,M., Hofmann,K.P., Jin,J., Jones,G.J., and Ripps,H. (1992) Light-dependent delay in the falling phase of the retinal rod photoresponse. *Vis.Neurosci.*, 8:9-18.

Pierce,G.N., Ward,R., and Philipson,K.D. (1986) Role for sulfur-containing groups in the  $\text{Na}^+ - \text{Ca}^{2+}$  exchange of cardiac sarcolemmal vesicles. *J.Membr.Biol.*, 94:217-225.

Pitts,B.J. (1979) Stoichiometry of sodium-calcium exchange in cardiac sarcolemmal vesicles. Coupling to the sodium pump. *J.Biol.Chem.*, 254:6232-6235.

Poon, S, Leach, S., Li, X-F, Tucker, J. E., Schnetkamp, P. P., and Lytton, J. Molecular Cloning and Functional Expresion of Alternatively Spliced isoforms of the Rat Eye Sodium-Calcium + Potassium Exchanger, NCKX1. Submitted . 2000.

Ref Type: Abstract

Porzig,H., Li,Z., Nicoll,D.A., and Philipson,K.D. (1993) Mapping of the cardiac sodium-calcium exchanger with monoclonal antibodies. *Am.J.Physiol*, 265:C748-C756.

Prinsen, C. F. M., Szerencsei, R. T., and Schnetkamp, P. P. Molecular Cloning and Functional Expression of the Potassium-Dependent Sodium-Calcium Exchanger from Human and Chicken Retinal Cone Photoreceptors. *Journal of Neuroscience* 20(4). 2-15-2000.

Ref Type: Abstract

Quednau, B.D., Nicoll, D.A., and Philipson, K.D. (1997) Tissue specificity and alternative splicing of the  $\text{Na}^+/\text{Ca}^{2+}$  exchanger isoforms NCX1, NCX2, and NCX3 in rat. *Am.J.Physiol*, 272:C1250-C1261.

Rebrik, T.I. and Korenbrot, J.I. (1998) In intact cone photoreceptors, a  $\text{Ca}^{2+}$ -dependent, diffusible factor modulates the cGMP-gated ion channels differently than in rods. *J.Gen.Physiol*, 112:537-548.

Reeves, J.P. and Sutko, J.L. (1979) Sodium-calcium ion exchange in cardiac membrane vesicles. *Proc.Natl.Acad.Sci.U.S.A*, 76:590-594.

Reeves, J.P. and Sutko, J.L. (1983) Competitive interactions of sodium and calcium with the sodium-calcium exchange system of cardiac sarcolemmal vesicles. *J.Biol.Chem.*, 258:3178-3182.

Reid, D.M., Friedel, U., Molday, R.S., and Cook, N.J. (1990) Identification of the sodium-calcium exchanger as the major ricin-binding glycoprotein of bovine rod outer segments and its localization to the plasma membrane. *Biochemistry*, 29:1601-1607.

Reilander, H., Achilles, A., Friedel, U., Maul, G., Lottspeich, F., and Cook, N.J. (1992) Primary structure and functional expression of the  $\text{Na}/\text{Ca}, \text{K}$ -exchanger from bovine rod photoreceptors. *EMBO J.*, 11:1689-1695.

Rozet, J.M., Gerber, S., Souied, E., Perrault, I., Chatelin, S., Ghazi, I., Leowski, C., Dufier, J.L., Munnich, A., and Kaplan, J. (1998) Spectrum of ABCR gene mutations in autosomal recessive macular dystrophies [published erratum appears in *Eur J Hum Genet* 1999 Jan;7(1):102]. *Eur.J.Hum.Genet.*, 6:291-295.

- Rudnicka-Nawrot, M., Surgucheva, I., Hulmes, J.D., Haeseleer, F., Sokal, I., Crabb, J.W., Baehr, W., and Palczewski, K. (1998) Changes in biological activity and folding of guanylate cyclase- activating protein 1 as a function of calcium. *Biochemistry*, 37:248-257.
- Saga, M., Mashima, Y., Akeo, K., Kudoh, J., Oguchi, Y., and Shimizu, N. (1998) A novel homozygous Ile535Asn mutation in the rod cGMP phosphodiesterase beta-subunit gene in two brothers of a Japanese family with autosomal recessive retinitis pigmentosa. *Curr.Eye Res.*, 17:332-335.
- Sambrook, J., Fritsch, E.F., and Maniatis, T. (1989) *Molecular Cloning*. Cold Spring Harbor Laboratory Press, Cold Spring Harbor.
- Sampath, A.P., Matthews, H.R., Cornwall, M.C., and Fain, G.L. (1998) Bleached pigment produces a maintained decrease in outer segment  $Ca^{2+}$  in salamander rods. *J.Gen.Physiol*, 111:53-64.
- Scheller, T., Kraev, A., Skinner, S., and Carafoli, E. (1998) Cloning of the multipartite promoter of the sodium-calcium exchanger gene NCX1 and characterization of its activity in vascular smooth muscle cells. *J.Biol.Chem.*, 273:7643-7649.
- Schnetkamp, P.P. (1980) Ion selectivity of the cation transport system of isolated intact cattle rod outer segments: evidence for a direct communication between the rod plasma membrane and the rod disk membranes. *Biochim.Biophys.Acta*, 598:66-90.
- Schnetkamp, P.P. (1986) Sodium-calcium exchange in the outer segments of bovine rod photoreceptors. *J.Physiol (Lond)*, 373:25-45.
- Schnetkamp, P.P. (1989) Na-Ca or Na-Ca-K exchange in rod photoreceptors. *Prog.Biophys.Mol.Biol.*, 54:1-29.
- Schnetkamp, P.P. (1991) Optical measurements of Na-Ca-K exchange currents in intact outer segments isolated from bovine retinal rods. *J.Gen.Physiol*, 98:555-573.



Schnetkamp, P.P. (1995a) Calcium homeostasis in vertebrate retinal rod outer segments. *Cell Calcium*, 18:322-330.

Schnetkamp, P.P. (1995b) How does the retinal rod Na-Ca+K exchanger regulate cytosolic free  $\text{Ca}^{2+}$ ? *J.Biol.Chem.*, 270:13231-13239.

Schnetkamp, P.P., Basu, D.K., Li, X.B., and Szerencsei, R.T. (1991a) Regulation of intracellular free  $\text{Ca}^{2+}$  concentration in the outer segments of bovine retinal rods by Na-Ca-K exchange measured with fluo-3. II. Thermodynamic competence of transmembrane  $\text{Na}^{+}$  and  $\text{K}^{+}$  gradients and inactivation of  $\text{Na}^{+}$ -dependent  $\text{Ca}^{2+}$  extrusion. *J.Biol.Chem.*, 266:22983-22990.

Schnetkamp, P.P., Basu, D.K., and Szerencsei, R.T. (1989)  $\text{Na}^{+}$ - $\text{Ca}^{2+}$  exchange in bovine rod outer segments requires and transports  $\text{K}^{+}$ . *Am.J.Physiol*, 257:C153-C157.

Schnetkamp, P.P., Li, X.B., Basu, D.K., and Szerencsei, R.T. (1991b) Regulation of free cytosolic  $\text{Ca}^{2+}$  concentration in the outer segments of bovine retinal rods by Na-Ca-K exchange measured with fluo-3. I. Efficiency of transport and interactions between cations. *J.Biol.Chem.*, 266:22975-22982.

Schnetkamp, P.P. and Szerencsei, R.T. (1991) Effect of potassium ions and membrane potential on the Na-Ca-K exchanger in isolated intact bovine rod outer segments. *J.Biol.Chem.*, 266:189-197.

Schnetkamp, P.P., Szerencsei, R.T., and Basu, D.K. (1991c) Unidirectional  $\text{Na}^{+}$ ,  $\text{Ca}^{2+}$ , and  $\text{K}^{+}$  fluxes through the bovine rod outer segment Na-Ca-K exchanger. *J.Biol.Chem.*, 266:198-206.

Schnetkamp, P.P., Basu, D.K., and Szerencsei, R.T., (1991d) The Stoichiometry of Na-Ca+K Exchange in Rod Outer Segments Isolated from Bovine Retinas. *Ann. N.Y. Acad. Sci.*, 639:10-20.

Schnetkamp, P.P., Tucker, J.E., and Szerencsei, R.T. (1995)  $\text{Ca}^{2+}$  influx into bovine retinal rod outer segments mediated by  $\text{Na}^{+}/\text{Ca}^{2+}/\text{K}^{+}$  exchange. *Am.J.Physiol*, 269:C1153-C1159.

Schnetkamp,P.P., Tucker,J.E., and Szerencsei,R.T. (1996) Regulation of the bovine retinal rod Na-Ca +K exchanger. *Ann.N.Y.Acad.Sci.*, 779:336-345.

Schwartz,E.A. (1981) First events in vision: the generation of responses in vertebrate rods. *J.Cell Biol.*, 90:271-278.

Schwarz,E.M. and Benzer,S. (1997) Calx, a Na-Ca exchanger gene of *Drosophila melanogaster*. *Proc.Natl.Acad.Sci.U.S.A*, 94:10249-10254.

Schwarzer, A. and Bauer, P. J. The complex of cGMP-gated channel and Na/Ca-K exchanger in rod plasma membrane. 1999 FASEB Summer Research Conferences: The Biology and Chemistry of Vision . 6-13-1999.

Ref Type: Abstract

Shady,S., Hood,D.C., and Birch,D.G. (1995) Rod phototransduction in retinitis pigmentosa. Distinguishing alternative mechanisms of degeneration. *Invest Ophthalmol.Vis.Sci.*, 36:1027-1037.

Shastry,B.S. (1994) Retinitis pigmentosa and related disorders: phenotypes of rhodopsin and peripherin/RDS mutations. *Am.J.Med.Genet.*, 52:467-474.

Shastry,B.S. and Trese,M.T. (1997) Identification of a polymorphic missense (G338D) and silent (106V and 121L) mutations within the coding region of the peripherin/RDS gene in a patient with retinitis punctata albescens. *Biochem.Biophys.Res.Comm.*, 231:103-105.

Short Protocols (1995) Short Protocols in Molecular Biology. John Wiley & Sons, Inc..

Shroyer,N.F., Lewis,R.A., Allikmets,R., Singh,N., Dean,M., Leppert,M., and Lupski,J.R. (1999) The rod photoreceptor ATP-binding cassette transporter gene, ABCR, and retinal disease: from monogenic to multifactorial. *Vision Res.*, 39:2537-2544.

Smith,W.C., Adamus,G., Van Der,W.H., Timmers,A., Palczewski,K., Ulshafer,R.J., Hargrave,P.A., and McDowell,J.H. (1995) Alligator rhodopsin: sequence and biochemical properties. *Exp.Eye Res.*, 61:569-578.

Smith,W.C., McDowell,J.H., Dugger,D.R., Miller,R., Arendt,A., Popp,M.P., and Hargrave,P.A. (1999) Identification of regions of arrestin that bind to rhodopsin. *Biochemistry*, 38:2752-2761.

Sokal,I., Haeseleer,F., Arendt,A., Adman,E.T., Hargrave,P.A., and Palczewski,K. (1999) Identification of a guanylyl cyclase-activating protein-binding site within the catalytic domain of retinal guanylyl cyclase 1. *Biochemistry*, 38:1387-1393.

Stryer,L. (1986) Cyclic GMP cascade of vision. *Ann.Rev.Neurosci.*, 9:87-119.

Subbaraya,I., Ruiz,C.C., Helekar,B.S., Zhao,X., Gorczyca,W.A., Pettenati,M.J., Rao,P.N., Palczewski,K., and Baehr,W. (1994) Molecular characterization of human and mouse photoreceptor guanylate cyclase-activating protein (GCAP) and chromosomal localization of the human gene. *J.Biol.Chem.*, 269:31080-31089.

Sugimoto,Y., Yatsunami,K., Tsujimoto,M., Khorana,H.G., and Ichikawa,A. (1991) The amino acid sequence of a glutamic acid-rich protein from bovine retina as deduced from the cDNA sequence. *Proc.Natl.Acad.Sci.U.S.A*, 88:3116-3119.

Sullivan,L.S., Heckenlively,J.R., Bowne,S.J., Zuo,J., Hide,W.A., Gal,A., Denton,M., Inglehearn,C.F., Blanton,S.H., and Daiger,S.P. (1999) Mutations in a novel retina-specific gene cause autosomal dominant retinitis pigmentosa. *Nat.Genet.*, 22:255-259.

Sun,H., Molday,R.S., and Nathans,J. (1999) Retinal stimulates ATP hydrolysis by purified and reconstituted ABCR, the photoreceptor-specific ATP-binding cassette transporter responsible for Stargardt disease. *J.Biol.Chem.*, 274:8269-8281.

- Szerencsei, R.T., Tucker, J.E., Cooper, C.B., Winkfein, R.J., Farrell, P.J., Iatrou, K., and Schnetkamp, P.P. (2000) Minimal domain requirement for cation transport by the potassium- dependent Na/Ca-K exchanger. Comparison with an NCKX paralog from *Caenorhabditis elegans*. *J.Biol.Chem.*, 275:669-676.
- Tachibanaki, S., Nanda, K., Sasaki, K., Ozaki, K., and Kawamura, S. (2000) Amino acid residues of S-modulin responsible for interaction with rhodopsin kinase [In Process Citation]. *J.Biol.Chem.*, 275:3313-3319.
- Tamai, M., Mizuno, K., and Chader, G.J. (1982) In vitro studies on shedding and phagocytosis of rod outer segments in the rat retina: effect of oxygen concentration. *Invest Ophthalmol.Vis.Sci.*, 22:439-448.
- Thorpe, D.S. and Garbers, D.L. (1989) The membrane form of guanylate cyclase. Homology with a subunit of the cytoplasmic form of the enzyme. *J.Biol.Chem.*, 264:6545-6549.
- Travis, G.H., Brennan, M.B., Danielson, P.E., Kozak, C.A., and Sutcliffe, J.G. (1989) Identification of a photoreceptor-specific mRNA encoded by the gene responsible for retinal degeneration slow (rds). *Nature*, 338:70-73.
- Tsien, R.Y., Rink, T.J. and Poenie, M. (1985) Measurement of cytosolic free  $\text{Ca}^{2+}$  in individual small cells using fluorescence microscopy with dual excitation wavelengths. *Cell Calcium*, 6(1-2): 145-157.
- Tsoi, M., Rhee, K.H., Bungard, D., Li, X.F., Lee, S.L., Auer, R.N., and Lytton, J. (1998) Molecular cloning of a novel potassium-dependent sodium-calcium exchanger from rat brain. *J.Biol.Chem.*, 273:4155-4162.
- Tucker, J.E., Winkfein, R.J., Cooper, C.B., and Schnetkamp, P.P. (1998b) cDNA cloning of the human retinal rod Na-Ca + K exchanger: comparison with a revised bovine sequence. *Invest Ophthalmol.Vis.Sci.*, 39:435-440.

- Tucker,J.E., Winkfein,R.J., Murthy,S.K., Friedman,J.S., Walter,M.A., Demetrick,D.J., and Schnetkamp,P.P. (1998a) Chromosomal localization and genomic organization of the human retinal rod Na-Ca+K exchanger. *Hum.Genet.*, 103:411-414.
- Washburn,T. and O'Tousa,J.E. (1989) Molecular defects in *Drosophila* rhodopsin mutants. *J.Biol.Chem.*, 264:15464-15466.
- Weil,D., Kussel,P., Blanchard,S., Levy,G., Levi-Acobas,F., Drira,M., Ayadi,H., and Petit,C. (1997) The autosomal recessive isolated deafness, DFNB2, and the Usher 1B syndrome are allelic defects of the myosin-VIIA gene. *Nat.Genet.*, 16:191-193.
- Weitz,D., Zoche,M., Muller,F., Beyermann,M., Korschein,H.G., Kaupp,U.B., and Koch,K.W. (1998) Calmodulin controls the rod photoreceptor CNG channel through an unconventional binding site in the N-terminus of the beta-subunit. *EMBO J.*, 17:2273-2284.
- Weng,J., Mata,N.L., Azarian,S.M., Tzekov,R.T., Birch,D.G., and Travis,G.H. (1999) Insights into the function of Rim protein in photoreceptors and etiology of Stargardt's disease from the phenotype in abcr knockout mice. *Cell*, 98:13-23.
- Wolbring,G. and Schnetkamp,P.P. (1995) Activation by PKC of the Ca(2+)-sensitive guanylyl cyclase in bovine retinal rod outer segments measured with an optical assay. *Biochemistry*, 34:4689-4695.
- Wolbring,G. and Schnetkamp,P.P. (1996) Modulation of the calcium sensitivity of bovine retinal rod outer segment guanylyl cyclase by sodium ions and protein kinase A. *Biochemistry*, 35:11013-11018.
- Yamamoto,S., Sippel,K.C., Berson,E.L., and Dryja,T.P. (1997) Defects in the rhodopsin kinase gene in the Oguchi form of stationary night blindness [see comments]. *Nat.Genet.*, 15:175-178.
- Yau,K.W. (1987) On presentation of the Proctor Medal of the Association for Research in Vision and Ophthalmology to Dr. Denis A. Baylor. *Invest Ophthalmol.Vis.Sci.*, 28:29-33.

Yau, K.W. and Nakatani, K. (1984b) Cation selectivity of light-sensitive conductance in retinal rods. *Nature*, 309:352-354.

Yau, K.W. and Nakatani, K. (1984a) Electrogenic Na-Ca exchange in retinal rod outer segment. *Nature*, 311:661-663.

Yu, A.S., Hebert, S.C., Lee, S.L., Brenner, B.M., and Lytton, J. (1992) Identification and localization of renal Na(+)-Ca<sup>2+</sup> exchanger by polymerase chain reaction. *Am.J.Physiol*, 263:F680-F685.

Zhaoping, L., Matsuoka, S., Hryshko, L.V., Nicoll, D.A., Bersohm, M.M., Burke, E.P., Lifton, R.P., and Philipson, K.D. (1994) Cloning of the NCX2 isoform of the plasma membrane Na<sup>+</sup>-Ca<sup>2+</sup> exchanger. *J.Biol.Chem.*, 269:17434-17439.

Zito, I., Thiselton, D.L., Gorin, M.B., Stout, J.T., Plant, C., Bird, A.C., Bhattacharya, S.S., and Hardcastle, A.J. (1999) Identification of novel RPGR (retinitis pigmentosa GTPase regulator) mutations in a subset of X-linked retinitis pigmentosa families segregating with the RP3 locus. *Hum.Genet.*, 105:57-62.

## Appendix I - Oligonucleotides

Bovcardsig1	TTGCGGCCGCAGCATGCTGCAGTTCAGTC	
Bovcardsig2	TTACTAGTTCCAAAGGAAGGGTCCTGGG	
Rod 5'	TTACTAGTGGACAGCCAGACCTGTACCC	
Rod 3'	CCACATCCTCAGAGATCTGC	
Rod Bandid1	CTAGGTGATCAGAATGCT	' for OF ligation
Rod Bandid2	CATTCTGATCAC	'
Bandid top	CTAGGTTTGATCATGAATGCT	' for IF construction
Bandid bott	CATTCATGATCAAAC	'
1-5'	TTCTCGAGTTGAATGCTGAAATTCAAGGTG	' for CCC construction
1-3'	AAGCGGCCGCTGATCAATTGCTTCCGCCTGGTCTCAGG	'
BaculovirusF	TTTACTGTTTTTCGTAACAGTTTTG	
BaculovirusR	CAACAACGCACAGAATCTAG	
λgt11 Forw	GGTGGCGACGACTCCTGGAGCCCG	' salamander attempt
λgt11 Rev	TTGACACCAGACCAACTGGTAATG	'
17-B	TCAACAACCTTCCCGTGCCACA	' salamander sequencing attempt
λgt10 Forw	AGCAAGTTCAGCCTGGTTAAG	
λgt10 Rev	CTTATGAGTATTTCTTCCAGGGTA	
λgt10-f-out	TCTATAGACTGCTGGGTAGTCC	
λgt10-r-out	ACAGTTTTTCTTGTGAAGATTGGG	
SeqPrimer1	TCCTCCTCTACCTCGTCCTCC	' for sequencing clone 27
Primer2	AGGCCAGTCCAGGGACAGAGG	' also
Nonsense1	AATTAAAGCCATATTTACCATCAT	' also, on the nonsense side
Nonsense2	TTCCCTTCCCACTCCACTCAA	' also
BB4mcs-S	GATCCTTGCGGCCGCTTGAATTCTTTCTAGATTA	' for BB4 cloning
BB4mcs-A	AGCTTAATCTAGAAAGAATTCAAGCGGCCGCAAG	' also
T <sub>7</sub>	TAATACGACTCACTATAGGG	
Sp6	TTAGGTGACACTATAGAATAG	
EHApach1	AATTCGGCGCCTTAAGCTTTTGACGTCC	
EHApach2	TCGAGGACGTCAAAAGCTTAAGGCGCCG	
Front	GGCAGCAGTCTCTTCTCATCAGCC	
Back	AGTTGGGGTGCTATCAAACATTCC	
SP1	CGCGAATTCCACCATGGGGAAAYTGATCAGGATGGG	
SP2	CCGGAATTCTCAGACAGATACAGGARCAAGGATAT	
ST1	TTACTACACCTCAACTTCAAGCAG	
180	TGATACACTGGTCCTGGGTGAAGG	
182	TTAGAAGATCGAATCATATCCTG	
R17 ?	AGCTGTTCTATTTCTAACGTGTCC	
Get 3'	TTGCGGCCGCCCCACTGTGGCTGACAGTCC	
Get 5'	TTGGTACCAAGGTGAAAACAAAAAACTTCCTA	
3' Race	TGAACCTCTGTCCCTGGACTGGC	
3 Sense	CGAATTCTTTGATCATTC	
3 Antisense	TCGAGAATGATCAAAGAATTCGGTAC	
H1-Rev	TTGTCTGTGATGACACCCAG	
H1-get cyto	CAYAT[CTA]TTYGGNATGATGTAYGT	
H5-get cyto	TTYACNATGAARTGGAAYCARCA	
H6-Rev	GCCATTCCAGGGACAGAGG	
H7-Forw	AGTTTTTTGTTATCACCTTCCTGG	
H7-Rev	CCNACYTGRTGNGCCCA	
H9-Forw	GGCCTGCCCCCTTCCTTGGATGCT	

H10-Rev	ATYTTTRTTCATYCTCCAYTTTRCA
FLAG-TOP	AATTCTTGACTACAAGGACGACGATGACAAGGT
FLAG-BOTT	CTAGACCTTGTTCATCGTCGTCCTTGTAGTCAAG
3'-UTR	GCATTCTTGGAATTTCCCTTT
Bovbuf	CAGACNTCAAGGGAGATCAGNAGG
JTG-1	CCTTCTGATCTCCCTTGATGTCTG
JTG-2	CCATGAAGTGGAACAAGCATATCGA
JTG-3	TCGATATGCTTGTTCCACTTCATGG
JTG-4	CTGGGTGTCATCACAGACAAGCT
JTG-5	TTCAGGCCAGTCCAGGGACAGAGG
JTG-6	CAGCACCATCTACCAGCTCATGCT
JTG-7	CTGGTTTGCTTTCTGCTTTGGCCT
JTG-8	TCAGCACTGAGTTCCTGGCTTTCA
JTG-8E	TTGAATTCAGCACTGAGTTCCTGGCTTTCA
JTG-9	GGATAGCCATGTTCTCATACCTCA
JTG-10	GAAGAGATCACAAACAGAAGCATG
JTG-11	GCTGACTGGAAGTGGCTGTAATCC
JTG-12	TAGGCTGATGAGAAGAGACTGCTG
JTG-13	CTGCTTGAAGTTGAGGTGTAGTAA
JTG-14	AGTAACAGCTCAGCCCATCCCTGG
JTG-15	CCAGGGATGGGCTGAGCTGTTACT
JTG-16	CCAGCACCTCAACAACCCCTACGG
JTG-17	AATCCTTGCAGCAGGCACATCAAT
JTG-18	CAATCACACTGGTGATGAGGTCAG
JTG-19	GCTCTCCCACCAGGCAATGAGGCT
JTG-20	TTCTCTTCAGTTTCACCTTCACCA
JTG-21	CATTTCCGAGCTAGGTTTTGAAGG
JTG-22	GCTTTGTCCGGAGTAACCACCTCTCTTGCG
JTG-23	TTGTTCAACTTCTTTGCTTTCTGC
JTG-24	TGCTCATTGTCTTCTTCCTGGACA
JTG-25	AGCATGAGCTGGTAGATGGTGCTG
JTG-26	AGGCCAAAGCAGAAAGCAAACC
JTG-27	AGCAGCTCAGCAGGAGGCCAGTGG
JTG-27E	TTGAATTCAGCAGCTCAGCAGGAGGCCAGTGG
JTG-28	CCACTGGCCTCCTGCTGAGCTGCT
JTG-29	GATGGGGCCATTGCGGTGGATGAG
JTG-30	TAGCTCATCCACCGCAATGGCCCC
JTG-31	TTCTTAGGAGCTTGCTGAGGTCTTCTAAGG
JTG-33	AGGAGCAGCTCAGCAGGAGGCCAG
JTG-34	GACCTCTGTGTTTCATATCTC
JTG-35	TTCTCCATGAAGCCCAGCCAG
JTG-35	TTCTCCATGAAGCCCAGCCAG
JTG-36	GTTTCCAGAGCTGAGAAGACAGCC
JTG-37	TGAGGTTCTTAATCCACAATGAGC
JTG-38	GCTCATTGTGGATTAAGAACCTCA
JTG-39	TCTAAGGATCCAAGGCTACAGA
JTG-40	GGCTGTCTTCTCAGCTCTGGAAAC
JTG-41	CTCCTCTTAGTGGTAAATAATCTC
JTG-42	CTAGAGAAACCTGAGCCAATTTGT
JTG-43	TCTAAGCTATGAGAATTGAGAGGT
JTG-44	CTTAATATCACTGGCTTCAGAGCA

\* replacement for JTG-27  
 \* for PAC-18 seq from T3 side  
 \* also, from JTG-12 side



JTG-45	AGGCCTAAAGGAAATCCTTGGTGT	
JTG-46	AAGATGGAATACTTGGAACACCTT	
JTG-47	GTCCACTGGATCTCTTACTTTATA	
JTG-48	CAATAAGAGTTAATGTAGTCCTCC	
JTG-50	TGGTGTGCAATGGCGTGATCTCGG	
JTG-60	GATGAAAATGAAGCAGAAGG	
JTG-61	TTAAGCTTGCTGAGGTCTTCTAAGGCCA	
JTG-62	TTAAGCTTGAAGATGTGGCTGAGGCCGA	
BovK	TTGGTACCGTTTTTCACCTTCAGCAGGAG	
BovB	TTAGATCTAGCAGCTCAACAAGAGGCCA	
dTanchor-B1	TGACTGGACTATGGTCTCGACATGGCGTAGTCGTTTTTTTTTTTTTTTTTT	
dTanchor-3'	CGACTACGCCATGTCTGAGACCATAGTCCAGTCACCCC	
Anchor1	GGGTGACTGGACTATGGTCTC	
Anchor2	GGGCTCGACATGGCGTAGTC	
Anchor3	GCAGGTCTCGACATGGCGTA	
Anchor4	GCAGGTCTCGACATGGCGTAGTCG	
RP1	ATGCTGCAGTTCAGTCTGTCACCC	
RP2	GAGCTGTTGGTTCCACTTCATGGT	' for Riboprobe for RPA, 1 <sup>st</sup> try

## Appendix II

## Human NCKX1 Transcript Sequence

cccttcacacccgaccagccttgaattaggattccataggagagctgggggcaggagaatgggggtgtccctgctgtccagcttcagacccactctttag  
 atattggattctgacaagtgtccagagctgagaagacagccagatgtcaaggctgaagggtgtggataccccctggctgggcttcagtgagaaatcttctc  
 gatcaccaacctgaatccagagtagcctccatcttaggacagaatgagaggccttctgtaaccagatataactggccagcATGGGGAAATTG  
 ATCAGGATGGGGCCGCAAGAGAGGTGGTTACTCCGGACAAAGCGGCTTCATTGGAGTCGCCT  
 CCTCTTCTTACTGGGAATGTTGATCATCGGTTCTACTTATCAGCACCTTAGGAGACCCCGGGG  
 CTTTCCTCATTGTGGGCAGCAGTCTTCTCATCAGCCTATAAACTGGCCAGTCGGGACCTCT  
 CCAGTGAAGAGATGATGATGATGAGCAGCAGCCCTTCAAAACCTAGCTCCGAAATGGGGGGT  
 AAGATGCTGGTACCCCAAGCCTCAGTGGGCAGTGATGAAGCAACACTGAGCATGACAGTGGA  
 GAATATCCCCAGTATGCCTAAAAGAACAGCCAAGATGATCCCAACAACAACCAAGAATAATT  
 ACAGCCCAACAGCAGCAGGTACAGAAAGAAGGAAGACACCCCAACATCCAGTAGAAC  
 ACTGACTTACACCTCAACTTCAAGCAGACAAATAGTAAAAAAGTATACCCCAACACCCA  
 GGGGAGAAATGAAGAGCTACAGCCCAACTCAAGTGAGGGAAAAGGTGAAGTATACTCCTTCC  
 CCACGTGGTAGAAGAGTAGGCACTTACGTGCCGTCCACATTCATGACAATGGAAACAAGCCA  
 TGCGATCACCCCCAGGACAACAGTGAAAGACAGTGACATTACAGCAACCTATAAAATACTCG  
 AAACCAACTCTCTTAAGAGAATAATGGAGGAAACCACCCCAACCACTCTCAAGGGAATGTTT  
 GATAGCACCCCAACTTTTCTGACACATGAGGTAGAAGCAAACGTCTTGACTTCTCCAAGGAGC  
 GTCATGGAAAAAACAACCTGTTTCCCCCAGAAGAGTGGAAGTAACAGCTCAGCCATCC  
 CTGGGGGTTAGTGGGAAAGAGCAACCCGAAGACTCCCCAGGGAACAGTCTGTTGCATACCC  
 CAGCCACCTCTGAGGGGCAGGTGACAATAAGCACCATGACAGGCAGCAGCCAGCAGAAACC  
 AAAGCCTTCACTGCTGCCTGGAGTCTTAGGAATCCTTCACCCAGGACCAGTGTATCAGCCATC  
 AAAACAGCCCCAGCCATAGTCTGGAGGCTGGCAAAGAAACCTTCCACAGCACCCAGCACCTC  
 AACAACCCCTACGGTCAGGGCAAAGCTGACCATGCAGGTCCATCACTGTGTGGTTGTGAAGCC  
 AACCCAGCCATGCTCACCACTCCCTCCCCAAGCCTCACAACAGCCCTGCTCCCAGAGGAGCT  
 CAGTCCTAGTCCCTCAGTGCTGCCTCCCAGCTTGCCAGACCTCCACCCCAAGGGAGAGTACCC  
 CCCAGATCTGTTCAGTGTGGAGGAGCGGCGGCAGGGCTGGGTGGTCTGCACGTTTTTGGCAT  
 GATGTATGTGTTTGTGGCCTTGCCATTGTTTGCACGAGTACTTCGTTCCAGCCCTGGGTGTC  
 ATCACAGACAAGCTGCAGATCTCCGAGGATGTGGCAGGCGCCACATTATGGCTGCTGGAGG  
 CTCTGCTCCTGAGCTCTTACCTCCCTCATCGGTGTCTTCAATTTCCACAGCAACGTGGGCATT  
 GGTACCATTTGTGGGCTCTGCTGTGTTCAACATTTCTTTGTCATTGGCACTTGTTCCTCTTCTC  
 CCGAGAGATCCTCAACCTCACCTGGTGCCCTTATTCGCTGATGTCTCCTTCTACATCCTTGAC  
 CTGATAGATGCTCATCCTCTTCTCCTGGACAGCCTCATTGCCTGGTGGGAGAGCCTGCTGCTGC  
 TGCTGGCCTATGCCTTCTATGTGTTACCATGAAGTGGAACAAGCATATCGAGGTCTGGGTGA  
 AGGAGCAGCTCAGCAGGAGGCCAGTGGCCAAGGTGATGGCCTTAGAAGACCTCAGCAAGCCG  
 GCGGATGGGGCCATTGCGGTGGATGAGCTACAGGATAACAAGAAGCTGAAGCTCCCGTCCTT  
 GCTGACCCGAGGGAGCAGCTCGACCTCTCTGCACAACAGCACCATCCGCAGCACCATCTACCA  
 GCTCATGCTCCACAGCCTGGACCCCTGAGGGAAGTTCGCTTGCCAAGGAGAAGGAGGAGG  
 AGAGCTTGAATCAAGGGGCCAGAGCCCAACCCAGGCCAAAGCAGAAAGCAAACCAGAAGA  
 GGAGGAGCCAGCCAAGCTCCCTGCGGTACGGTCACACCAGCCCTGTTCCAGACATCAAGG  
 GAGATCAGAAGGAGAATCCAGGCGGTACAGGAAGATGTGGCTGAGGCCGAGAGCACAGGTGA  
 AATGCCAGGCGAAGAGGGCGAAACTGCTGGTGAAGGTGAAACTGAAGAGAAAAGTGAGGT  
 GAAACTCAACCAGAAGGTGAAGGTGAAACTGAAACACAAGGAAAAGGAGAAGAATGTGAAG  
 ATGAAAATGAAGCAGAAGGAAAAGGAGACAATGAAGGTGAAGATGAGGGTGAATCCACGC  
 AGAAGATGGTGAATGAAGGTGAATGAAGGTGAAACTGAAAGCCAGGAACTCAGTGCTGAA  
 AATCACGGTGAAGCCAAAAATGATGAGAAAGGTGTAGAAGATGGAGGGGGAAAGTATGGAG  
 GGGATAGCGAAGAGGAGGAAGAGGAGGAGGAAGAGCAGGAGGAAGAGGAGGAGGAGGAAG  
 AGCAGGAGGAAGAGGAGGAGGAGGAGGAGGAAGAGGAGGAGAAGGGAAATGAAGAGCCTC  
 TGTCCCTGGACTGGCCTGAAACCAGGCAGAAAGCAGGCCATTTACCTCTTCTCTGCCCATCG  
 TGTTCCTCACTGTGGCTGACAGTCCCCGACGTCCGAAGGCAGGAGTCTAGGAAGTTTTTTT  
 CACCTTCTGGATCTATCATGTGGATAGCCATGTTCTCATACCTCATGGTGGTGGGCTCAC  
 CAGGTTGGTGAAACAATAGGATTTCTGAAGAGATCATGGGCCTGACAATCCTTGACGAGG  
 CACATCAATTCCTGACCTCATCACCAGTGTGATTGTGCTCGAAAAGGCCTGGGAGACATGGC  
 TGTGTCAAGCTCTGTGGGCAGTAACATATTTGATATCACTGTGGGCTTGCCTGTTCTTGGTTG  
 CTTTTCTCTTATCAATGGATTACAGCCAGTTCAGTCAGCAGCAATGGCTTGTGTTGTGCAA



**Appendix II****Partial sequences of mouse retinal NCKX1 cDNA**

GCAGATCTCCGAGGATGTGGCAGGGGCCACATTCATGGCTGCCGGAGGCTCGGC  
CCCGGAGCTCTTCACCTCTCTCATTGGTGTCTTTATCTCCCACAGCAATGTGGGTA  
TTGGTACCATCGTGGGCTCTGCTGTGTTCAACATCCTTTTTGTCATCGGCACCTGT  
GCCCTCTTCTCCCGGGAGATCCTCAACCTCACCTGGTGGCCCCTGTTCCGAGACG  
TCTCCTTCTACATCCTTGACTTGTCTATGCTCATTGTCTTCTTCTGACAGC

GCCTGGTGGGAGAGCCTGCTGCTGCTGTTGGCCTACGCTCTCTATGTGTTACCA  
TGAAGTGGAACAAGCAGATTGAGCTCTGGGTGAAAGAGCAGCTTAGCAGGAGGC  
CCGTAGCCAAAGTCATGGCCCTGGGAGACCTCAGCAAGCCCAGTGAGGATGCTG  
TCGAGGAAGAACGAGCAACAGGACAGCAAGAACTGAAGCTCCGTC

GAACAAGAAGGGAACTGAGGCAGAAGGAAAAAGAAGATGAACAAGAAGGGGAA  
ACTGAGGCAGAAGGCAAAGAGGAACAAGAAGGGGAACTGAGGCAGAAAGCAA  
AGAAGTTGAACAAGAAAGGGAACTGAGGCAGAAGGCAAAGATAAGCATGAAG  
GGCAAGGTGAAACCCAACCAGACGACACTGAGGTGAAAGATGGTGAGGGTGAAA  
CAGAAGCCAATGCTGAAGATCAATGTGAGGCCACCCAAGGTGAGAAGGGTGACAG  
ACGGTGGAGGGGGAAGTGATGGAGGGGACAGTGAGGAAGAGGAGGATGAAGAA  
GATGAAGAGGAGGAAGAGGAGGAAGATGAGGAAGAGGAGGAGGAGGAAAATGA  
GGAG